DEVELOPMENT OF THE HUMAN NEOCORTEX

A REVIEW AND INTERPRETATION OF THE HISTOLOGICAL RECORD

Joseph Altman and Shirley A. Bayer

A Free eBook from the
Laboratory of Developmental Neurobiology, Inc.

www.neurondevelopment.org

PREFACE

This book is a sequel to an earlier publication of ours, *Neocortical Development* (Bayer and Altman, 1991), which dealt mainly with the development of the rat neocortex. That book was based to a large extent on an analysis of several large collections of brains prepared in our own laboratory. The first one was a collection of paraffin embedded and cell-body stained histological sections of complete embryos or dissected brains, ranging in age at daily intervals from embryonic day 11 (E11) until birth (E23/postnatal day 0). We used that material for easy visualization of the development of the neocortex and some related forebrain structures at low magnification as a function of prenatal age. The second was a collection of thinner sections of brains embedded in methacrylate, systematically cut in the coronal, sagittal and horizontal planes and providing better cellular detail, which allowed visualization of the growth and differentiation of neocortical neurons at higher magnification. The third was a vast collection of brains from rats that were injected with ^{3}H-thymidine during the prenatal period to label the DNA of multiplying precursors of neurons and glia. Specimens were killed 2 hours after injection, at 24 hour intervals after injection, or as adults after multiple injections. The thymidine autoradiographic material was prepared with three variants of the technique. The first survival set (2 hrs), referred to as short-survival autoradiography, allowed us to identify the site and time of origin of forebrain and neocortical neurons from proliferative precursor cells in the neuroepithelium (NEP) with their regional gradients. The second survival set (24 hr intervals), referred to as sequential survival autoradiography, allowed us to track the migration and settling pattern of the differentiating neocortical neurons. This led to the identification of the stratified transitional field (STF), the transient region between the neuroepithelium and the cortical plate (gray matter), where the migrating neurons sojourn before proceeding to settle in the cortical plate (also called the intermediate zone). We hypothesized that the differentiating “unspecified” neurons become ”specified” in the STF in terms of their modality and topographic identity. The third set, called long survival autoradiography after multiple injections of ^{3}H-thymidine, allowed us to quantify the time of origin of neurons that settled in different layers of the neocortex in adult rats. The multiple injections nearly eliminated the label dilution problem and enabled us to divide neuronal populations into either unlabeled (neurons generated before injections began) or labeled (neurons generated after injections began).

With that background in the analysis of some aspects of the morphogenetic development of the simpler, smooth (lissencephalic) neocortex of the rat, we turn now to an investigation of the development of the far more complex foliated (gyrencephalic) human neocortex. The brains that we have used for that purpose and illustrate in this book were not prepared in our laboratory. Rather, we turned to other sources. One was the published gross-anatomical and histological studies of the developing human neocortex, dating back as far as the end of the 19th century, much of it unavailable and forgotten by contemporary researchers. These included the large collection of developing human brains by Gustaf Retzius towards the end of the 19th century; the work of Cecilie and Oscar Vogt early in the 20th century concerned with the fiber development and myelination of the infant brain; and the 8 volumes on postnatal brain development early in the second half of the 20th century by Leroy Conel. The other source was the large archive of photographs that we have collected in the 1980s, using the Collections of histologically prepared developing human brains, housed at the National Museum of Health and Medicine, at that time located on the campus of the Walter Reed Army Hospital, in Bethesda, Maryland. The three Collections that we have used were prepared by Charles Minot early in the 20th century, the staff of the Carnegie Institution a few decades later, and by Paul Yakovlev early in the second half of the 20th century. We found many of the sections fading and becoming useless and sought to salvage the best preserved of them for future use by photographing them and digitizing the photos.

Our knowledge of the development and organization of the brain comes from many sources. Embryologists, neuroanatomists, and neuropathologists have been studying the morphological development of the brain and the formation of the its circuitry in animals and humans for over 150 years, ever since techniques have become available to preserve postmortem neural tissue and use stains to visualize nerve cell bodies and their axons and dendrites. The earlier studies focused on the dissection of the brains of animals and humans at different stages of development and analysis of the morphogenesis of different brain structures. That was followed by selective destruction of different brain regions in experimental animals and subsequently tracing the trajectory of degenerating fibers, some of them originating in the neocortex, others targeting it. A highly successful later technique included the injection of anterograde and retrograde tracers into selected brain regions of experimental animals, followed by a postmortem analysis of the origins, trajectories and targets of the tagged fibers. These experimental methods could not be used in humans. The major source of information that we have about the structural organization of the developing human central nervous system (CNS) in general, and the neocortex in particular, had to come from the brains of aborted embryos, fetuses, stillborn neonates, and infants that died from causes other than brain pathology. These specimens were histologically prepared for microscopic analysis and we present some of them here.

The last few decades has seen the introduction of minimally-invasive approaches to study brain development in living preterm babies, neonates, infants and young children using scanning techniques such as magnetic resonance imaging (MRI), positron emission tomography (PET), and diffusion tensor imaging (DTI). As of the present time, the most rewarding procedure has been MRI scanning and visualization, which is based on the computerized determination of the substantial difference in the free water content of three components of the brain: the ventricles filled with cerebrospinal fluid; the soft cortical gray matter; and the more compact white matter. That differential provides useful images of the changing material composition of the developing

brain as a function of age. However, the resolution that MRI currently provides is macroscopic rather than microscopic, hence it is limited to visualization of gross changes in brain development. MRI cannot be used for the study of morphogenetic changes at the cellular level, and it is not suitable for tracking intrauterine brain development. (Ultrasonic scanning has been a good source of following intrauterine body growth and movement but not of the development of the soft brain tissue.) These new "high-tech" based "modern" approaches have greatly advanced the diagnosis of early brain abnormalities and are proving to be a promising approach in the neuropsychological study of brain-behavior correlations in adults. They have yet to become a rewarding research technique to further our knowledge of human brain development at the microscopic level of resolution. As a matter of fact, most of what we currently know about human prenatal and early postnatal brain development on the cellular and subcellular level is based on classical postmortem studies using various histological and cytological staining techniques. The purpose of this book is to review that information and encourage research scientists to pursue that "low-tech" and rewarding "classical" approach.

This book is divided into an introductory section and two parts. Part I consists mainly of photographic illustrations of microscopic transformations, and at later stages also visible changes in the development of the neocortex, beginning with the initial emergence of the neocortex in embryos during the mid-first trimester of gestation through the fetal stages of the second and third trimesters, and ending with infants and young children. We provide each illustration with extensive commentaries, with emphasis on highlights of developments taking place during each stage. Part II offers interpretations and hypotheses based on the illustrations presented, as well as information that comes from other sources, with much of it carried out in experimental animals. Thanks to the availability of computerized resources, we have been able in the last few decades to prepare our books as camera-ready copies that were printed and distributed by different publishers. Their sale was a source of revenue that financed the preparation of those books. We have recently received some unsolicited funds (an award from the Prince of Asturias Foundation in 2011, and another from the Japan Society for the Advancement of Science in 2012) and are in a position to bypass the publishers and put this book directly on the Internet, thus making it available free of charge by students, researchers, and perhaps the occasional layman, social worker or official interested in the topic of early human brain development.

INTRODUCTION AND BACKGROUND

The structural and functional organization of the mature human central nervous system (CNS) in general and of the neocortex in particular is the end product of a complex developmental process. As in other vertebrates, that development consists of a series of sequential morphogenetic transformations that begins with the proliferation of the precursors of neurons and glia; the migration and differentiation of young neurons; followed by the neurons sprouting axons and dendrites and forming synapses; and ending with the myelination of the axons of the fiber tracts. That partially overlapping sequence is uniform throughout much of the CNS but with a different timetable for its different components from caudal to rostral—the spinal cord, medulla, hindbrain, and forebrain—with the neocortex being among the latest-maturing brain regions.

The first event in CNS development is the proliferation of the precursor cells of neurons and neuroglia in a specialized germinal matrix, the *neuroepithelium*. Initially flat, the neuroepithelium (NEP) folds and fuses, and forms the fluid filled neural tube caudally and the brain ventricles rostrally. The next developmental event is *neurogenesis*, the progressive differentiation of many NEP precursor cells into postmitotic neurons. The young neurons leave the NEP and migrate along radial and tangential routes to settle in various terminal locations. Other precursor cells leave the NEP to form secondary (subventricular or subpial) germinal matrices, while still others retain their proliferative potential and multiply in the maturing or mature brain parenchyma as supporting glial cells. The second event in CNS development is the maturation of neurons and glia throughout the parenchyma of the brain and spinal cord. Neurons differentiate in four phases that may occur either simultaneously or in sequence. Part one of this differentiation is *axonogenesis*. Some neurons sprout long afferent axons that convey information from the sense organs to projection areas of the CNS. Other neurons sprout shorter axons that feed-forward and feedback information from one processing center to another. Still other neurons sprout long efferent axons that carry commands from motor brain regions in the brain and spinal cord to the muscular system. Part two of this differentiation is *dendrogenesis*, when neurons sprout dendrites that assume different regionally specific configurations to intercept incoming signals from axons in the neighborhood. Part three of differentiation is *synaptogenesis* when axon terminal branches establish contacts with dendrites in specialized structures called *synapses*. The fine circuitry of the nervous system develops and is modified as synaptic connections form and disappear during brain activity. The fourth step in differentiation is *myelogenesis*. Specialized glial cells encase long axons of the afferent, efferent, associational, and commissural fiber tracts of the CNS circuitry. Myelination is a particularly important step in turning the maturing sensory, integrative and motor networks of the CNS in general and of the neocortex in particular into a functional system by regulating the speed of afferent and efferent impulse transmission, timely access to storage sites, and the synchronization of feed-forward and feedback information processing.

SOURCES OF THE ILLUSTRATED SPECIMENS

The illustrations of human brain specimens used in this book, tracking the sequence of embryonic, fetal and early postnatal neocortical development. were drawn from multiple sources. The oldest illustrations are from Paul Flechsig's work on the myelination of the human cerebral cortex, as summarized by Ariëns Kappers et al. (1936). Flechsig began to publish his pioneering papers on

"myeloarchitectonics" of the cerebral cortex in the 1870s, using the newly invented technique of staining the myelin sheath of nerve fibers. He presented evidence for the sequential postnatal myelination of the "projection areas" and "association areas" of the cerebral cortex, and sought to correlate that in his *Gehirn und Seele* (Flechsig, 1896) with the mental maturation of children. Another old source was Gustaf Retzius' photographic reproduction of his large collection of the prenatally developing human brain in his *Das Menschenhirn* (Retzius, 1896). Next in line was the work of Cecilie Vogt and Oscar Vogt who published their findings of the myelination of the human cerebral cortex during the first four months of postnatal life in two volumes of their *Beiträge zur Hirnfasernlehre* (Vogt and Vogt, 1902, 1904). A more recent source of published illustrations has been Leroy Conel's 8 volumes of *The Postnatal Development of the Human Cerebral Cortex* (Conel, 1939-1967). The work contains a wealth of information about the cytology of the developing neocortex, using a variety of staining techniques, from birth to six years of age. But the bulk of the illustrations presented in this book are from our archive of photomicrographs that we collected a few decades ago of cell-, fiber- and myelin-stained embryonic, fetal and early postnatal brain specimens stored at the National Museum of Health and Medicine in the United States. We examined hundreds of specimens in the earlier Minot and Carnegie Collections, and the more recent Yakovlev Collection. Our archive contains more than 10,000 photomicrographs, a portion of which has been digitized and some published (Altman and Bayer, 2001; Bayer and Altman, 2002-2008). The selection of specimens presented in this book to illustrate neocortical development at different gestational ages was not a random one. We could not use the specimens that have deteriorated over the decades, those that were not accurately cut in the coronal, sagittal or horizontal planes, and those that have appeared to us to be pathological.

The large Carnegie Collection (designated here by the **C** prefix) originated in the Department of Embryology of the Carnegie Institution of Washington. They were prepared under the stewardship of Franklin P. Mall (1862-1917), George L. Streeter (1873-1948), and George W. Corner (1889-1981). The human embryos were collected over a span of 40 to 50 years and were histologically prepared with a variety of fixatives, embedding media, cutting planes, section thickness, and histological stains. Descriptions and analyses of that material, much of that dealing with other facets of embryonic development than that of the brain, were published in issues of *Contributions to Embryology, Carnegie Institution of Washington,* in the early 1900s. Detailed analyses of brain development, mostly of first trimester embryos of the Carnegie Collection, were carried out and published by O'Rahilly and Müller (1987, 1994). We also made use of the Minot Collection in illustrating neocortical development during the first trimester (designated here by the prefix **M**). Charles S. Minot (1852-1914), an embryologist at Harvard University, collected and meticulously prepared about 100 human embryos. The sections were cut at 10 μm and stained with aluminum cochineal. Most of the brains of the second and third trimester fetuses, and those of neonates, infants and young children that we present in this book come from the Yakovlev Collection (designated by the prefix **Y**). Over a period of about 40 years, Paul I. Yakovlev (1894-1983) collected about 1500 normal and pathological brains, ranging in age from the early second trimester period through old age (Haleem, 1990). All of the specimens were fixed in formalin, embedded in celloidin, cut in 36 μm thickness, and stained with various techniques to visualize cell bodies, fibrous processes and myelin.

DATING GESTATIONAL AGES

Most of the brain sections we illustrate here were accompanied by some information about their origin, such as the crown-rump length (CR) and estimated gestational age of the embryos and fetuses. However, in some cases gestational age was not available or was uncertainly indicated in days, weeks or months. In order to more reliably date gestational age, we opted to rely on the most straightforward measure provided, the CR of the specimens, and indicated their age in gestational week (GW) on the basis of the large data base that has currently become available with the intrauterine ultrasonic scanning technique (Fig. 1). There is apparently a close relationship between CR and GW during the first trimester (Fig. 2). Of significance in this context, is also the regular relationship between estimated GW and measures of head circumference (Fig. 3).

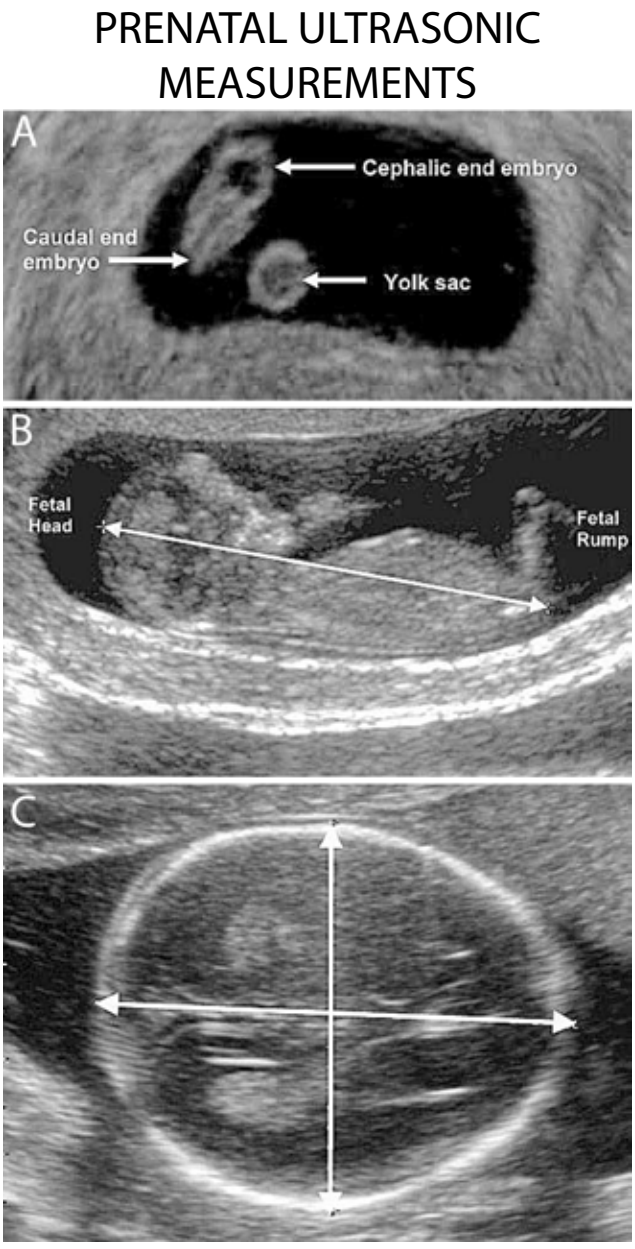

Fig. 1. A. Ultrasonic visualization of early intrauterine embryonic development. **B.** Method of determining head and body length, known as crown-rump (CR) length. **C**. Measurement of head circumference, occipito-frontal diameter, and biparietal diameter After Lougha et al. (2009).

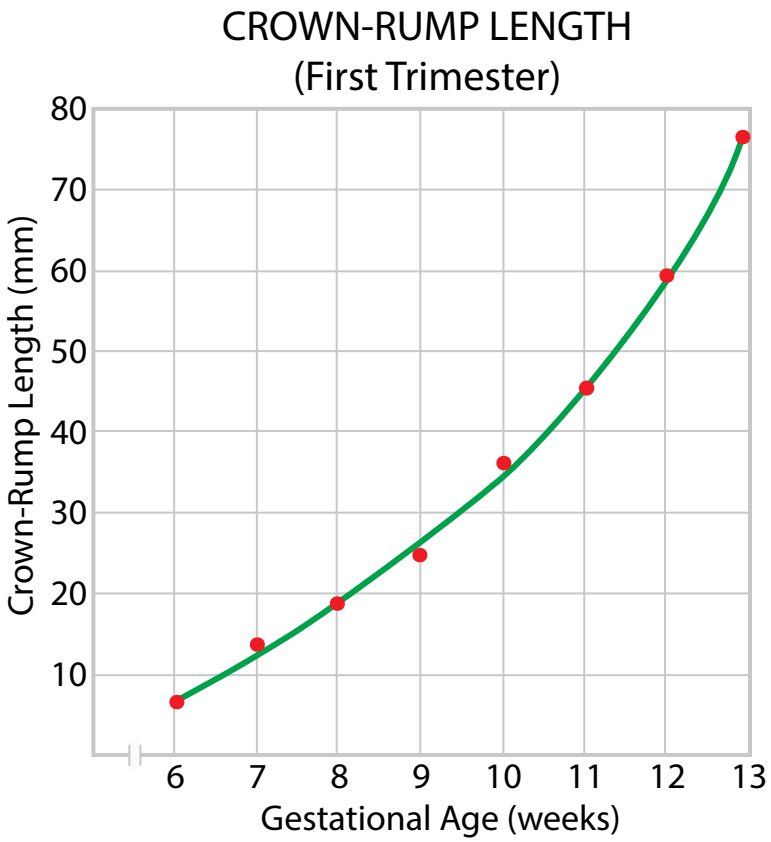

Fig. 2. The relationship between the intrauterine CR of first trimester human embryos and their estimated gestational ages in weeks (GW). Based on data by Lougha et al. (2009).

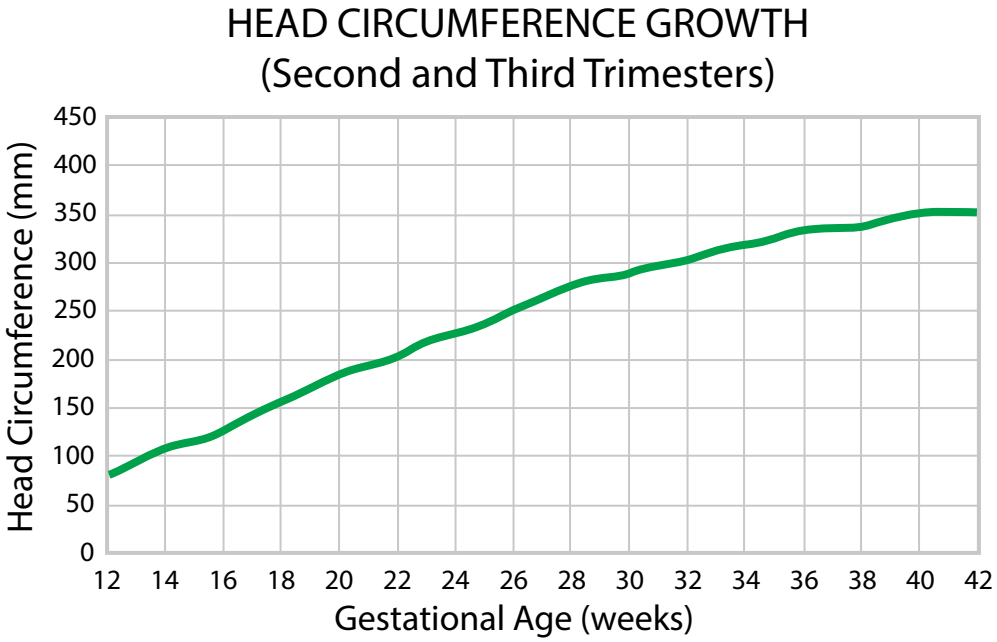

Fig. 3. The relationship between the intrauterine growth of head circumference of human embryos and fetuses (means) and their estimated gestational age. Based on data by Lougha et al. (2009).

OVERVIEW OF PRENATAL NEOCORTICAL DEVELOPMENT

The regular growth of head circumference is paralleled by the progressive expansion of the human cerebral cortex between the late first trimester (GW10) and the neonatal period (GW41) as it is visible to the naked eye (Fig. 4). This frequently reproduced plate by Larroche (1966) summarizes the highlights of the most obvious features of prenatal cortical development: its progressive growth during the first and second trimester (between GW10 and GW24) as a lissencephalic (smooth-surfaced) structure (column I), and its subsequent immense expansion during the third trimester (between GW28 and GW41), coupled with progressive gyrification (columns II and III).

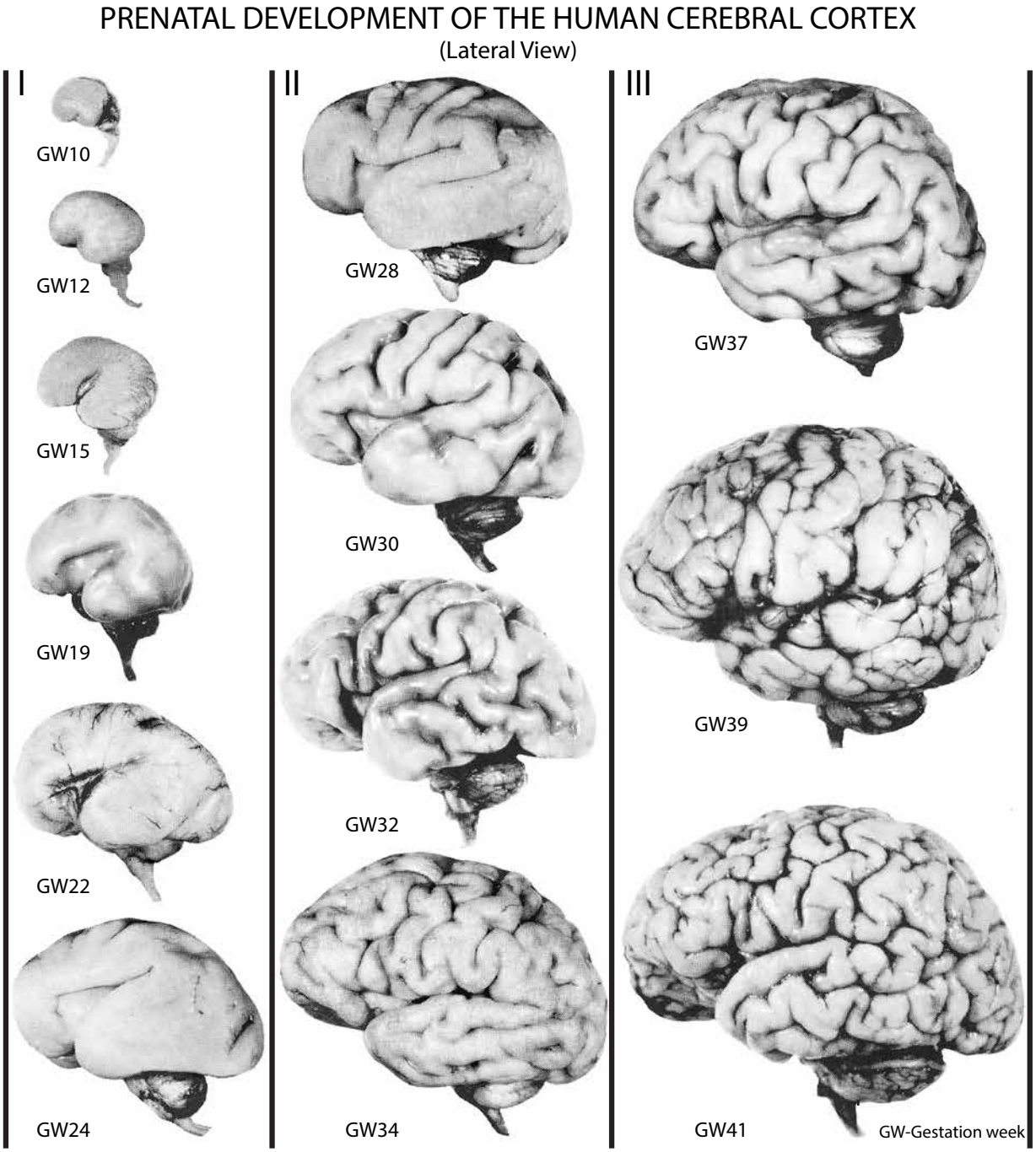

Part I

ILLUSTRATIONS WITH COMMENTS

A. NEOCORTICAL DEVELOPMENT DURING THE FIRST TRIMESTER

Prospectus. Based on the data summarized by Lougha et al. (2009), we used the following measurements to estimate the gestational age of first trimester embryos in weeks (Table 1). (We present the less consistent relationship between CR length and the age of second and third trimester fetuses in weeks or months in Table 2 in Part 2.)

TABLE 1
FIRST TRIMESTER CROWN RUMP LENGTH (CR)
AND ESTIMATED GESTATIONAL AGE (GW)

CR (mm)	GW (weeks)
3-4	5
5-9	6
10-15	7
16-22	8
23-31	9
32-41	10
42-53	11
54-66	12
67-80	13

Fig. 4. Overview of the prenatal growth of the human cerebral cortex. The gestational ages in weeks are uncorrected, as given by the author. The photographs were taken at the same magnification and are illustrated at about half the normal size. After Larroche (1966).

In the photomicrographs that we present in Figs. 5 to 17, we will illustrate with detailed comments the morphogenetic development of the neocortex during the first trimester from GW5 to GW12 as revealed by the histological evidence. We begin with a GW5 (CR 4.0 mm) embryo, which as yet has an undivided (unicameral) telencephalon, composed entirely of its neuroepithelial (NEP) rudiment (Fig. 5). That undivided NEP—considered by some authors, together with the diencephalon, to be the prosencephalon—is situated anterior to the bilateral optic vesicle (Fig. 5), which is a transient component of the diencephalon and will give rise to the retina and the supporting elements of the optic tract. At this gestational age, the unicameral NEP is surrounded anteriorly by the bilateral olfactory placode, and the optic vesicles by the bilateral optic placode. The relatively small size of the primordial telencephalon is evident in the computer reconstruction of the entire CNS in another GW5 embryo, shown in three views. The undivided primordial telencephalon expands somewhat by the next week, as seen in a GW6 (CR 7.1 mm) embryo (Fig. 6). The olfactory placodes are becoming transformed into the bilateral olfactory epithelium; the optic placodes are forming the lens of the two eyes, and the optic vesicles are forming into the retina. The bicameral telencephalic NEP forms during the 7th week postconception, as seen in a CR 15 mm embryo (Fig. 7). By this age the separation of the dorsal neocortical NEP and the ventral basal ganglionic NEP is becoming evident, and a parenchyma composed of differentiating neurons begins to surround the latter but not the former. The neocortical NEP expands during the next week, as seen in the GW8 (CR 17.5 mm) embryo (Fig. 8). But unlike the basal ganglionic NEP, which is surrounded by an expanding neuronal parenchyma by this age, the neocortical NEP is only surrounded by a thin white band containing the earliest differentiating neurons. Differentiating neurons leave the neocortical NEP in larger numbers early during the 9th week postconception, as seen in a GW9 (CR 25 mm) embryo, and begin to form a thin cortical plate, the rudiment of the future gray matter in the future paracentral area dorsolaterally (Fig. 9). That development is associated with the formation of the choroid plexus in the expanded lateral ventricles. The cortical plate has expanded anteriorly and posteriorly in an older (CR 31 mm) GW9 embryo (Fig. 10). The developing stratified transitional field (STF) in the developing neocortex of the latter is shown at higher magnification in Fig. 11, together with the expanded choroid plexus.

A landmark development in a young (CR 32 mm) GW10 embryo is the penetration of ascending thalamic fibers through the diencephalic-telencephalic boundary into the neocortex. Descending corticospinal fibers form the internal capsule and pass through the basal ganglia (Fig. 12). The reconstructed model of an older (CR 38mm) GW10 embryo, and a sagittal section of a 40 mm embryo show the extent to which the neocortex has expanded posteriorly, covering the thalamus (Fig. 13B). A horizontal section of a young GW11 embryo (CR 42 mm) shows the descending corticospinal fibers reaching the level of the subthalamus (Fig. 13D). Another significant development by this age is the ballooning of the primitive choroid plexus in the expanding lateral ventricles. That development is associated with two extraneural processes, the hypertrophy of the meninges and the onset of vascularization of the neocortex (Fig. 14). The descent of corticofugal fibers has continued in a GW 12 (CR 60 mm) embryo (Fig. 15). A series of horizontal cut combined cell- and fiber-stained sections of another GW12 (CR 57 mm) embryo provides an overview of many of the developments that have taken place by the end of the first trimester (Fig. 16). Much of the expanding neocortex is encased in a hypertrophied meninges; the expanded choroid plexus fills much of the lateral ventricles; a large complement of corticofugal fibers traverse the basal ganglia; and the thalamocortical, somatosensory radiation can be seen penetrating the neocortex

and the visual radiation can be seen of making its turn in what is known as Meyer's loop. We end this survey of neocortical development with a series of high magnificaton microphotographs of the transformations of the neocortical NEP and the formation of the cortical gray matter during the first trimester (Fig. 17). The stockbuilding NEP with its proliferative precursor neural cells is expanding during this period as differentiating neurons leave it to sojourn in the stratified transitional field (STF) or migrate toward and settle in the expanding cortical gray.

ANNOTATED ILLUSTRATIONS OF EMBRYONIC BRAINS

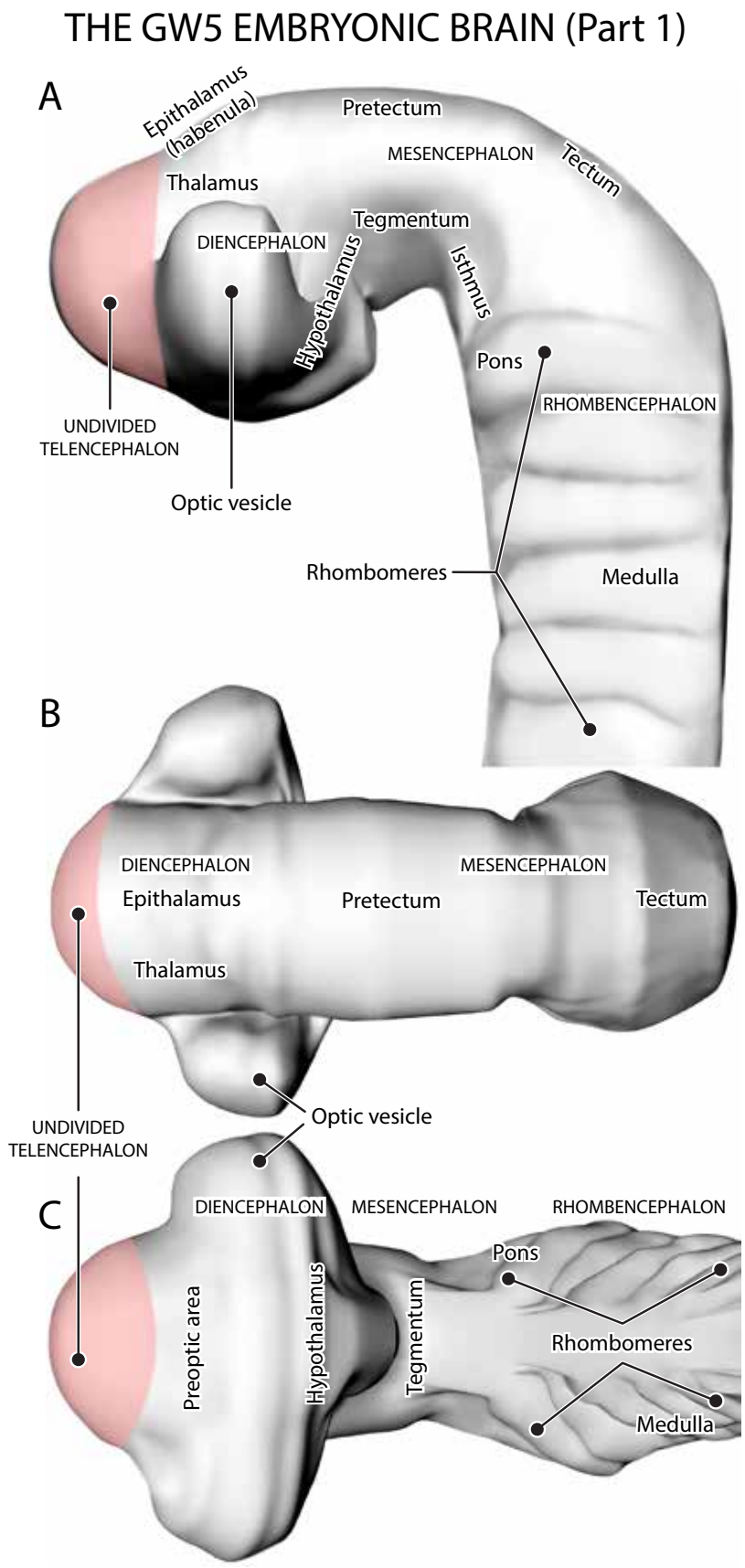

Fig. 5 (facing pages). 3D computer reconstruction of the brain of a CR 4.0 mm, GW5 embryo (C836), shown in lateral (**A**), dorsal (**B**) and ventral (**C**) views. The small, undivided (unicameral) telencephalon is colored pink. **D**. Photomicrograph of the brain of a CR 3.5 mm embryo of about the same age (C7724) cut in the sagittal plane. **E** and **F** are, respectively, coronal sections of the C836 brain cut through the primordial telencephalon anteriorly and the diencephalon more posteriorly. At this stage of development the small primordial telencephalon consists exclusively of a neuroepithelium composed of proliferating neural precursor cells. There is as yet no parenchyma composed of differentiating neurons present outside the NEP. The olfactory placodes surrounding the primordial telencephalon and the optic placodes surrounding the diencephalic optic recess have yet to give rise to the peripheral tissues that will form the bilateral nostrils and the bilateral eyes.

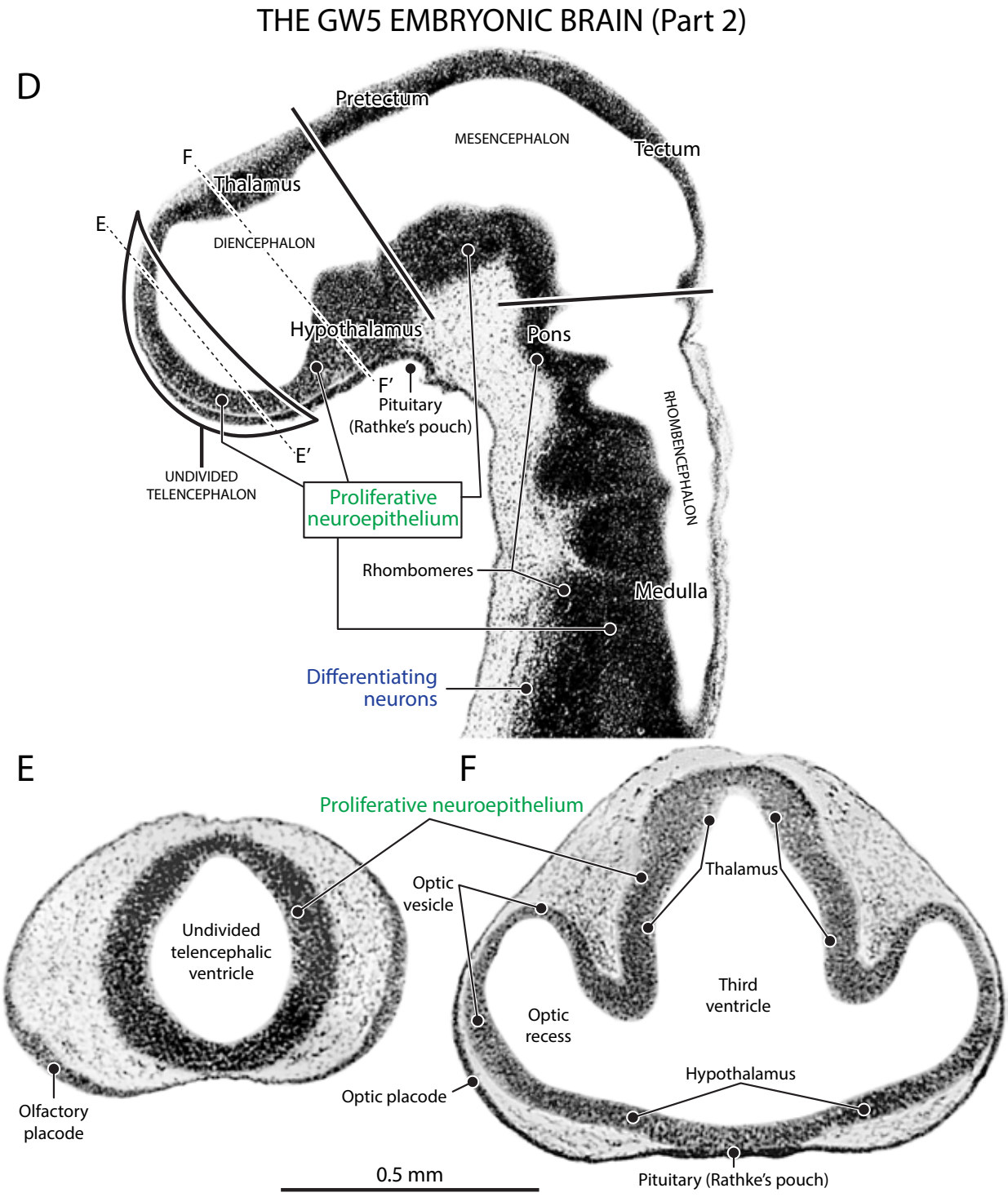
THE GW5 EMBRYONIC BRAIN (Part 2)
D
Pretectum
MESENCEPHALON
Tectum
F
Thalamus
E
DIENCEPHALON
Hypothalamus
Pons
F′
Pituitary
(Rathke's pouch)
RHOMBENCEPHALON
E′
UNDIVIDED
TELENCEPHALON
Proliferative
neuroepithelium
Rhombomeres
Medulla
Differentiating
neurons
E
F
Proliferative neuroepithelium
Thalamus
Optic
vesicle
Undivided
telencephalic
ventricle
Third
ventricle
Optic
recess
Hypothalamus
Optic placode
Olfactory
placode
0.5 mm
Pituitary (Rathke's pouch)

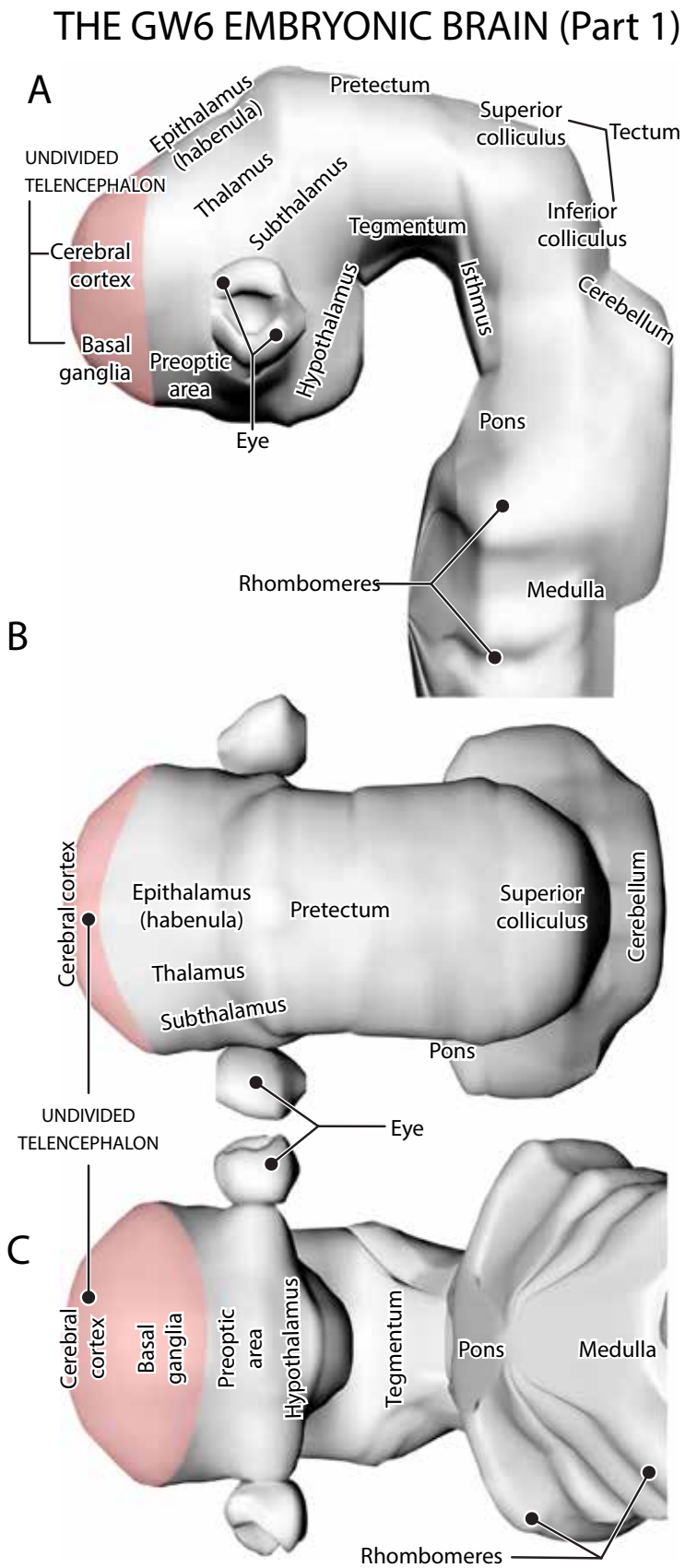

Fig. 6 (facing pages). 3D reconstruction of the brain of a CR 8.0 mm, GW6 embryo (C8314), shown in lateral (**A**), dorsal (**B**) and ventral (**C**) views. **D**. Photomicrograph of the brain of a CR 7.1 mm, GW6 embryo (C8966) in the sagittal plane. **E** and **F** are, respectively, coronal sections cut through the oval-shaped unicameral telencephalon of C8314 anteriorly and the diencephalon posteriorly. The embryonic brain still consists only of a proliferative NEP. Note the onset of transformation of the olfactory placode into the olfactory epithelium (**E**), and of the lens placode (**F**) becoming surrounded by the NEP of the optic recess, split into the thin outer pigment epithelium and the thick internal retina (**F**). Among other developments, is the formation of the pia surrounded peripherally by blood vessels.

THE GW6 EMBRYONIC BRAIN (Part 2)

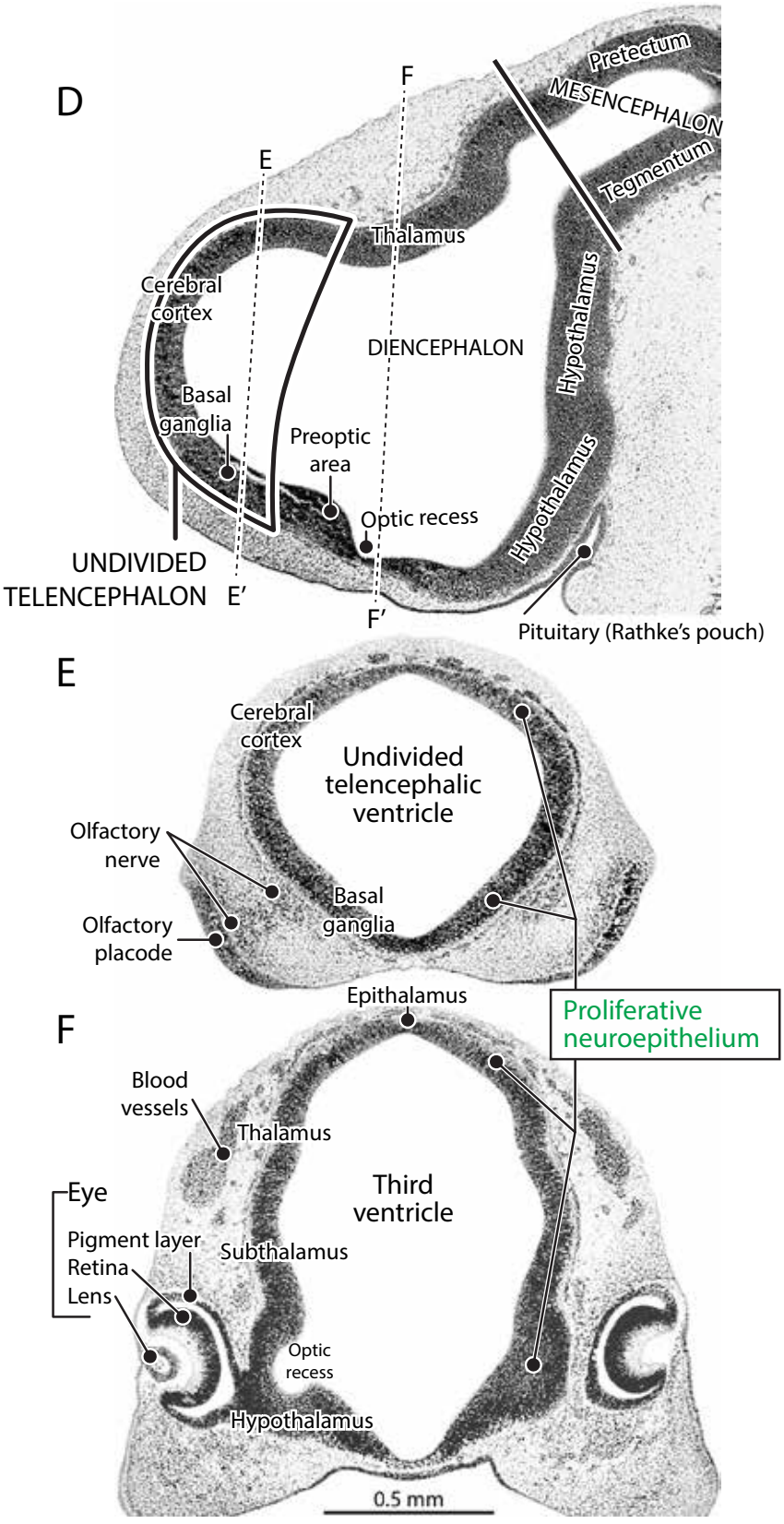

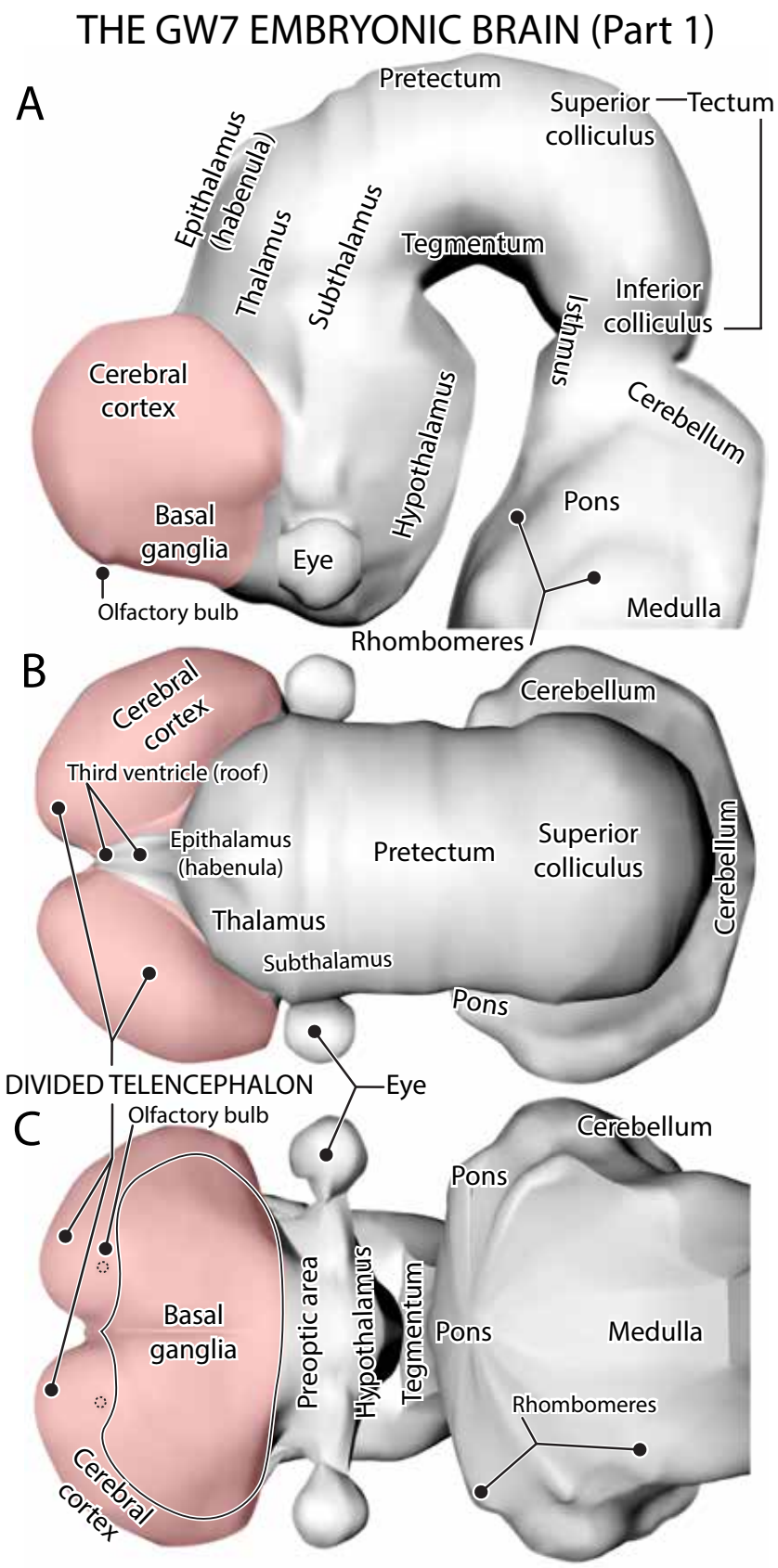

Fig. 7 (facing pages). 3D reconstruction of the brain of a CR 10.0 mm, GW7 embryo (M1000), shown in lateral (**A**), dorsal (**B**) and ventral (**C**) views. The ofactory bulb and the eye are beginning to form.
D. Photomicrograph of a CR 15.0 mm embryo (late GW7, C9247) cut in the sagittal plane. **E** and **F** are, respectively, coronal sections of the M2051 (late GW7, CR 15.0 mm) brain cut through the now paired (bicameral) telencephalon. Note the relative uniformity of the densely cell-packed NEP stretching from the future frontal pole anteriorly to the future occipital pole posteriorly. Differing from the basal telencephalon, which is surrounded by a parenchyma of differentiating neurons, there are only a few differentiating cells leaving the neocortical NEP.

THE GW7 EMBRYONIC BRAIN (Part 2)

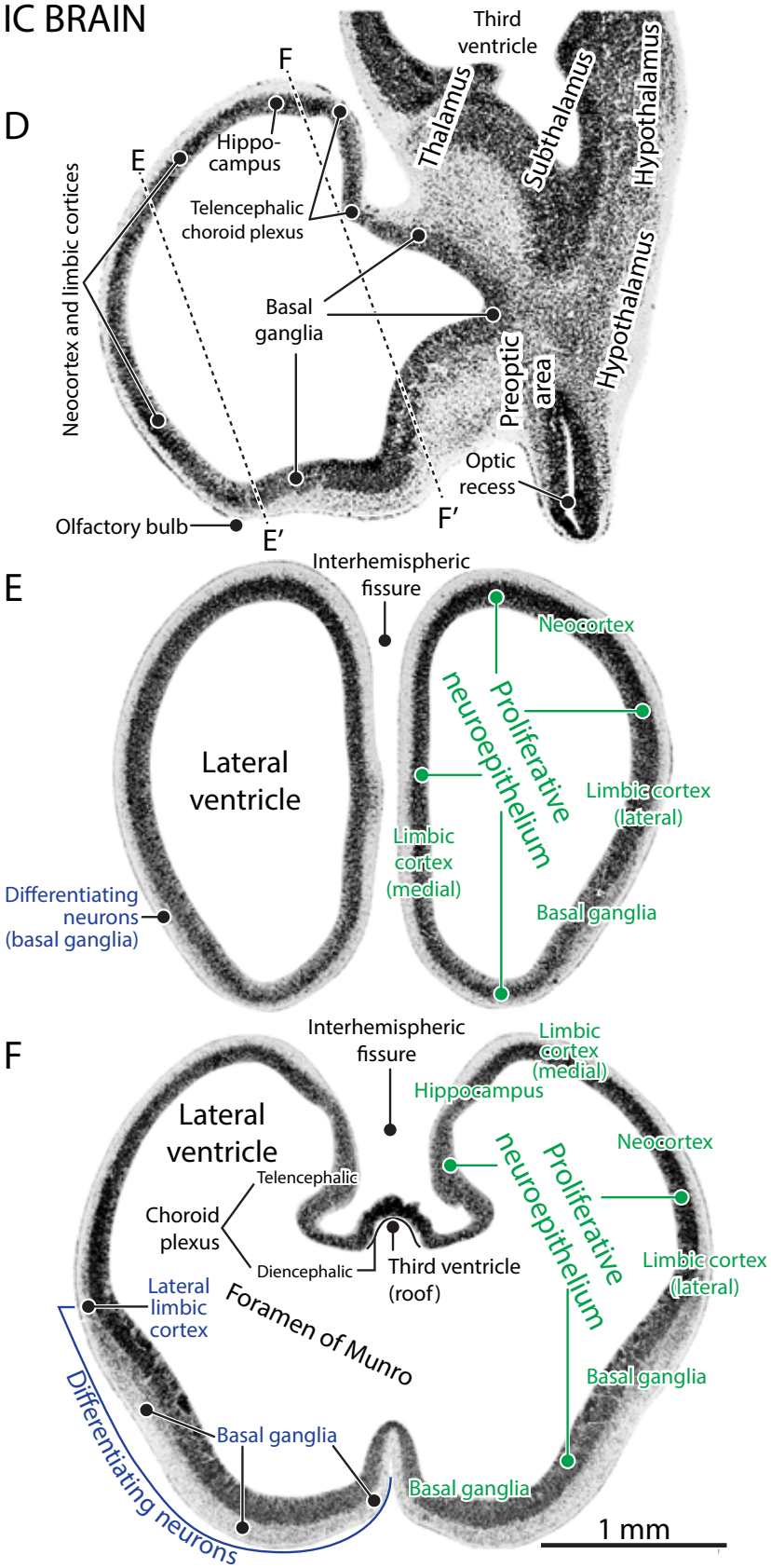

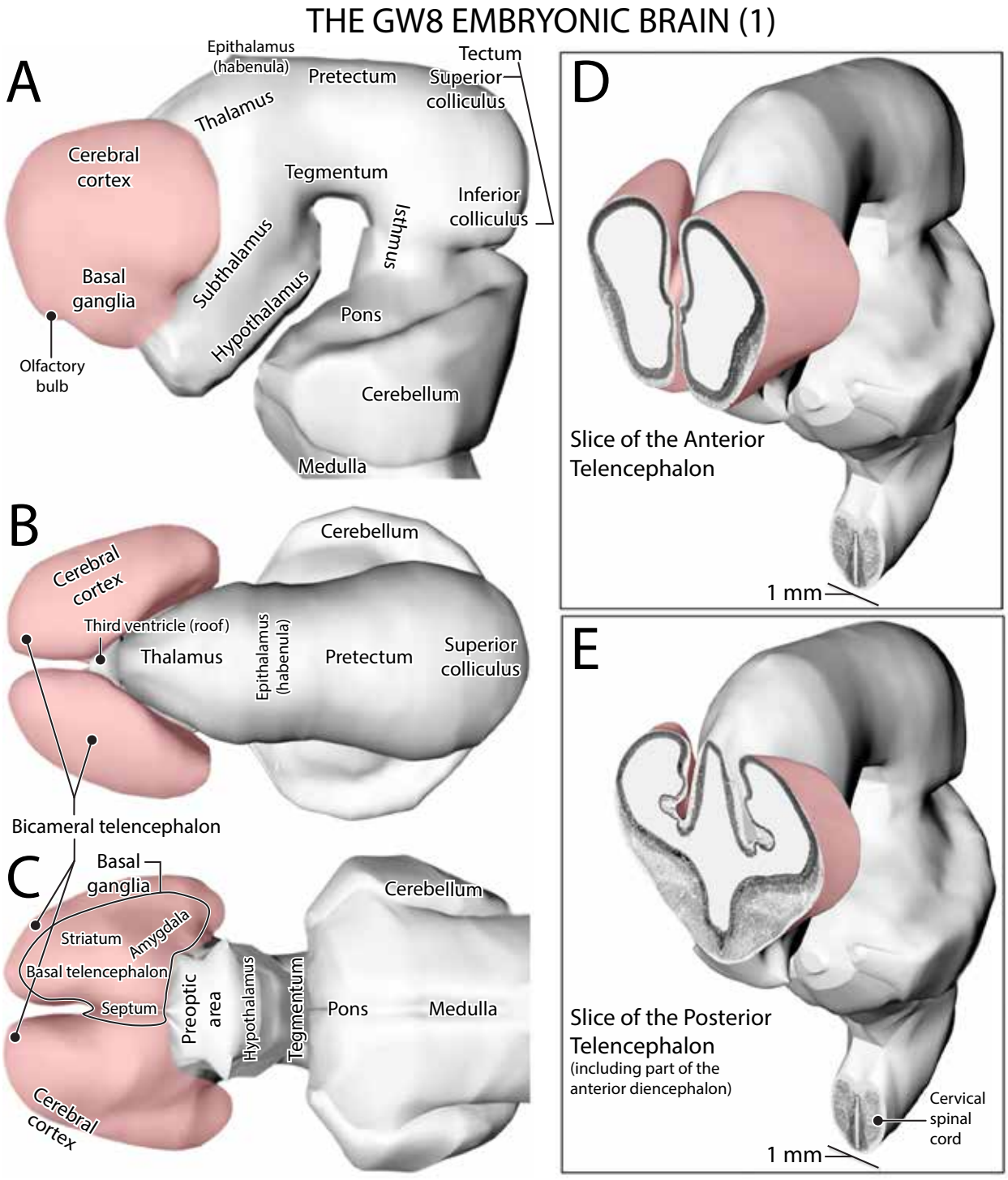

Fig. 8 (facing pages). 3D reconstruction of the brain of a CR 17.5 mm, GW8 embryo (M2155), shown in lateral (**A**), dorsal (**B**), ventral (**C**), and two angled anterior (**D)** and posterior (**E**) views. The expansion of the neocortex and basal telencephalon are evident. Photomicrograph of a CR 21.0 mm GW8 embryo (C6202) cut in the sagittal plane (**F**). The expanding neocortical NEP, which now caps the thalamus, has assumed an oval shape, with an olfactory evagination forming anteriorly. Coronal sections of the M2155 forebrain from anterior (**G**) to

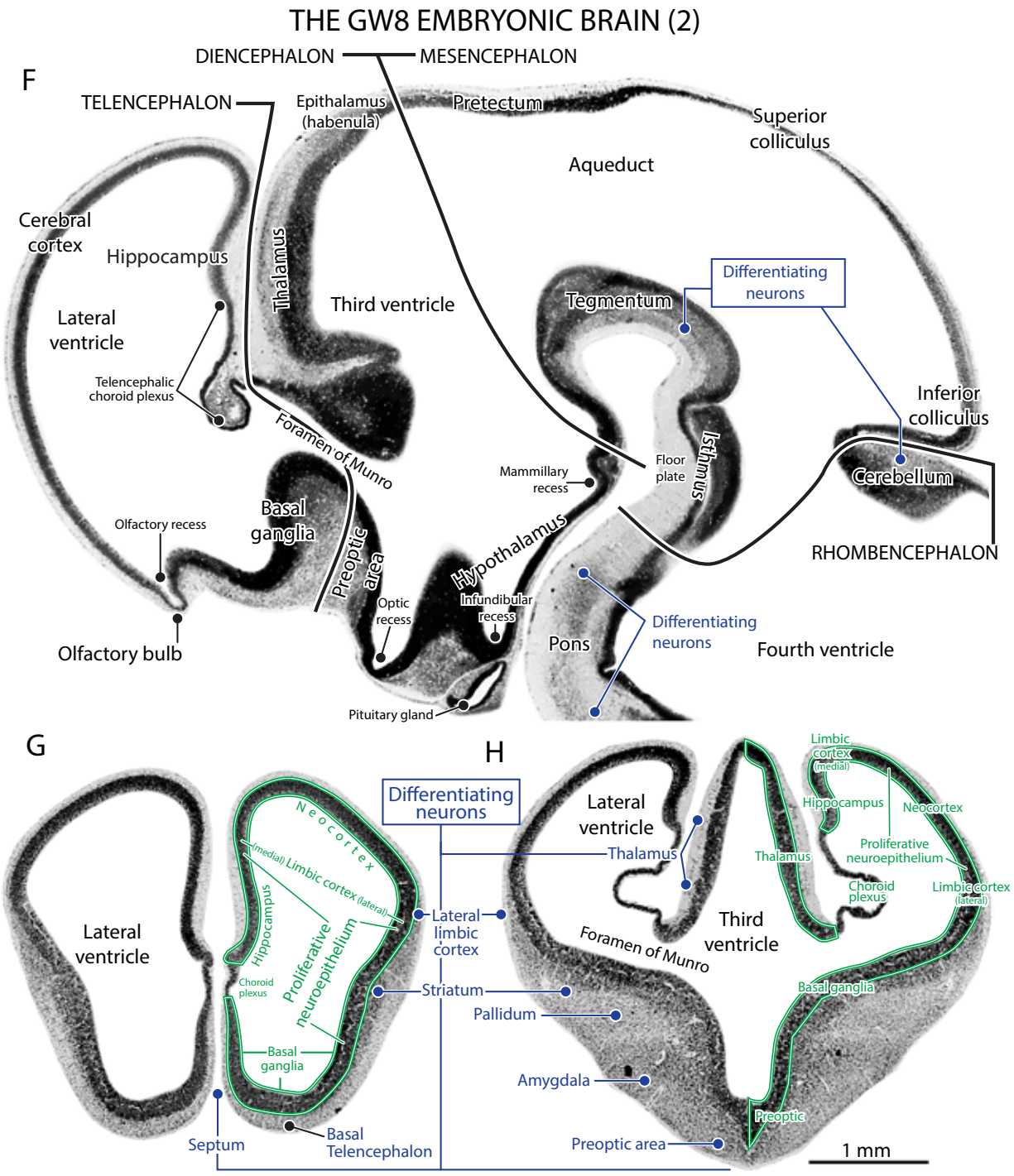

posterior (**H**). The dorsally positioned formative neocortex (the alar plate) is still devoid of differentiating neurons but neurons have left the ventral part of the telencephalic NEP (the basal plate) in appreciable numbers to form the expanding basal ganglia. A vascular bed medially beneath the developing hippocampus marks the site where the choroid plexus is beginning to invaginate into the the ventricles (**H**).

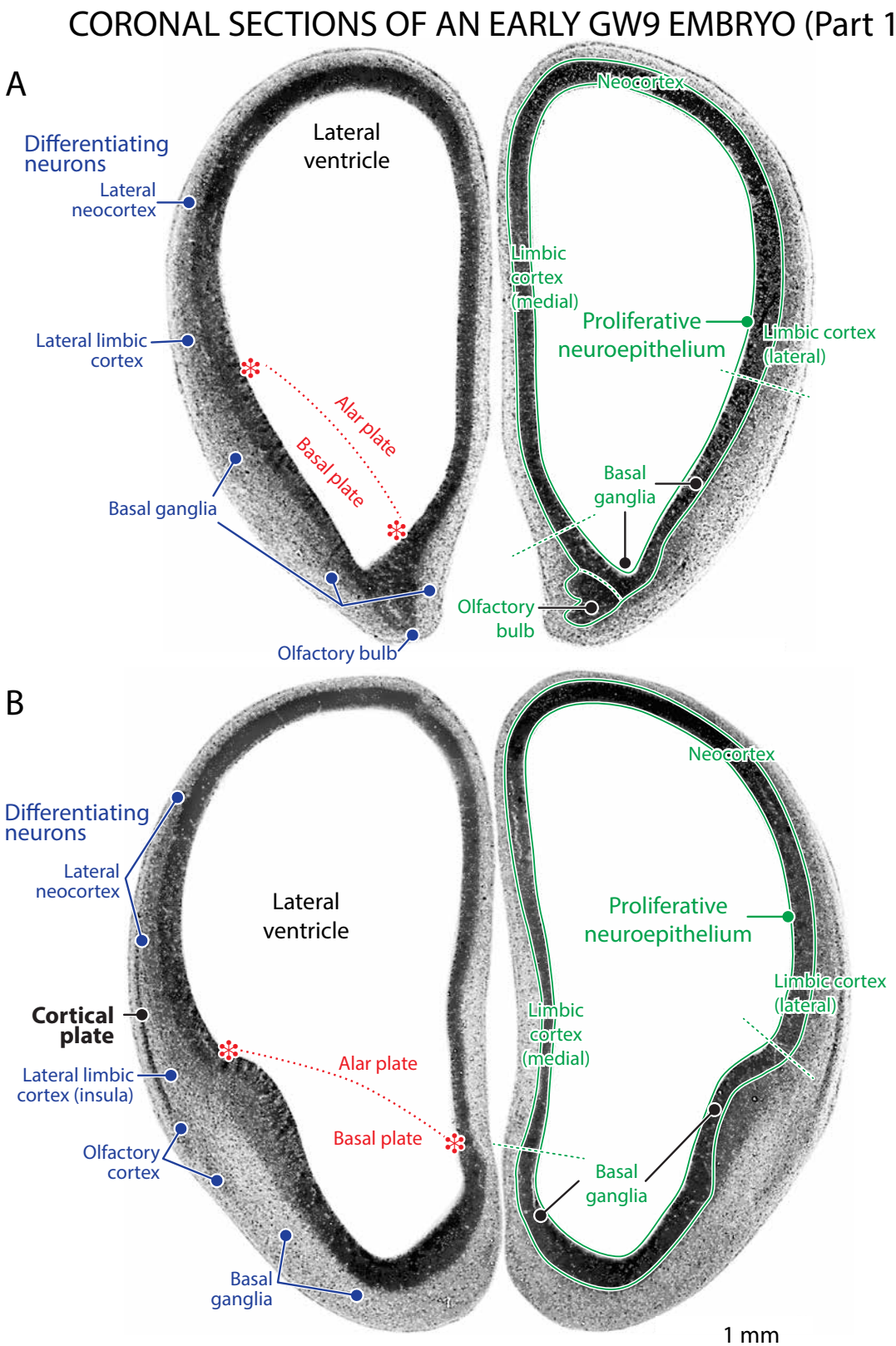

Fig. 9. Coronal sections of the forebrain of M2042 (CR 25 mm, GW9) from anterior (**A**) to posterior (**D**), showing the emergence of a new structure in the neocortex, the *cortical plate*, the future gray matter. The cortical plate, composed of postmitotic (differentiating) neurons, is still absent anteriorly in the presumptive frontal cortex (**A**)

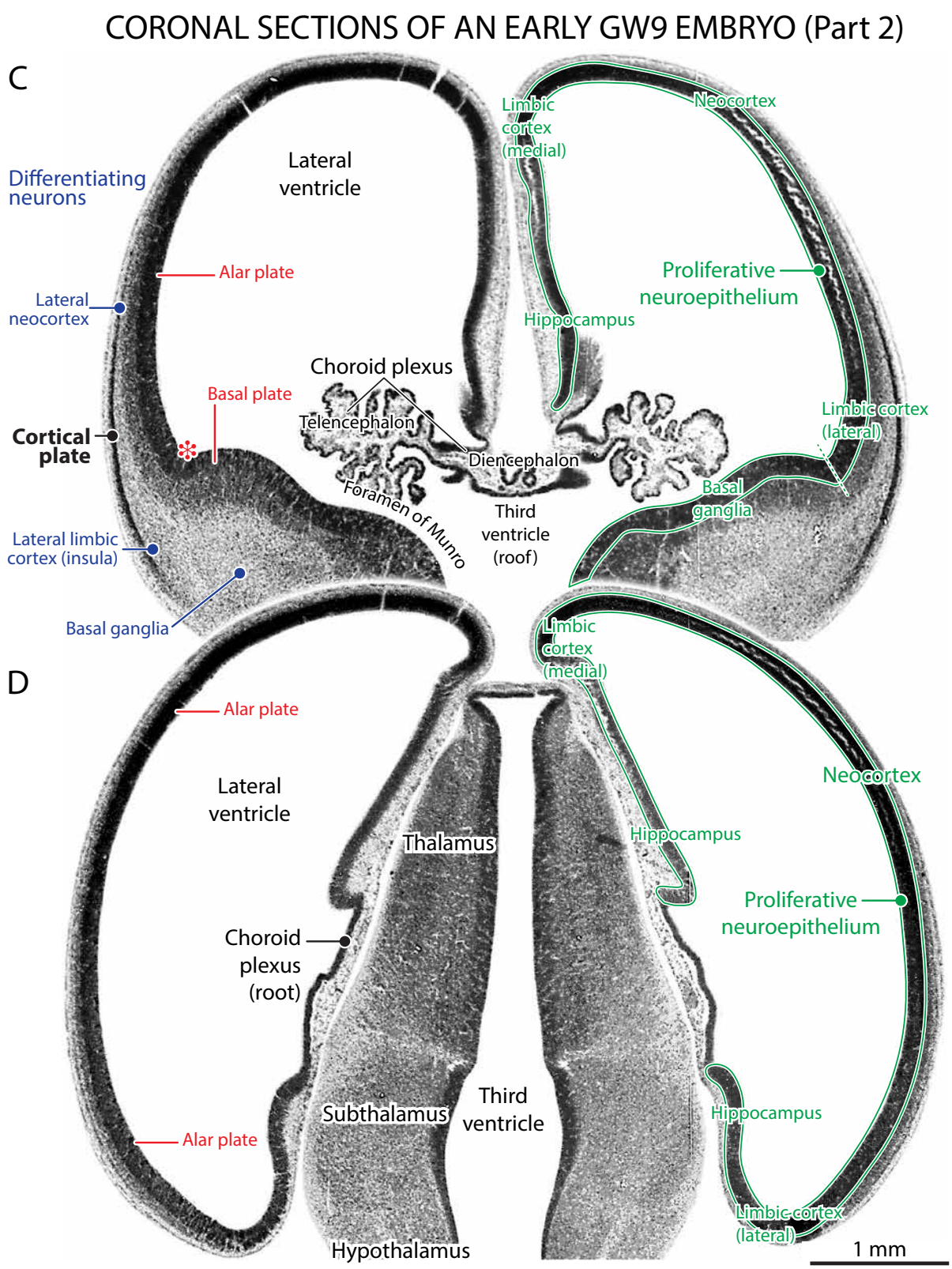

but begins to form ventrolaterally in the mid-anterior posterior extent of the neocortex (**B**, **C**). The cortical plate is absent more caudally, at the level of the thalamus and the hypothalamus (**D**). Note the continuing uniformity of the lateral neocortical NEP, in contrast to the heterogeneity of the NEP in the medial limbic telencephalon and the diencephalon. In association with the formation of the cortical plate, the choroid plexus has begun to "bloom" in **C**.

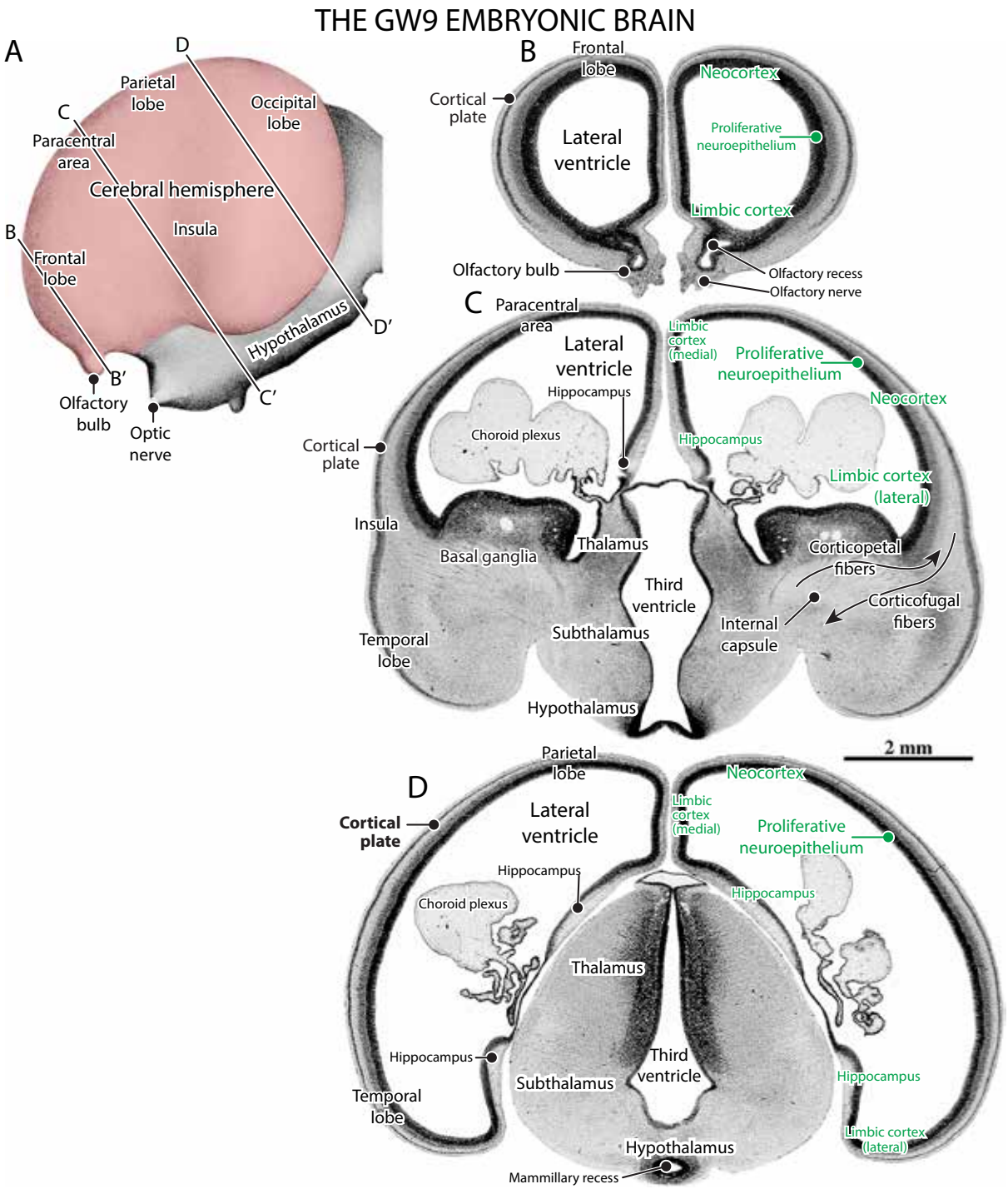

Fig. 10. **A**. Model of the brain of an older, CR19.4 mm GW9 embryo (HA3, reproduced from Hochstetter, 1919, Fig. 37, Table VI). Note the formative olfactory bulb and optic nerve and the great expansion of the neocortical hemisphere. The other illustrations are photomicrographs of horizontal sections of the brain of still older, CR 31 mm GW9, embryo (C9226) from anterior to posterior. The cortical plate has spread anteriorly into the future frontal lobe (**B**) and the primitive choroid plexus fills much of the lateral ventricles at the level of the anterior thalamus (**C**), and has spread into the posterior neocortex (**D**). New developments are the presence of descending corticofugal fibers passing trough the basal ganglia and indications of ascending thalamocortical fibers penetrating the neocortex (*arrows*, **C**).

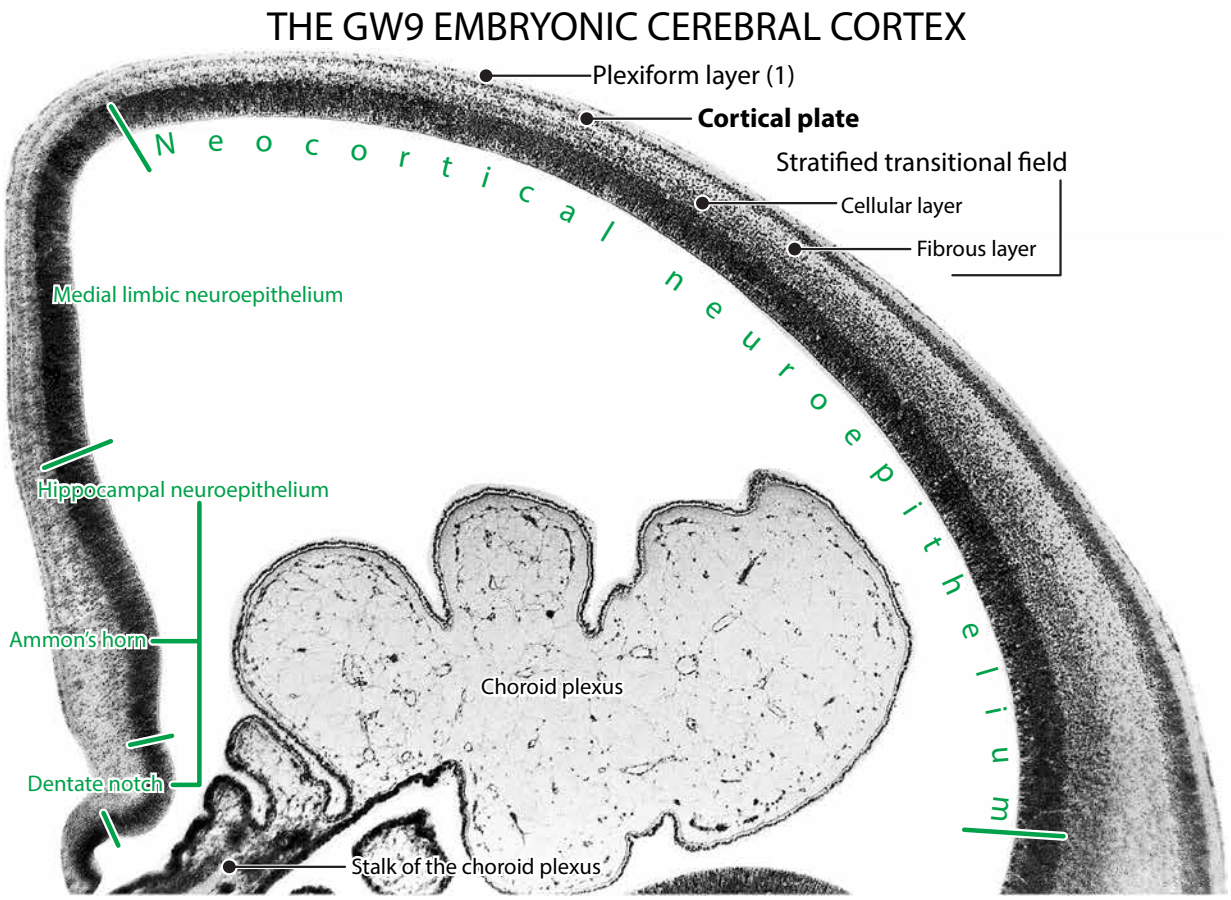

Fig. 11. Higher magnification detail showing the organization of the neocortex in C9226, the GW9 embryo pictured in **Fig. 10.** Note the uniformity of neuroepithelial thickness from lateral to medial. In contrast, the two-layered (cellular and fibrous) stratified transitional field (STF) has decreasing widths from lateral to dorsal. The STF is absent outside the medial limbic neuroepithelium, but definite cellular and fibrous layers are outside the hippocampal neuroepithelium. The expanding embryonic choroid plexus is surrounded by a double membrane and its spongy interior is filled with capillaries.

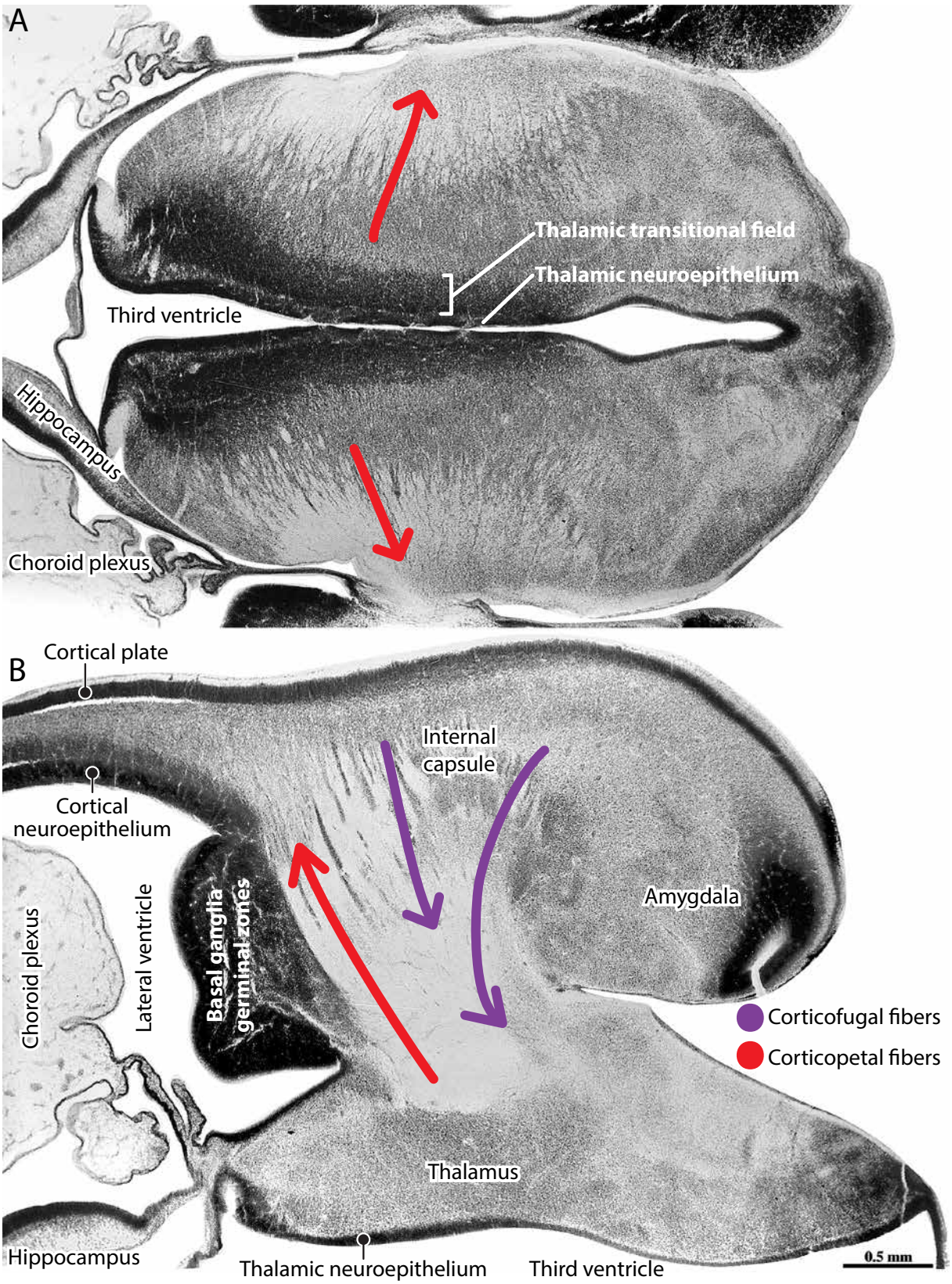
FIBERS BETWEEN THALAMUS AND CORTEX ON GW10
A
Thalamic transitional field
Thalamic neuroepithelium
Third ventricle
Hippocampus
Choroid plexus
B
Cortical plate
Internal capsule
Cortical neuroepithelium
Choroid plexus
Lateral ventricle
Basal ganglia germinal zones
Amygdala
Corticofugal fibers
Corticopetal fibers
Thalamus
Hippocampus
Thalamic neuroepithelium
Third ventricle
0.5 mm

Fig. 12. **A**. The horizontally-sectioned thalamus of a young GW 10 (C609, CR 32 mm) fetus illustrating many fibers apparently radiating laterally from the thalamic transitional field toward the developing neocortex (*red arrows*). **B**. In a more ventral horizontal section the fiber-rich formative internal capsule seems to contain ascending thalamocorical (corticopetal) fascicles that emanate from the thalamus (*red arrow*) and descending corticospinal (corticofugal) fibers that originate in the cerebral cortex (*purple arrows*).

THE LATE GW10/EARLY GW11 EMBRYONIC BRAIN (Part 1)

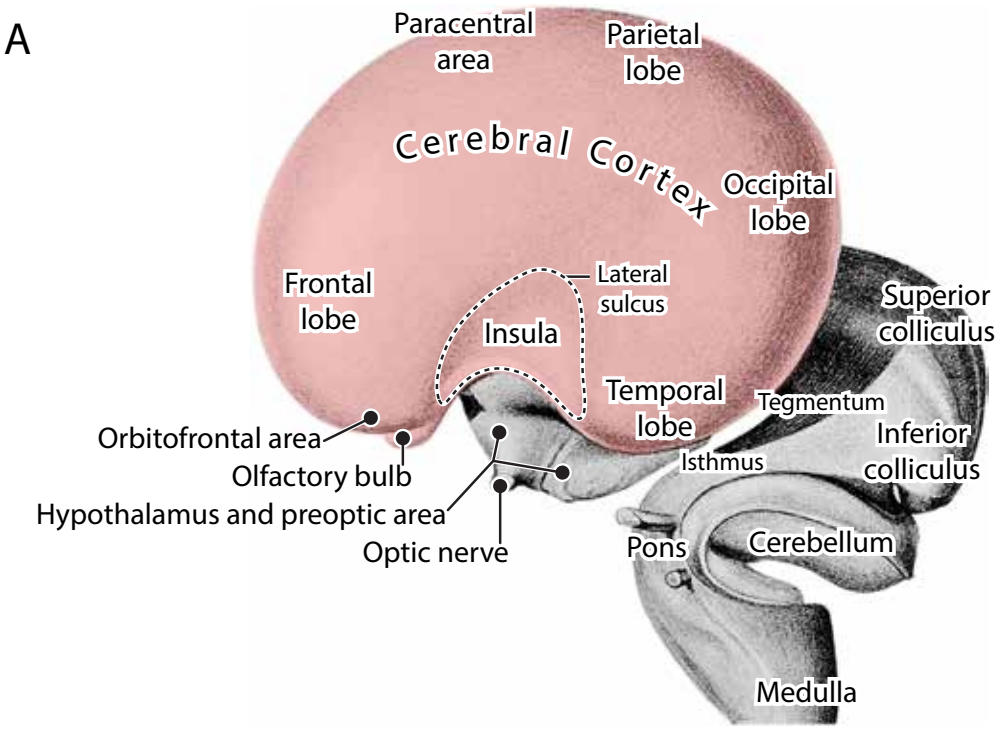

Fig. 13A. A Model of the brain of an older GW10 embryo (CR 38 mm, Fig.43, Table VII, Hochstetter, 1919). Note the ventral invagination of the greatly enlarged cerebral cortex at this stage of development. This is the beginning of the separation of the frontal and parietal lobes from the temporal lobe. The cerebral hemisphere changes from an ovoid to a croissant shape, with the formative insula buried in its depth.

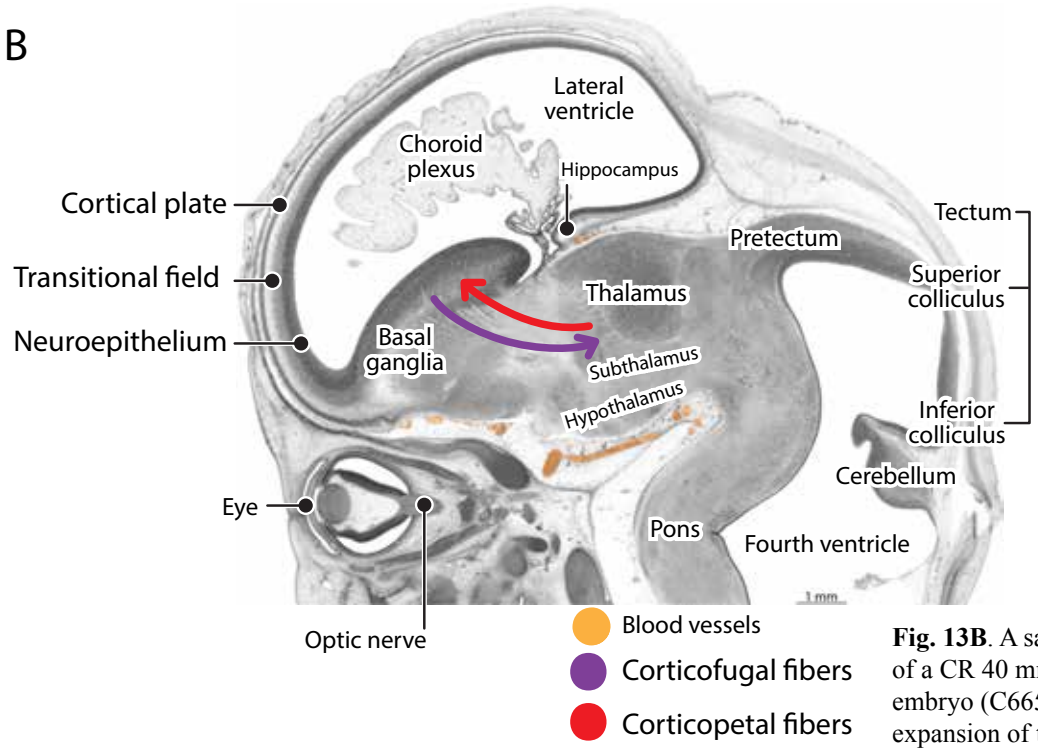

Fig. 13B. A sagittal section of a CR 40 mm, GW10 embryo (C6658). Note the the expansion of the choroid plexus and the presumptive ascending thalamocortical (*red arrow*) and descending corticospinal fibers (*purple arrow*).

THE LATE GW10/EARLY GW11 EMBRYONIC BRAIN (Part 2)

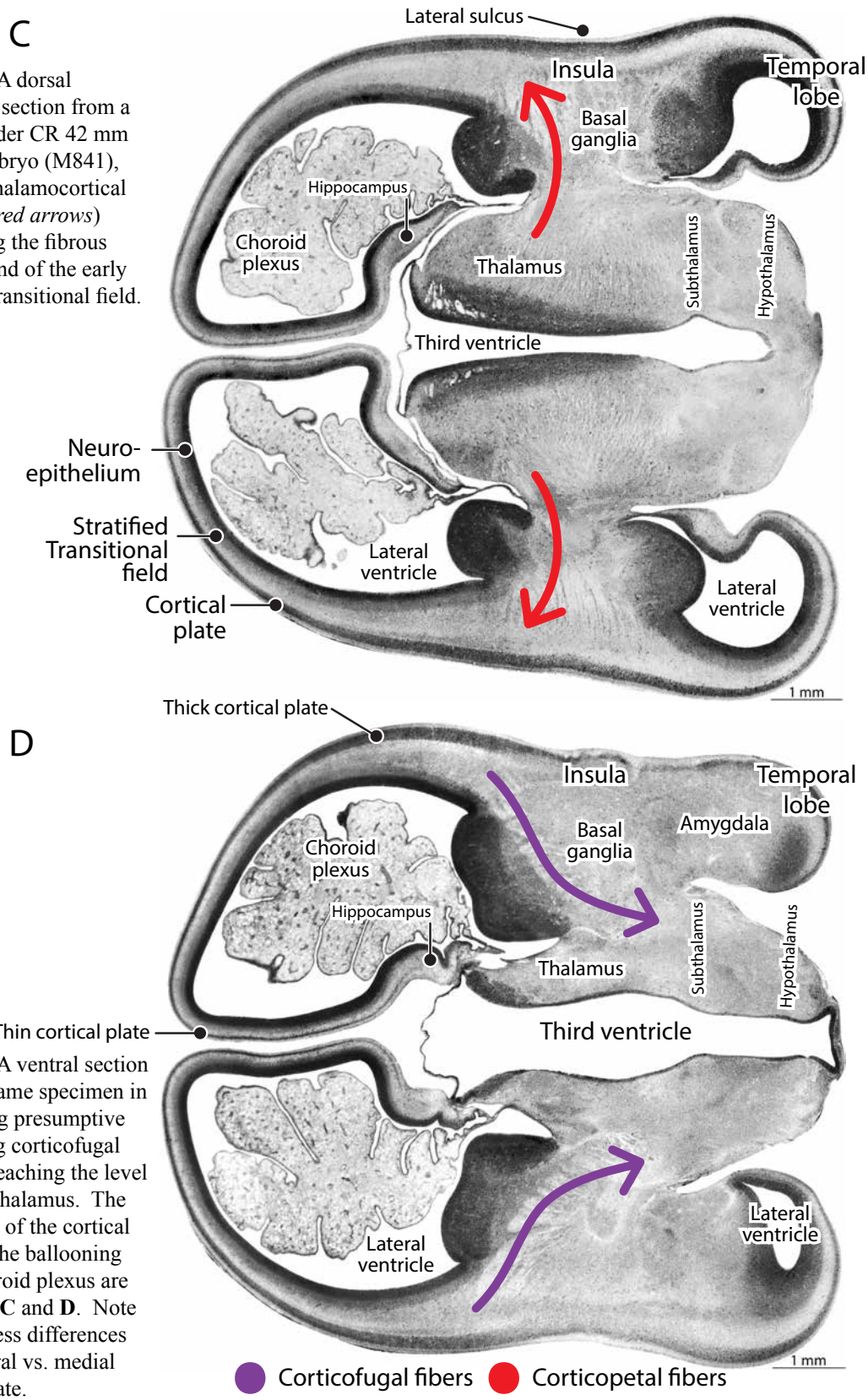

Fig. 13C. A dorsal horizontal section from a slightly older CR 42 mm GW10 embryo (M841), showing thalamocortical fascicles (*red arrows*) penetrating the fibrous (white) band of the early stratified transitional field.

Fig 13D. A ventral section from the same specimen in **C**, showing presumptive descending corticofugal fascicles reaching the level of the subthalamus. The thickening of the cortical plate and the ballooning of the choroid plexus are evident in **C** and **D**. Note the thickness differences in the lateral vs. medial cortical plate.

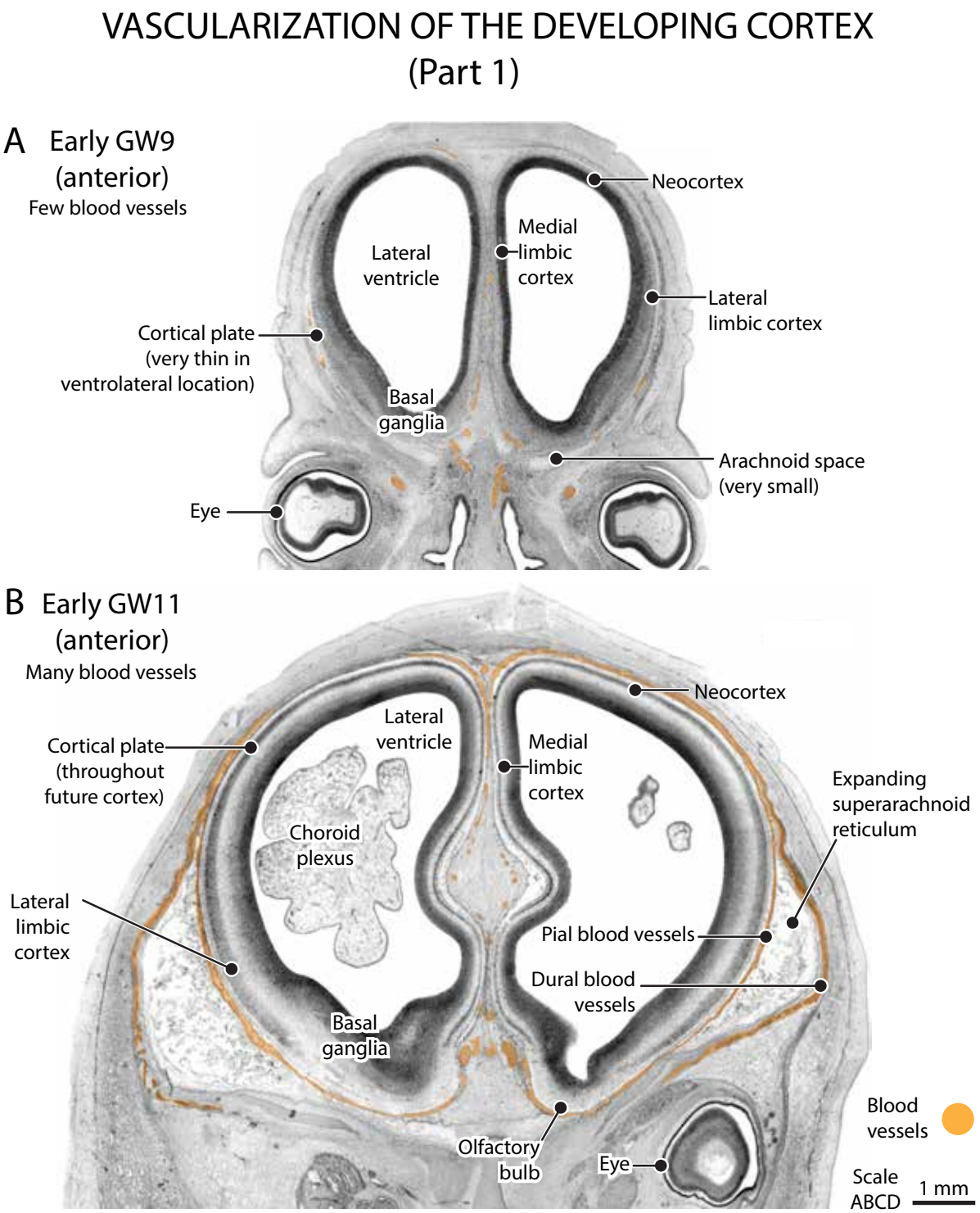

Fig. 14 (facing pages). The vascularization of the neocortex between **GW9** and **GW11** is illustrated by comparing two sets of coronal sections through the heads of a CR 25 mm embryo (**A**, **C**, M2042) and a CR 42 mm embryo (**B**, **D**, M841). **A**. In the younger embryo, there is only a trace of the cortical plate and no blood vessels surrounding the cortex. **B**. In the older embryo, there is an expanding cortical plate, and many blood vessels (presumably branches of the anterior cerebral artery) pass from the midline to the lateral surface of the cortex (*orange*). **C** and **D**. The same pattern of vasculalization, with a gradient from posterior to anterior, is evident at more posterior coronal levels. Two other notable differences are visible between the younger and older brains. One is the enlargement of the

VASCULARIZATION OF THE DEVELOPING CORTEX (Part 2)

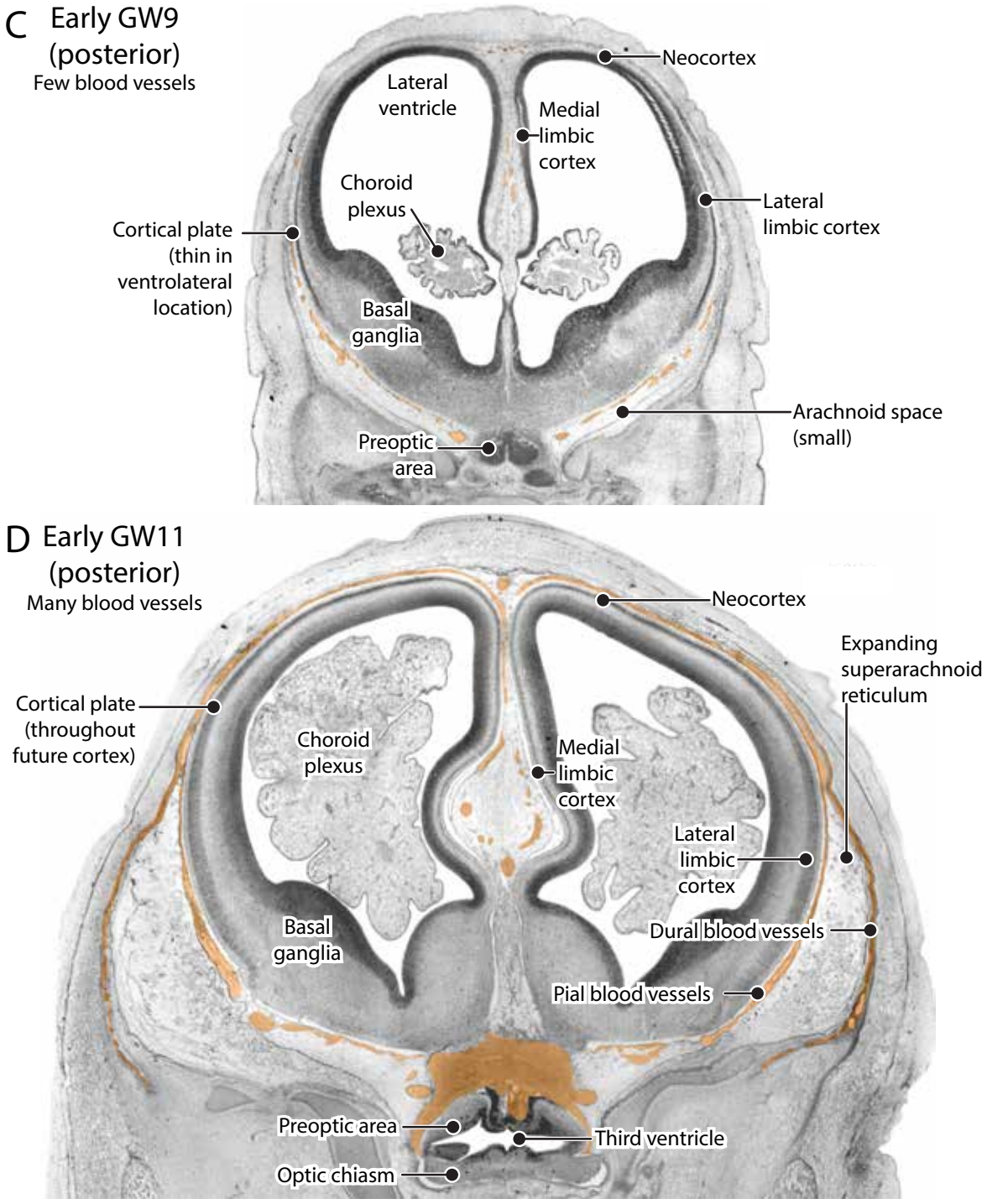

spongy choroid plexus in the older embryo; the other is the great expansion of the similarly spongy arachnoid space. Apparently, cortical plate formation is supported not only by growing vascularization but the formation of two transient trophic structures, the large embryonic choroid plexus and the large embryonic superarachnoid reticulum.

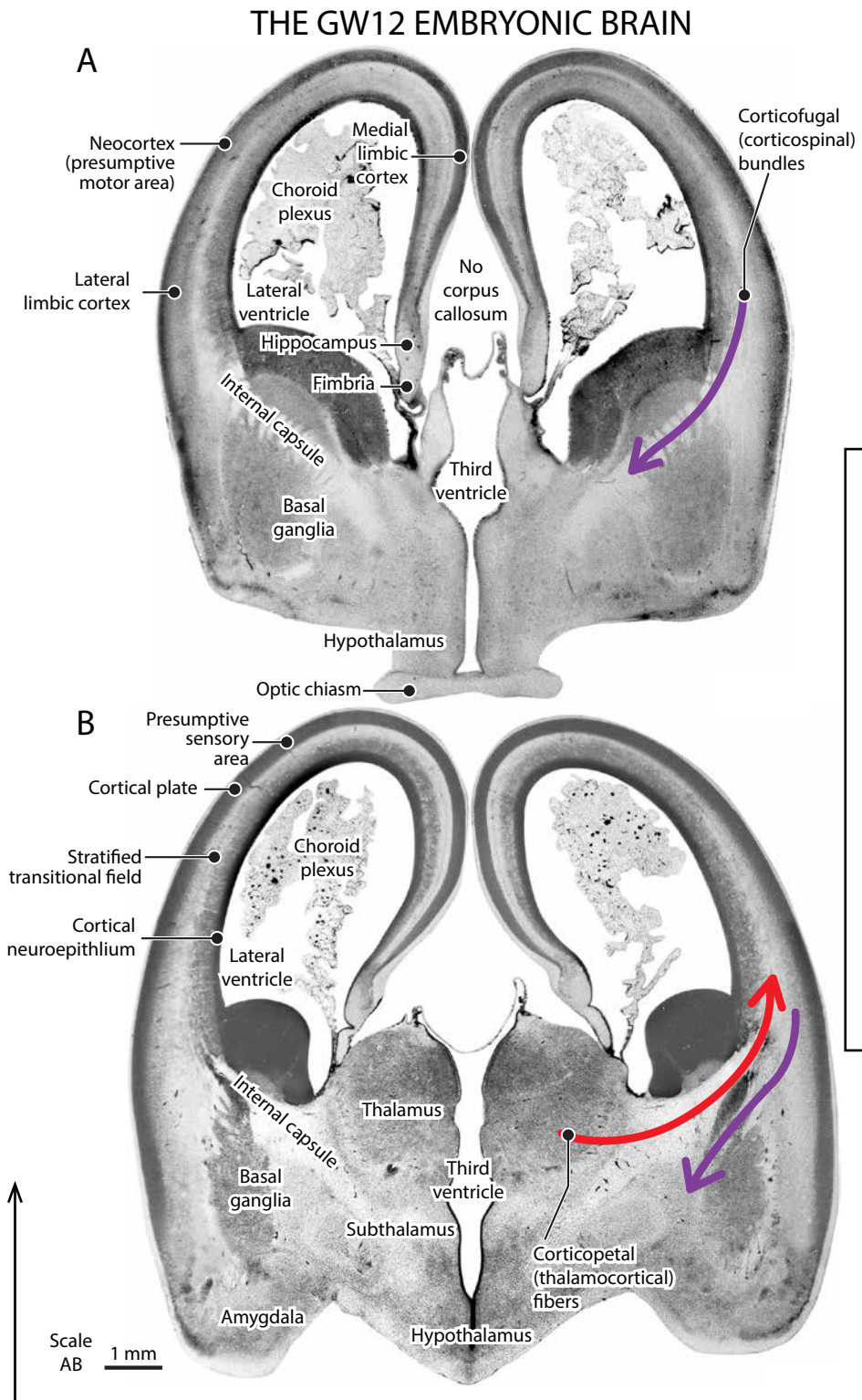

Fig. 16. The following 7 pages show horizontally cut, combined cell- and fiber-stained sections of the brain of a CR 56.5 mm, GW12 embryo (C1500) at 7 levels from dorsal (**A**) to ventral (**H**). The tissues surrounding the brain—presumptive skin and bone, and components of the meningeal brain coverings—have been preserved and illustrate an important facet of embryonic cortical development, the presence of a superarachnoid reticulum.

Fig. 15. Coronal sections of the brain of a CR 60 mm, GW12 embryo (Y1-59) at an anterior level cut across the basal ganglia and presumptive motor cortex (**A**), and more posteriorly at the presumptive sensory cortex and thalamus (**B**). The illustrations indicate presumptive continuity of the undifferentiated fibrous layer below the cortical plate with the corticospinal tract (*purple arrows*) and with the ascending thalamocortical fibers (*red arrow*). This is the first hint that cortical connections are being established by the end of the first trimester.

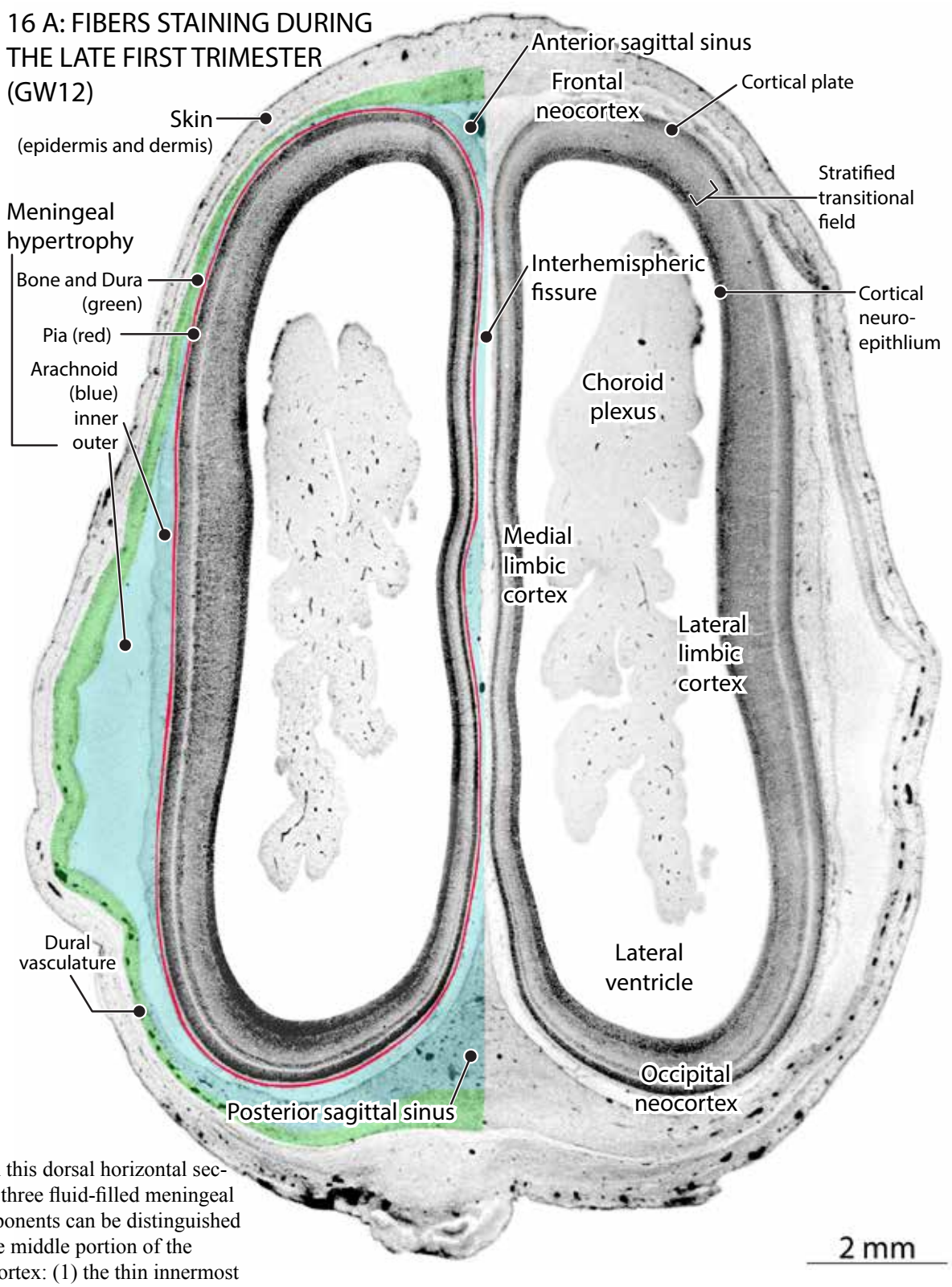

A. In this dorsal horizontal section, three fluid-filled meningeal components can be distinguished in the middle portion of the neocortex: (1) the thin innermost pial matrix (*red*); (2) two intermediate hypertrophied arachnoid matrices (*blue*, the superarachnoid); and (3) the outer dural matrix (*green*), which contains blood vessels that are assumed to be associated with the developing neocortical arterial and venous vasculature. The dural meninx is encased in the primordia of bone and skin.

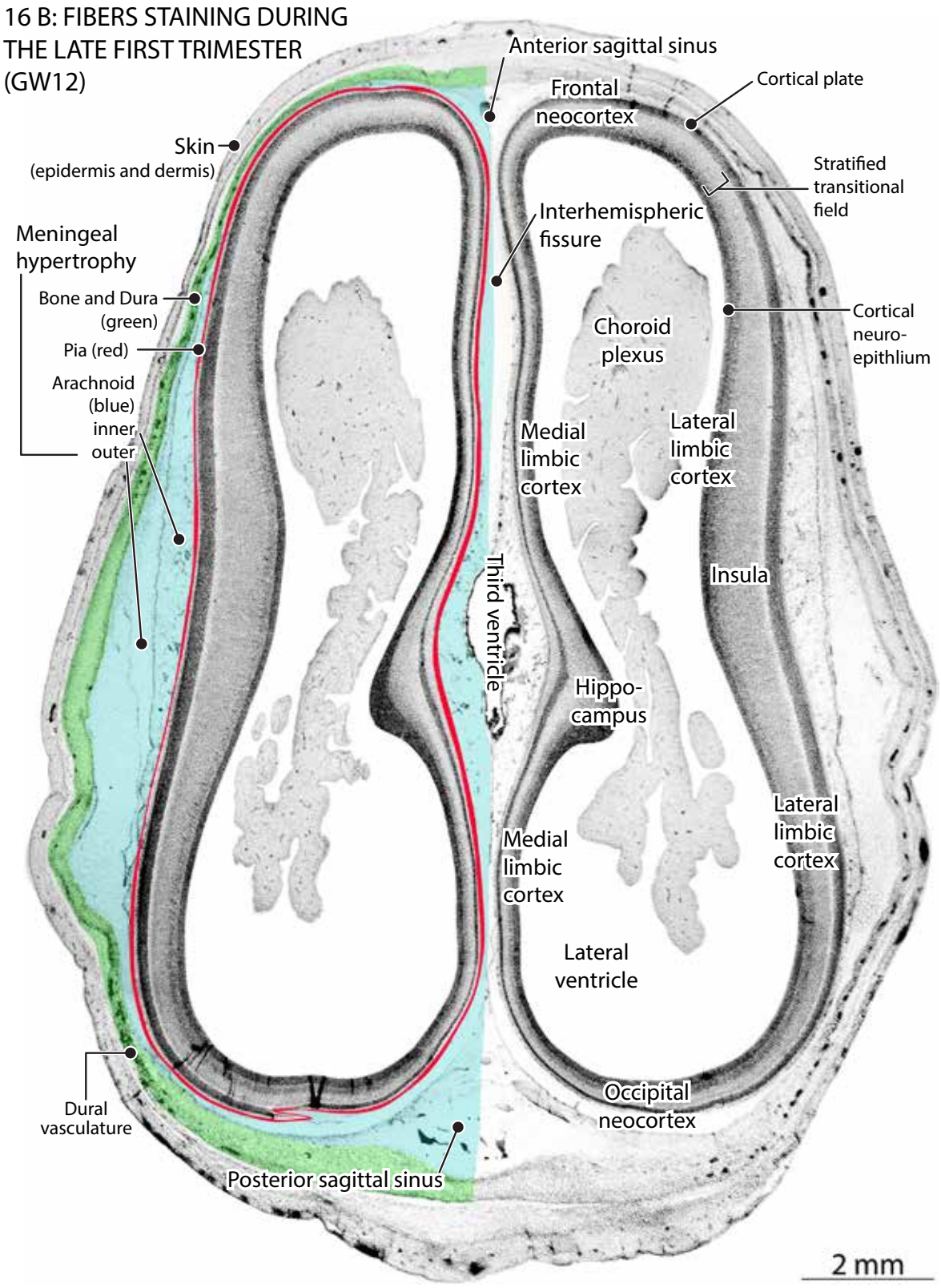

B. Perusal of the this section suggests that presumed fluid pressure exerted by the hypertrophied arachnoid meninx leads to middle constriction of the neocortex (insula) and its separation into an anterior (frontal) and a posterior (temporal/occipital) component.

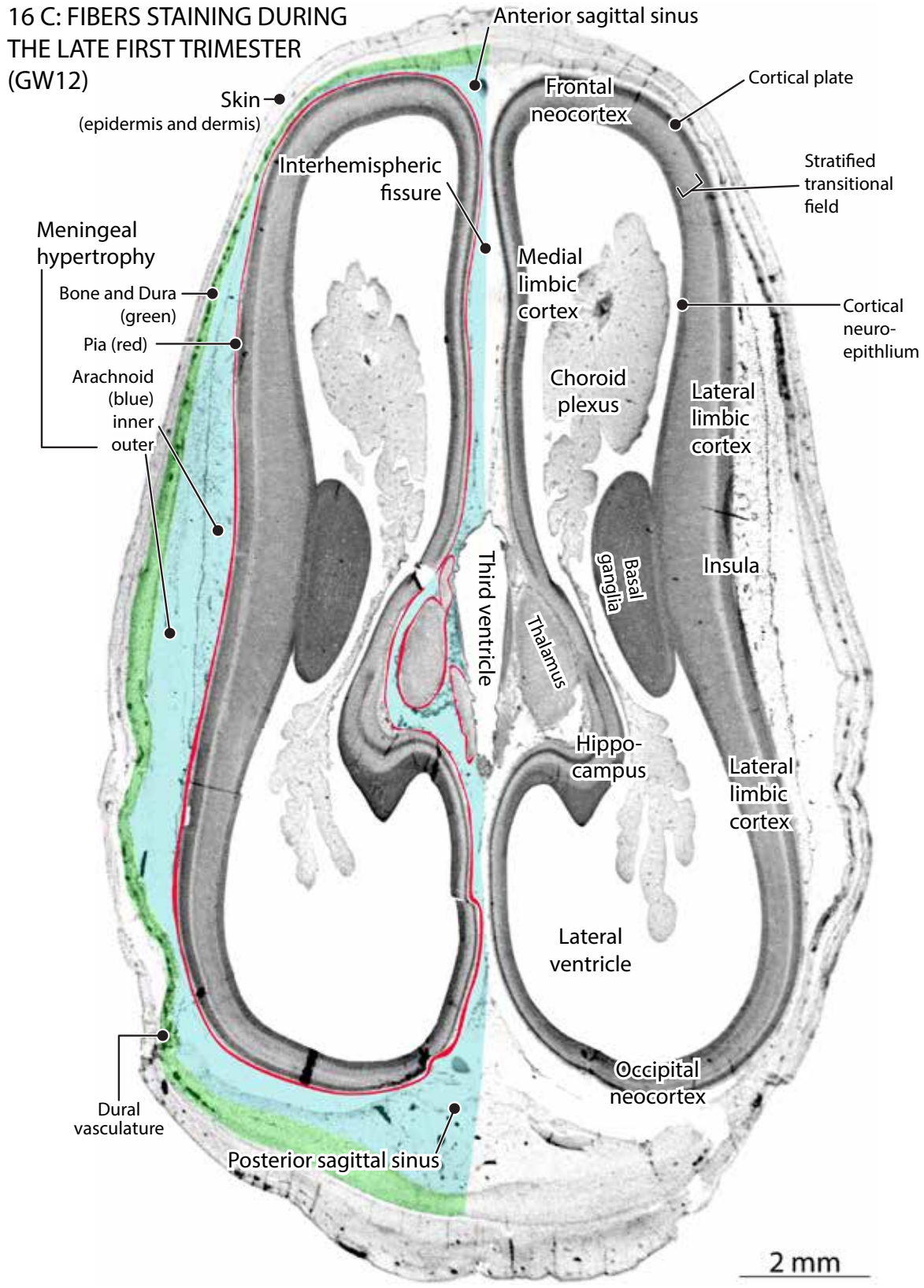

C. The separation is more pronounced in this horizontal section where constriction of the neocortex at the insula is accompanied by the inward expansion of the basal ganglia and the hippocampus.

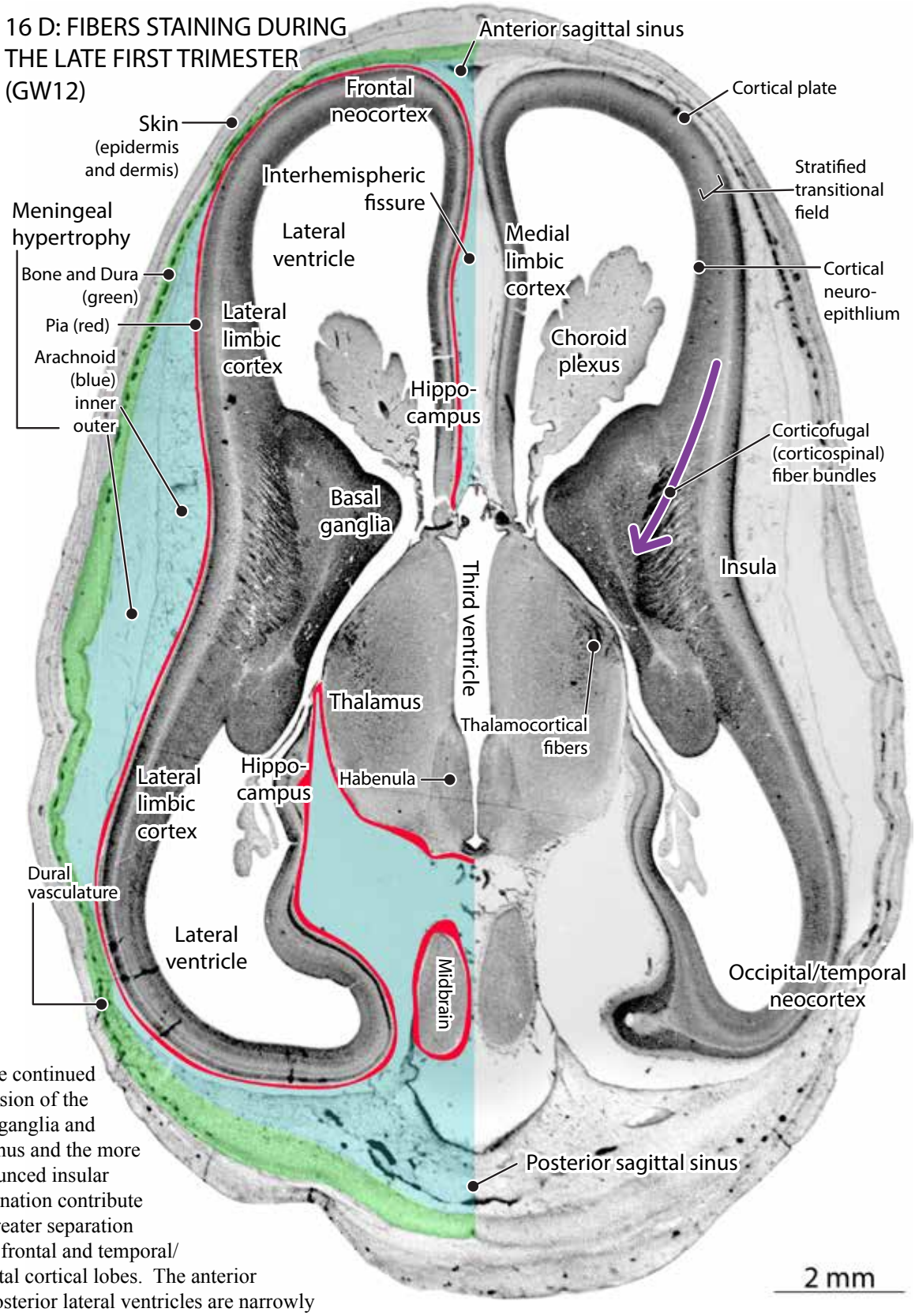

D. The continued expansion of the basal ganglia and thalamus and the more pronounced insular invagination contribute to a greater separation of the frontal and temporal/ occipital cortical lobes. The anterior and posterior lateral ventricles are narrowly continuous in a channel between the thalamus and the basal ganglia. Darkly-staining anterior corticofugal fiber bundles (*purple arrow*) from the neocortex are traversing the basal ganglia at this level.

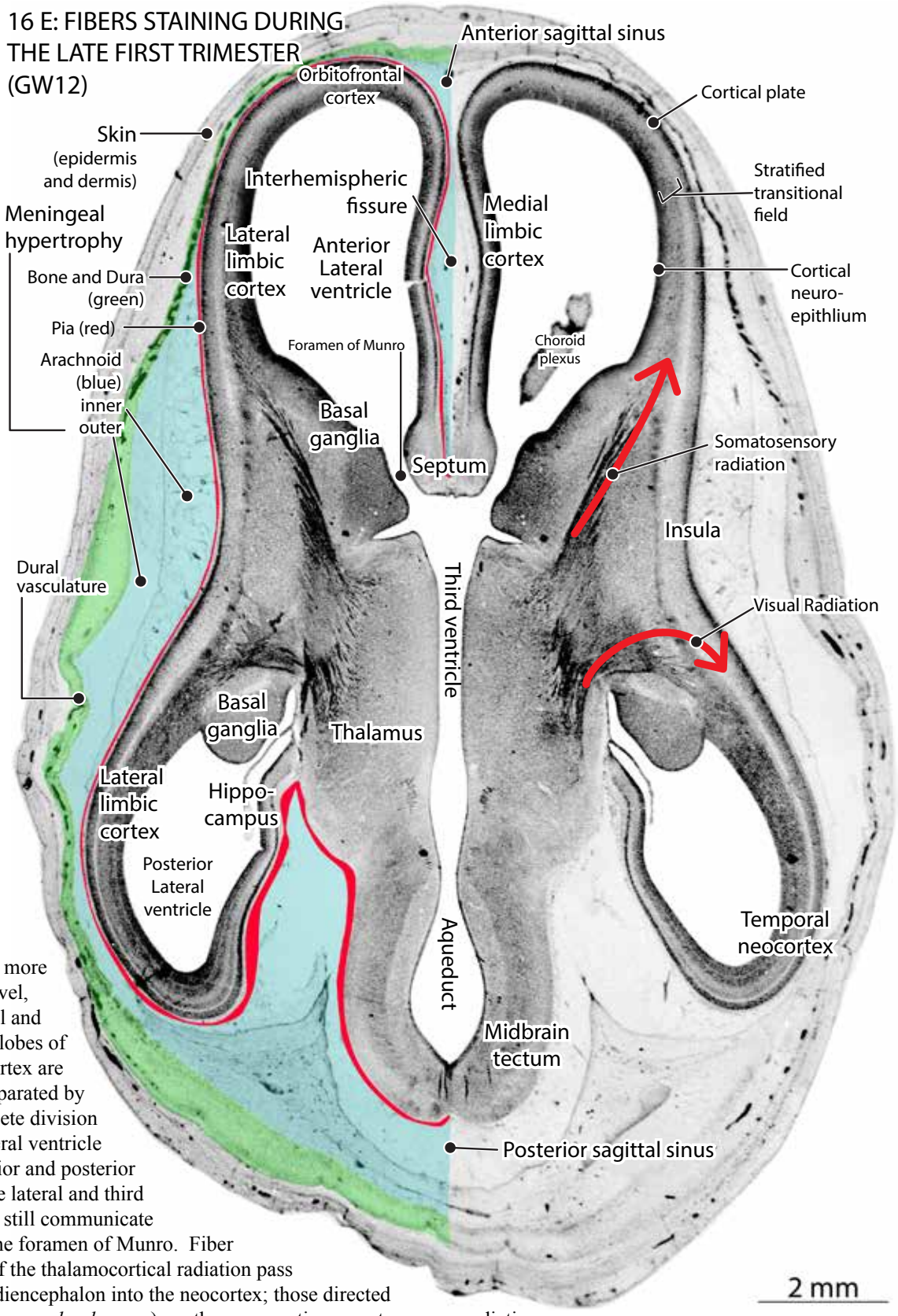

E. At this more ventral level, the frontal and temporal lobes of the neocortex are further separated by the complete division of the lateral ventricle into anterior and posterior parts. The lateral and third ventricles still communicate through the foramen of Munro. Fiber bundles of the thalamocortical radiation pass from the diencephalon into the neocortex; those directed rostrally (*upward red arrow*) are the presumptive somatosensory radiation; those the turning caudally form the presumptive visual radiation (Meyer's loop, *downward red arrow*).

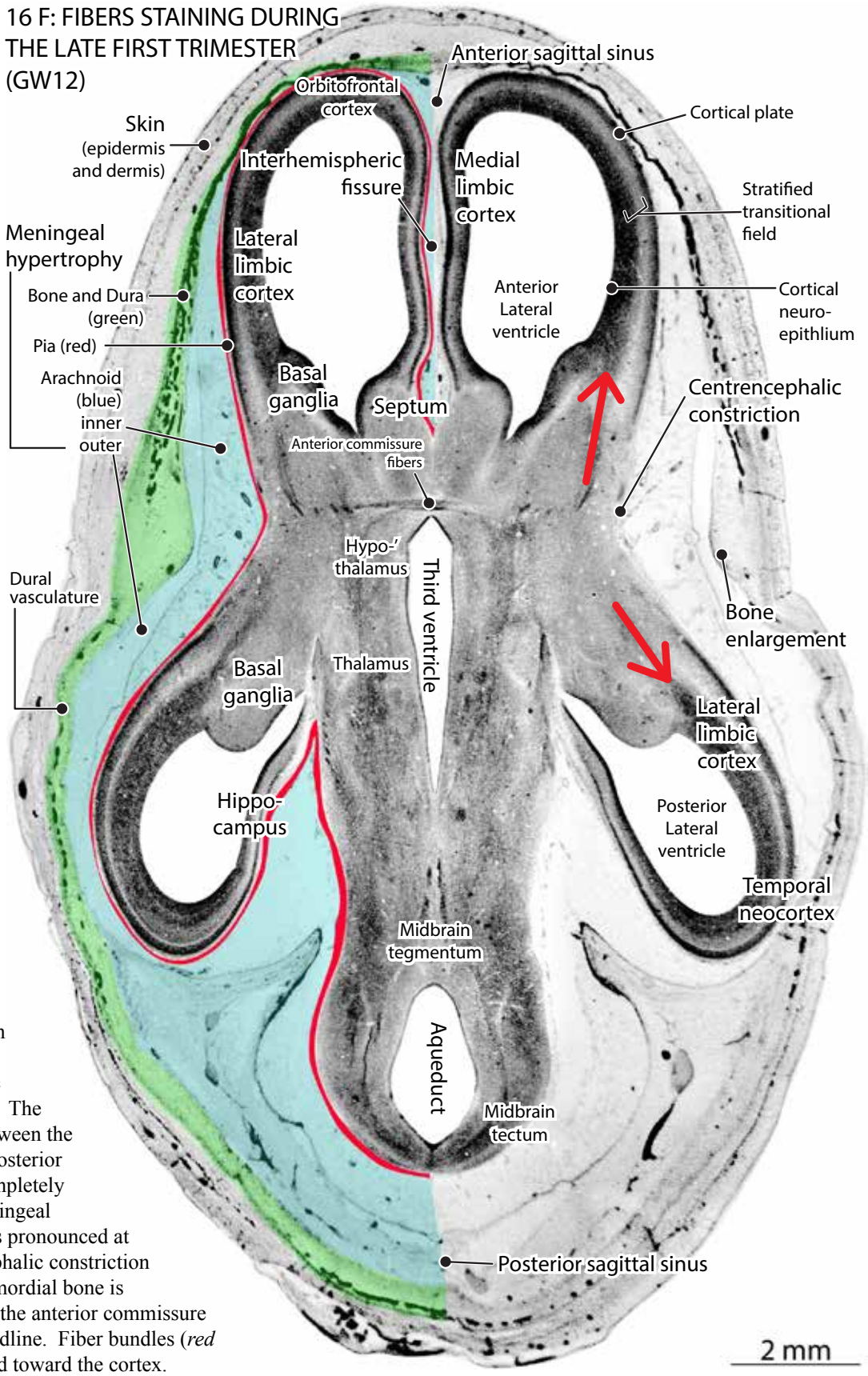

F. This section is just below the embryonic lateral fissure. The continuity between the anterior and posterior cortices is completely severed. Meningeal hypertrophy is pronounced at the centrencephalic constriction where the primordial bone is enlarging and the anterior commissure crosses the midline. Fiber bundles (*red arrows*) extend toward the cortex.

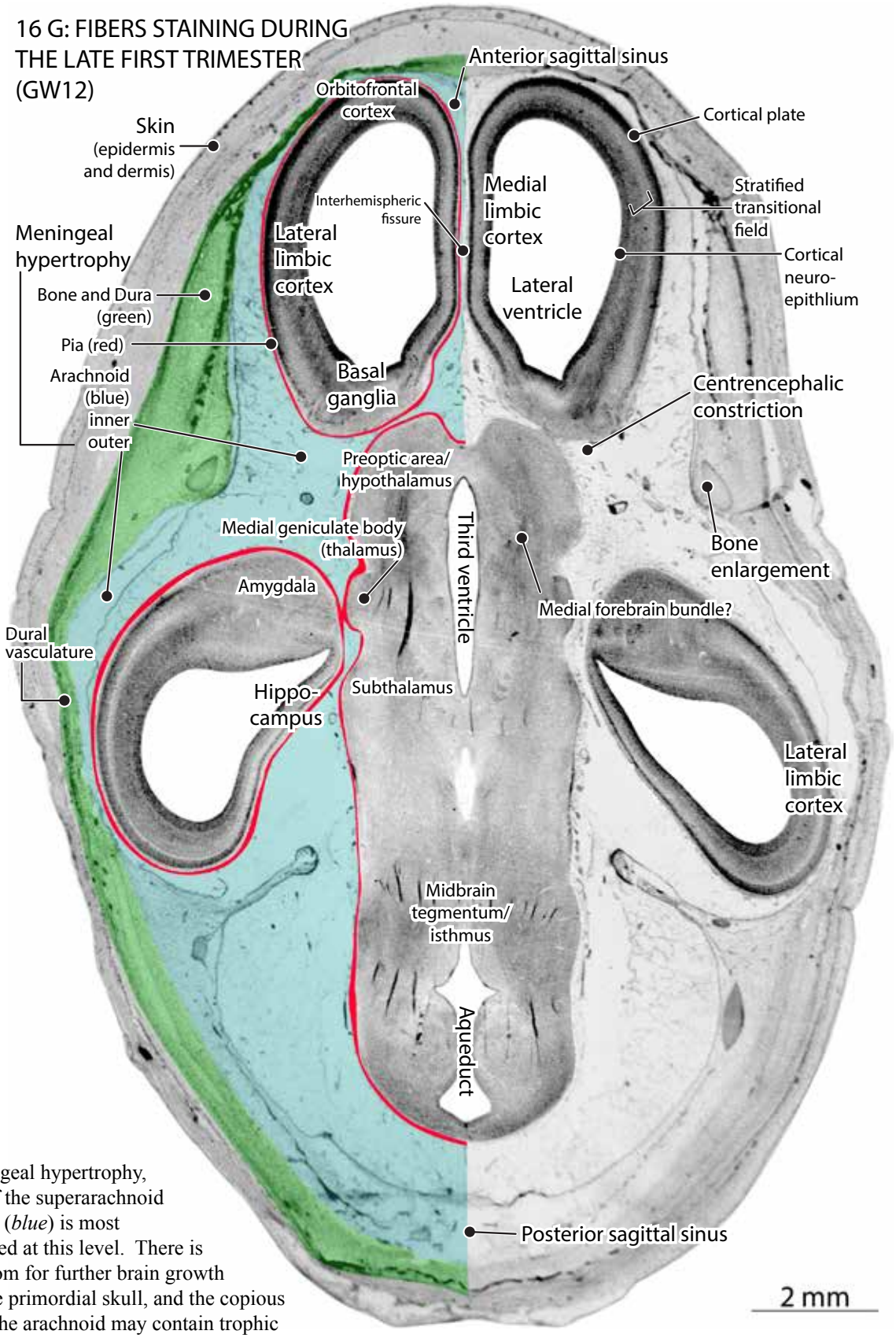

G. Meningeal hypertrophy, mainly of the superarachnoid reticulum (*blue*) is most pronounced at this level. There is ample room for further brain growth within the primordial skull, and the copious fluids in the arachnoid may contain trophic factors to enhance brain growth.

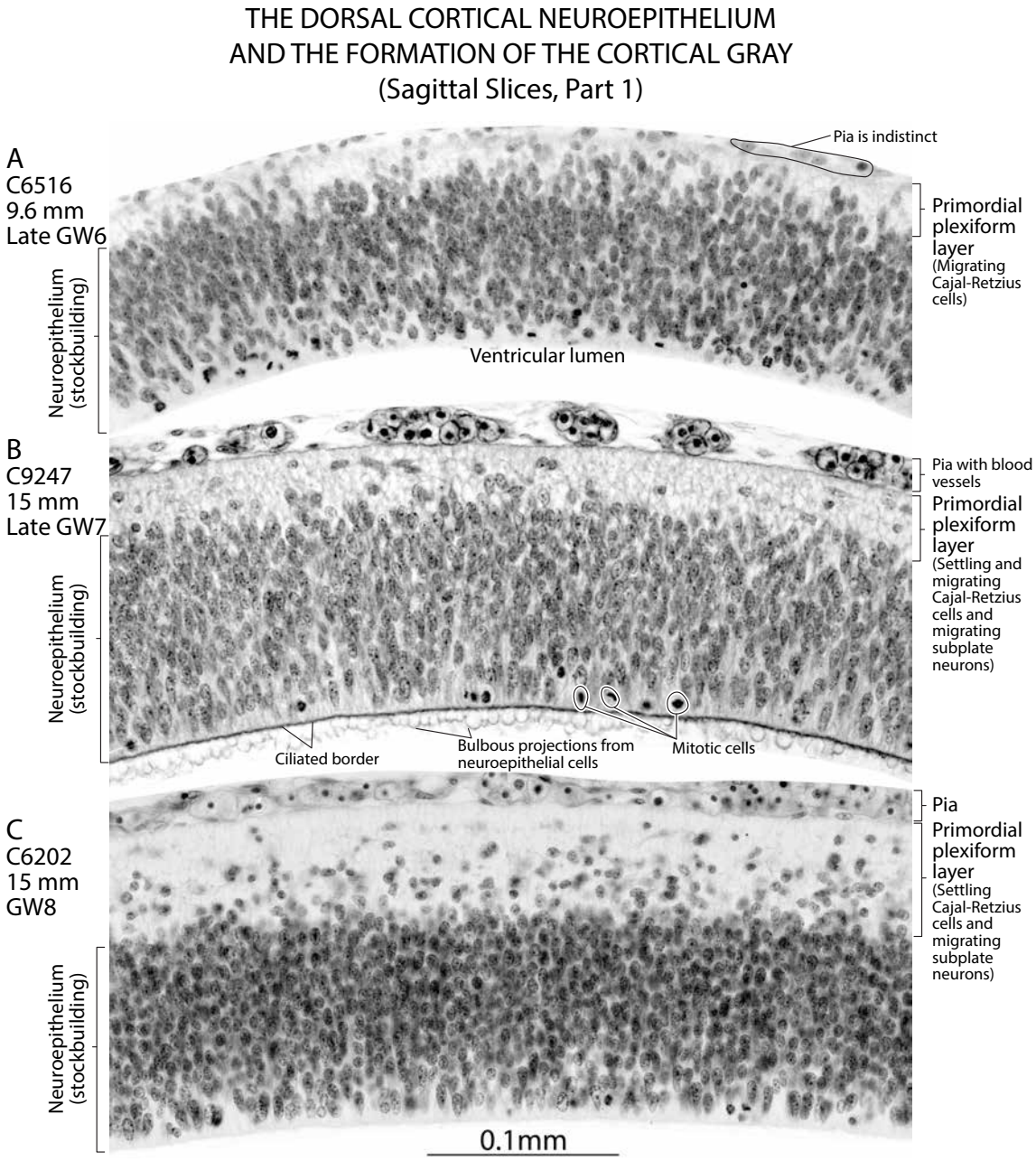

Fig. 17 (facing pages). High magnification photomicrographs of the developing dorsal neocortex in sagittally-cut first trimester embryos. **A.** In the CR 9.6 mm GW6 embryo (C6516), the proliferating neuroepithelial (NEP) cells have their nuclei undergoing mitosis at the lumen of the lateral ventricle, increasing their numbers (stockbuilding). The few migrating cells, presumably Cajal-Retzius, enter the thin fibrous primordial plexiform layer. As yet, there is no distinct pial covering. **B.** In this CR 11.7 mm GW7 cortex (C8789), the primordial plexiform layer has become wider and contains densely packed round extracellular vesicles that may be a conduit for ingrowing fibers. The cells in the plexiform layer may be the earliest differentiating Cajal-Retzius neurons settling superficially, while subplate neurons are migrating from the NEP. The pia, with its many blood islands, has formed. **C**. In the CR 15.0 mm GW8 cortex (C6202), there are more neurons settling and migrating into the expanding primordial plexiform layer. **D**. Several new developments are evident in the neocortex of the CR 28.8 mm GW9 embryo (M1598). (i) The most obvious is the formation of the thin, compact band of cells, the cortical plate, containing the earliest settling neurons of the future laminated cortical gray matter. (ii) The cortical plate is sandwiched between the superficial fibrous layer 1, containing aligned Cajal-Retzius cells, and a deep fibrous layer. The neurons settling neurons in the

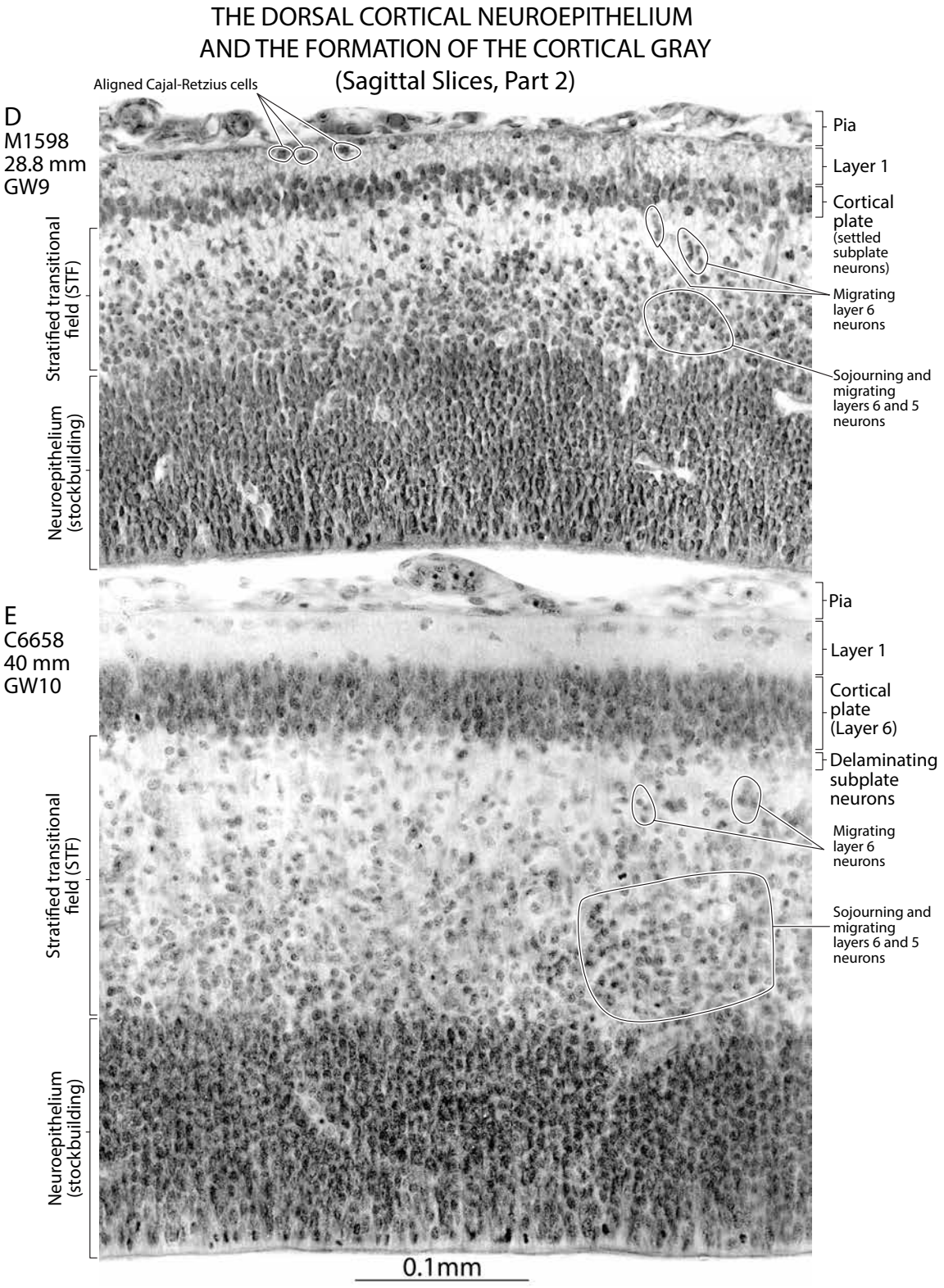

cortical plate may be subplate neurons, the future layer 7. (iii) A widening band of cells flanking the expanding NEP contains migrating and sojourning neurons (mainly layer 6). **E**. The progressive thickening of the cortical plate, the stratified transitional field, and the NEP (still in stockbuilding phase) continues in the neocortex of the CR40 mm GW10 embryo (C6658). The ragged base of the cortical plate contains delaminating subplate neurons.

B. NEOCORTICAL DEVELOPMENT DURING THE SECOND AND THIRD TRIMESTERS

The second trimester specimens we illustrate in this chapter are mostly from the Yakovlev Collection. Information is available in most instances about the estimated age and size of the fetuses but in a few cases we have corrected the dates on the basis of the large data file presented by Lougha et al. (2009), based on *in vivo* ultrasound imaging about the relationship between the crown-lump length of fetuses (CR), and their estimated gestational age in weeks (GW) or months (Table 2).

TABLE 2
SECOND TRIMESTER CROWN RUMP LENGTH (CR)
AND ESTIMATED GESTATIONAL AGE (GW)

CR (mm)	GW (weeks)	Months
100-145	14-17	4
150-190	18-21	5
195-230	22-24	6

The neocortex is undergoing major developmental changes during the second trimester, which is often considered the beginning of the early fetal period. As seen in a photograph of a 4 months-old fetus (Fig. 18A-D), the cerebral cortex is lissencephalic, lacking in convolutions, with the exception of a deep ventrolateral invagination at the mid antero-posterior level where the branches of the internal carotid arteries (anterior cerebral and middle cerebral) fan out and are distributed over the surface of the cerebral hemispheres (Fig. 18E). We call this invagination, the insular cleavage. This cleavage, originally a dimple, separates the frontal lobe from the temporal lobe and is the base of the formative lateral fissure.

Fig. 18. The brain of a 4 months-old fetus in lateral (**A**), dorsal (**B**) and ventral views (**C**), and the brain of another fetus (**D**) of the same age in midline view. **E**. The same brain in **A**, after its vascular system was injected with ink. This lateral view shows the partitioning of the frontal lobe from the temporal lobe ventrally by the wide-based insular cleavage (the incipient lateral fissure). That primordial partitioning of the cerebral cortex serves as the passageway for the distribution of cerebral arteries from the internal carotid artery into the developing cerebral cortex (**E**). (After Retzius, 1896. Color and labeling added).

THE 4-MONTHS-OLD FETAL NEOCORTEX

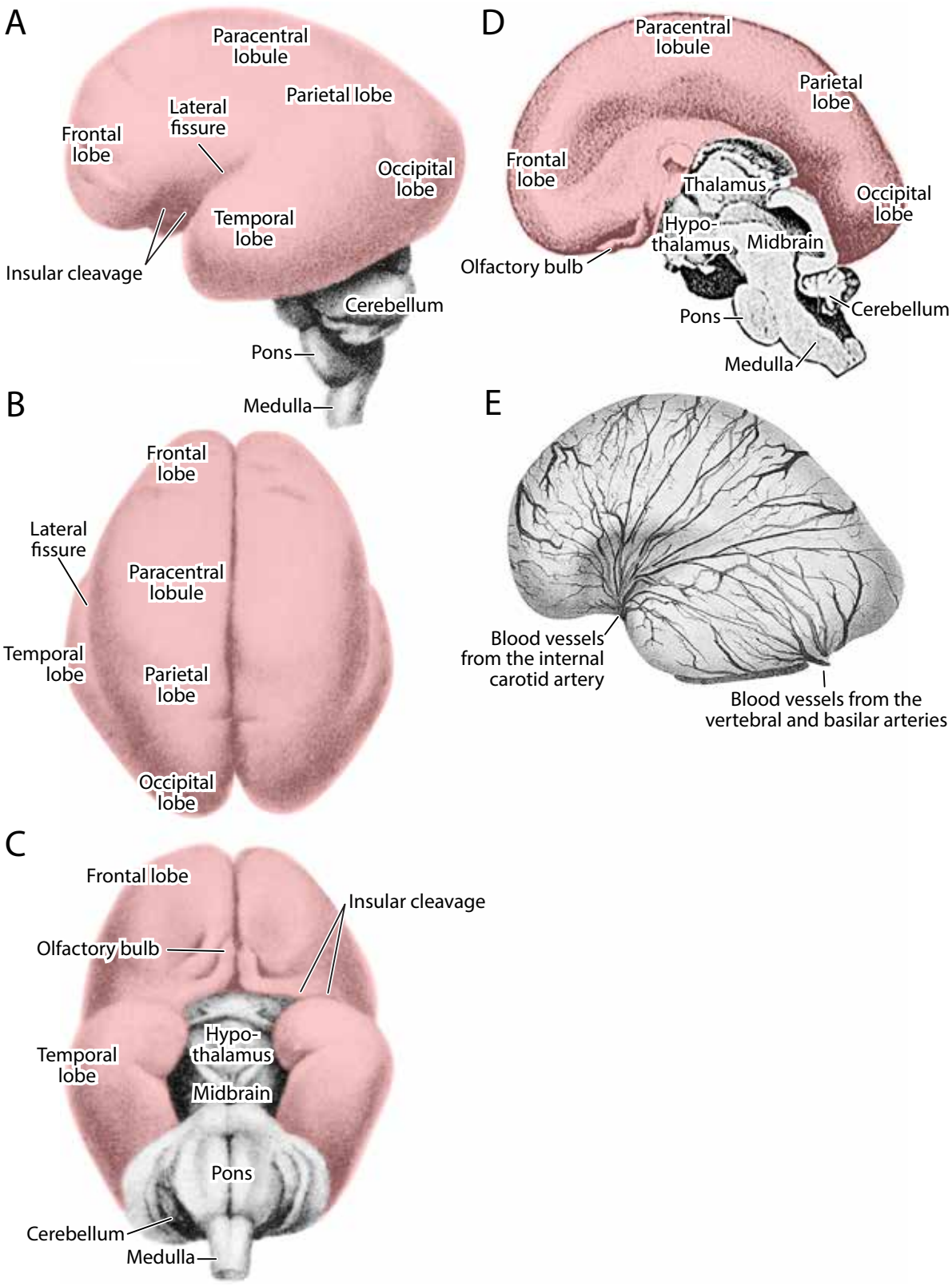

Figures 19 through 37 (see list on facing page) show neocortical development in second and third trimester fetal brains. The following text is an abstract of the major changes.

A comparison of photomicrographs of the brain of a second trimester (GW14) and an early third trimester (GW18) fetus (Fig. 19) indicates that a major event during this period is the expansion of the stratified transitional field (STF), with pronounced regional differences in the lamination pattern from the frontal cortex rostrally to the occipital cortex caudally. The corticofugal tract traversing the basal ganglia expands during this period but as yet few of these descending fibers have reached the pontine gray in the younger fetus (Fig. 19E) but many more so in the older fetus (Fig. 19F). It is also during this period that the corpus callosum is in the process of crossing to the opposite side. Regional differences in STF lamination are becoming more pronounced during the 5th month of fetal life, as seen in a GW20 fetus (Fig. 20). This important morphogenetic event is associated with a large complement of corticofugal fibers that leave the anterior neocortex and another large complement of thalamocortical fibers that penetrate the paracentral and posterior neocortex. A remarkable feature in the latter region is the STF honeycomb matrix, which is most pronounced in the occipital lobe (Figs. 20, 21, 22). We postulate that the STF honeycomb matrix is the site where fascicles of thalamocortical sensory relay fibers specify cortical neurons migrating and sojourning there. It is postulated that the thalamocortical fibers carry markers of their topographic (retinotopic, somatotopic and cochleotopic) origin and transmit that information to the unspecified ascending differentiating neurons in STF layer 3 before these neurons resume their migration to the cortical plate (Fig. 23).

Cortical gyrification begins at about the 5th month of fetal life, as the parieto-occipital and calcarine fissures are beginning to form posteriorly in the occipital lobe (Fig. 20). But gyrification in the lateral convexity does not start until the 6th month of fetal life (Figs. 24 to 28) and does not become pronounced until the 7th month in early third trimester fetuses (Figs. 29 to 30). The deepening fissures come to separate different components of the neocortex: the lateral fissure separates the frontal lobe from the temporal lobe; the central fissure separates the motor precentral gyrus from the somatosensory postcentral gyrus (paracentral area); the occipito-parietal fissure separates the visual cortex from the haptic (touch sense) parietal cortex; and the calcarine fissure separates the dorsal visual cortex from the ventral visual cortex. It is during the middle and late third trimester that the frontal lobe, temporal lobe, parietal lobe and occipital lobe gradually undergo secondary and tertiary foliation (Fig. 31). That increased cortical gyrification is associated with three developments: (i) the gradual dissolution of the STF (Fig. 30); (ii) a great increase in white matter volume (a sign of increased axonogenesis, Fig. 31); (iii) the expansion of the cortical plate as it differentiates into regionally distinctive gray matter.

There is little difference in the thickness and cellular organization of the cortical plate in the presumptive motor cortex and visual cortex in the GW18 fetus (Fig. 32). A pronounced difference emerges in the thickness of the motor cortex and the visual cortex in the GW20 fetus (Fig. 33). The relationship between the dissolution of the STF, the increasing depth of the white matter, and the incipient lamination of the gray matter is illustrated in a comparison of the neocortical organization at different levels in a GW21 fetus and a GW26 fetus (Fig. 34). We illustrate the development of regional differences in the cytoarchitectonics of the cortical gray matter at higher magnification at 5 months, 7 months and at birth in Figs. 35-37.

ANNOTATED ILLUSTRATIONS OF FETAL BRAINS

→

Fig. 19. On the following 6 pages. Coronal sections of the brain from anterior to posterior of a 4 months-old fetus (Y144-63, GW14, CR 100 mm) and an early 5 months-old fetus (Y15-63, GW 19, CR 150 mm). A series of developmental changes are visible in the cerebral cortex at these two ages and in comparison with late first trimester fetuses shown earlier (**Figs. 15-17**). Among these changes are some of the following. The cortical plate is progressively widening during this period, indicating ongoing neuronal migration and settling. However, that migration is an interrupted process as large populations of sojourning neurons form alternating cellular layers with fibrous bands in the transient neocortical stratified transitional field (*STF*). These distinctive layers in different cortical areas are shown in insets at higher magnification.

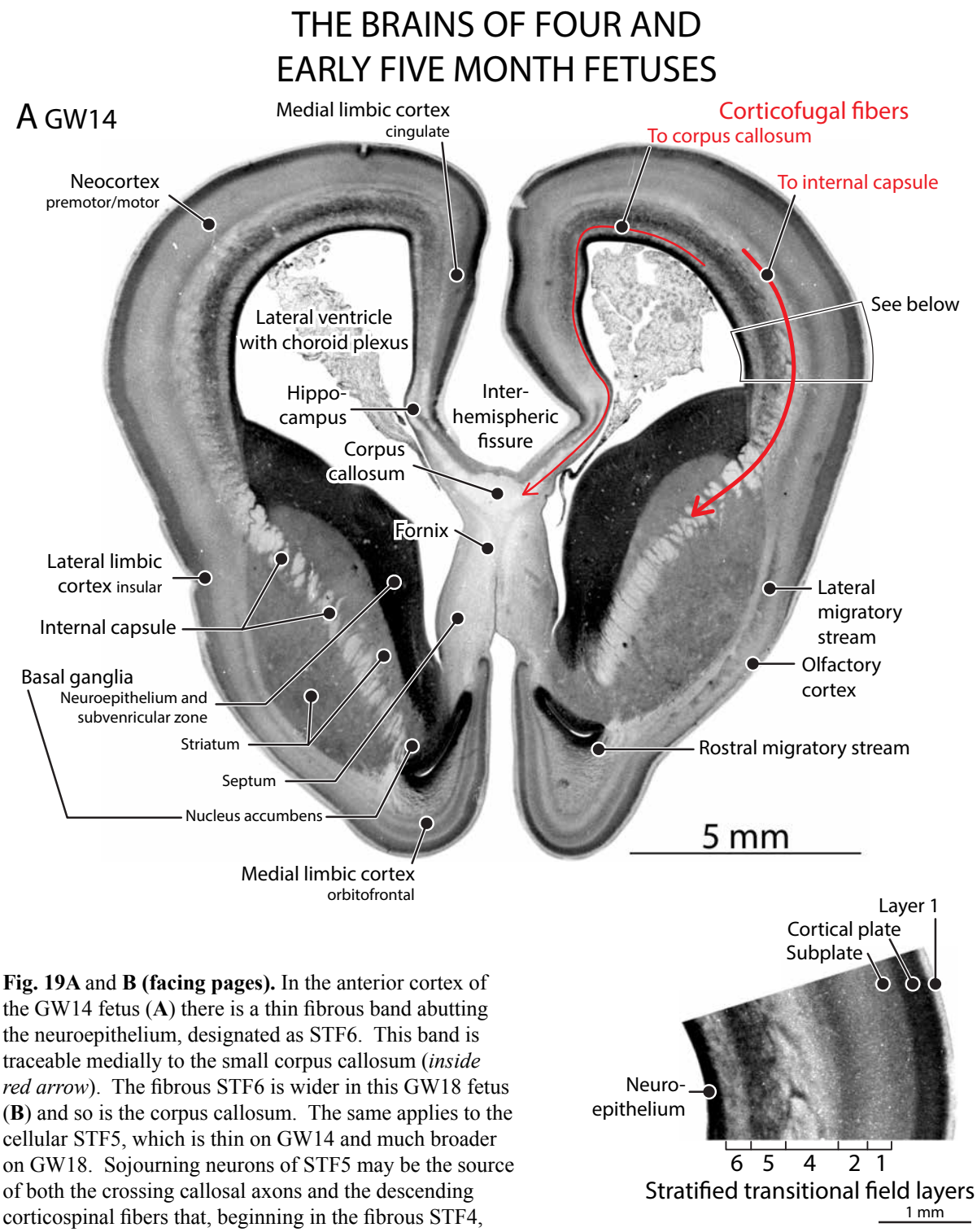

Fig. 19A and **B (facing pages).** In the anterior cortex of the GW14 fetus (**A**) there is a thin fibrous band abutting the neuroepithelium, designated as STF6. This band is traceable medially to the small corpus callosum (*inside red arrow*). The fibrous STF6 is wider in this GW18 fetus (**B**) and so is the corpus callosum. The same applies to the cellular STF5, which is thin on GW14 and much broader on GW18. Sojourning neurons of STF5 may be the source of both the crossing callosal axons and the descending corticospinal fibers that, beginning in the fibrous STF4, form discrete fascicles as they transit through the basal ganglia (*outside red arrow*).

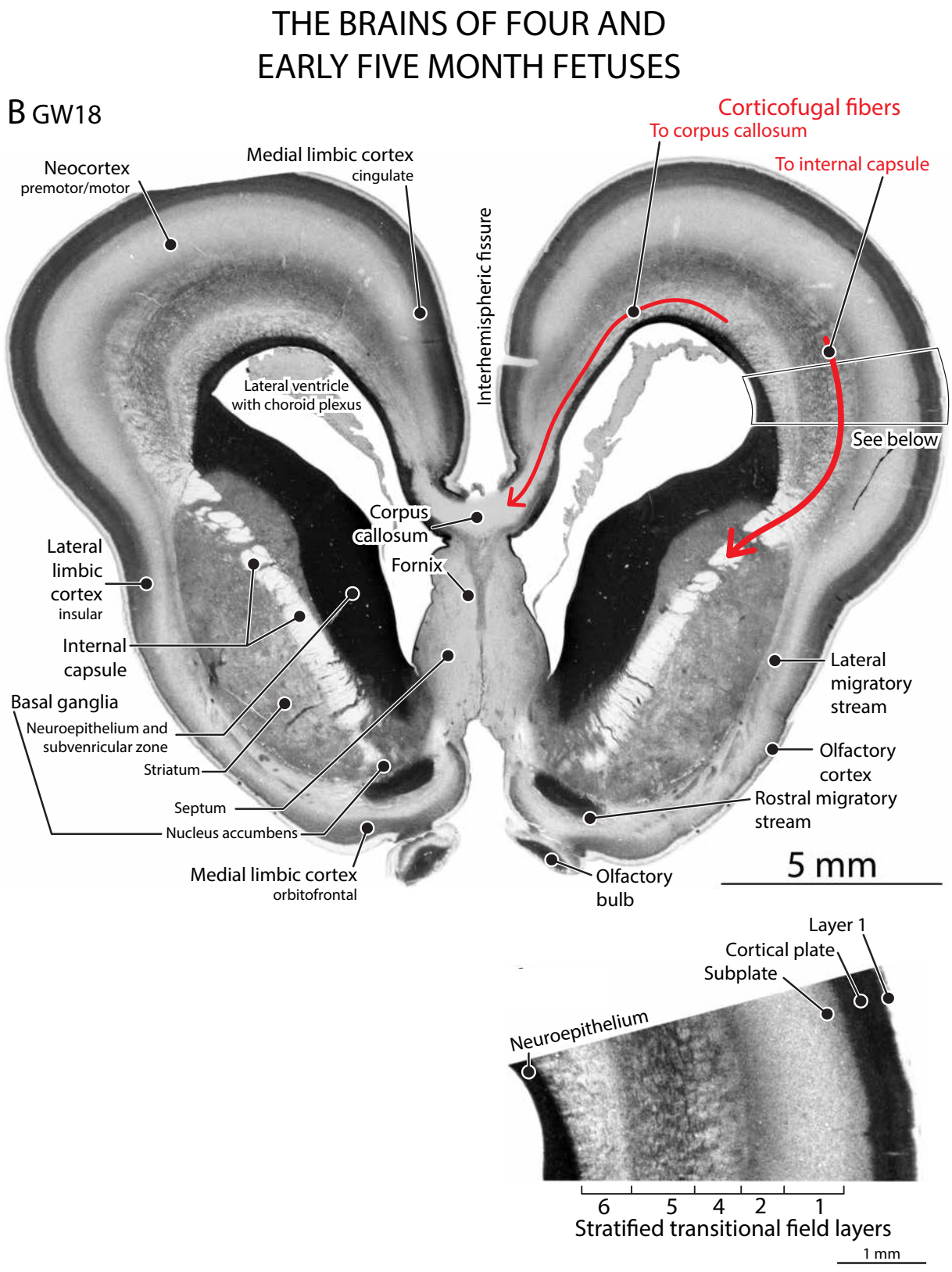
THE BRAINS OF FOUR AND
EARLY FIVE MONTH FETUSES
B GW18
Corticofugal fibers
To corpus callosum
To internal capsule
Neocortex
premotor/motor
Medial limbic cortex
cingulate
Interhemispheric fissure
Lateral ventricle
with choroid plexus
See below
Corpus
callosum
Fornix
Lateral
limbic
cortex
insular
Internal
capsule
Basal ganglia
Neuroepithelium and
subventricular zone
Striatum
Septum
Nucleus accumbens
Medial limbic cortex
orbitofrontal
Lateral
migratory
stream
Olfactory
cortex
Rostral migratory
stream
Olfactory
bulb
5 mm
Layer 1
Cortical plate
Subplate
Neuroepithelium
6
5
4
2
1
Stratified transitional field layers
1 mm

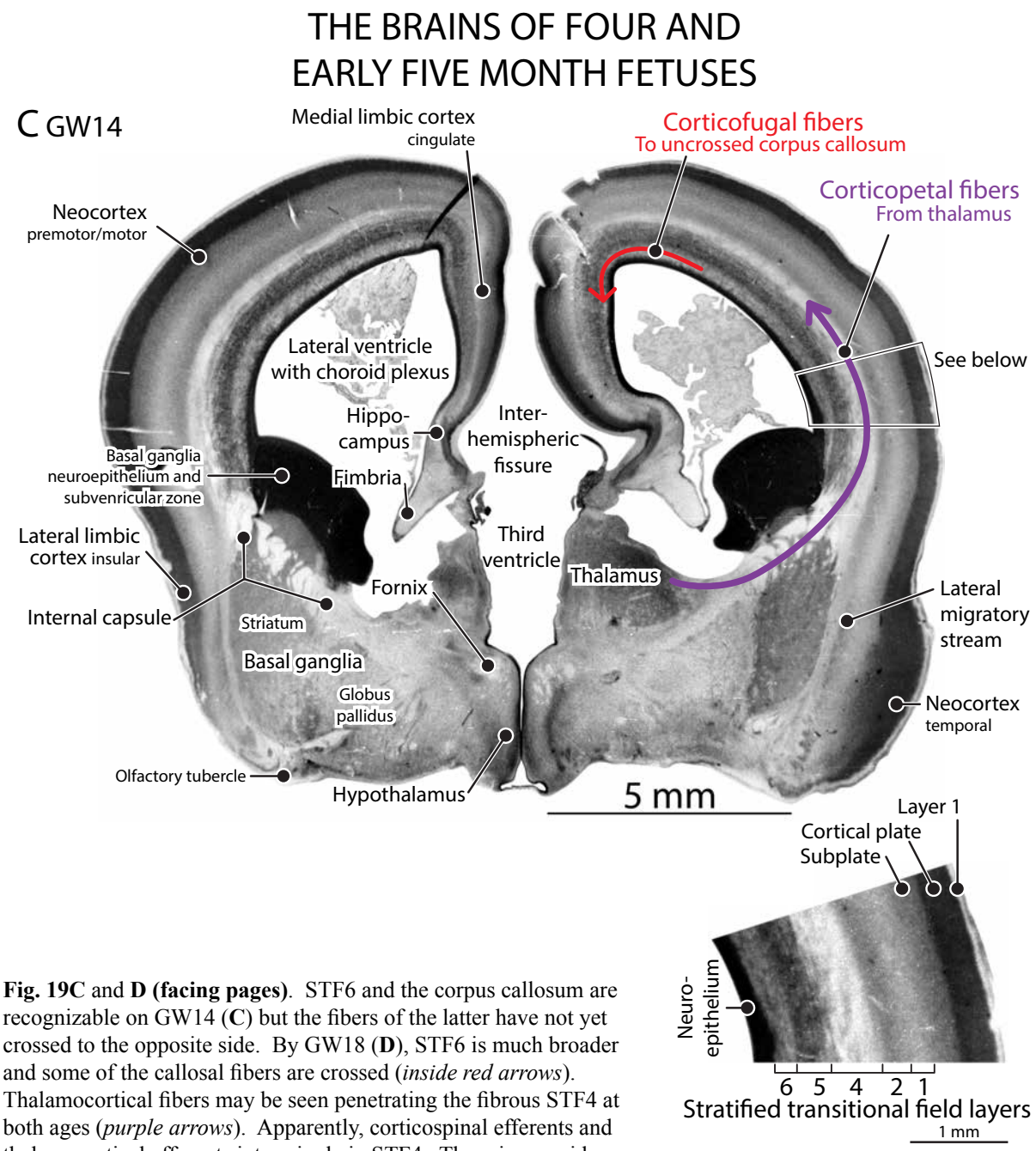

Fig. 19C and **D (facing pages)**. STF6 and the corpus callosum are recognizable on GW14 (**C**) but the fibers of the latter have not yet crossed to the opposite side. By GW18 (**D**), STF6 is much broader and some of the callosal fibers are crossed (*inside red arrows*). Thalamocortical fibers may be seen penetrating the fibrous STF4 at both ages (*purple arrows*). Apparently, corticospinal efferents and thalamocortical afferents intermingle in STF4. There is no evidence of a cellular STF3 in these anterior sections.

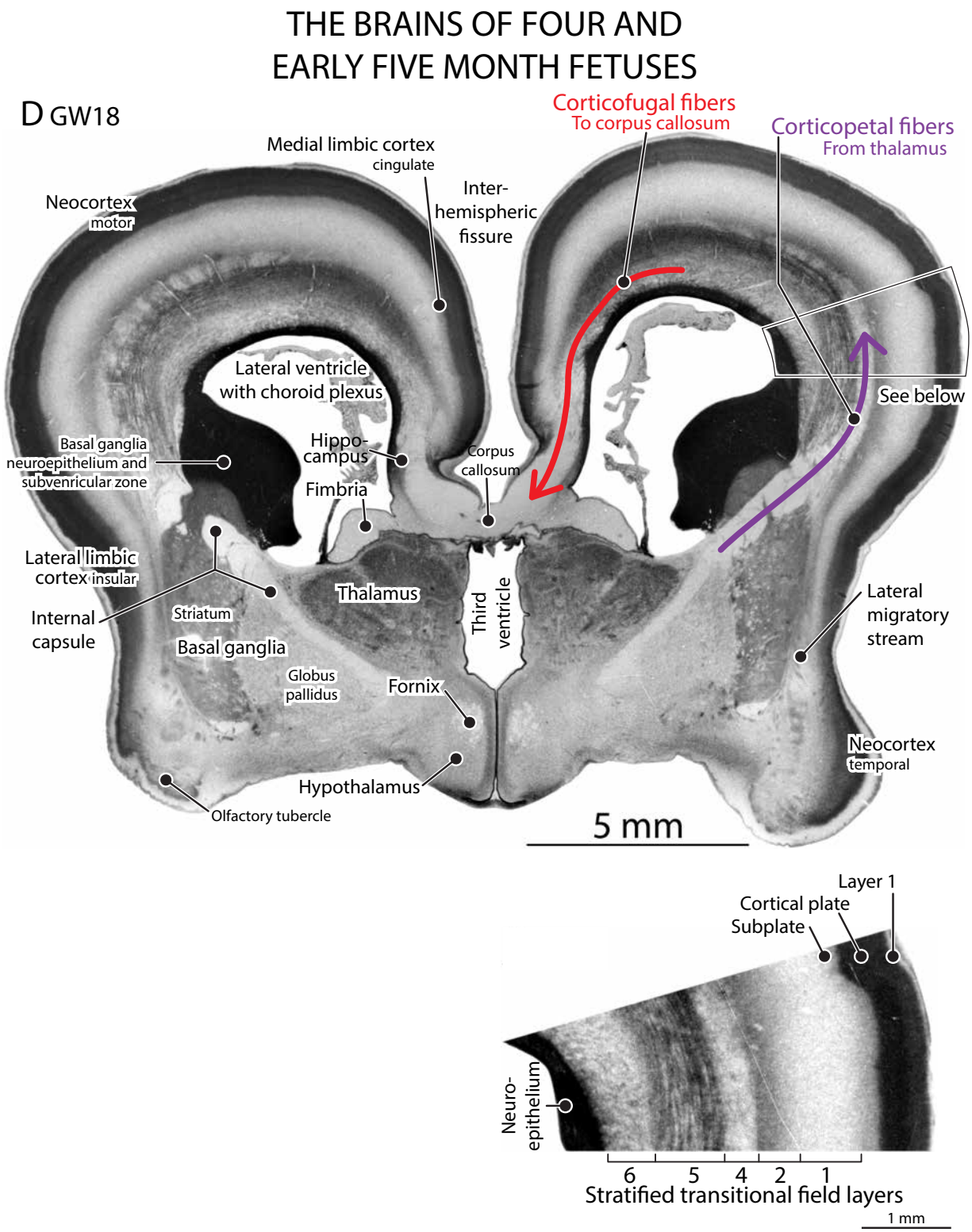
THE BRAINS OF FOUR AND
EARLY FIVE MONTH FETUSES
D GW18
Corticofugal fibers
To corpus callosum
Corticopetal fibers
From thalamus
Medial limbic cortex
cingulate
Neocortex
motor
Inter-
hemispheric
fissure
Lateral ventricle
with choroid plexus
See below
Basal ganglia
neuroepithelium and
subventricular zone
Hippo-
campus
Corpus
callosum
Fimbria
Lateral limbic
cortex insular
Thalamus
Third
ventricle
Lateral
migratory
stream
Internal
capsule
Striatum
Basal ganglia
Globus
pallidus
Fornix
Neocortex
temporal
Hypothalamus
Olfactory tubercle
5 mm
Layer 1
Cortical plate
Subplate
Neuro-
epithelium
6
5
4
2
1
Stratified transitional field layers
1 mm

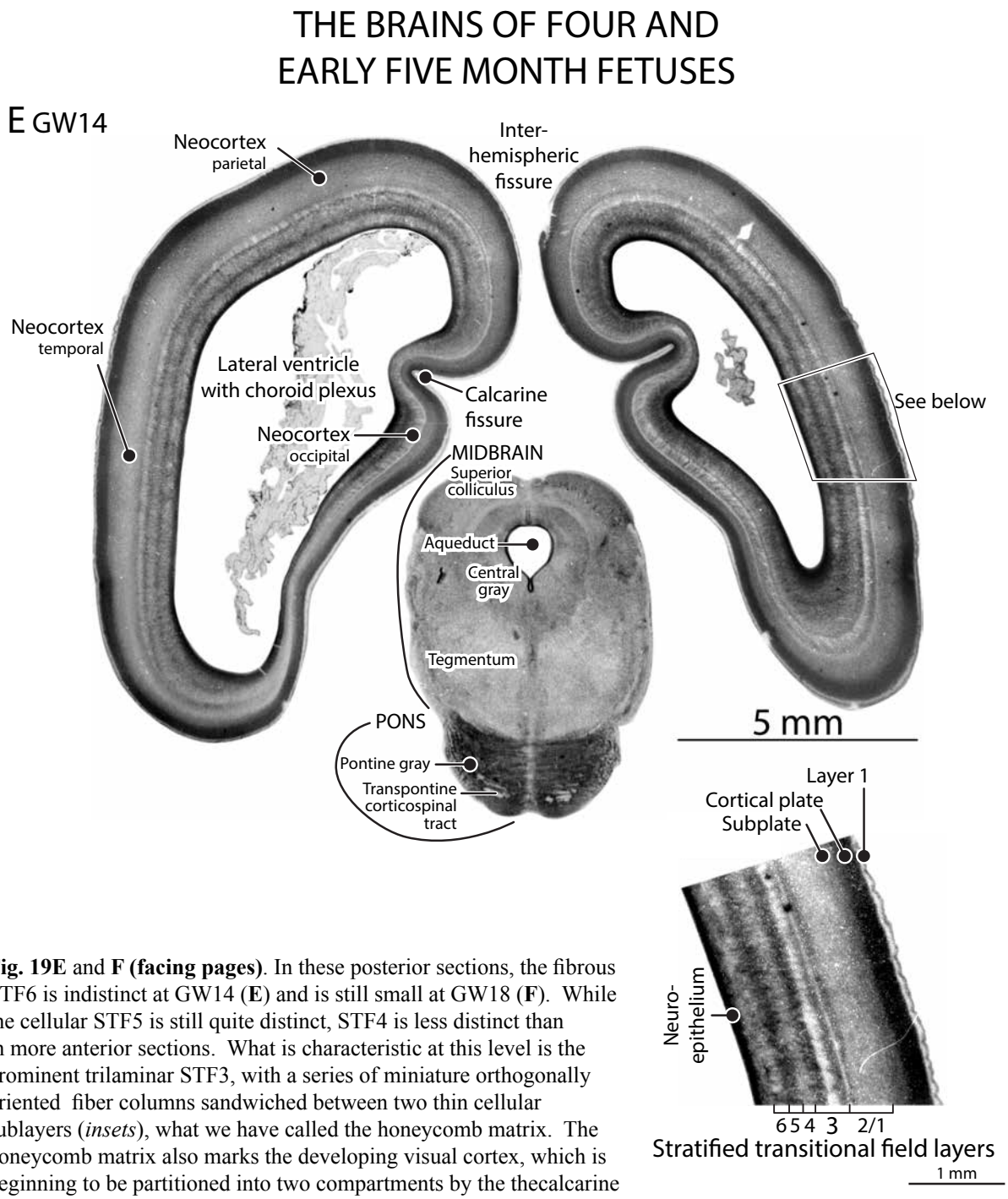

Fig. 19E and **F (facing pages)**. In these posterior sections, the fibrous STF6 is indistinct at GW14 (**E**) and is still small at GW18 (**F**). While the cellular STF5 is still quite distinct, STF4 is less distinct than in more anterior sections. What is characteristic at this level is the prominent trilaminar STF3, with a series of miniature orthogonally oriented fiber columns sandwiched between two thin cellular sublayers (*insets*), what we have called the honeycomb matrix. The honeycomb matrix also marks the developing visual cortex, which is beginning to be partitioned into two compartments by the thecalcarine fissure in both specimens. Also noteworthy is the few descending transpontine corticospinal fibers passing through the pons on GW14 and their abundance on GW18.

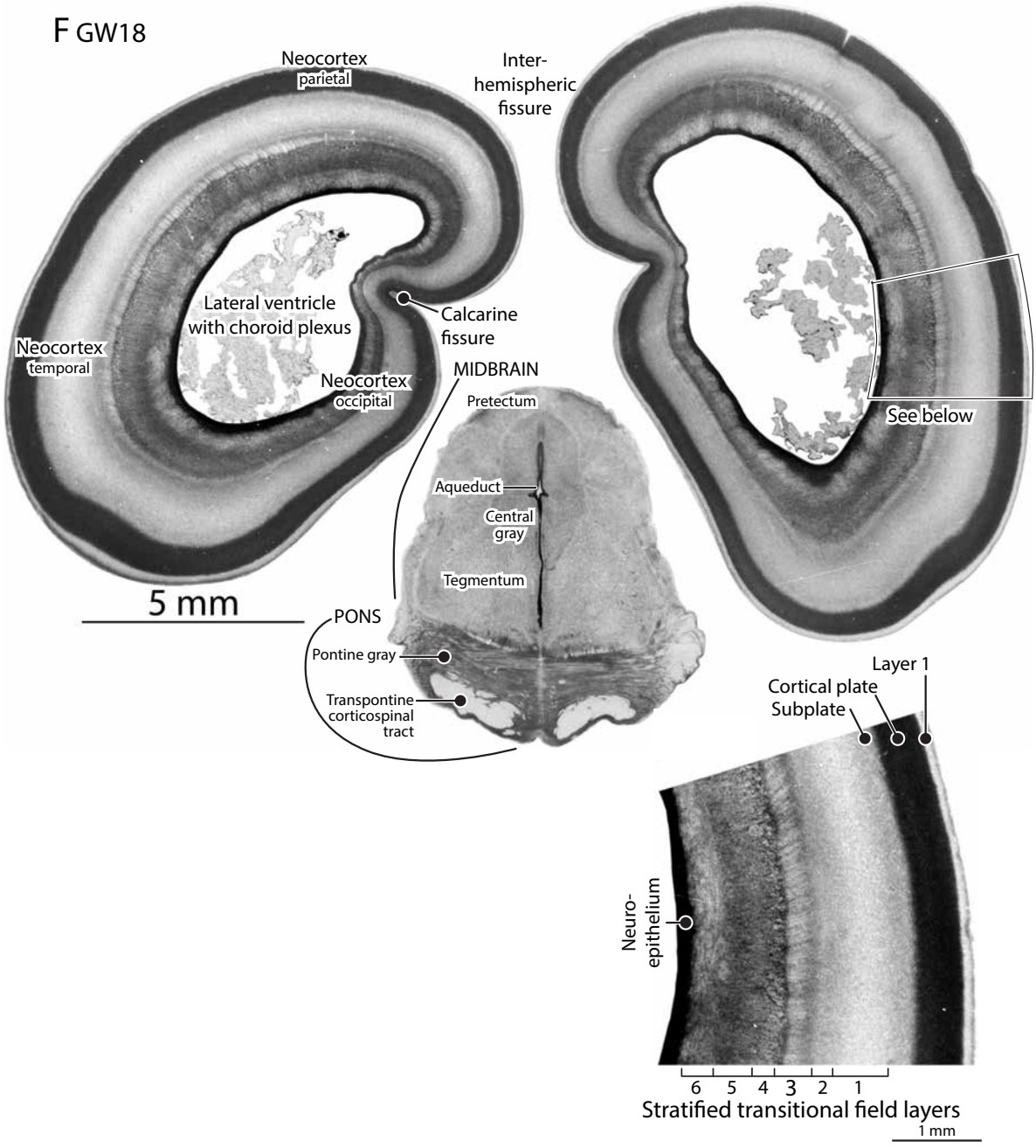
THE BRAINS OF FOUR AND
EARLY FIVE MONTH FETUSES
F GW18
Neocortex
parietal
Inter-
hemispheric
fissure
Lateral ventricle
with choroid plexus
Calcarine
fissure
Neocortex
temporal
Neocortex
occipital
MIDBRAIN
Pretectum
See below
Aqueduct
Central
gray
Tegmentum
5 mm
PONS
Pontine gray
Transpontine
corticospinal
tract
Layer 1
Cortical plate
Subplate
Neuro-
epithelium
6 5 4 3 2 1
Stratified transitional field layers
1 mm

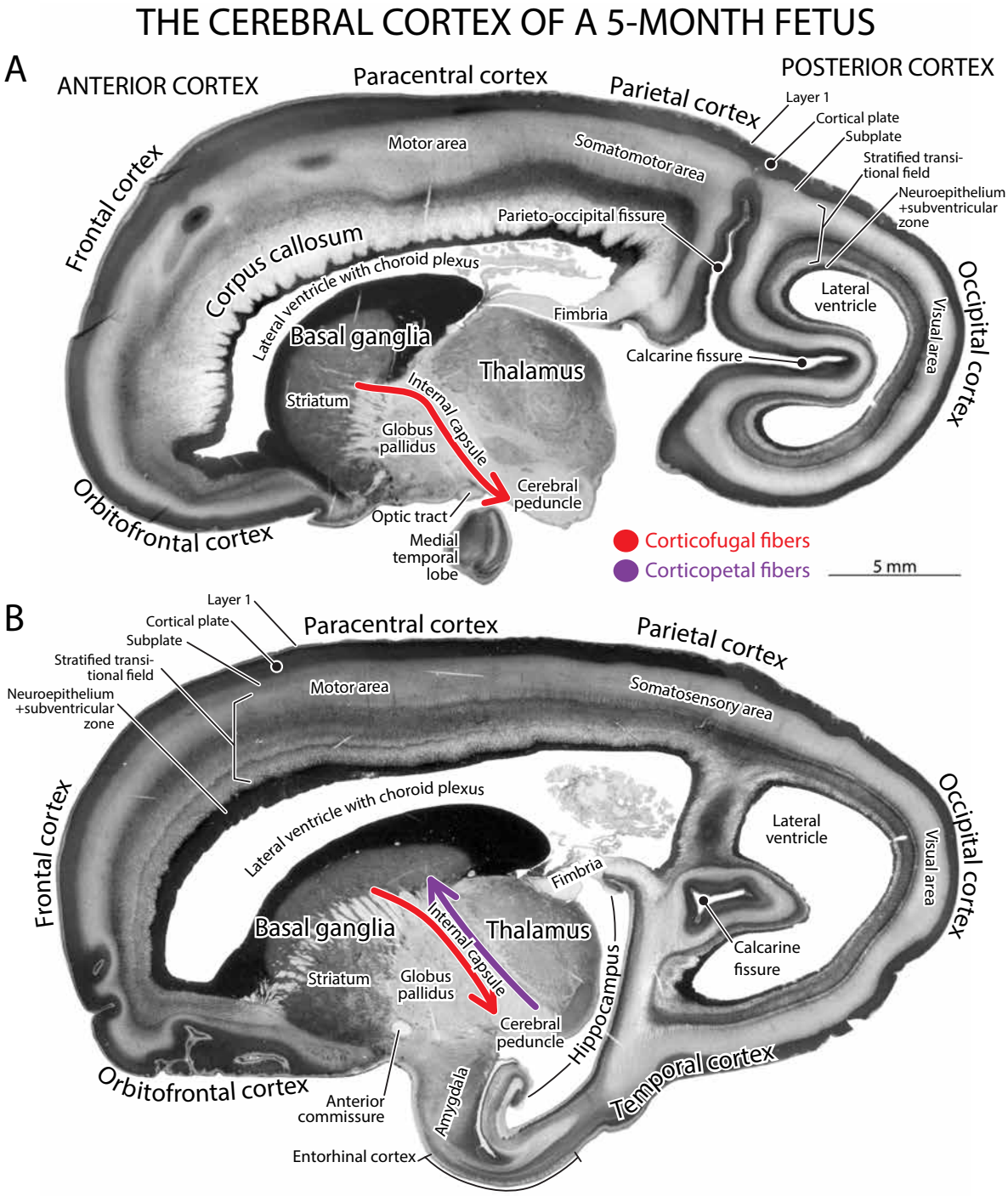

Fig. 20 (facing pages). Parasagittal sections of the brain of a 5 months-old fetus (Y27-60, GW20, CR160 mm) from medial (**A**) to lateral (**D**), showing the organization of the developing neocortex and the stratified transtional field (STF) from anterior to posterior in relation to the descending corticospinal tract (*downward red arrows*) and the ascending thalamocortical radiation (*upward purple arrows*). There is little indication for systematic regional differences in the thickness or cell-packing density of the cortical plate in the different areas (as there is in the mature cortical gray matter). However, there are distinct differences in the configuration of

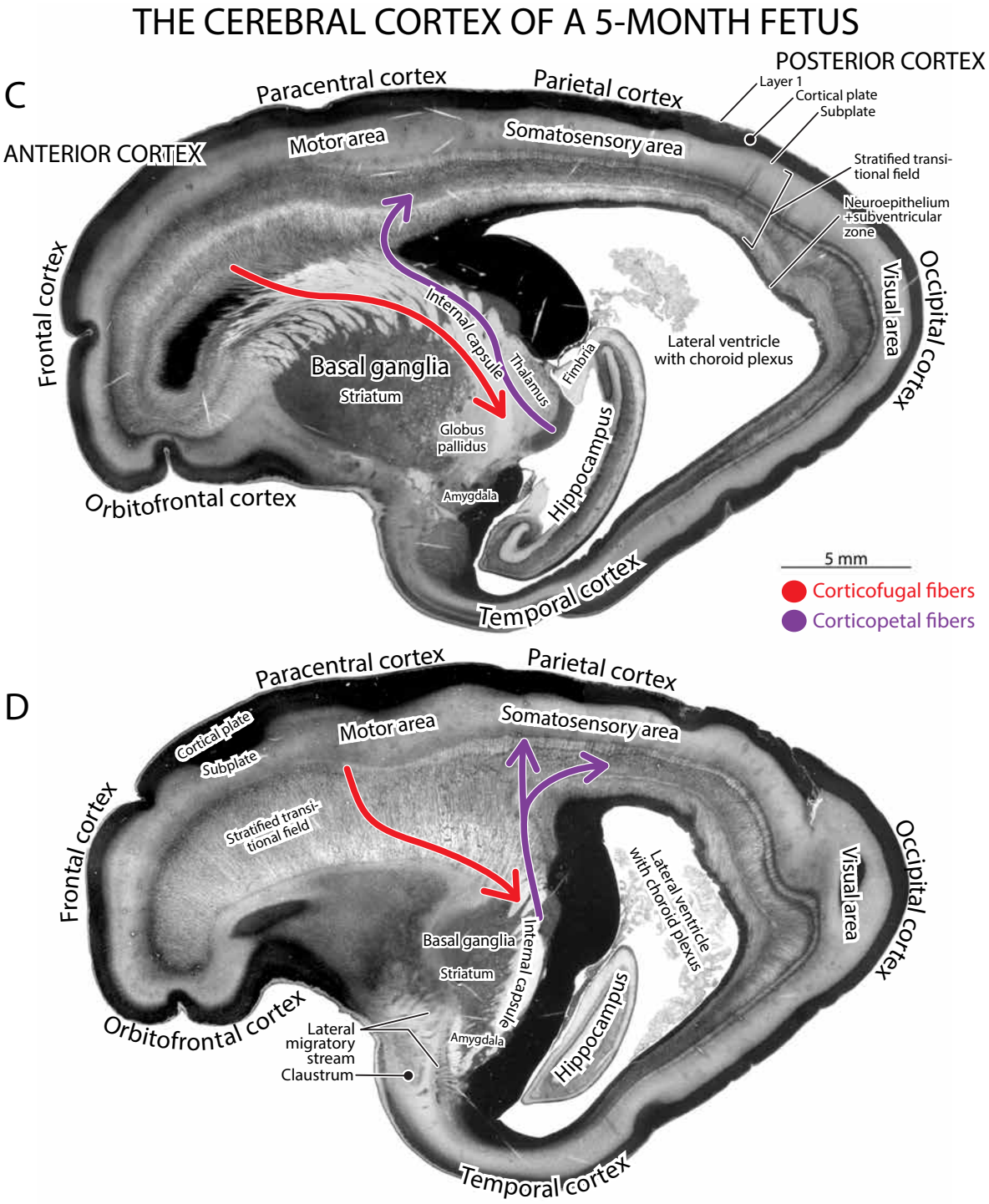

the STF in the different presumptive cortical areas. Most marked is the presence of an STF3 in the posterior (sensory) cortex and its absence in the anterior (motor) cortex. There are differences in STF3 organization in the presumptive somatosensory and parietal cortices, and in the occipital cortex. It is only in the visual occipital cortex that the radially oriented, miniature fibrous columns are sandwiched between two compact cellular layers. A notable feature of this brain is the deepening of the calcarine fissure (**A** and **B**) and the formation of the parieto-occipital fissure most medially (**A**).

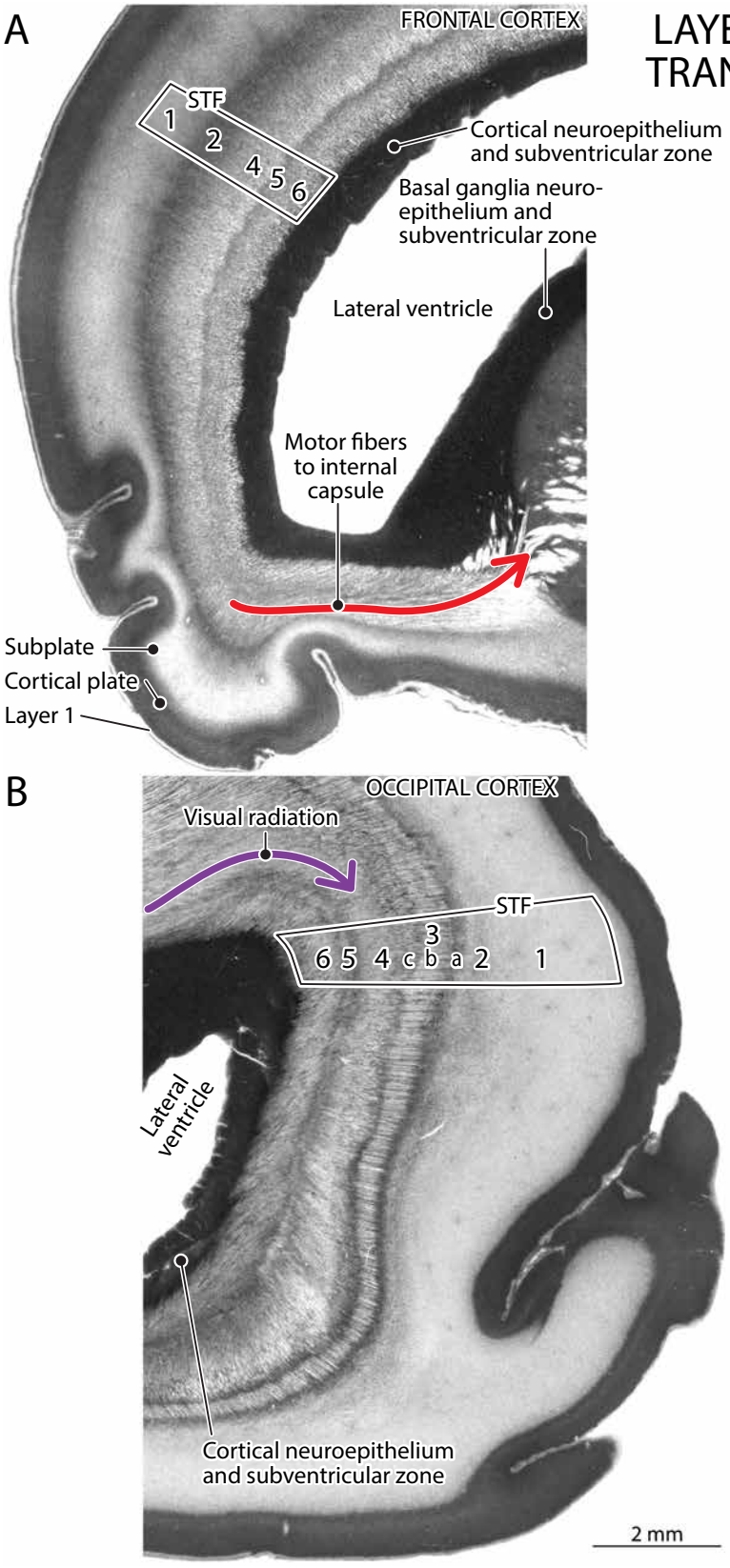

Fig. 21. These higher magnification photomicrographs illustrate the differences between STF organization in the frontal cortex (**A**) and the occipital cortex (**B**) in this 5-months-old fetus (Y27-60, GW20, CR 160 mm). STF3 is absent anteriorly and is prominent posteriorly. STF5 is thinner anteriorly, and STF1, the formative white matter, is less prominent in the frontal cortex than in the occipital cortex, but that difference may simply be due to the cutting angle of the sections rather than actual differences.

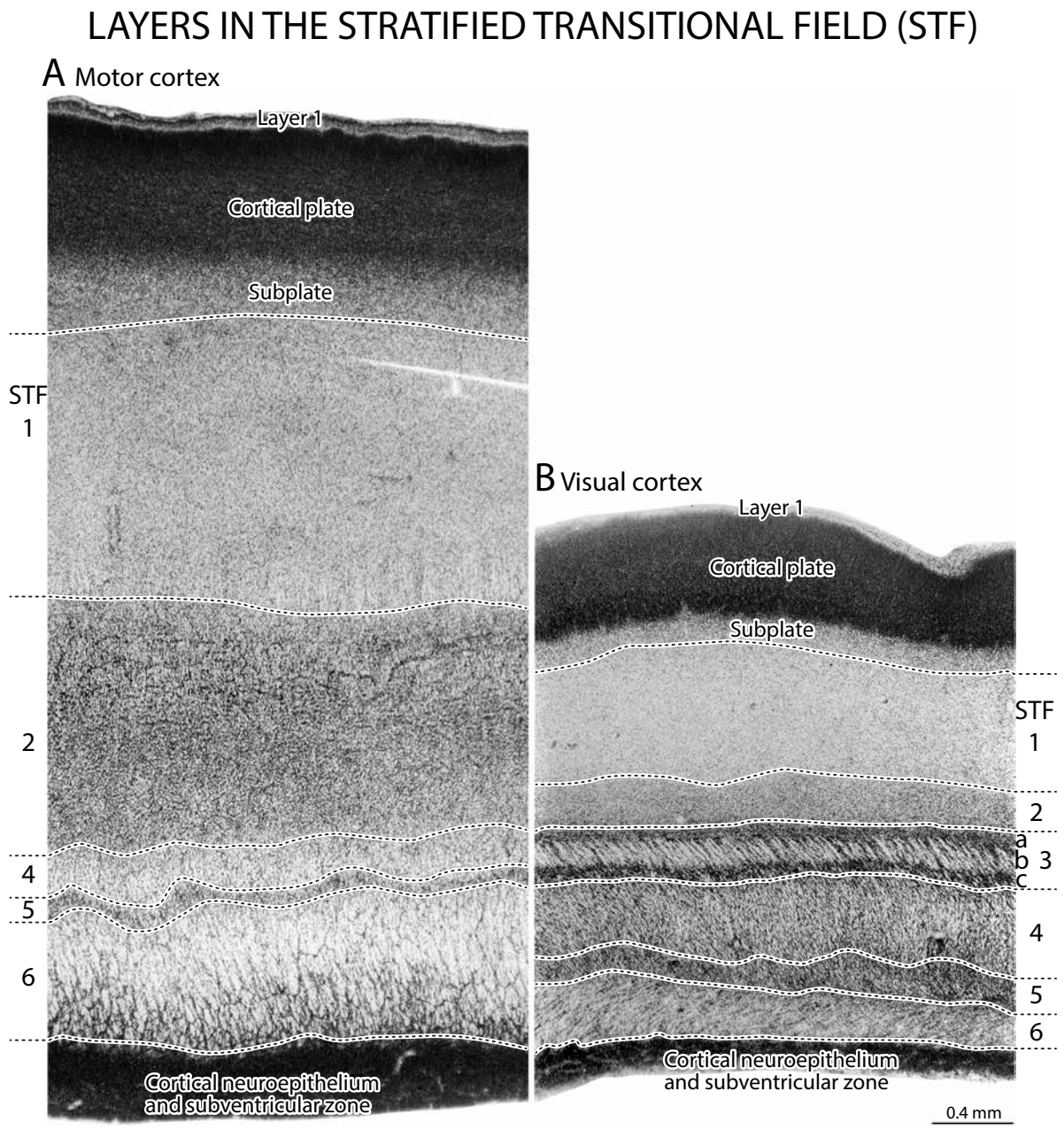

Fig. 22. A comparison of the presumptive motor cortex (**A**) and visual cortex (**B**) in the preceding 5 months-old fetus at higher magnification. Both areas show an indistinct layer of diffuse cells beneath the cortical plate (the subplate), but the thicker cortical plate in the motor cortex compared to visual cortex may be due to differences in cutting angles. But most important and most pronounced are the differences in STF lamination patterns between the two areas. STF1 (the formative white matter) and STF2 (the zone of migrating neurons) are much thicker in the motor cortex that in the visual cortex. The trilaminar STF3, the distinctive feature of the occipital lobe and sensory cortex, is absent in the motor cortex. The greater concentration of fibers in STF4 and cells STF5 in the visual cortex may indicate the later maturation of the visual cortex compared to motor cortex.

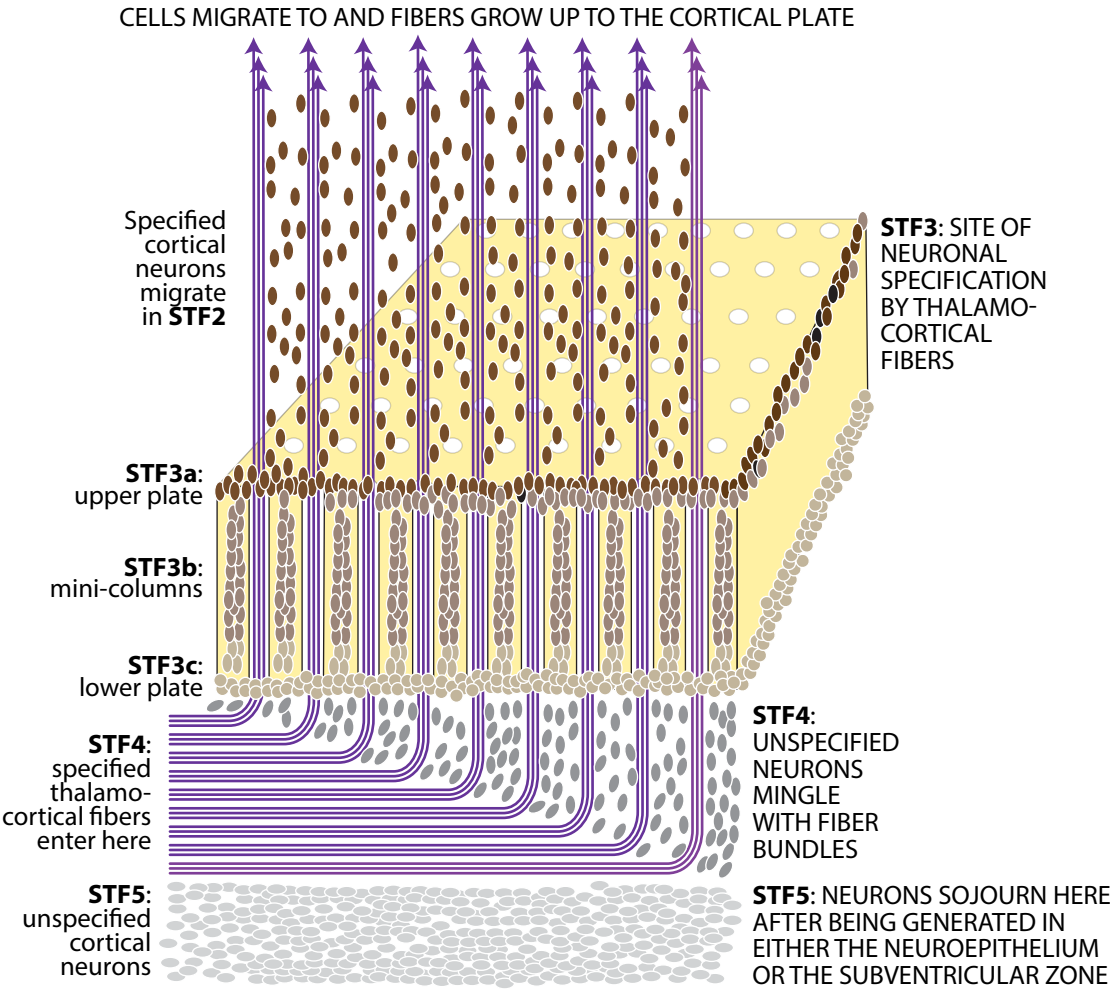

Fig. 23. A diagram of the organization and hypothetical function of STF3 in the developing visual cortex. The two horizontal cell-dense bands (STF3a and STF3c) form an upper plate and a lower plate parallel to the cortical surface, with vertical minicolumns of cells and fibers between them (STF3b). We postulate that the segregated fiber bundles from the lateral geniculate nucleus (in STF4) carry specific information, such as, location of retinal origin, on-center or off-center excitability, etc., and that these fibers interact with the nonspecified neurons moving out of STF5 into STF3. As neurons migrate through STF3c, STF3b, STF3a, they intermingle with the thalamic fibers and enter STF2 as specified neurons, possibly migrating to specific regions in the cortical plate with their associated fibers.

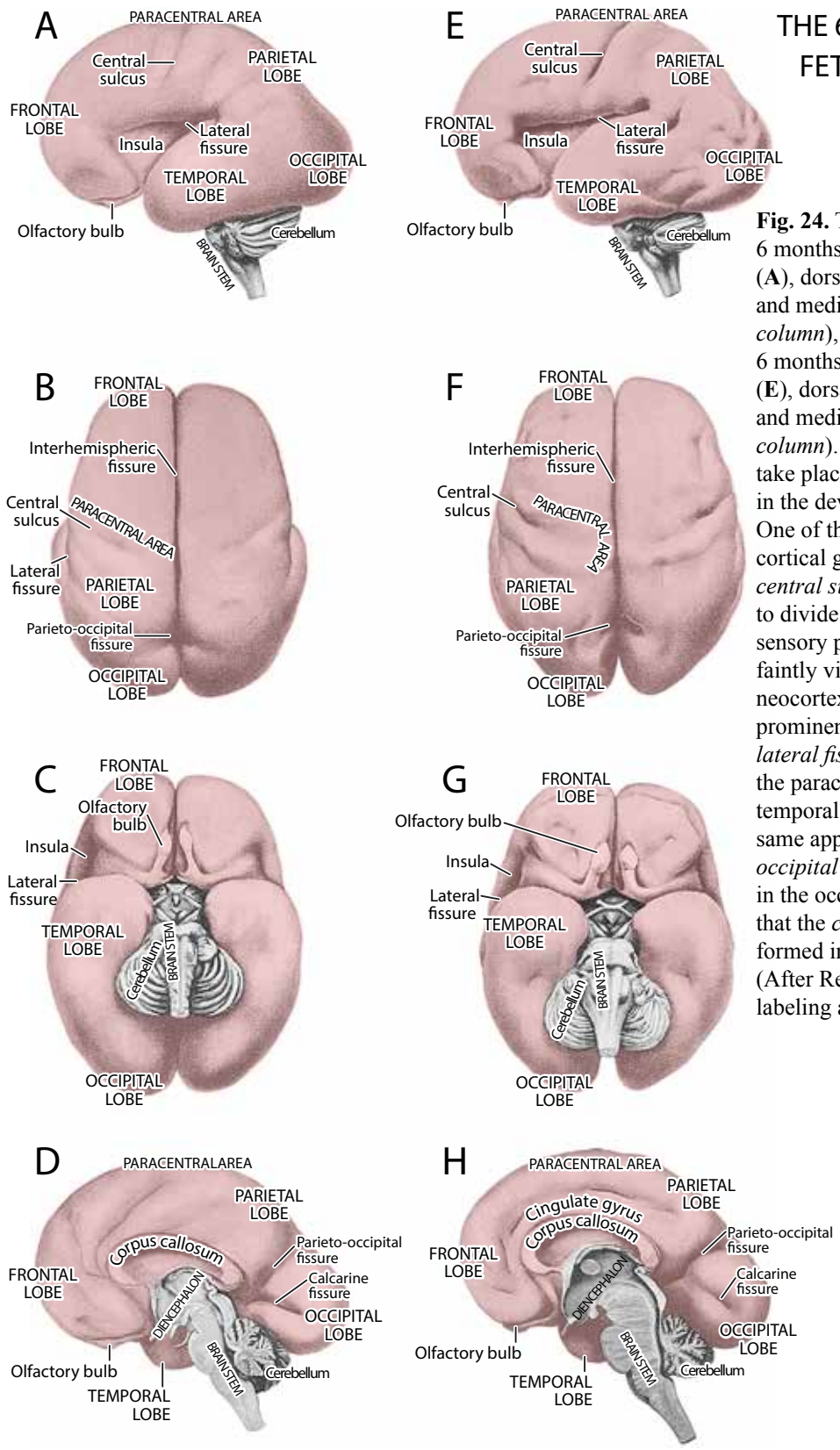

THE 6-MONTHS-OLD FETAL NEOCORTEX

Fig. 24. The brain of a younger 6 months-old fetus in lateral (**A**), dorsal (**B**), ventral (**C**) and medial (**D**) view (*left column*), The brain of an older 6 months-old fetus in lateral (**E**), dorsal (**F**), ventral (**G**) and medial (**H**) view (*right column*). Several changes take place during this period in the developing neocortex. One of them is the onset of cortical gyrification. The *central sulcus*, which comes to divide the motor and sensory projection areas, is faintly visible in the younger neocortex and becomes prominent in the older. The *lateral fissure* that divides the paracentral area from the temporal lobe expands, and the same applies to the *parieto-occipital* and *calcarine fissures* in the occipital lobe. Note also that the *cingulate gyrus* is well formed in the older fetus (**H**). (After Retzius, 1896; color and labeling added).

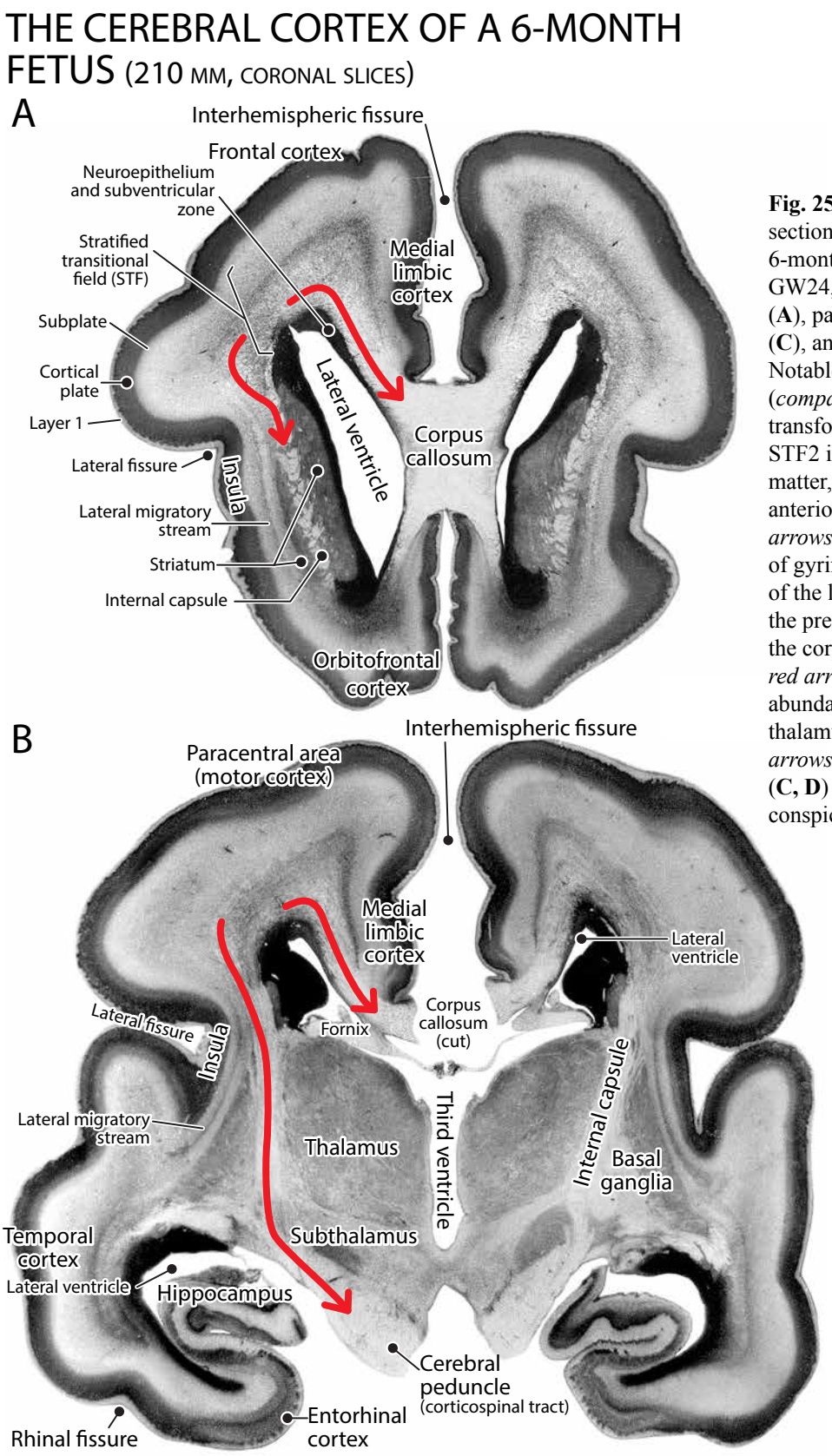

Fig. 25 (facing pages). Coronal sections of the brain in a 6-months-old fetus (Y94-62; GW24, CR, 210 mm) at frontal (**A**), paracentral (**B**), parietal (**C**), and occipital (**D**) levels. Notable developmental changes (*compare with* **Fig. 19**) are the transformation of STF1 and STF2 into a thick layer of white matter, more fibers leaving the anterior cortex (*outward red arrows* in **A** and **B**), the onset of gyrification, the shrinkage of the lateral ventricles, and the presence of more fibers in the corpus callosum (*inward red arrows*, **A, B, C**). **C** shows abundant fibers between the thalamus and cortex (*purple arrows*). STF3 is still present (**C, D**) but is becoming less conspicuous.

THE CEREBRAL CORTEX OF A 6-MONTH FETUS (210 MM, CORONAL SLICES)

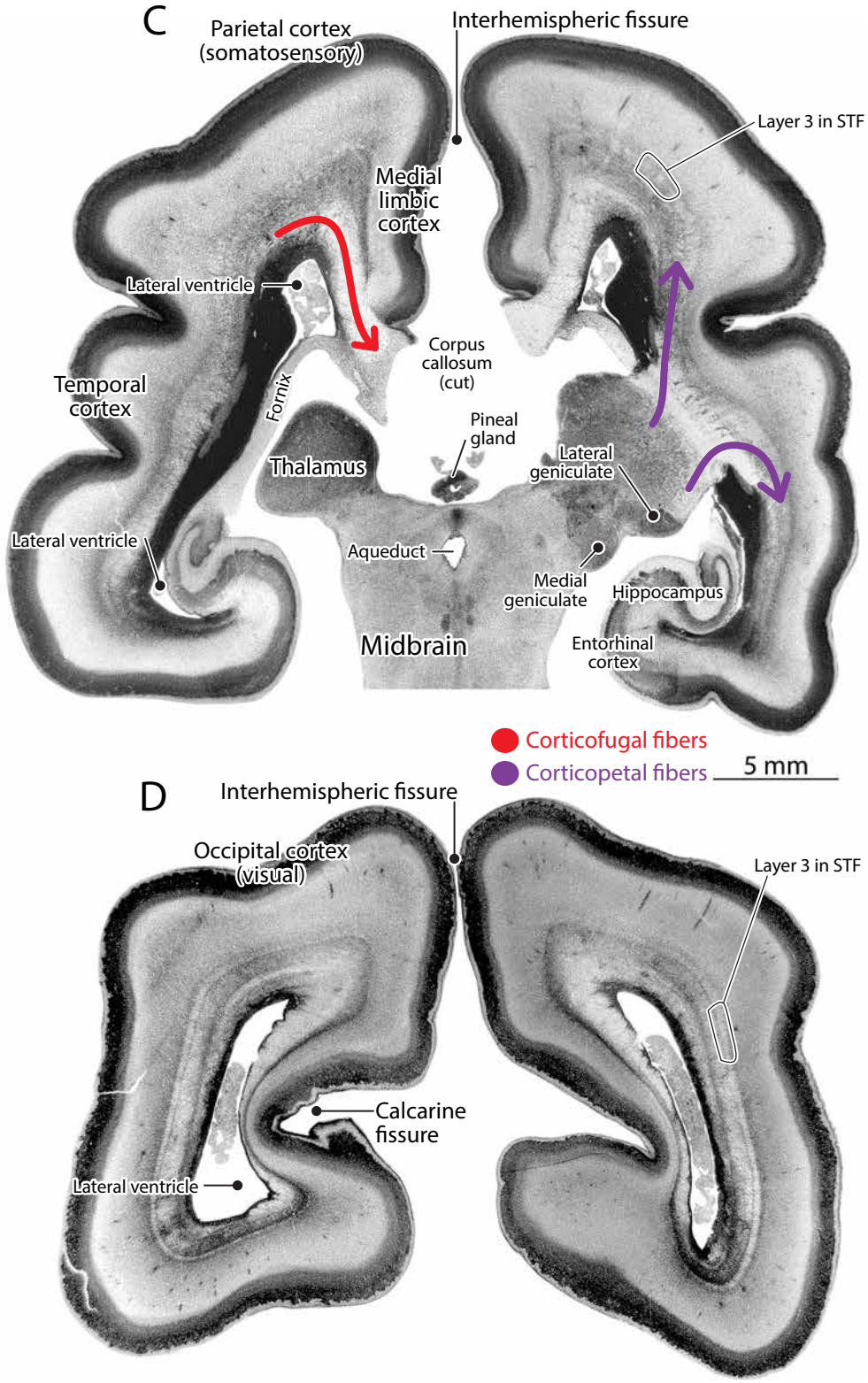

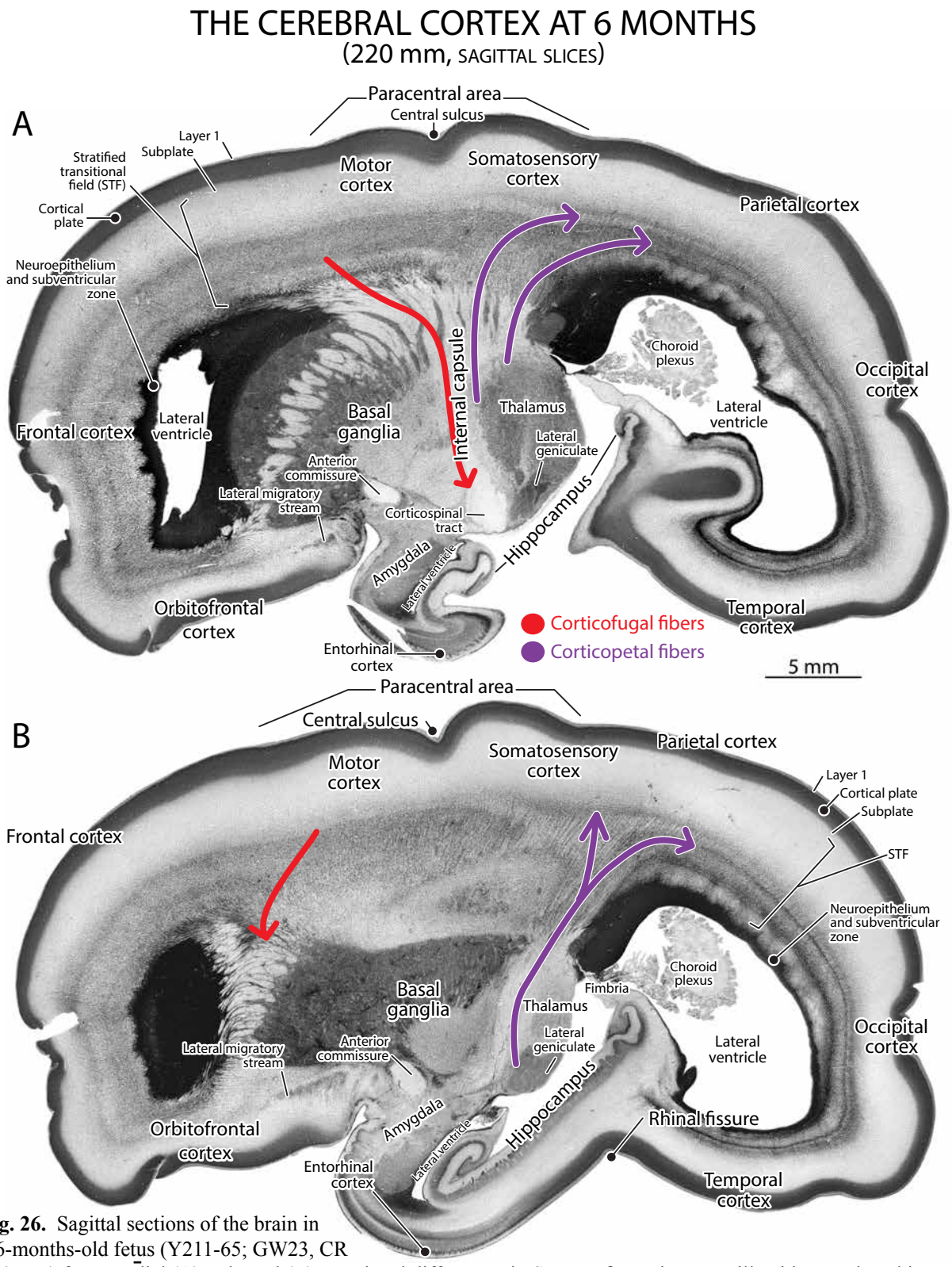

Fig. 26. Sagittal sections of the brain in a 6-months-old fetus (Y211-65; GW23, CR 220 mm) from medial (**A**) to lateral (**B**). Regional differences in STF configuration are still evident as the white matter (STF1) widens considerably, some gyri are beginning to form, and the lateral ventricle shrinks (*compare with* **Fig. 20**). There are indications for the separation of ascending thalamocortical fibers (*upward purple arrows*) posteriorly from the descending corticofugal fibers anteriorly (*downward red arrows*).

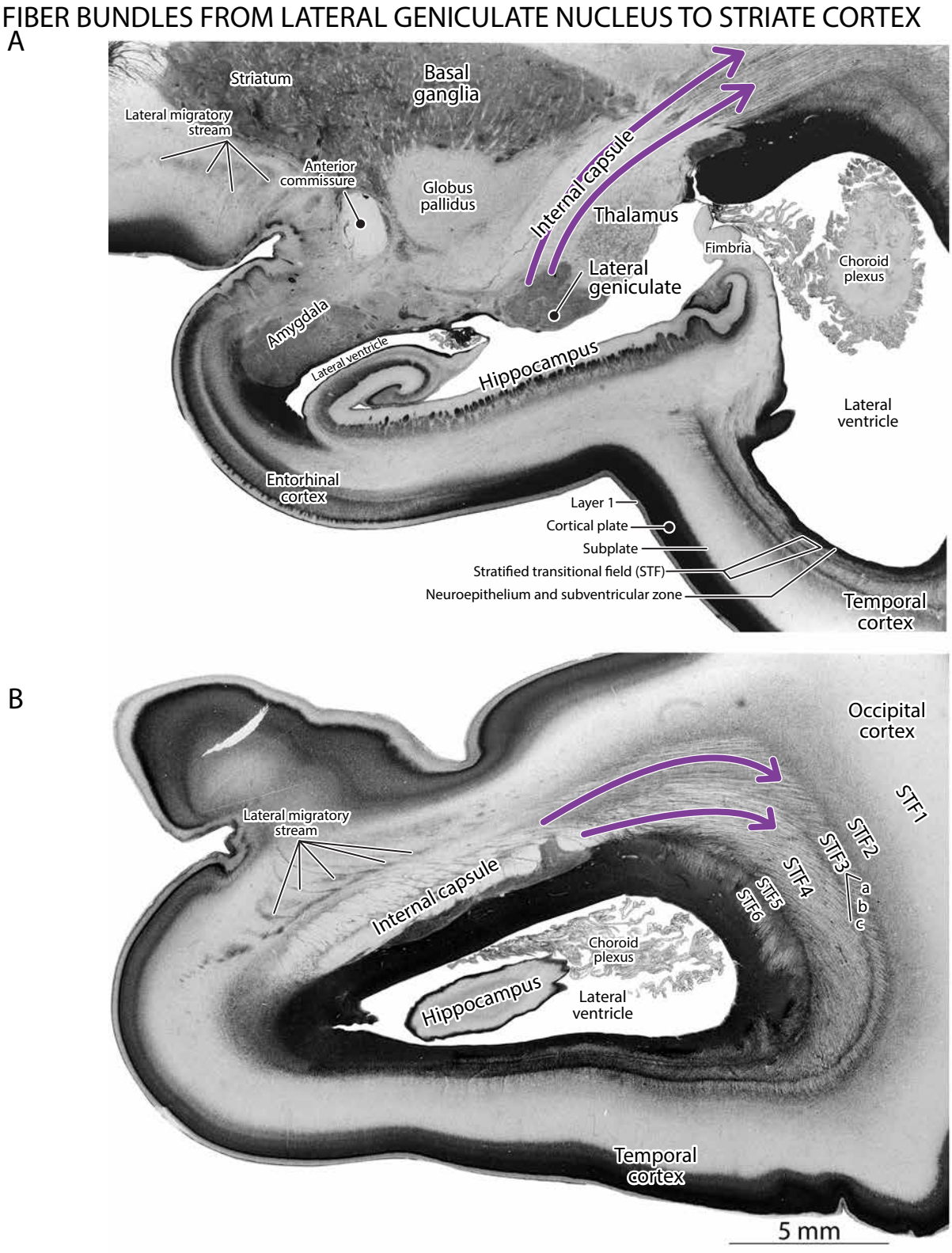

Fig. 27. Two farther lateral sagittal sections from the preceding 6 months-old fetus (Y211-65) at higher magnification, showing visual radiation fibers (*purple arrows*) leaving the dorsal lateral geniculate nucleus (**A)** and terminating in STF4 and STF3 of the occipital cortex (**B)**. The beginning transformation of the choroid plexus can be seen from the early spongy type in **A** to the more mature chain-like configuration in **B**.

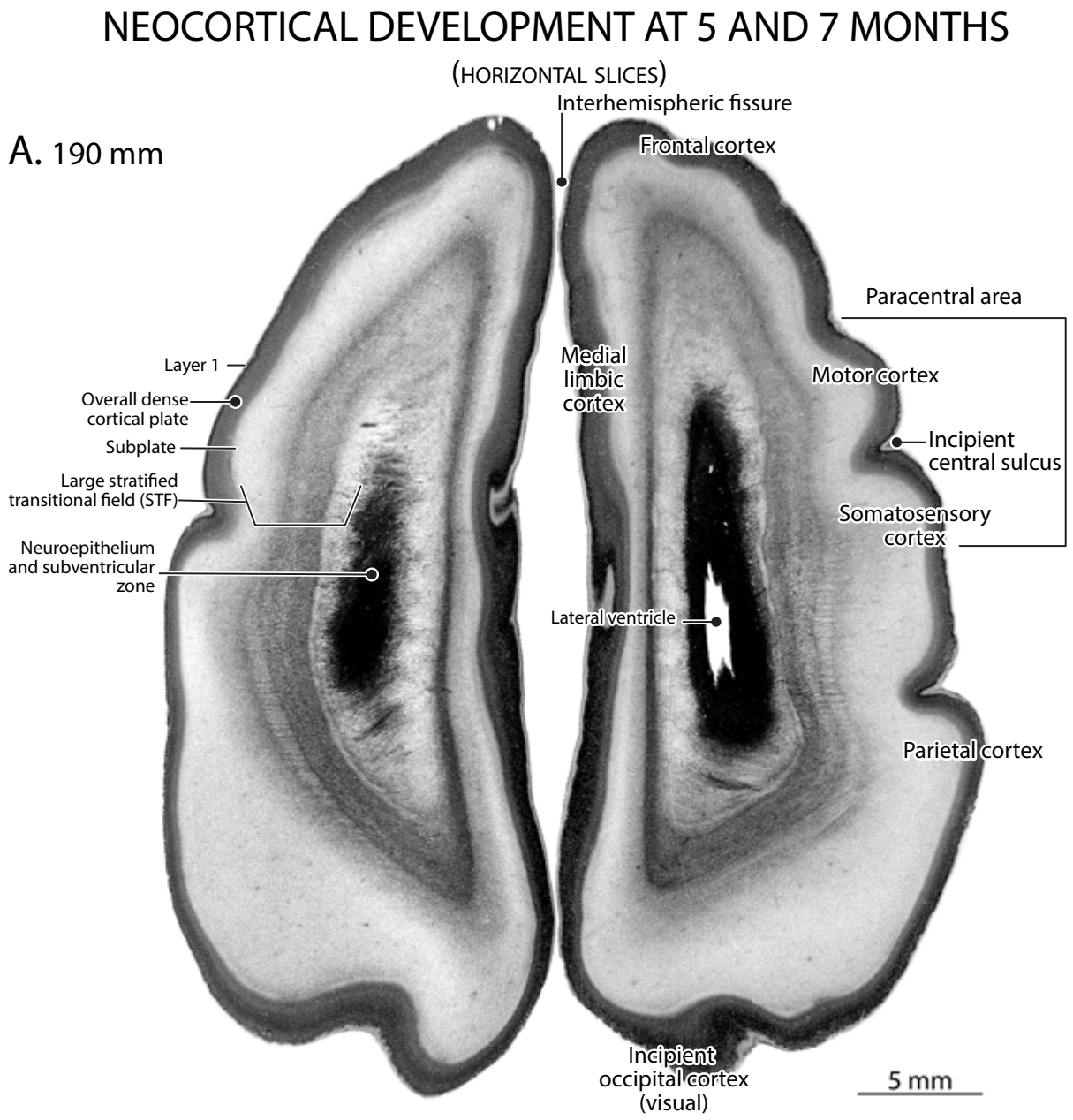

Fig. 28 (On these 2 pages and the following 6 pages). Changes in neocortical development are illustrated in a comparison of a series of matched horizontal brain sections, from dorsal to ventral, in a 5 months-old fetus (Y197-65, GW23, CR 190 mm) and a young third trimester, 7 months-old fetus, (Y16-59, GW26, CR 235 mm). **A** and **B**. In this dorsal pair of sections slicing through the paracentral area the following developmental changes are evident: The STF is prominent in the younger fetus but is in the process of dissolution in the older fetus. The depth and expanse of the white matter has increased in the older fetus. The uniformly cell-dense cortical plate seen in the younger fetus has changed into a laminated one (superficial and central cell dense bands) in the older fetus. Finally, there is a considerable increase in number and depth of the gyri in the older fetus.

NEOCORTICAL DEVELOPMENT AT 5 AND 7 MONTHS

(HORIZONTAL SLICES)

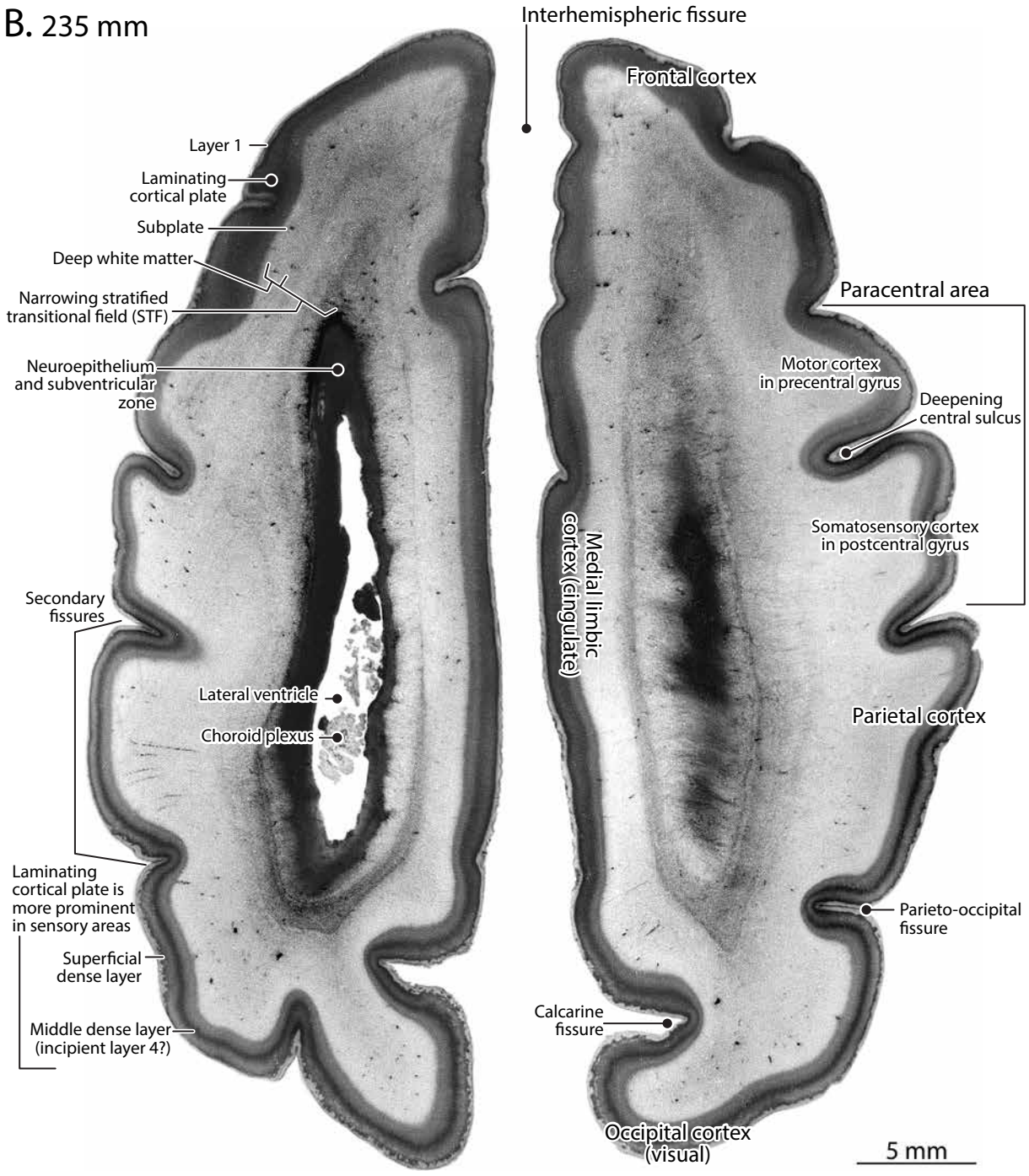

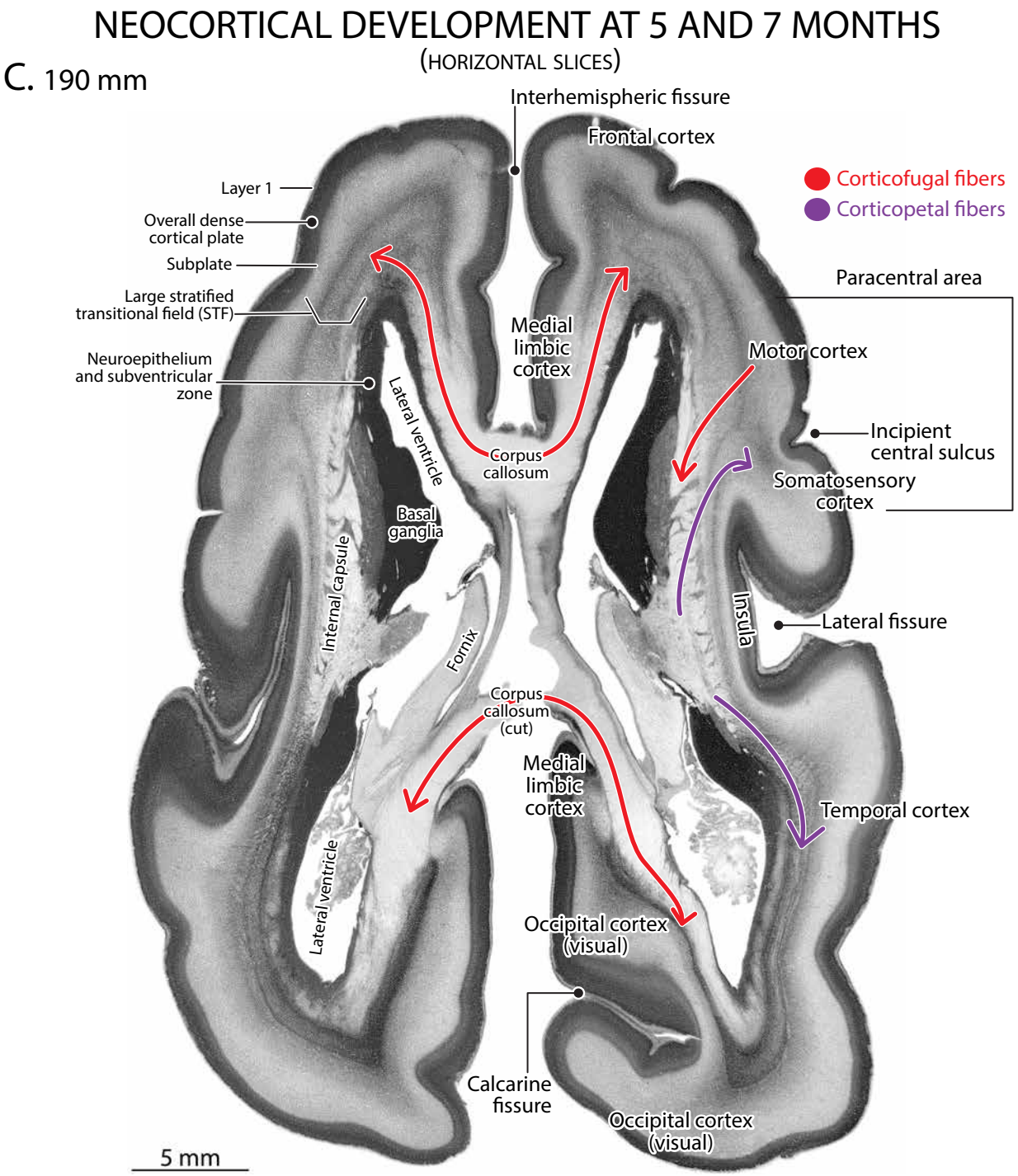

Fig. 28 C and D. The same changes seen in **A** and **B** are evident at lower horizontal levels that transect the basal ganglia. More fibers are present at this level. *Red arrows* indicate cortical fibers crossing in the corpus callosum or entering the internal capsule. *Purple arrows* are postulated thalamic fibers flowing out of the internal capsule to enter the anterior and posterior cortex in STF4.

NEOCORTICAL DEVELOPMENT AT 5 AND 7 MONTHS

(HORIZONTAL SLICES)

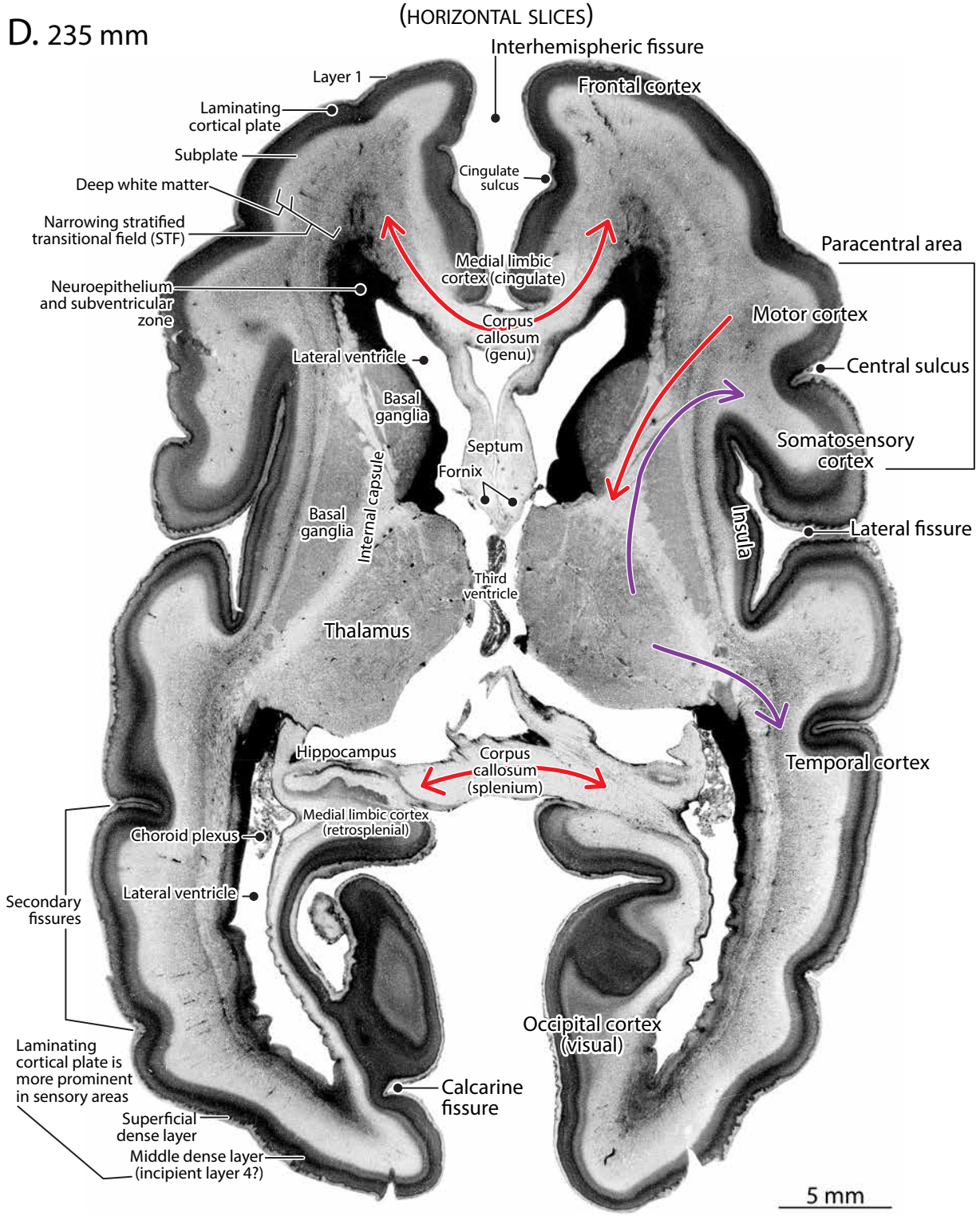

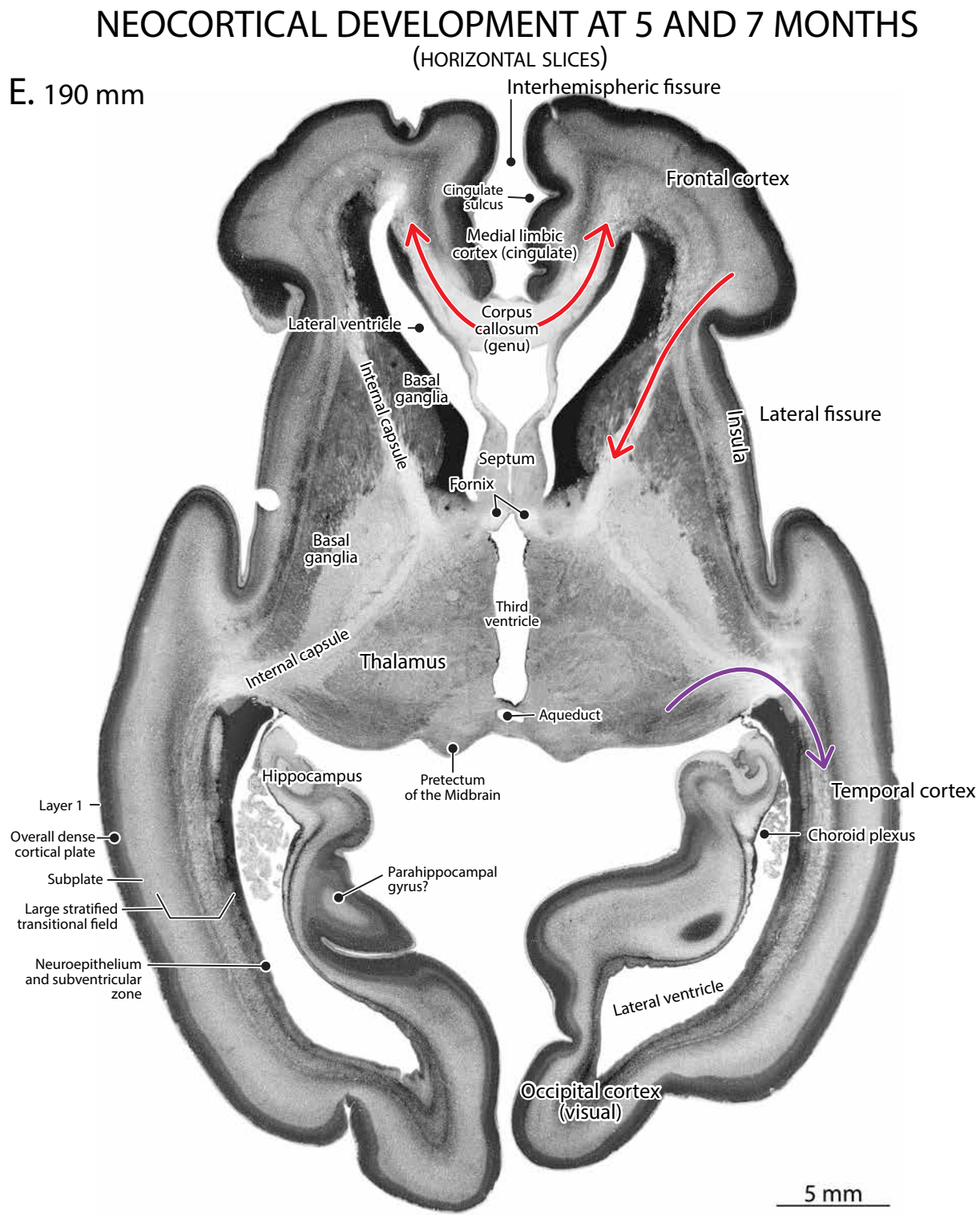

Fig. 28 E and F. The same changes seen in the preceding levels are evident at lower horizontal levels that transect the thalamus. *Colored arrows* indicate the postulated trajectory of fibers to (*purple*) and from (*red*) the cortex.

NEOCORTICAL DEVELOPMENT AT 5 AND 7 MONTHS

(HORIZONTAL SLICES)

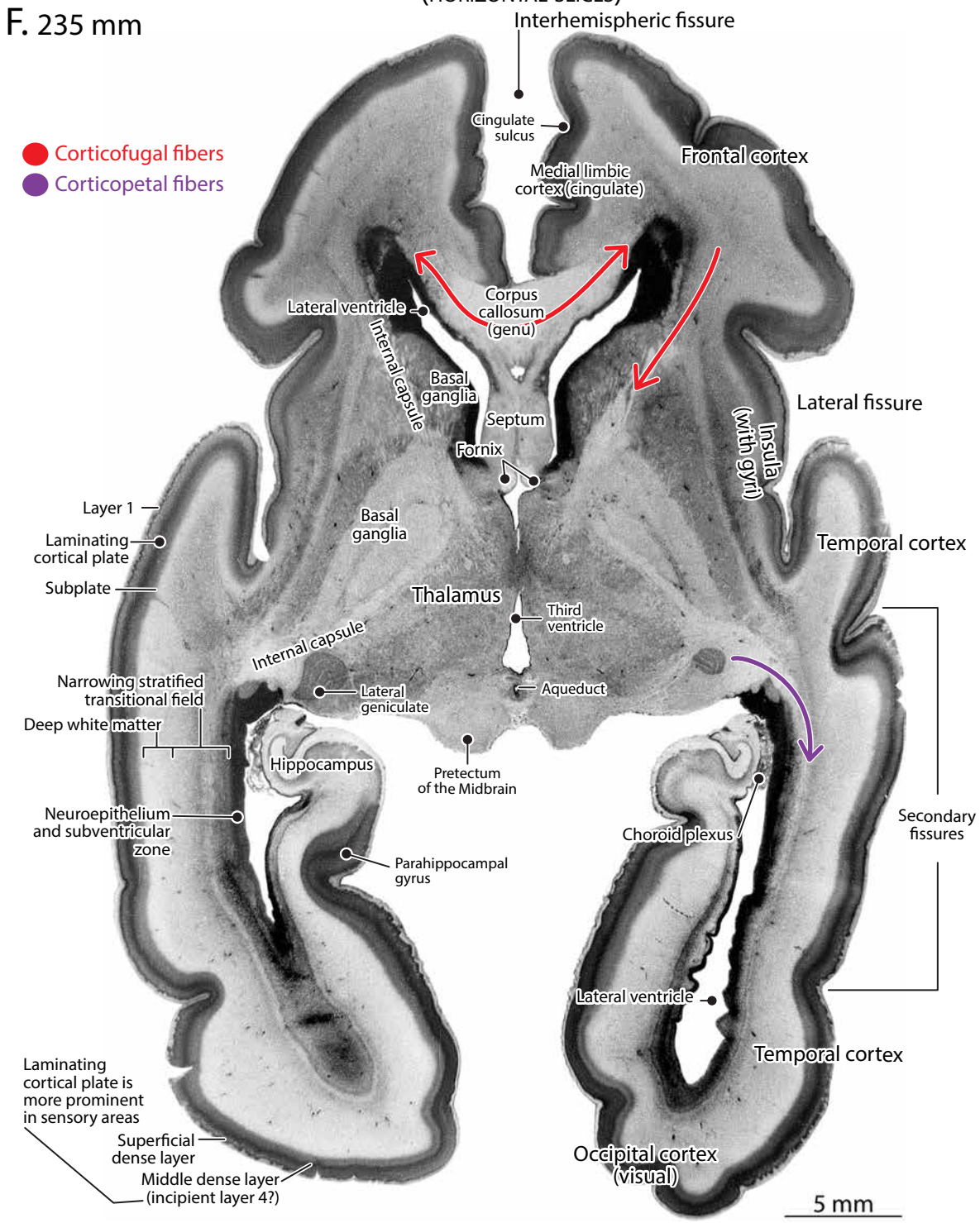

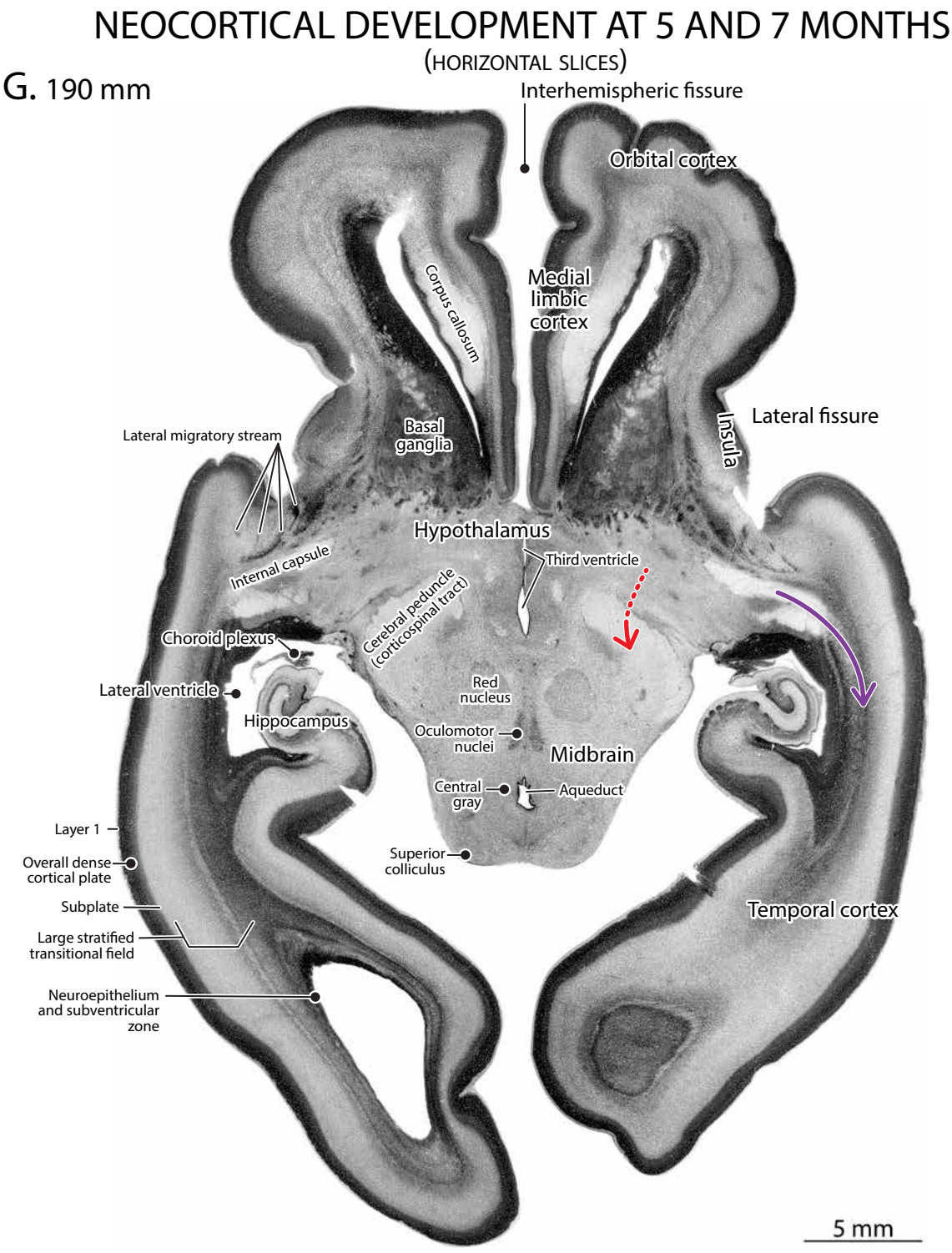

Fig. 28 G and H. The same changes seen in the preceding levels are evident at lower horizontal levels that transect the midbrain. Note that at all levels of the older specimen (**B, D, F,** and **H**), the *deep white matter* tends to be thinner in the depths of the developing fissures—an important point that we will emphasize later.

NEOCORTICAL DEVELOPMENT AT 5 AND 7 MONTHS

(HORIZONTAL SLICES)

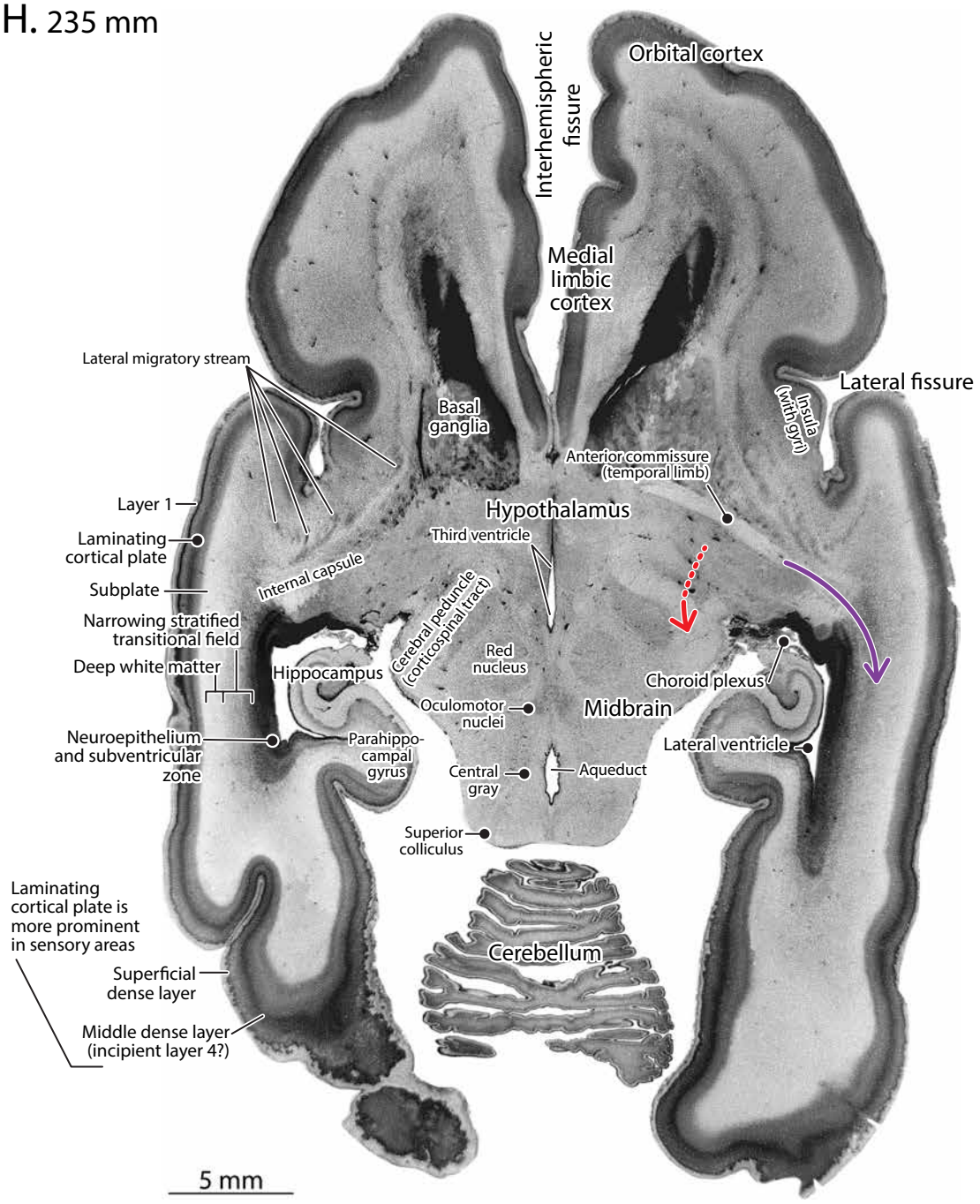

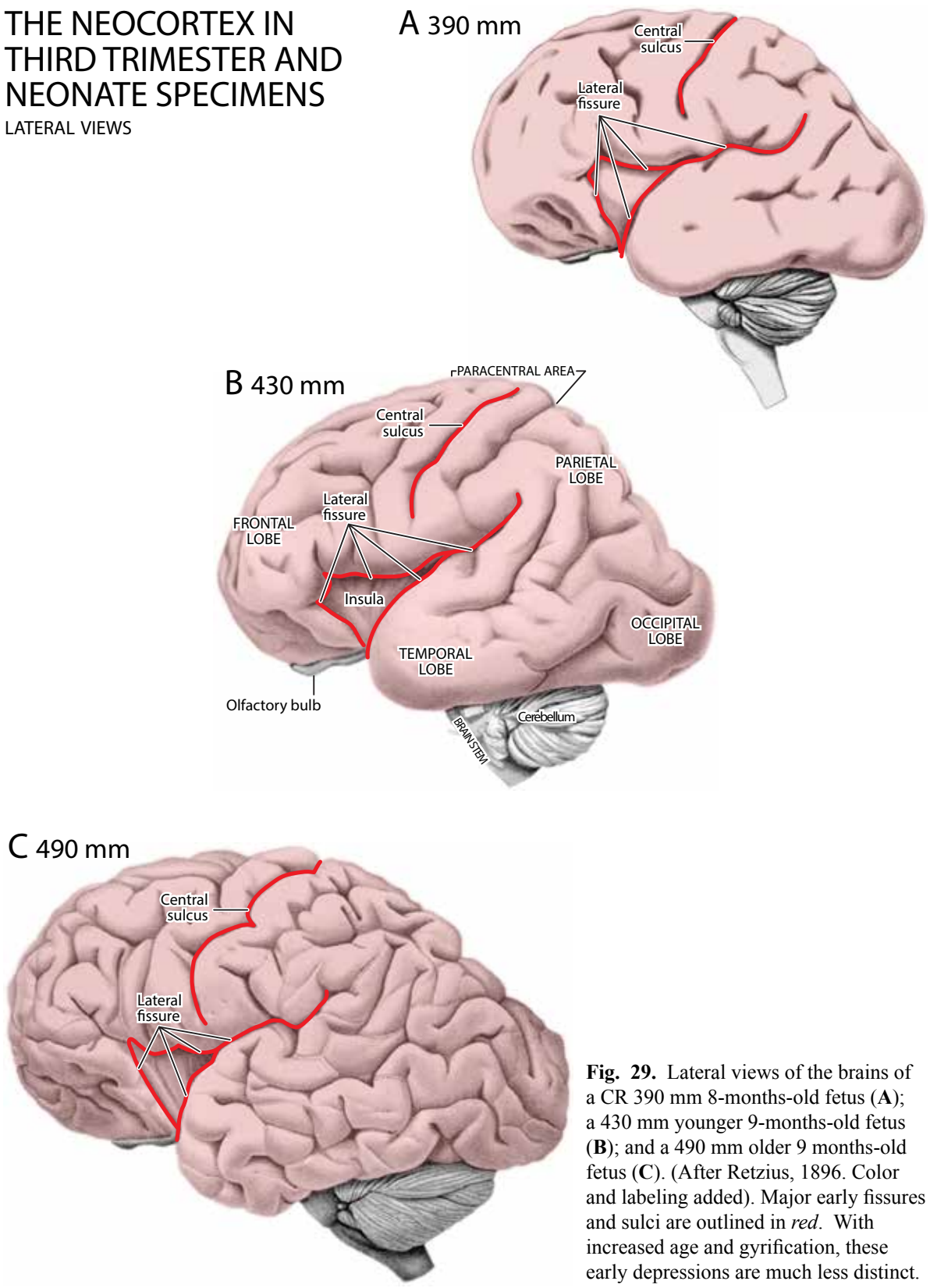

Fig. 29. Lateral views of the brains of a CR 390 mm 8-months-old fetus (**A**); a 430 mm younger 9-months-old fetus (**B**); and a 490 mm older 9 months-old fetus (**C**). (After Retzius, 1896. Color and labeling added). Major early fissures and sulci are outlined in *red*. With increased age and gyrification, these early depressions are much less distinct.

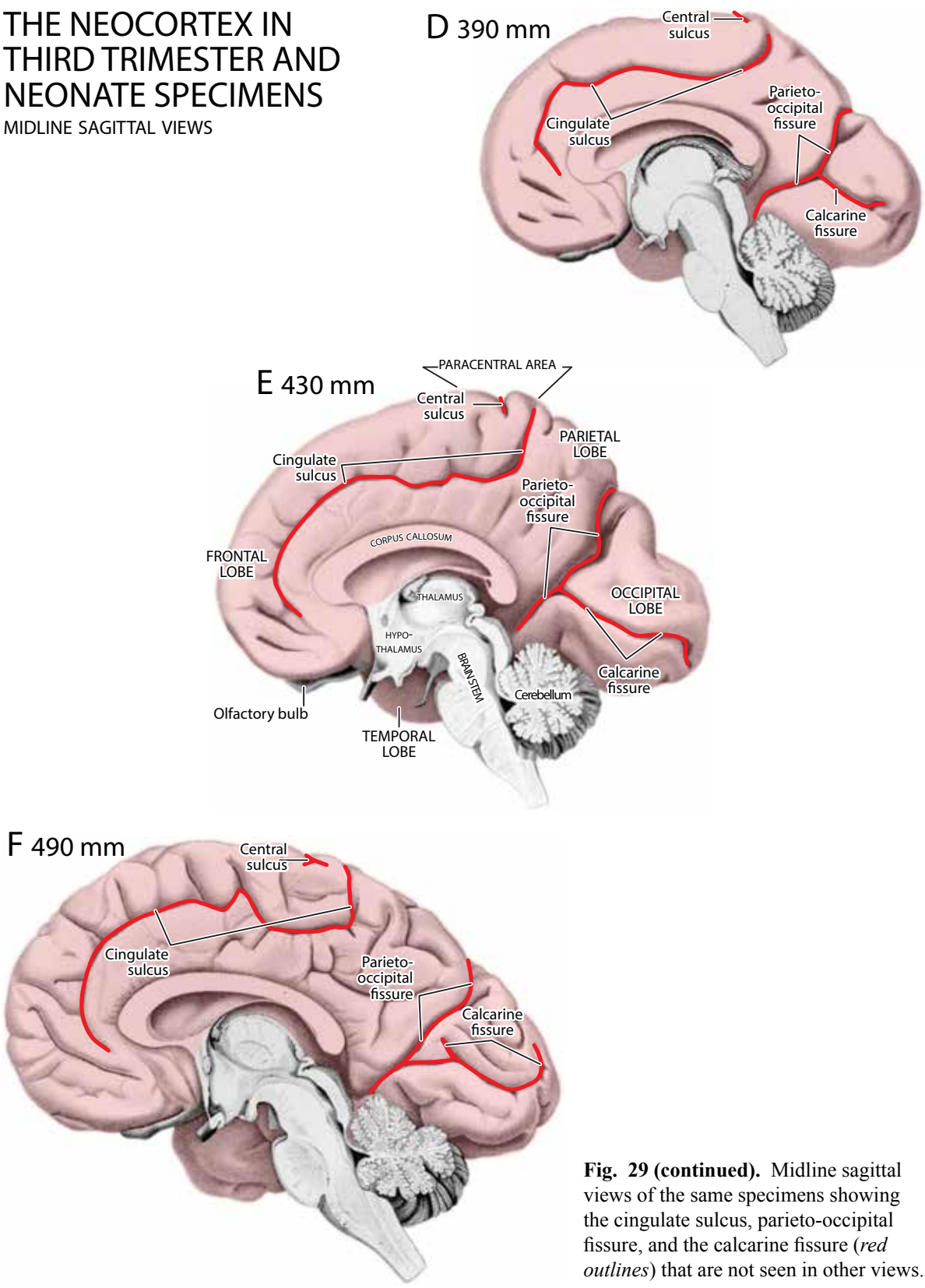

Fig. 29 (continued). Midline sagittal views of the same specimens showing the cingulate sulcus, parieto-occipital fissure, and the calcarine fissure (*red outlines*) that are not seen in other views.

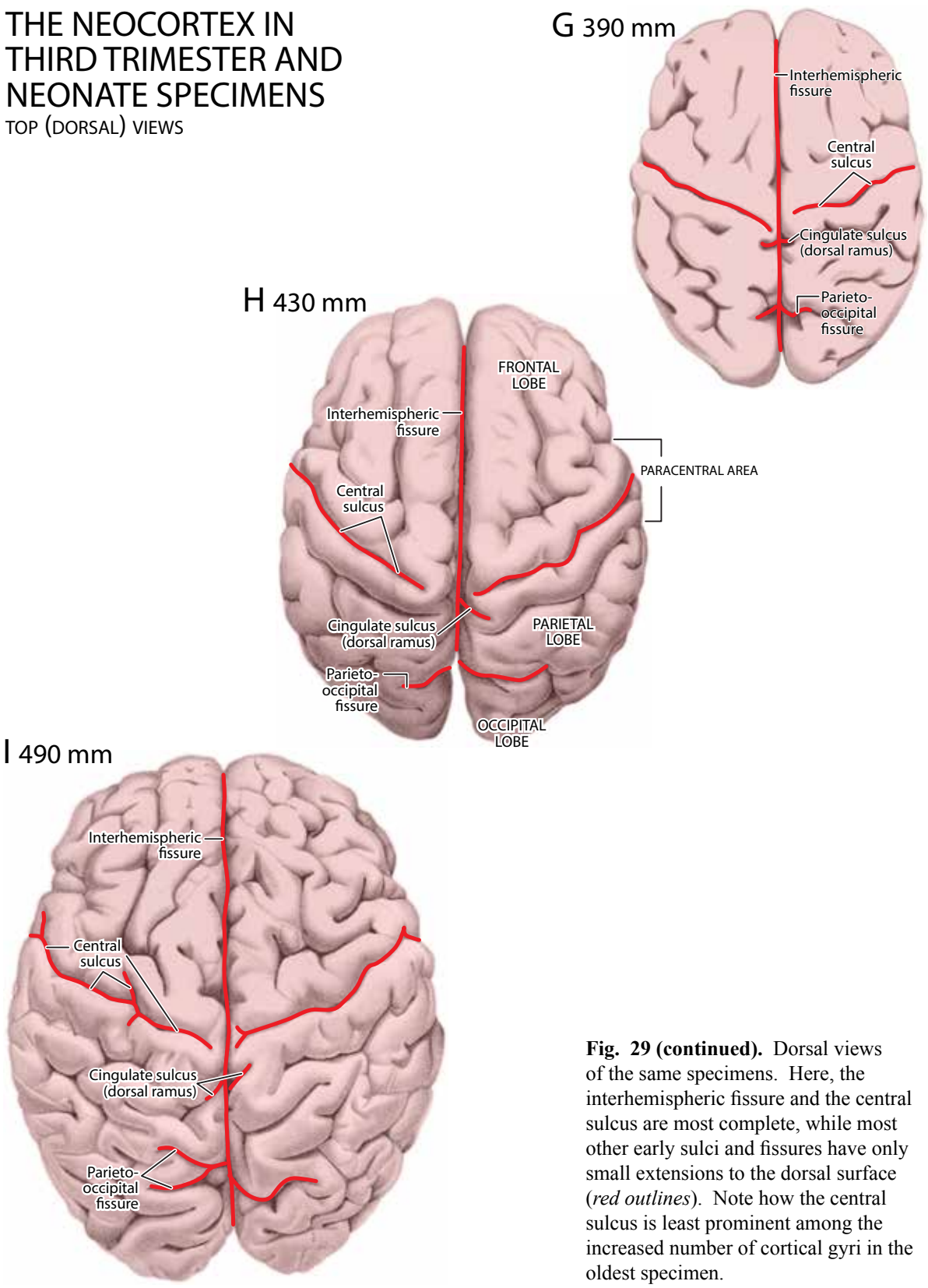

Fig. 29 (continued). Dorsal views of the same specimens. Here, the interhemispheric fissure and the central sulcus are most complete, while most other early sulci and fissures have only small extensions to the dorsal surface (*red outlines*). Note how the central sulcus is least prominent among the increased number of cortical gyri in the oldest specimen.

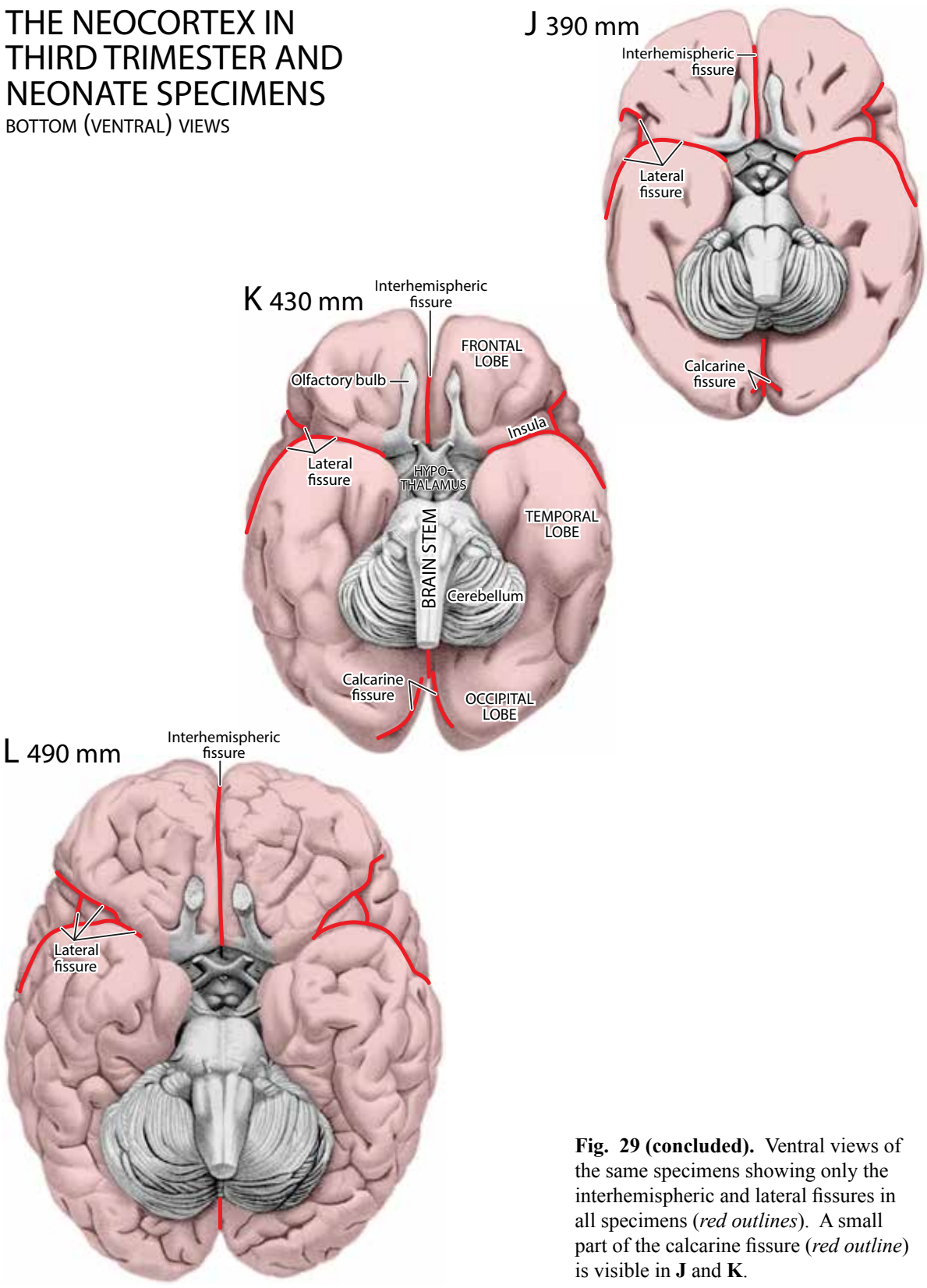

Fig. 29 (concluded). Ventral views of the same specimens showing only the interhemispheric and lateral fissures in all specimens (*red outlines*). A small part of the calcarine fissure (*red outline*) is visible in **J** and **K**.

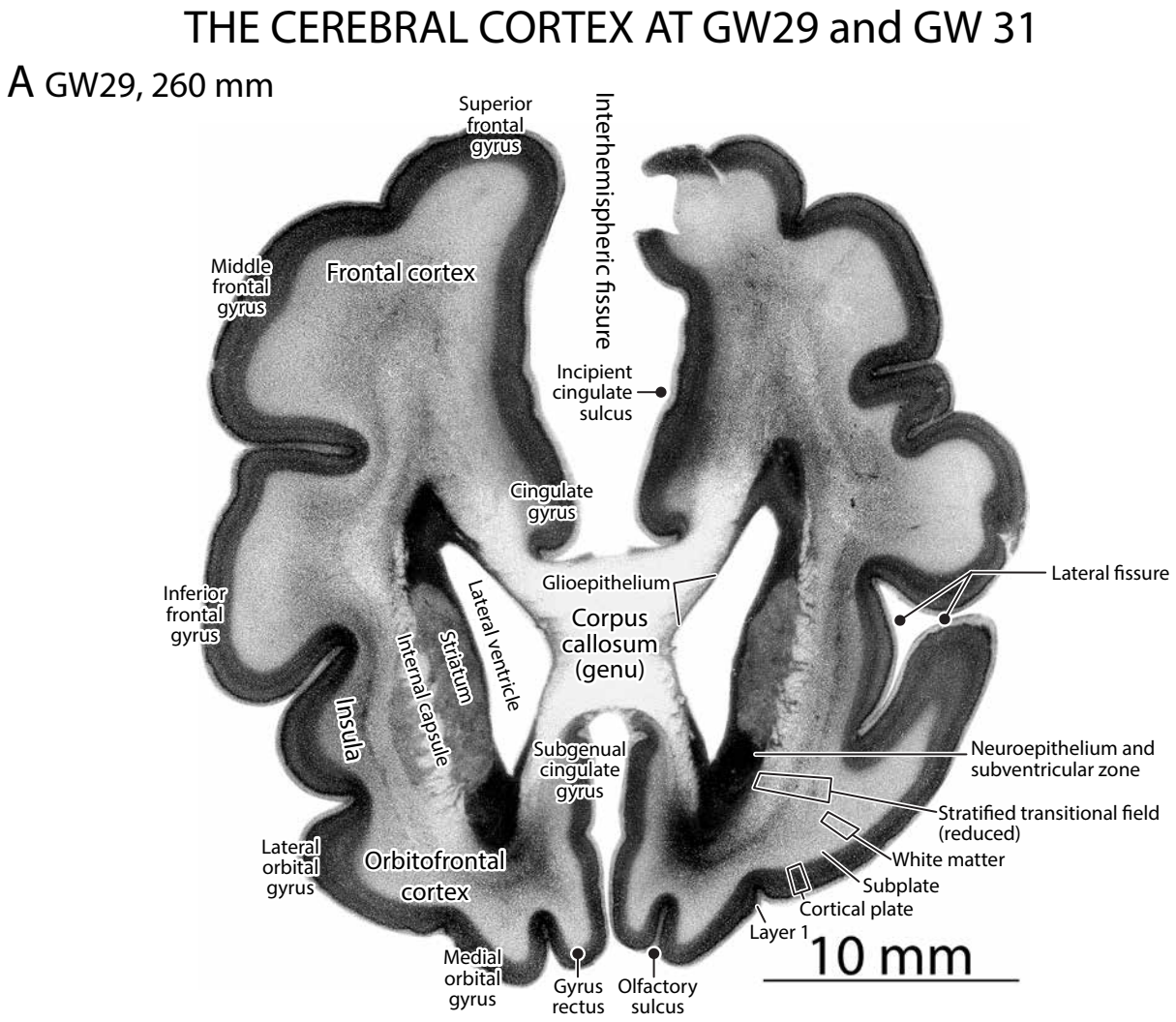

Fig. 30 (on this, and the following 5 pages. Neocortical development as seen in three sets of coronal sections from anterior to posterior in a younger third trimester fetus (GW29, Y14-59, CR 260 mm), and an older third trimester fetus (GW31, Y13-59, CR 295 mm). In these anterior sections that transect the frontal lobe, the major developmental changes in the older fetus (**B**) are the expansion of the white matter, an increase in gyrification in the prefrontal, orbitofrontal and cingular cortices, and the beginning of laminar differentiation of the cortical plate. compared to the younger fetus (**A**)

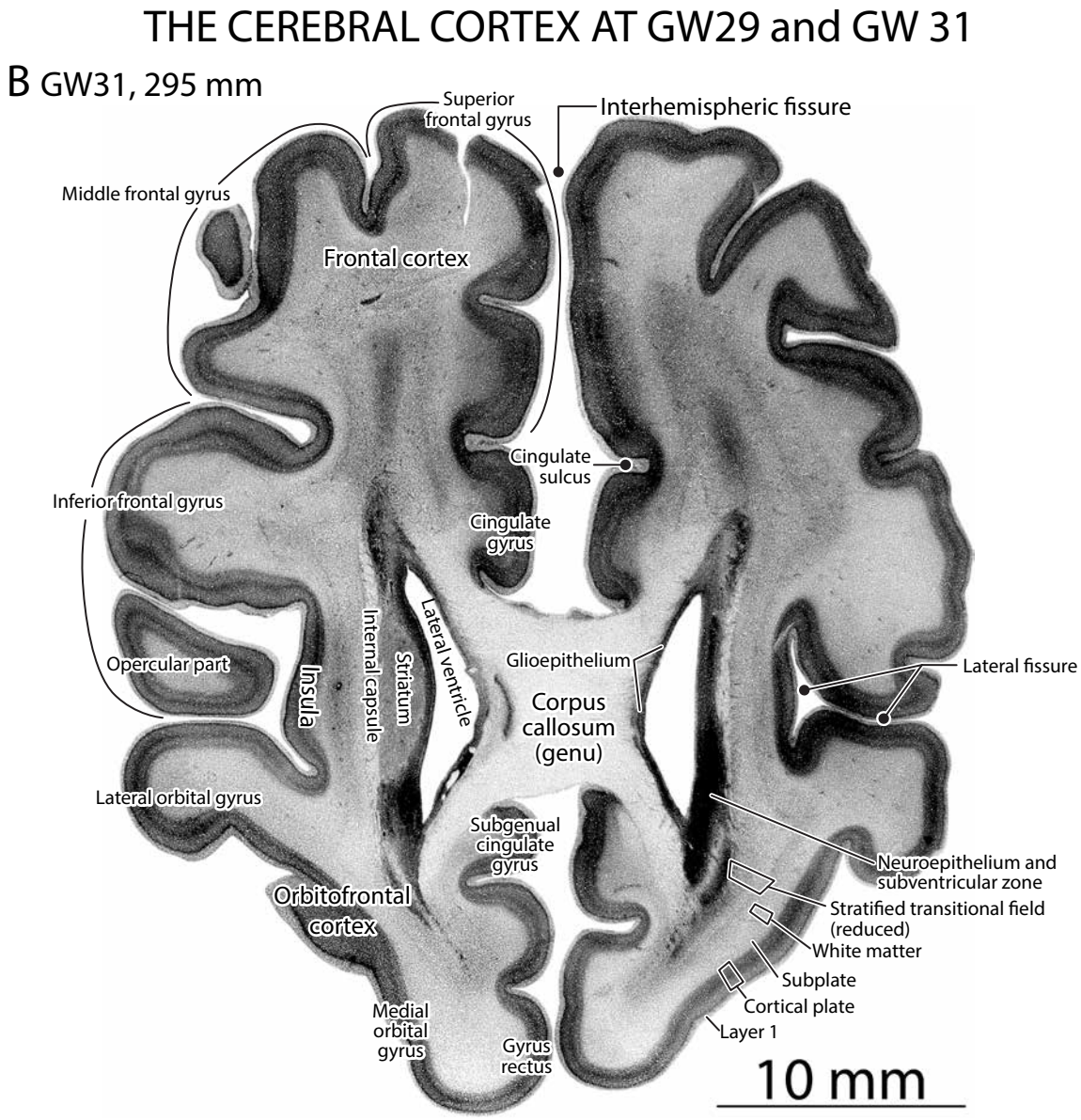
THE CEREBRAL CORTEX AT GW29 and GW 31
B GW31, 295 mm
Superior frontal gyrus
Interhemispheric fissure
Middle frontal gyrus
Frontal cortex
Cingulate sulcus
Inferior frontal gyrus
Cingulate gyrus
Lateral ventricle
Internal capsule
Striatum
Insula
Opercular part
Glioepithelium
Lateral fissure
Corpus callosum (genu)
Lateral orbital gyrus
Subgenual cingulate gyrus
Neuroepithelium and subventricular zone
Orbitofrontal cortex
Stratified transitional field (reduced)
White matter
Subplate
Cortical plate
Layer 1
Medial orbital gyrus
Gyrus rectus
10 mm

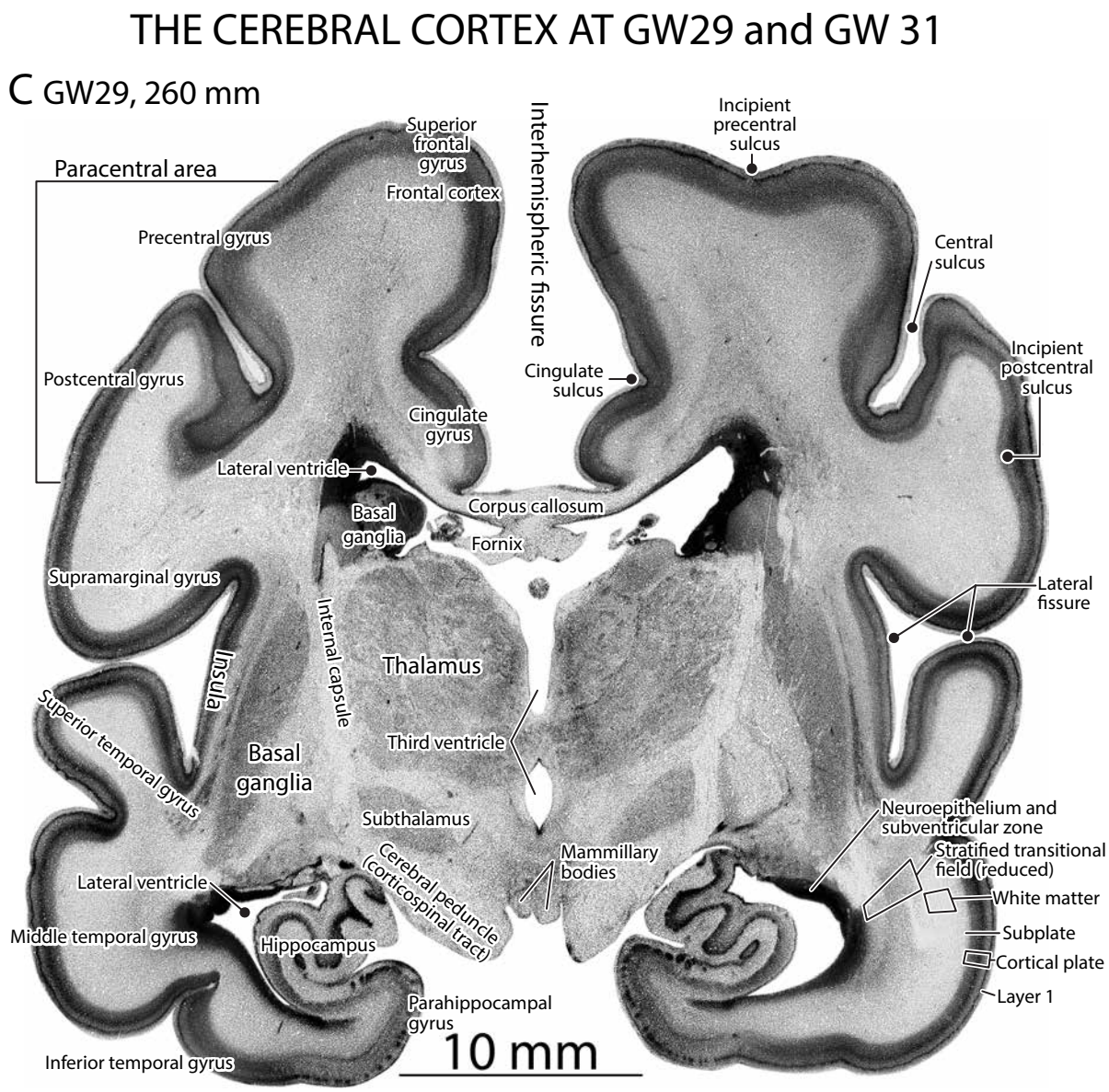

Fig. 30 C and **D**. The same changes are evident in these sections that transect the paracentral area and the anterior temporal lobe. Note the considerable increase in gyrification of the older specimen. The stratified transitional field is much reduced in both specimens and the white matter is considerably expanded in the older specimen.

THE CEREBRAL CORTEX AT GW29 and GW 31

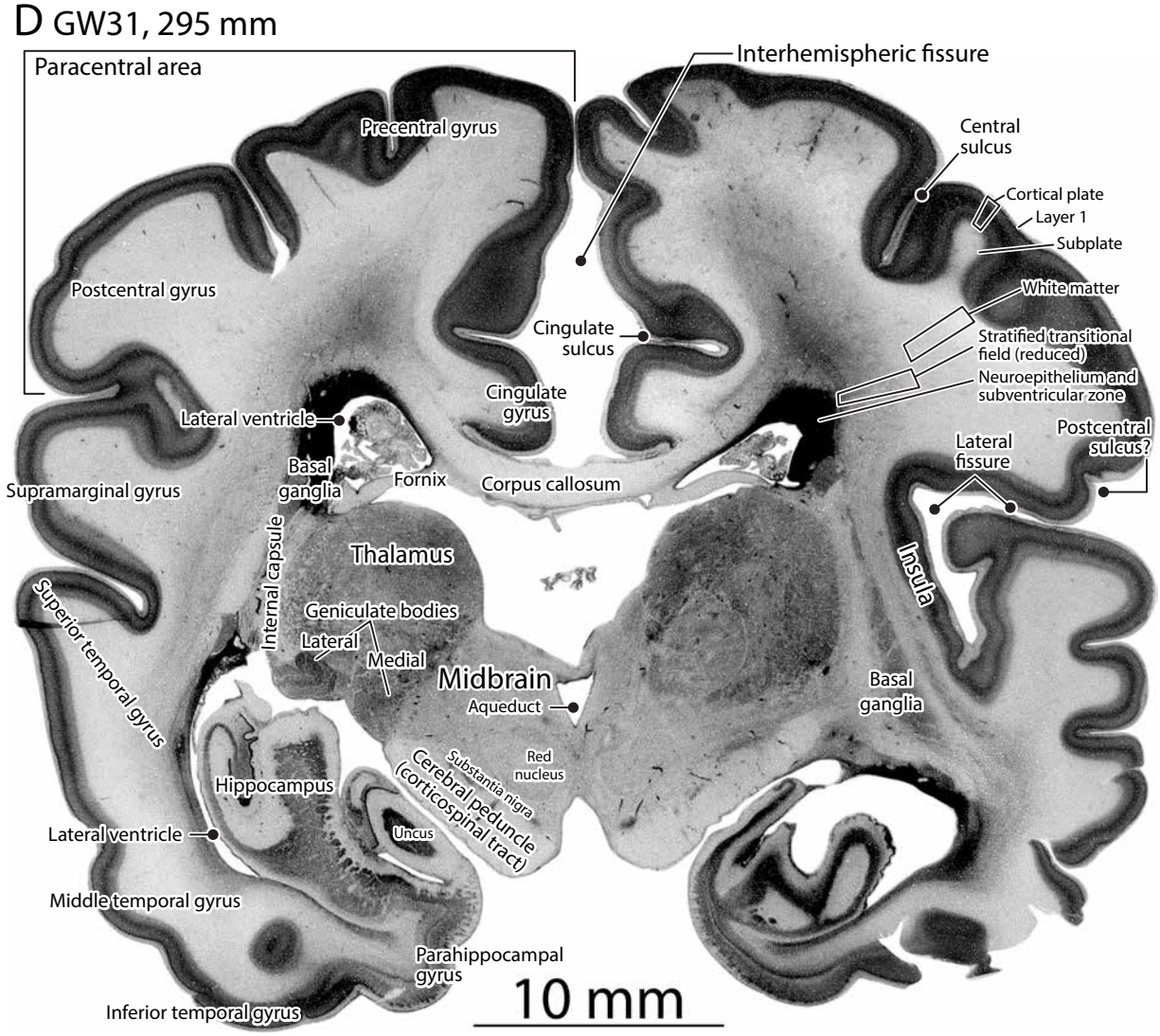

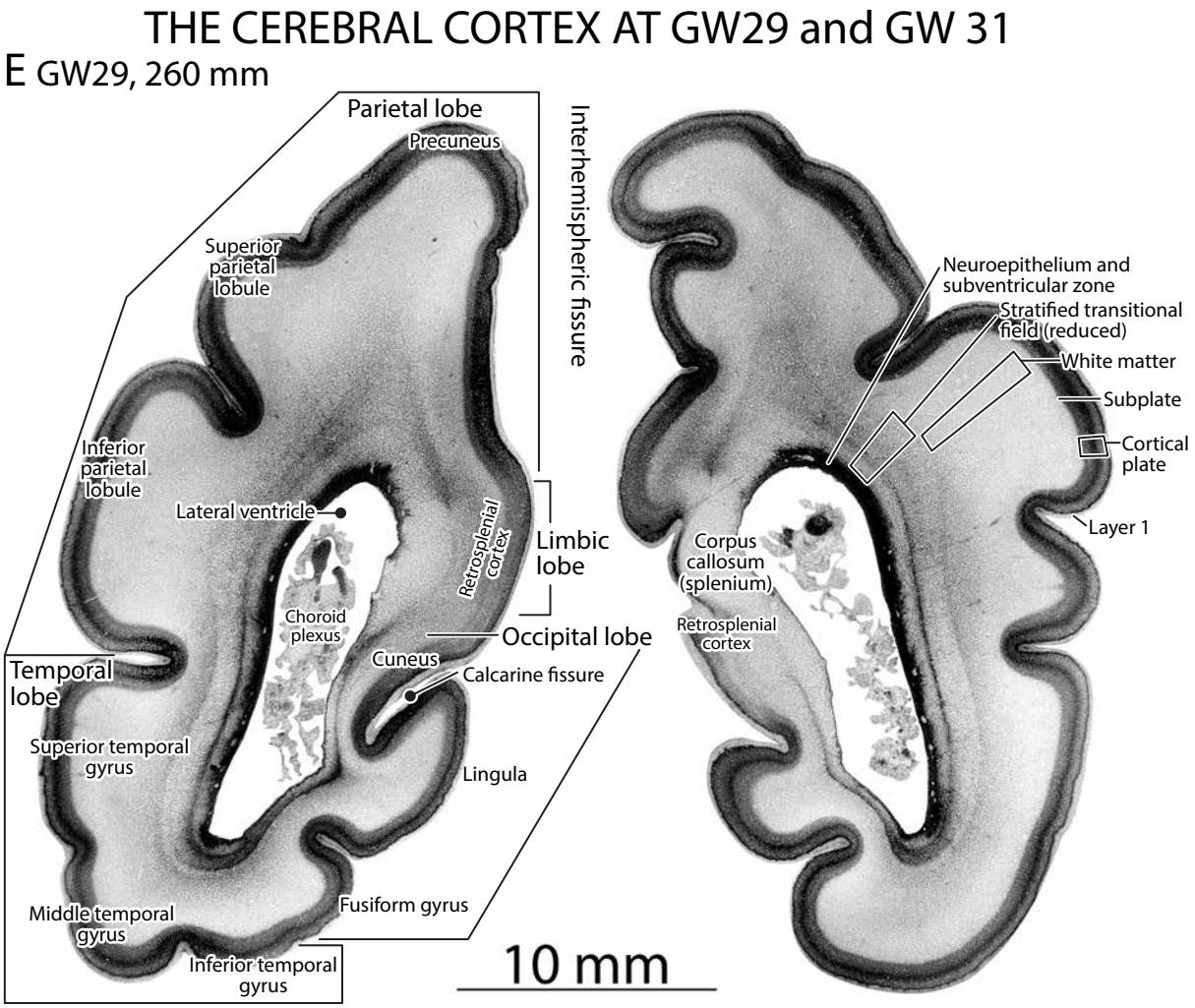

Fig. 30E and **F,** are sections that transect posterior parietal and temporal lobes and the anterior occipital lobe. The increase in gyrification is very evident in the older specimen, but note that the white matter in the depths of each gyrus remains thin in the older specimen. By comparing both specimens, the reduction in the stratified transitional field correlates with expansion of the overlying white matter.

THE CEREBRAL CORTEX AT GW29 and GW 31

F GW31, 295 mm

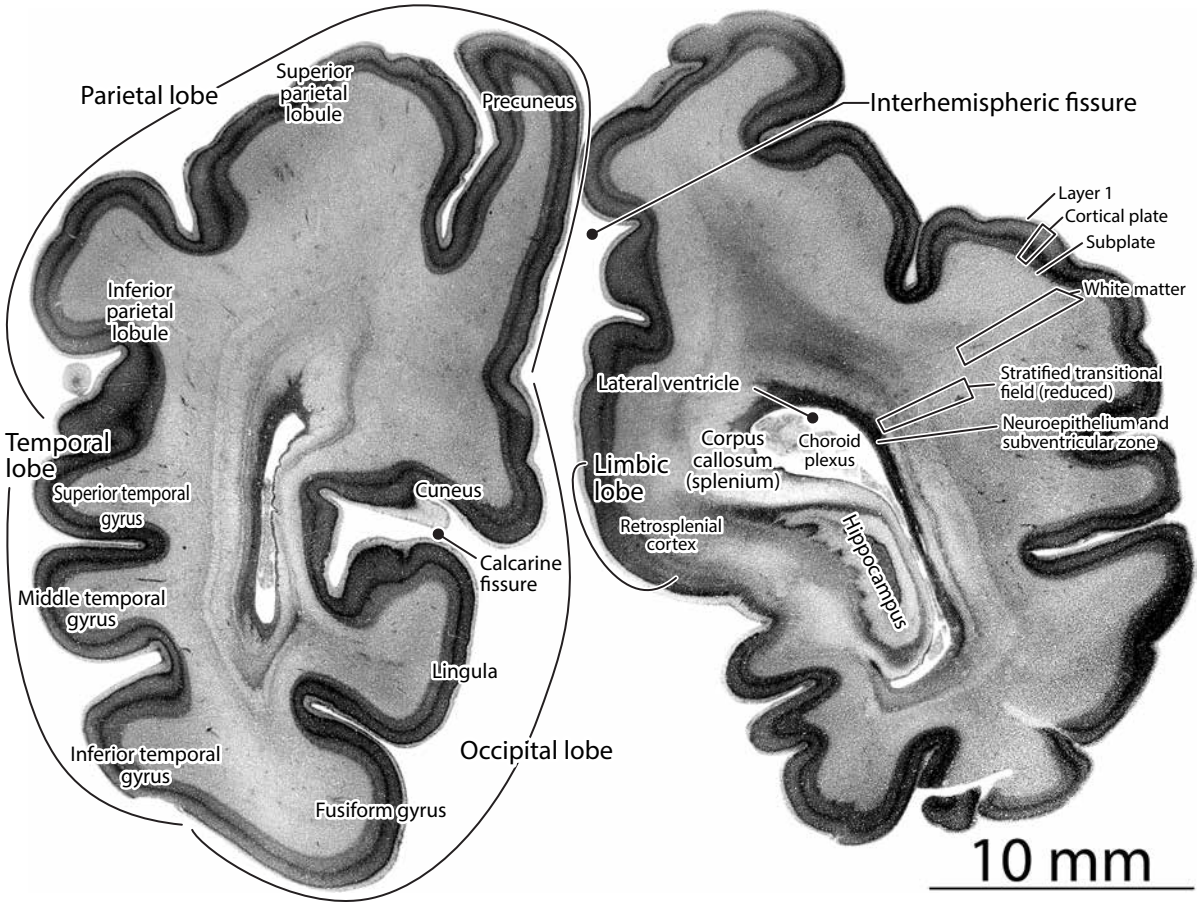

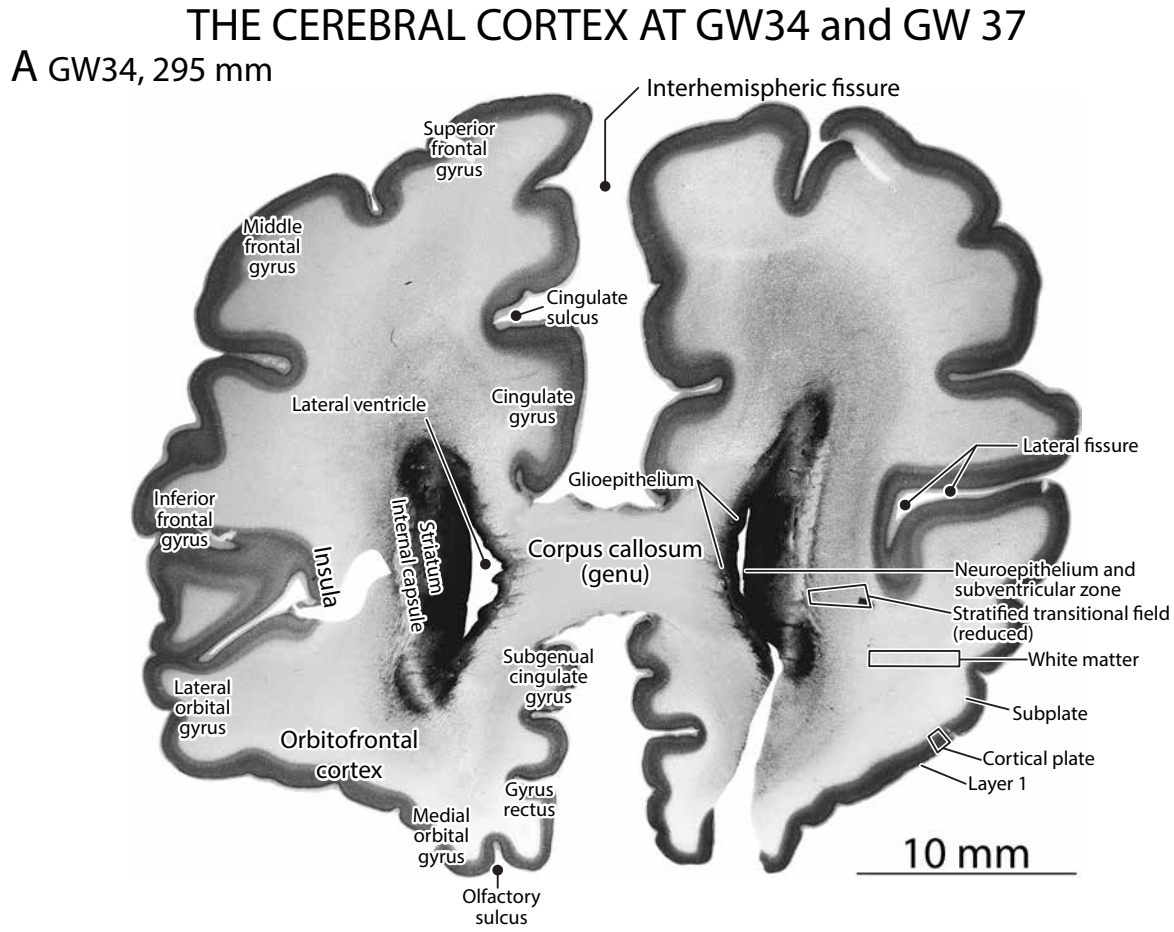

Fig. 31 (on this and the following 5 pages). A comparison of neocortical development in two older third trimester fetuses—GW34 (Y232-66, CR 295 mm) and GW37 (Y217-65, CR 350 mm)—at three coronal levels. The sections on these pages (**A** and **B**) transect only the frontal lobes.

Notable developmental differences between the two specimens are the great expansion in the older fetus of both the cortical white matter and the gray matter (the fibrous component of the neocortex versus its cellular component) by the outward massive expansion of the white matter and the consequent deepening of the fissures. There is by these ages only traces left of the stratified transitional field (STF).

Hence, the expansion the cortical plate reflects the combined outcome of two coordinated developmental processes: First, sojourning neurons—initially residing in the STF—have migrated into the cortical plate increasing neuron numbers. Second, the invasion of corticopetal fibers and the growth of axons from the cortical neurons themselves—part of the ongoing organization of the brain's circuitry—causes the neurons to spread farther apart, initially increasing the linear extent of the cortical plate rather than its depth.

THE CEREBRAL CORTEX AT GW34 and GW 37

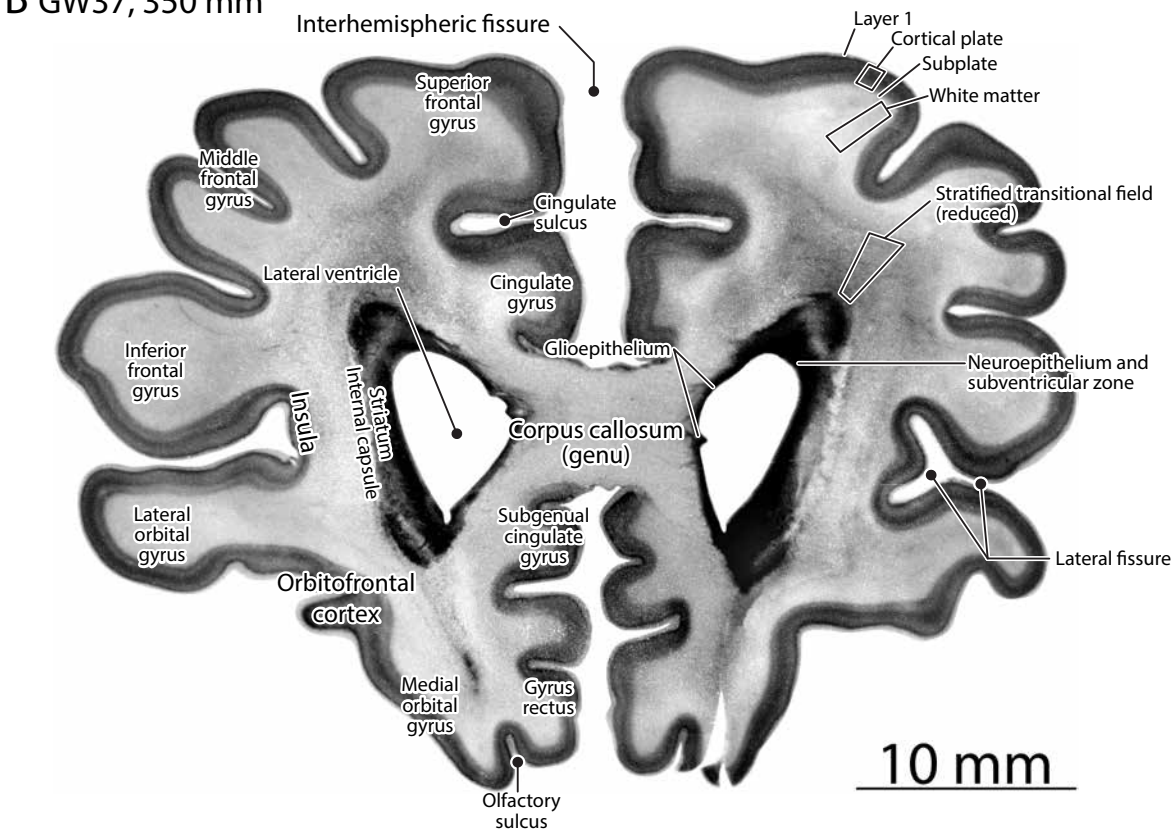

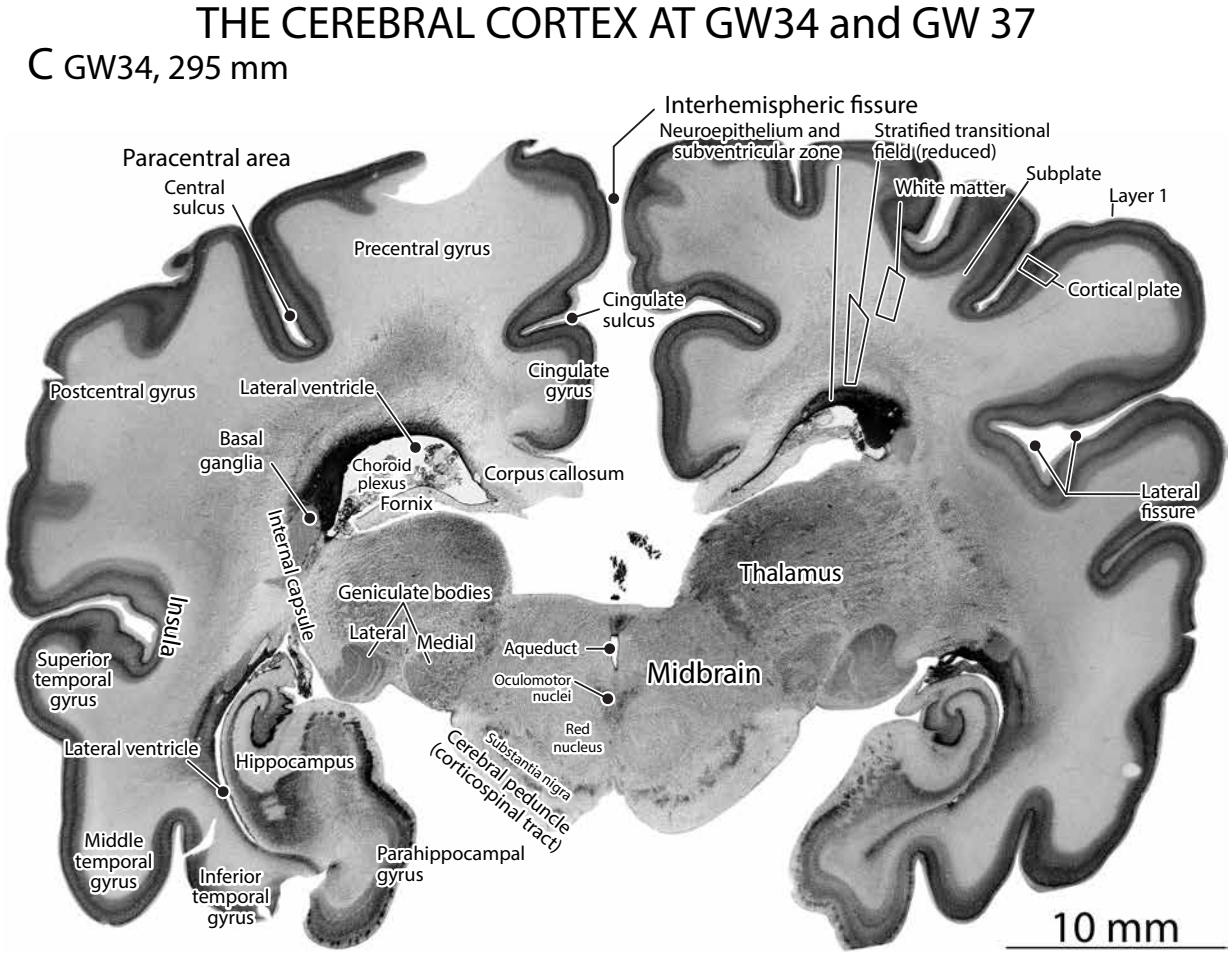

Fig. 31C and **D.** The sections on these pages transect the paracentral area around the central sulcus and the temporal lobe. The same developmental differences between the two specimens seen the the anterior sections (**A** and **B**) are evident at this middle level of cortex.

THE CEREBRAL CORTEX AT GW34 and GW 37

D GW37, 350 mm

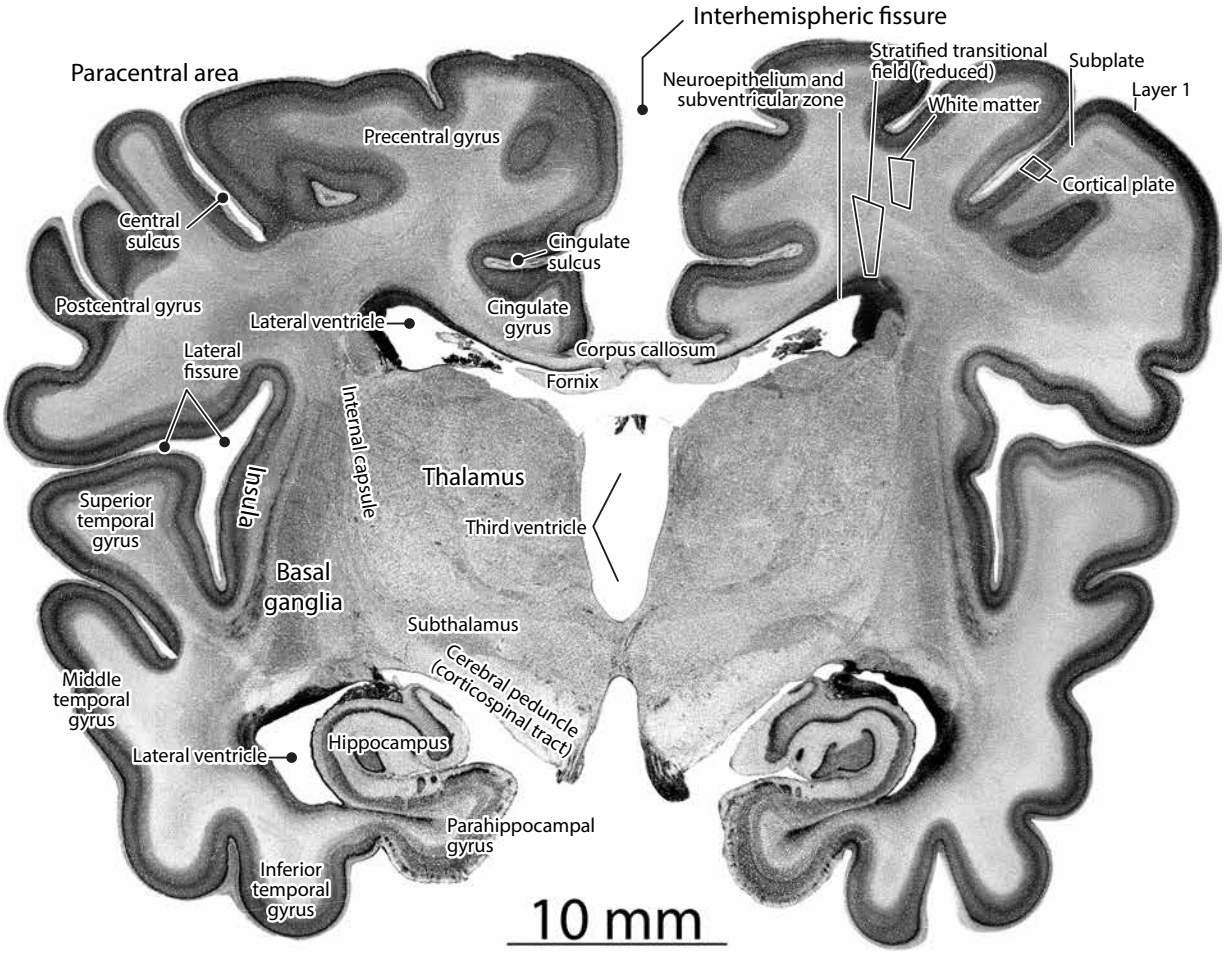

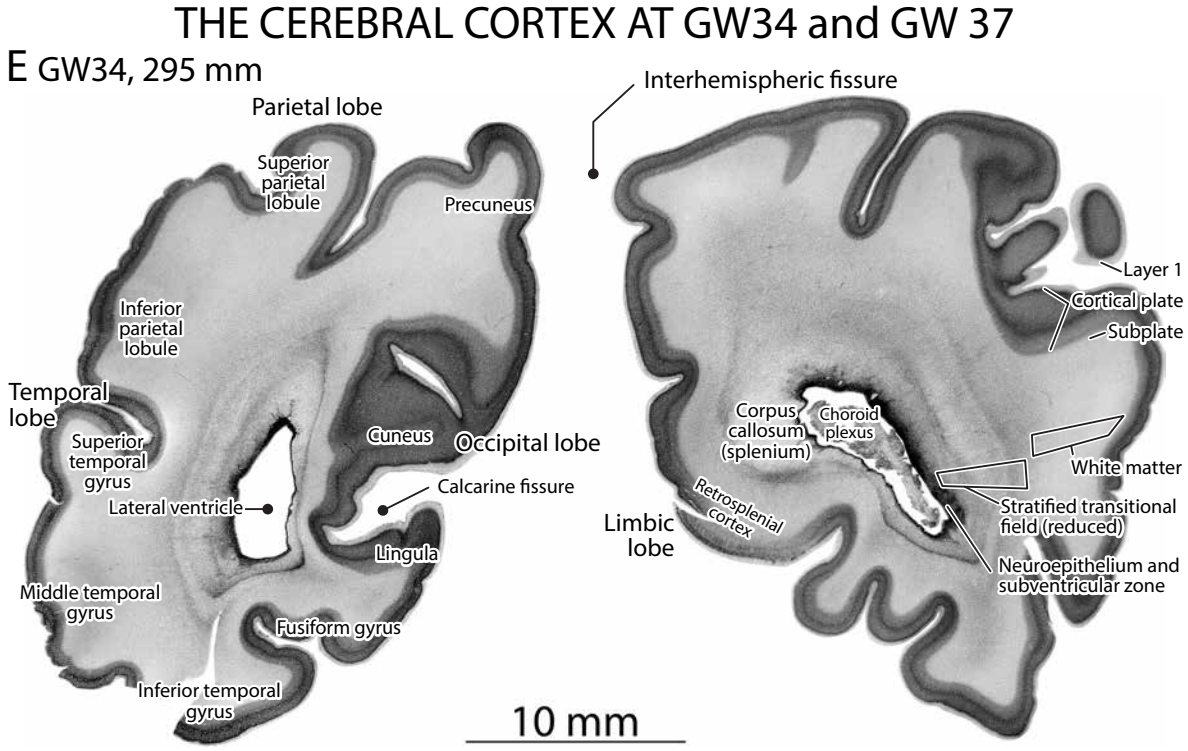

Fig. 31E and **F.** The sections on these pages transect the posterior parietal and temporal lobes and the anterior occipital lobe. The same developmental differences between the two specimens seen in the anterior and mid-level sections (**A** through **D**) are evident at this posterior level of cortex.

THE CEREBRAL CORTEX AT GW34 and GW 37

F GW37, 350 mm

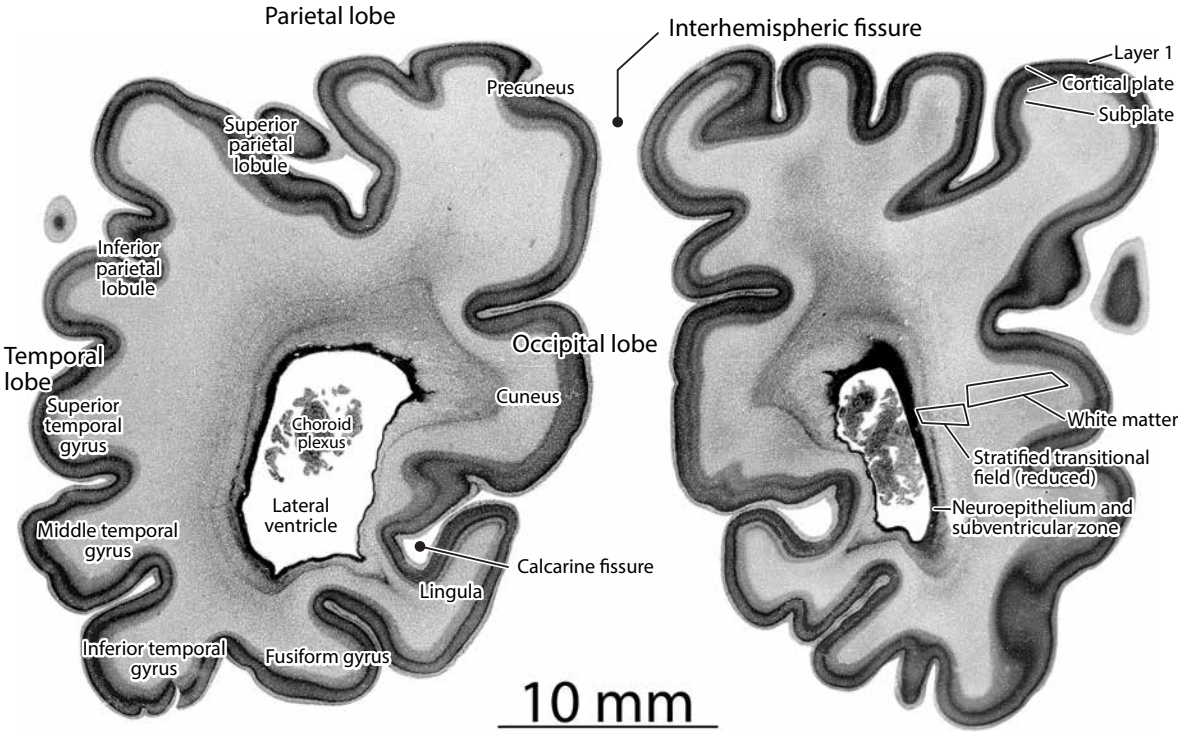

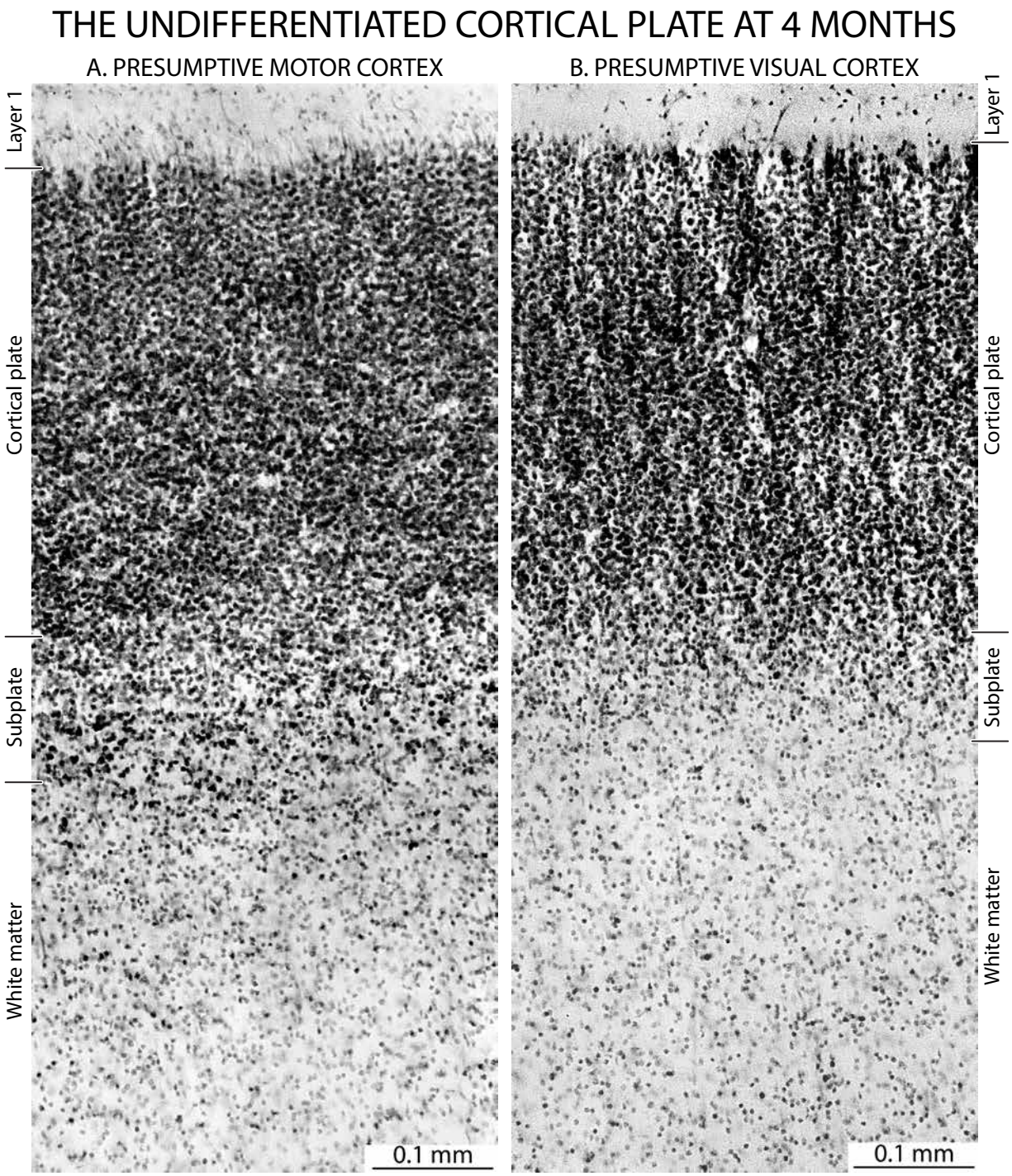

Fig. 32. High magnification photomicrographs of the cortical plate—the future gray matter—in the presumptive motor cortex (**A**) and visual cortex (**B**) of a GW17 (Y37-63, CR 145 mm) fetus. The cells are tightly packed with no indication of a columnar organization, and with little difference in the depth of the plate in the two regions.

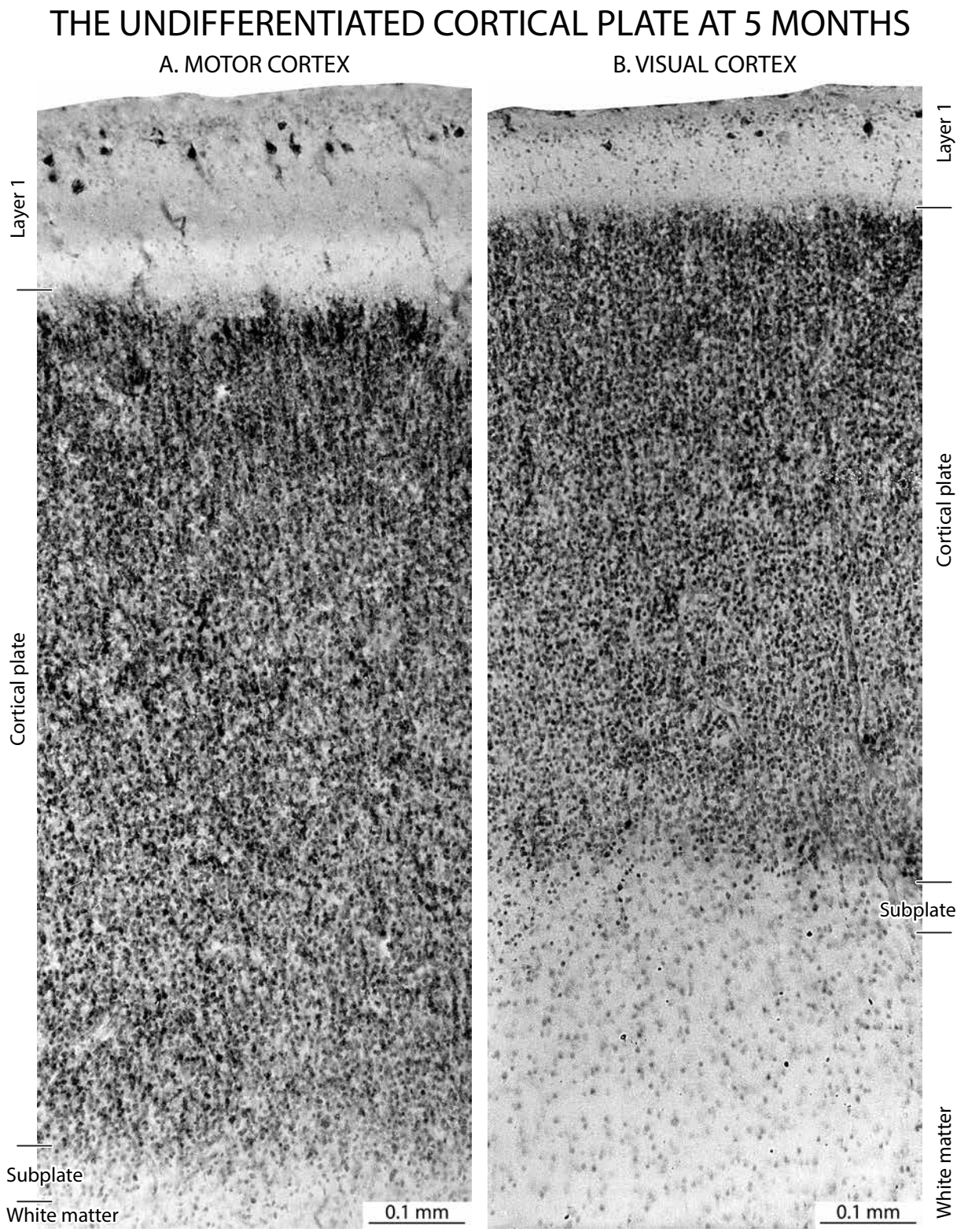

Fig. 33. In this GW20 (Y189-61, CR 160 mm) fetus there is considerable increase in the depth of the cortical plate in the motor cortex (**A**) and some also in the shallower visual cortex (**B**), suggesting migration and settling of young neurons from the sojourn zones of the STF. There is also a notable difference in the width and organization of layer 1 (the plexiform layer) beneath the pia in the two regions.

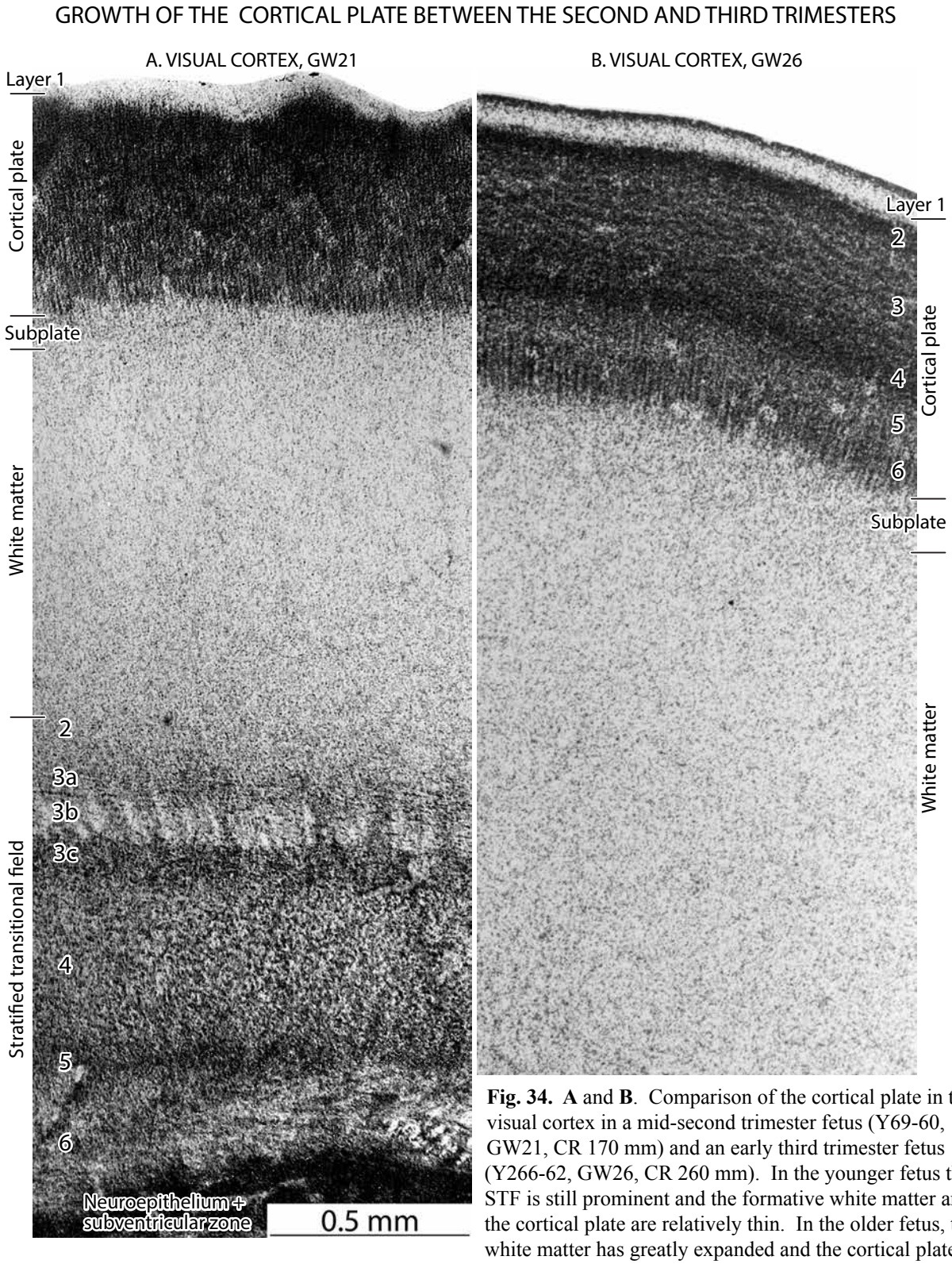

Fig. 34. A and **B**. Comparison of the cortical plate in the visual cortex in a mid-second trimester fetus (Y69-60, GW21, CR 170 mm) and an early third trimester fetus (Y266-62, GW26, CR 260 mm). In the younger fetus the STF is still prominent and the formative white matter and the cortical plate are relatively thin. In the older fetus, the white matter has greatly expanded and the cortical plate is thickening with the onset of lamination. **C** and **D (facing page)** similar changes are seen in the motor cortex in a comparison of the cortical plate in a mid-second trimester fetus (Y27-60, GW20,CR 160 mm) and an early third

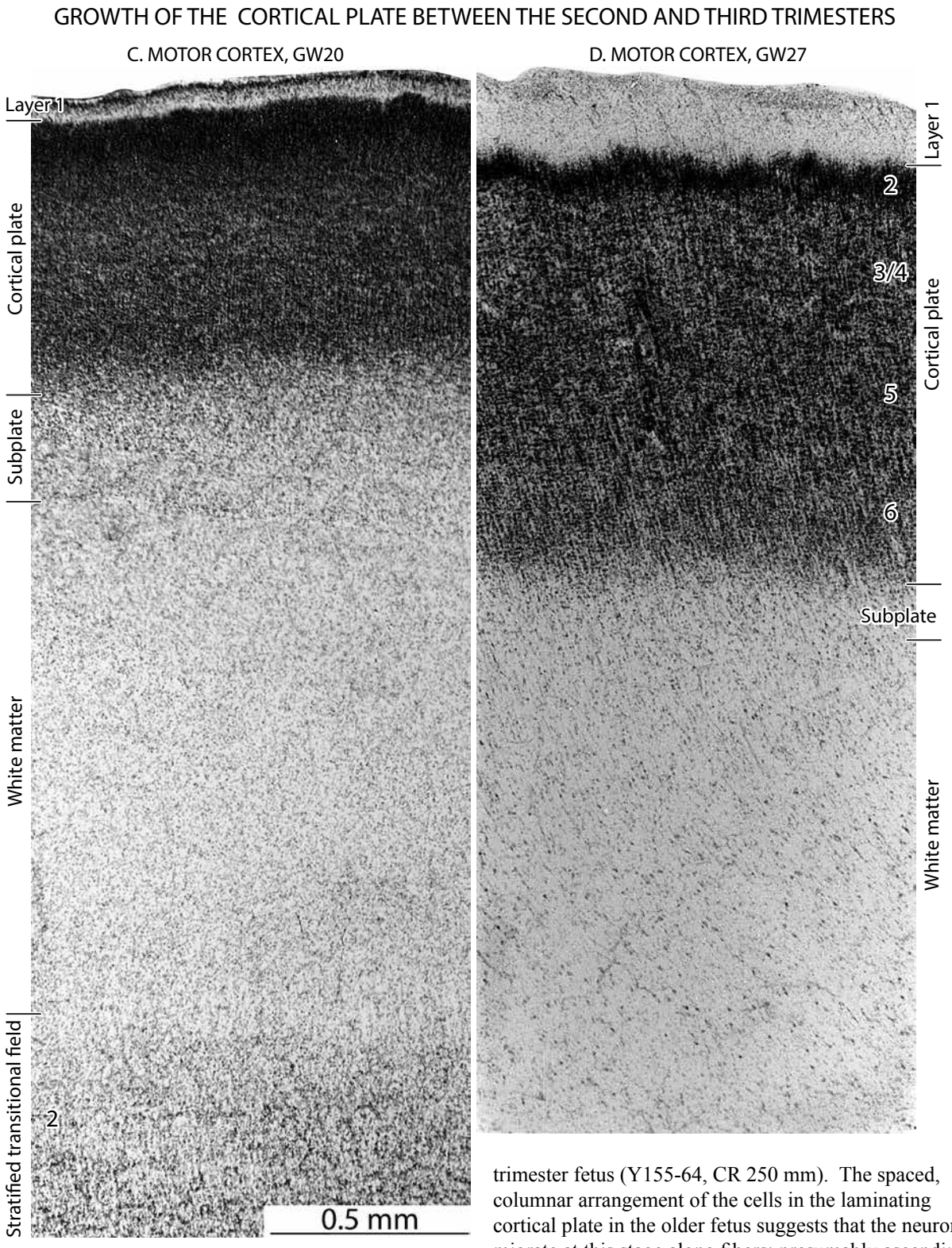

trimester fetus (Y155-64, CR 250 mm). The spaced, columnar arrangement of the cells in the laminating cortical plate in the older fetus suggests that the neurons migrate at this stage along fibers; presumably ascending axons in the visual cortex and descending axons in the motor cortex. The presence of a subpial cellular band in **B** and **C** is an inconsistent feature of the developing neocortex in different specimens.

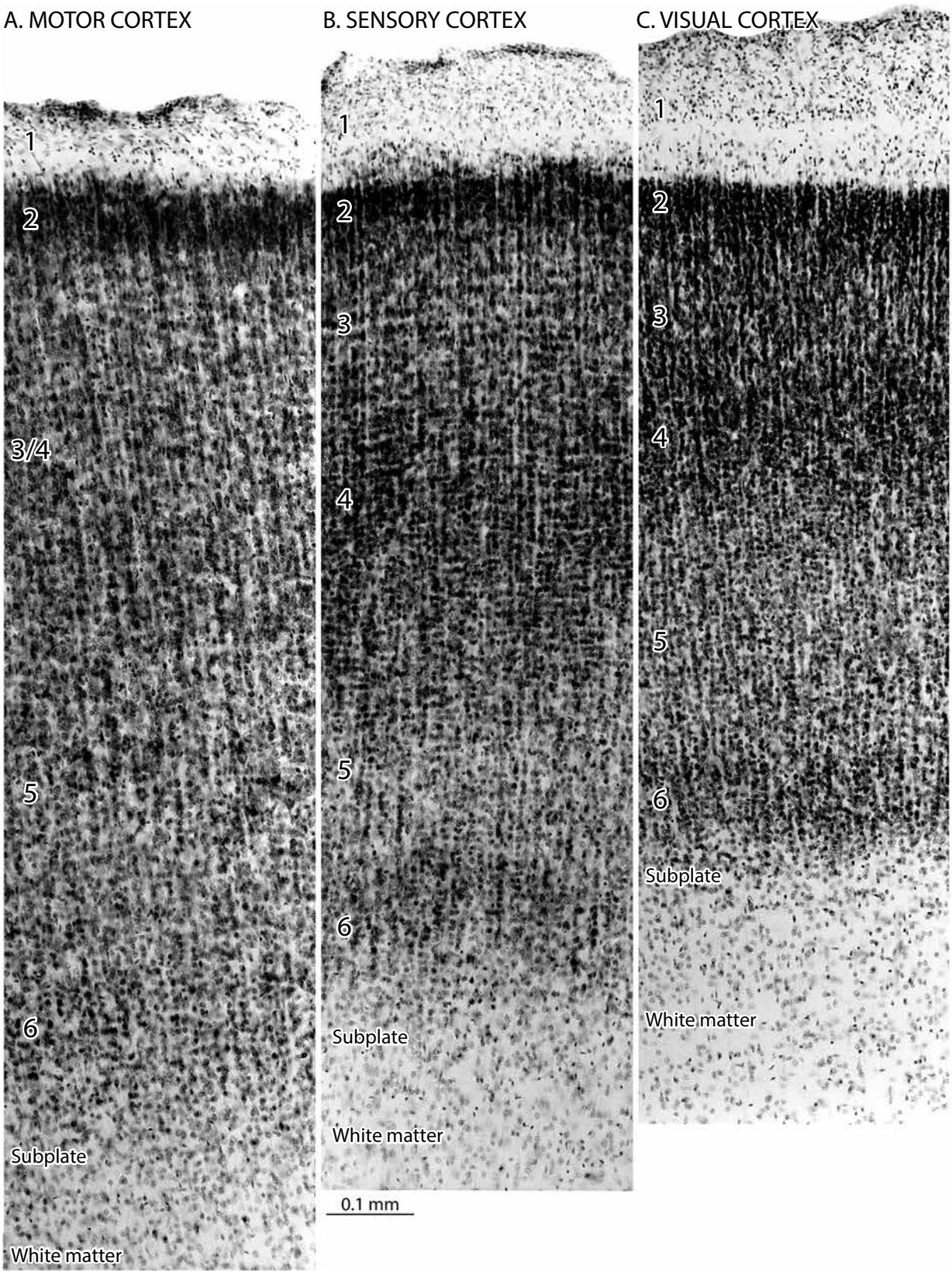
REGIONAL DIFFERENCES IN THE CORTICAL GRAY AT 6 MONTHS
A. MOTOR CORTEX
B. SENSORY CORTEX
C. VISUAL CORTEX
1
2
3/4
5
6
Subplate
White matter
1
2
3
4
5
6
Subplate
White matter
0.1 mm
1
2
3
4
5
6
Subplate
White matter

Fig. 35. Differentiation of the cortical gray matter in the motor (**A**), somatosensory (**B**) and visual areas (**C**) in a 6-months-old fetus (Y211-65, GW23, 220 mm) shown at higher magnification. (For low-power views of the brain of this specimen, see **Fig. 26**.) There are differences in the width of the gray matter in the different areas, a pronounced columnar alignment of neuronal cell bodies along radial fibers in all of them, as well as an incipient horizontal stratification. The compactly packed cells of layer 2 may be the least differentiated neurons that are settling in the cortical gray matter in an inside-out sequence.

Fig. 36 (on the following 3 pages). Illustrations of the ongoing differentiation of the cortical gray matter in a 7 months-old fetus (Y14-59, GW29, CR 260 mm) at six levels. The distinctive cytoarchitectonic organization of the gray matter in the different areas is becoming more evident.

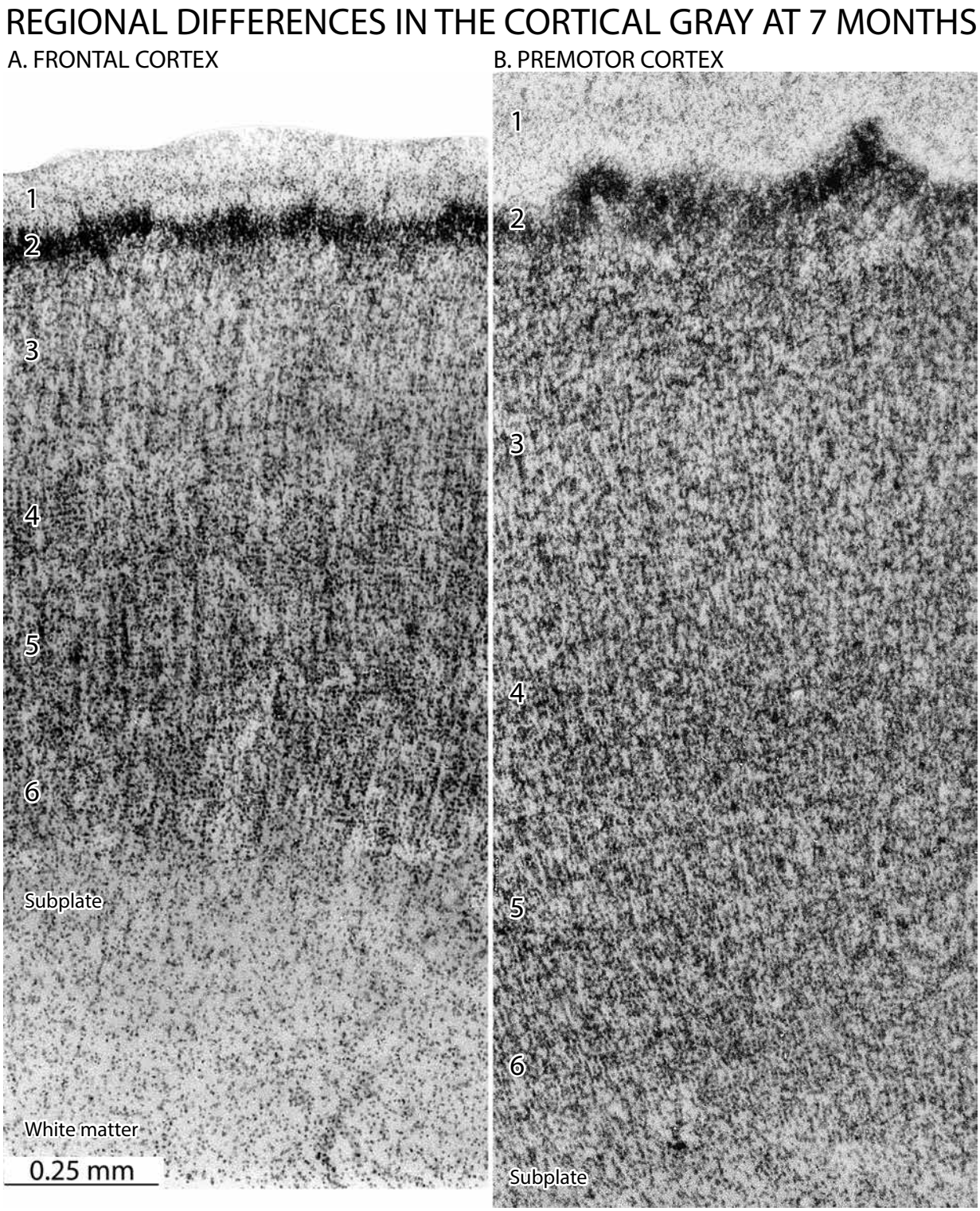

Fig. 36A. The granular frontal associational area.

Fig. 36B. The dysgranular premotor area.

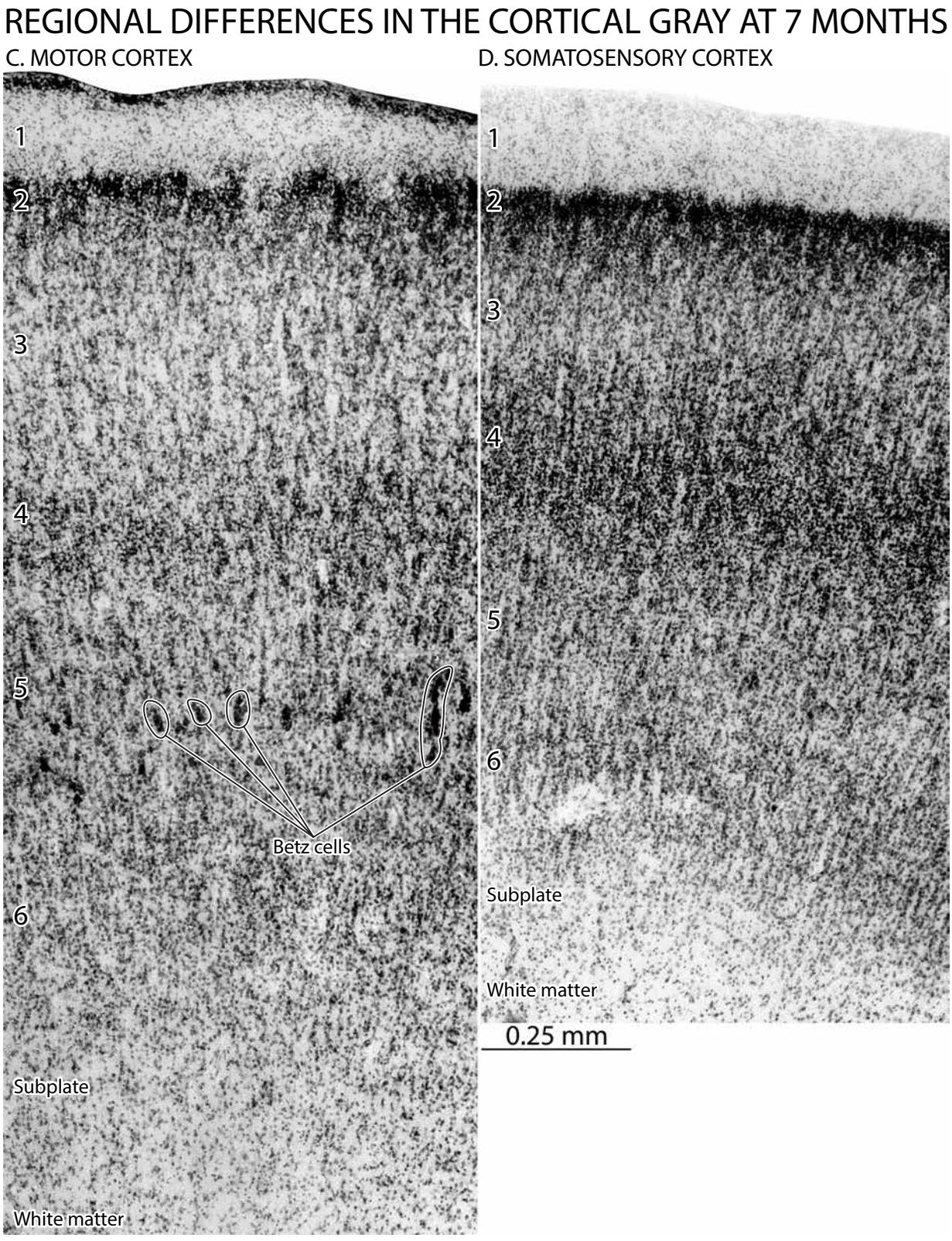

Fig. 36C. The agranular motor projection area with large Betz cells.

Fig. 36D. The granular somatosensory projection area.

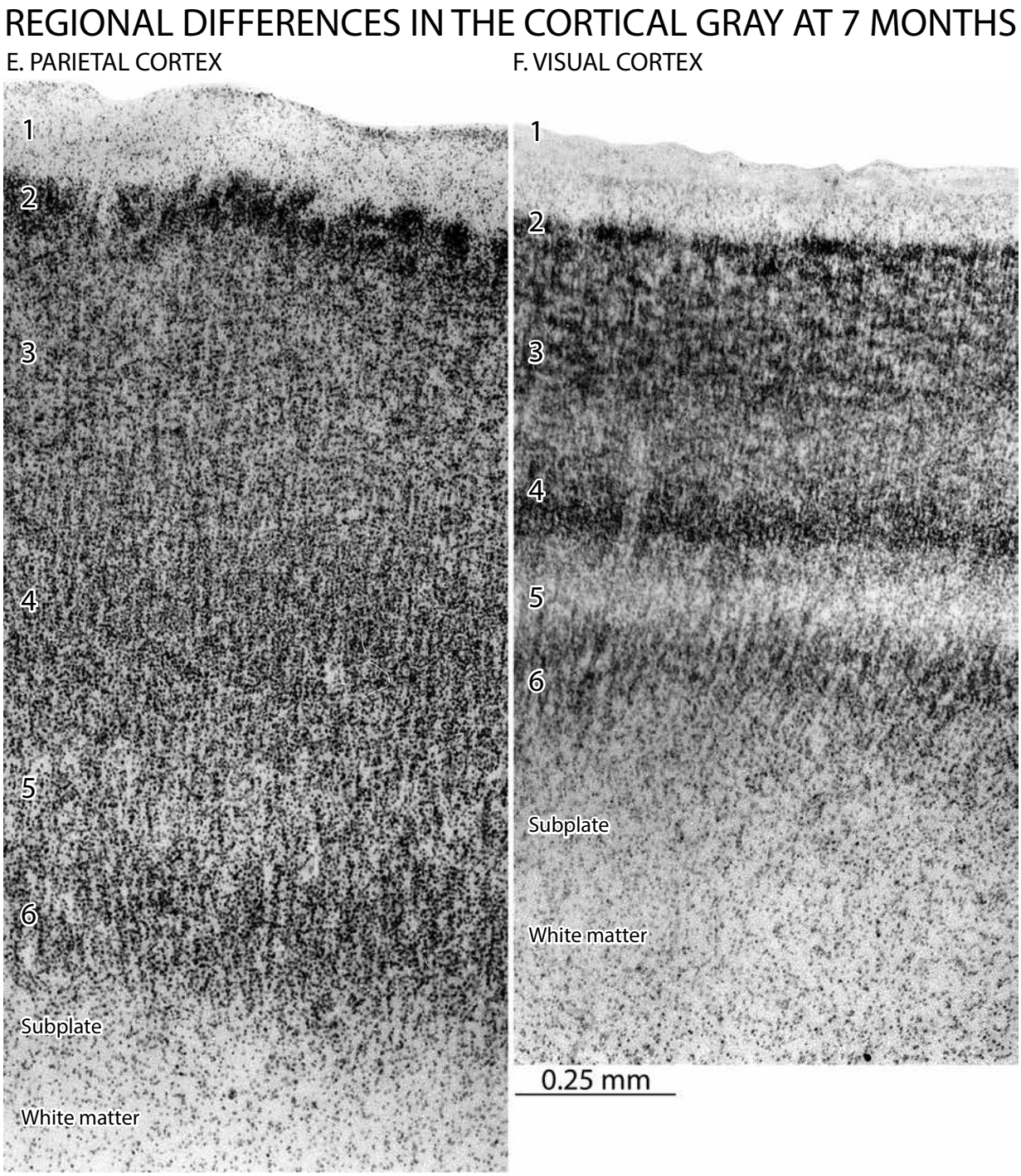

Fig 36E. The granular parietal associational area.

Fig. 36F. The super-granular and distinctly laminated visual projection area.

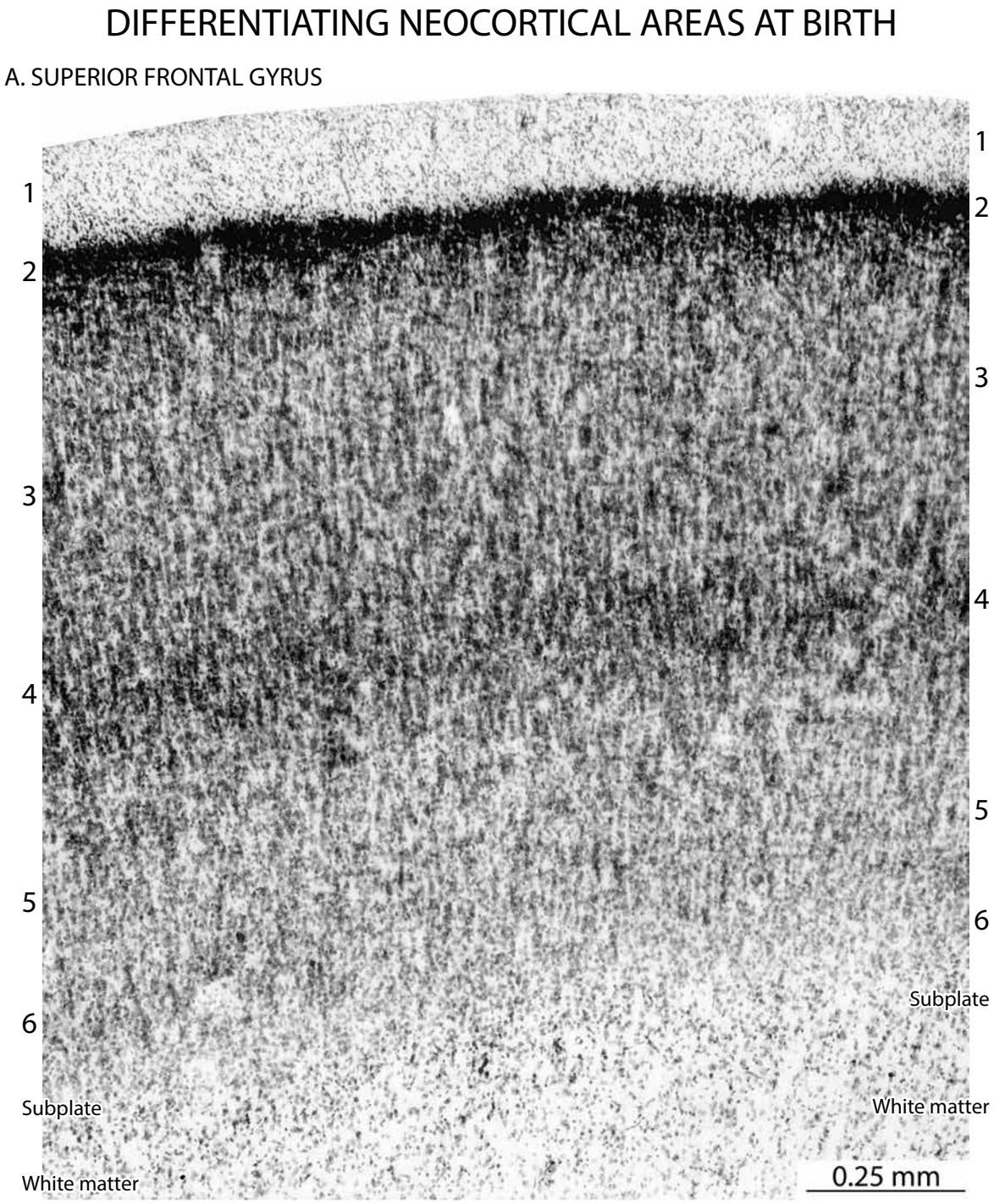

Fig. 37 (on this page and the next three pages). Illustration of the close resemblance in the laminar differentiation of four neocortical areas in a 9 months-old, full-term newborn (Y217-65, CR 350 mm) to that seen in postnatal specimens.
A. The superior frontal gyrus, an association area, with large upper layers 3 and 4.

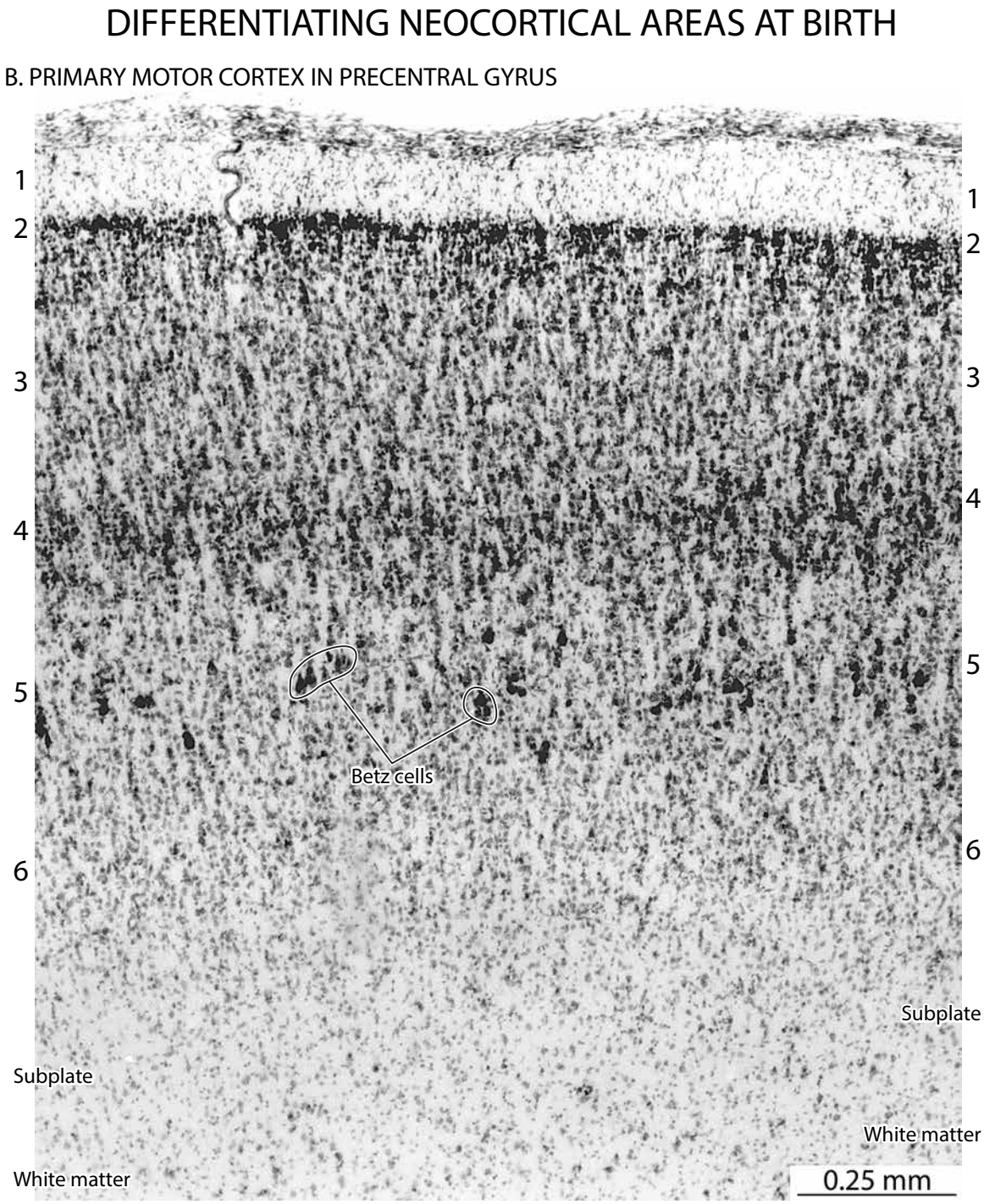

Fig. 37B. The precentral gyrus, the motor projection area, with large lower layers 5 and 6.

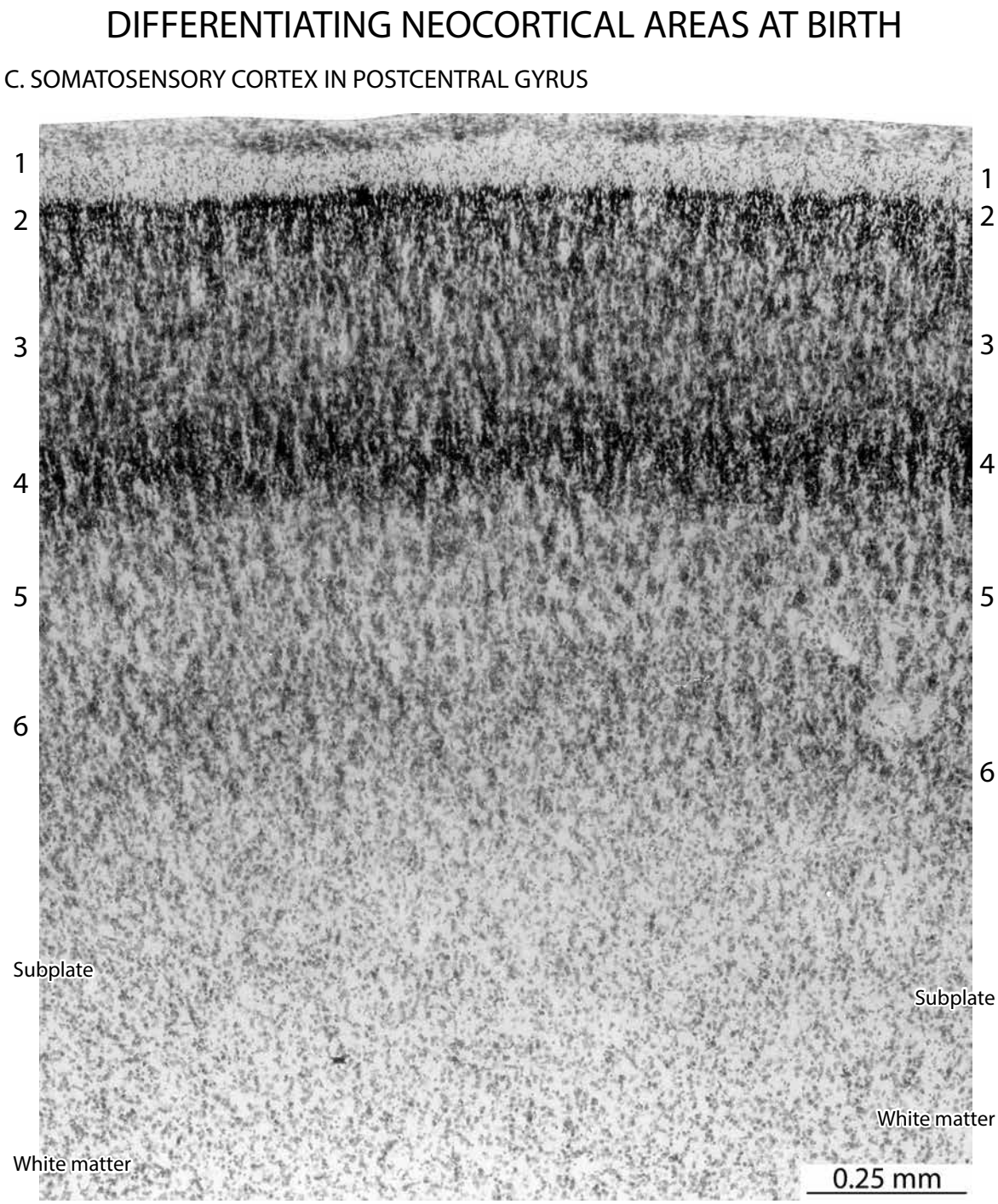

Fig. 37C. The postcentral gyrus, the somatosensory projection area, with densely packed cells in upper layers 3 and 4.

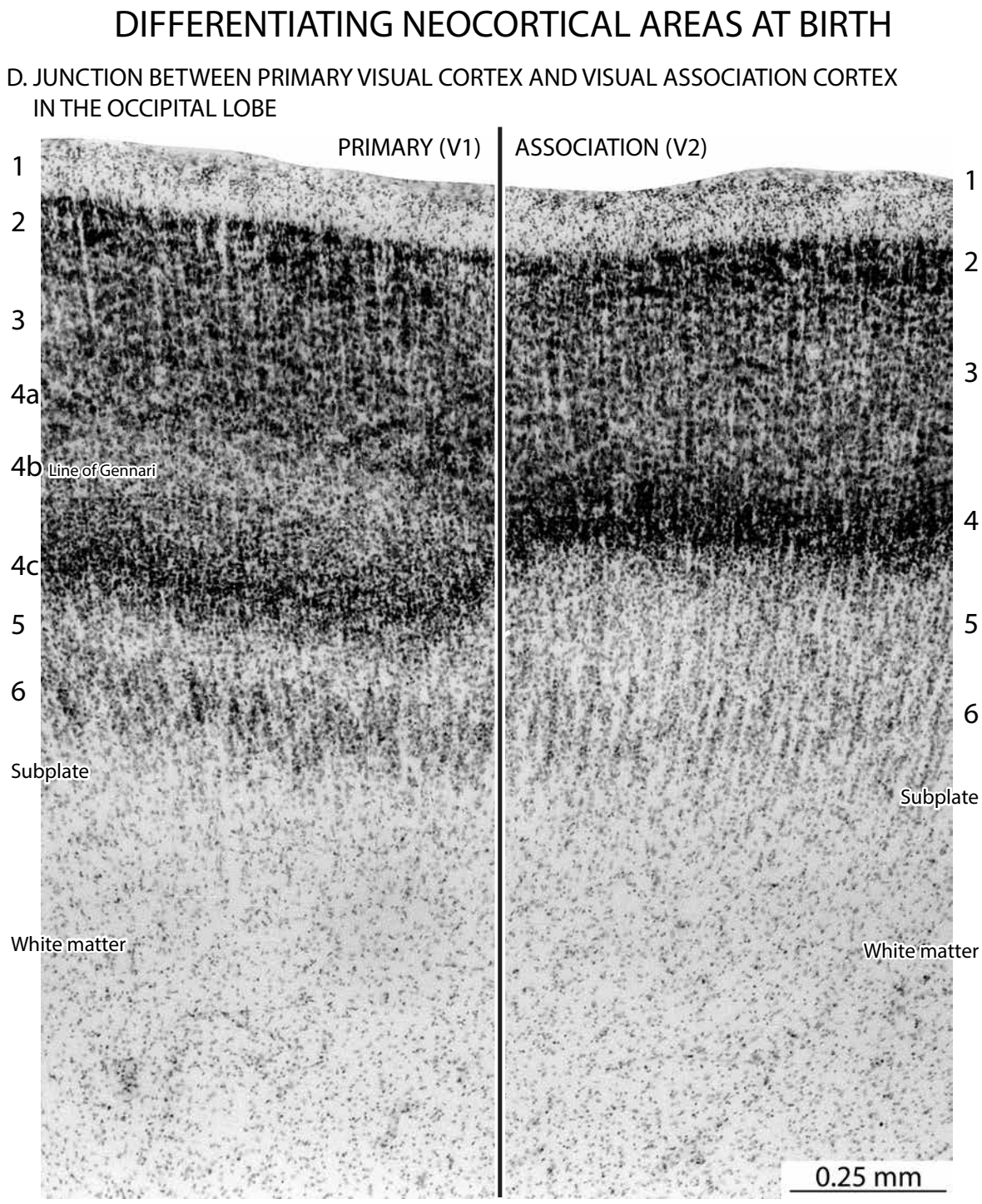

Fig. 37D. The junction between areas 17 and 18, the primary visual projection area (*V1, left*) and the first-order visual association area (*V2, right*), with the thick upper layer 3 and 4 and distinctive lamination patterns (*note the line of Gennari in layer 4b of V1*).

C. NEOCORTICAL DEVELOPMENT FROM BIRTH THROUGH EARLY CHILDHOOD

Neocortical Foliation. In its external appearance, the highly foliated neocortex of the full-term neonate closely resembles the neocortex of the adult (Fig. 38). However, it is much smaller. Brain weight increases about three-fold from birth through early childhood, then more modestly during late childhood and early adolescence, and begins to diminish slowly during adulthood (Fig. 39).

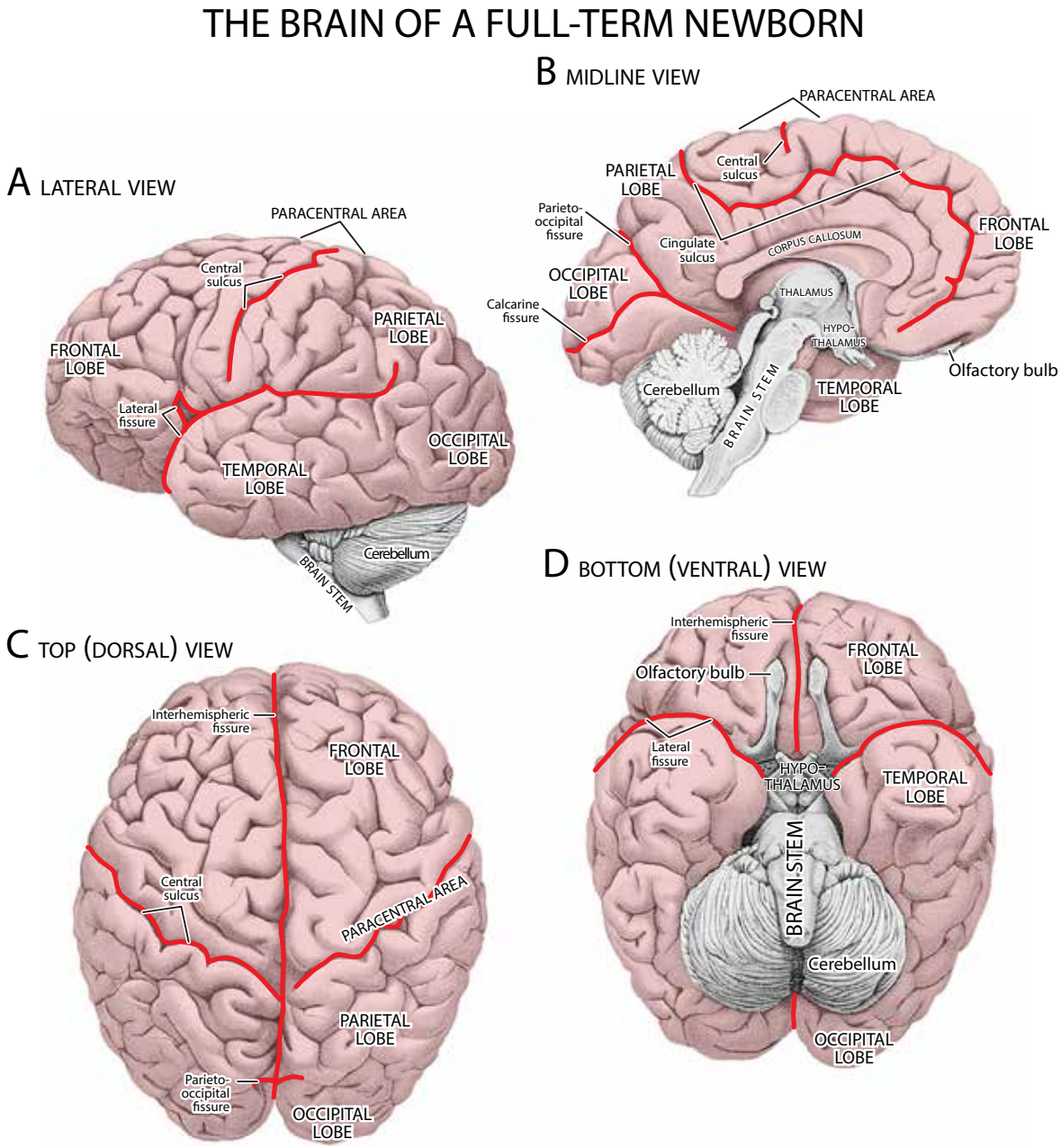

Fig. 38. The neocortex of a full-term newborn in lateral (**A**), sagittal (**B**), dorsal (**C**), and ventral (**D**) views. After Retzius (1896). Although much smaller, the convolutions of all the lobes resemble those seen in adults. Coloration and labeling in this and the following illustrations are ours.

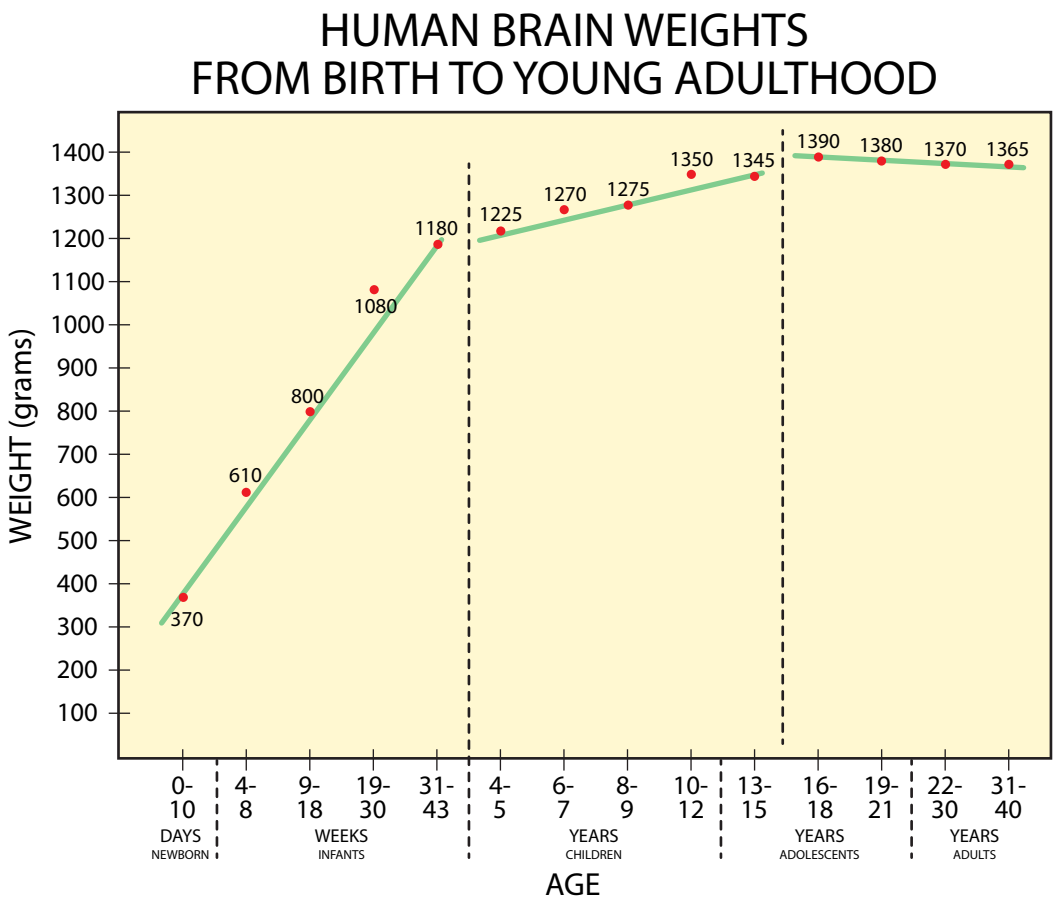

Fig. 39. Increase in brain weight (in grams) from birth to middle age. Based on the fresh weight of 2,773 male and 1,963 female brains, with the two here combined. Based on data by Dekaban and Sadowsky (1978). The largest increase in brain weight occurs during the first 3 years of postnatal life, with the rate of growth slowing during adolescene, and beginning to decline during early adulthood.

While that postnatal growth is partly attributable to the expansion of some subcortical structures, the primary contributor to that growth is the expansion of both the gray matter and the white matter of the neocortex. According to an older histological survey (Blinkov and Glezer, 1968), the postnatal expansion of the neocortex is far more pronounced in the frontal and temporal lobes than in the occipital lobe (Fig. 40). That pattern is also suggested by Conel's (1939-1967) photographs of the expanding cerebral cortex between 1 month and 6 years of age, as seen in lateral (Fig. 41) and medial (Fig. 42) views. Paralleling that cortical expansion is the progressive growth of the corpus callosum during that period (Fig. 42).

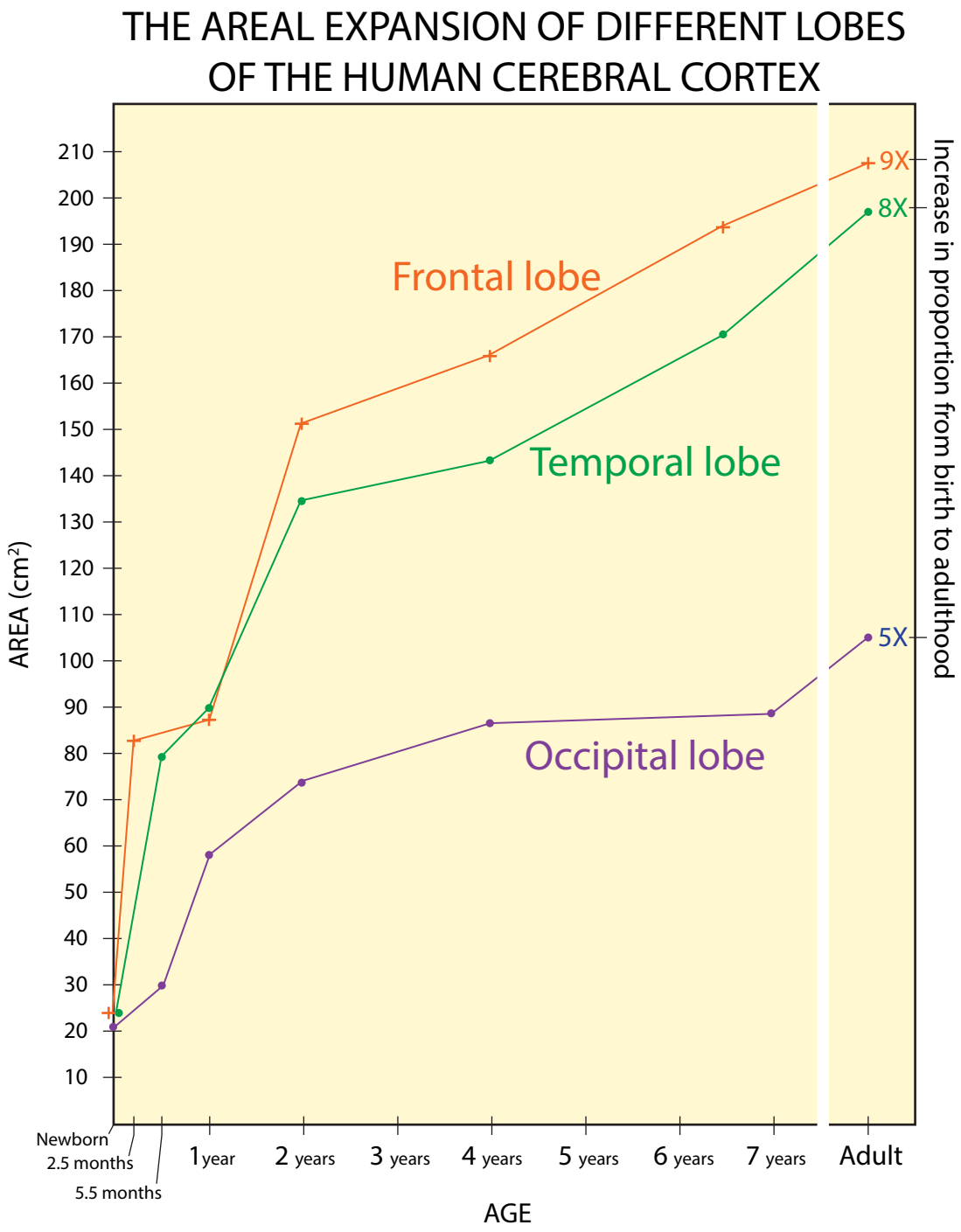

Fig. 40. The growth of the surface area of the neocortex (in cm^2), from birth to adulthood in three regions, the frontal, temporal and occipital lobes. The occipital lobe expands 5-times, the temporal lobe 8-times, and the frontal lobe 9-times. Based on data by Blinkov and Glezer (1968).

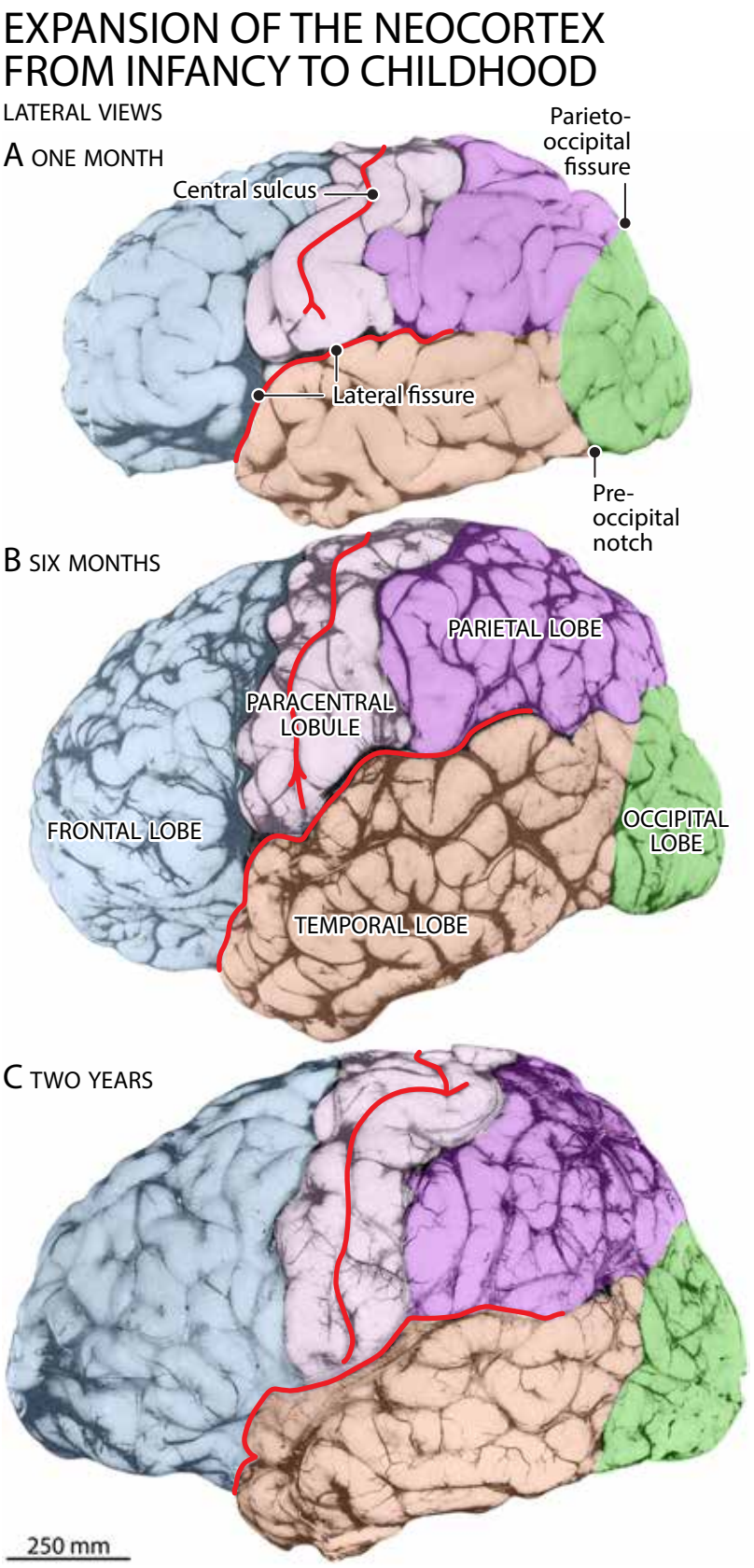
EXPANSION OF THE NEOCORTEX
FROM INFANCY TO CHILDHOOD
LATERAL VIEWS
A ONE MONTH
Parieto-
occipital
fissure
Central sulcus
Lateral fissure
Pre-
occipital
notch
B SIX MONTHS
PARIETAL LOBE
PARACENTRAL
LOBULE
FRONTAL LOBE
OCCIPITAL
LOBE
TEMPORAL LOBE
C TWO YEARS
250 mm

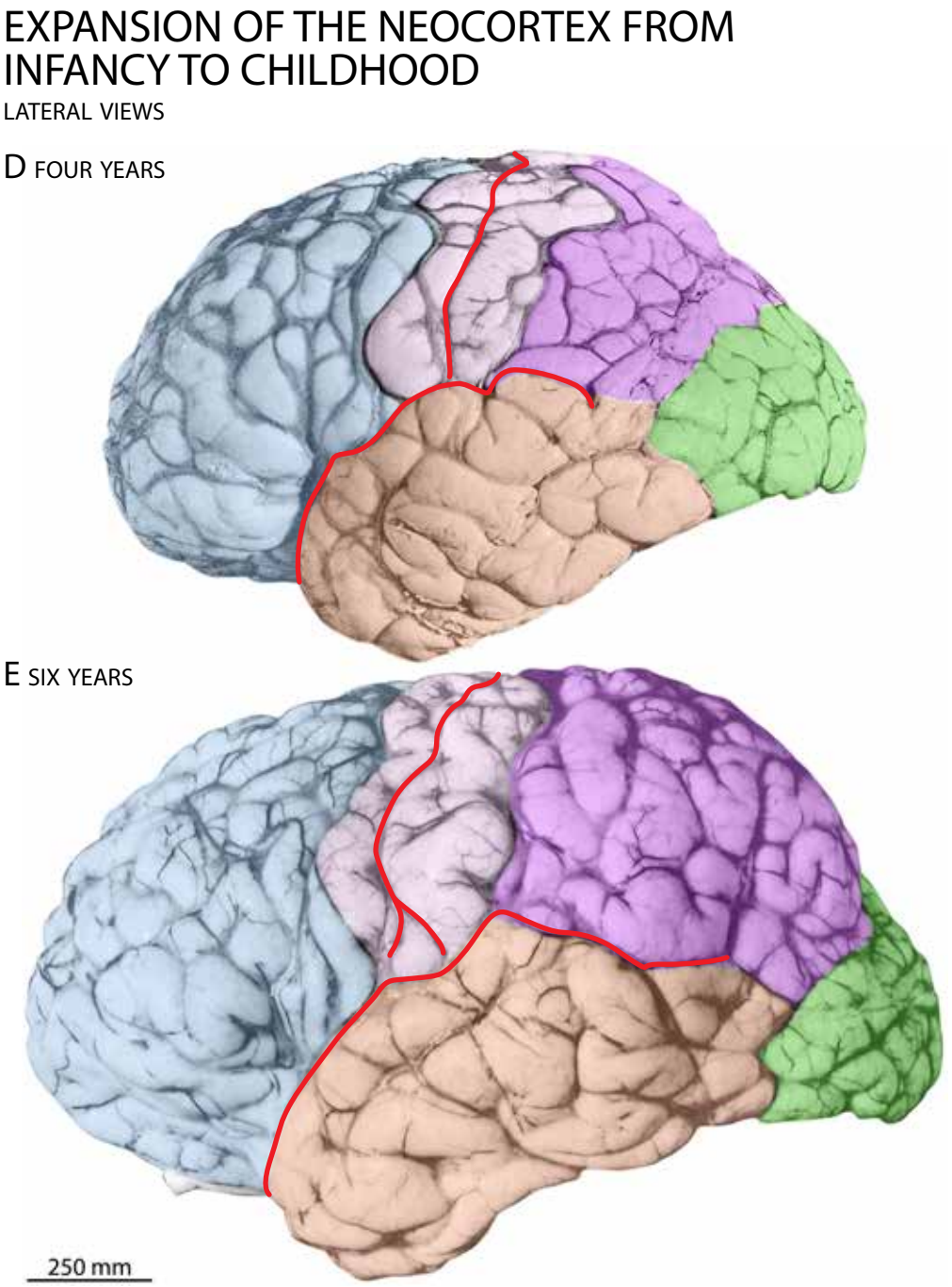

Fig. 41 (on facing pages). Lateral views of the postnatally expanding neocortex at the following postnatal ages:
A, 1 month; **B**, 6 months; **C**, 2 years; **D**, 4 years; **E**, 6 years. (From Conel's Figure 3 in volumes 2, 4, 6, 7, and 8).
Conel's photographs have been colored to delineate the different lobes: frontal lobe, *blue*; paracentral lobe, *pink*; parietal lobe, *violet*; occipital lobe, *green*; temporal lobe, *orange*. That delineation of the different lobes has been aided by the preservation of the surface blood vessels. The age-related expansion of the neocortex appears to be most pronounced in the association areas of the frontal, temporal and parietal lobes.

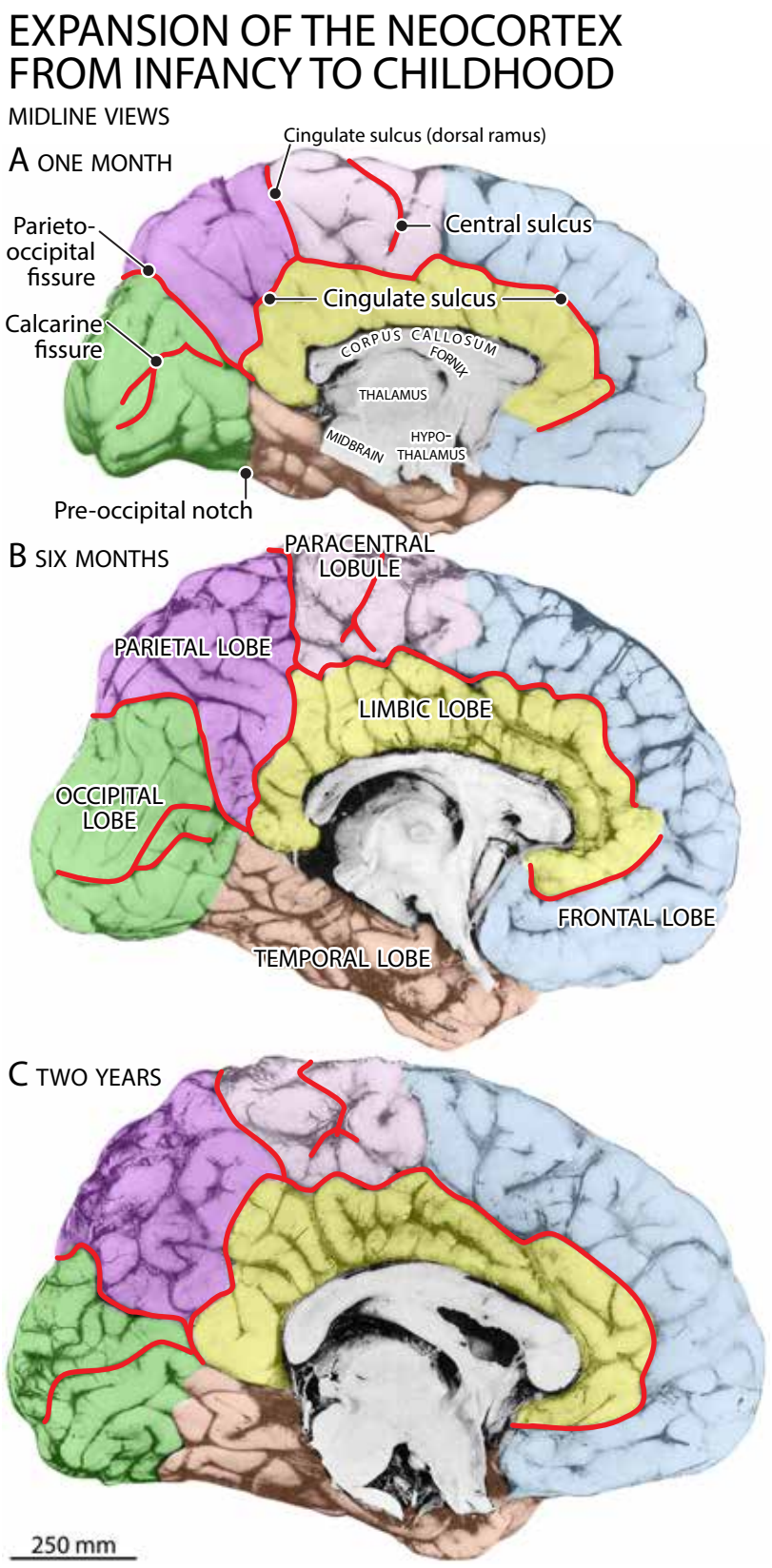
EXPANSION OF THE NEOCORTEX
FROM INFANCY TO CHILDHOOD
MIDLINE VIEWS
A ONE MONTH
Cingulate sulcus (dorsal ramus)
Central sulcus
Parieto-
occipital
fissure
Cingulate sulcus
Calcarine
fissure
CORPUS CALLOSUM
FORNIX
THALAMUS
MIDBRAIN
HYPO-
THALAMUS
Pre-occipital notch
B SIX MONTHS
PARACENTRAL
LOBULE
PARIETAL LOBE
LIMBIC LOBE
OCCIPITAL
LOBE
FRONTAL LOBE
TEMPORAL LOBE
C TWO YEARS
250 mm

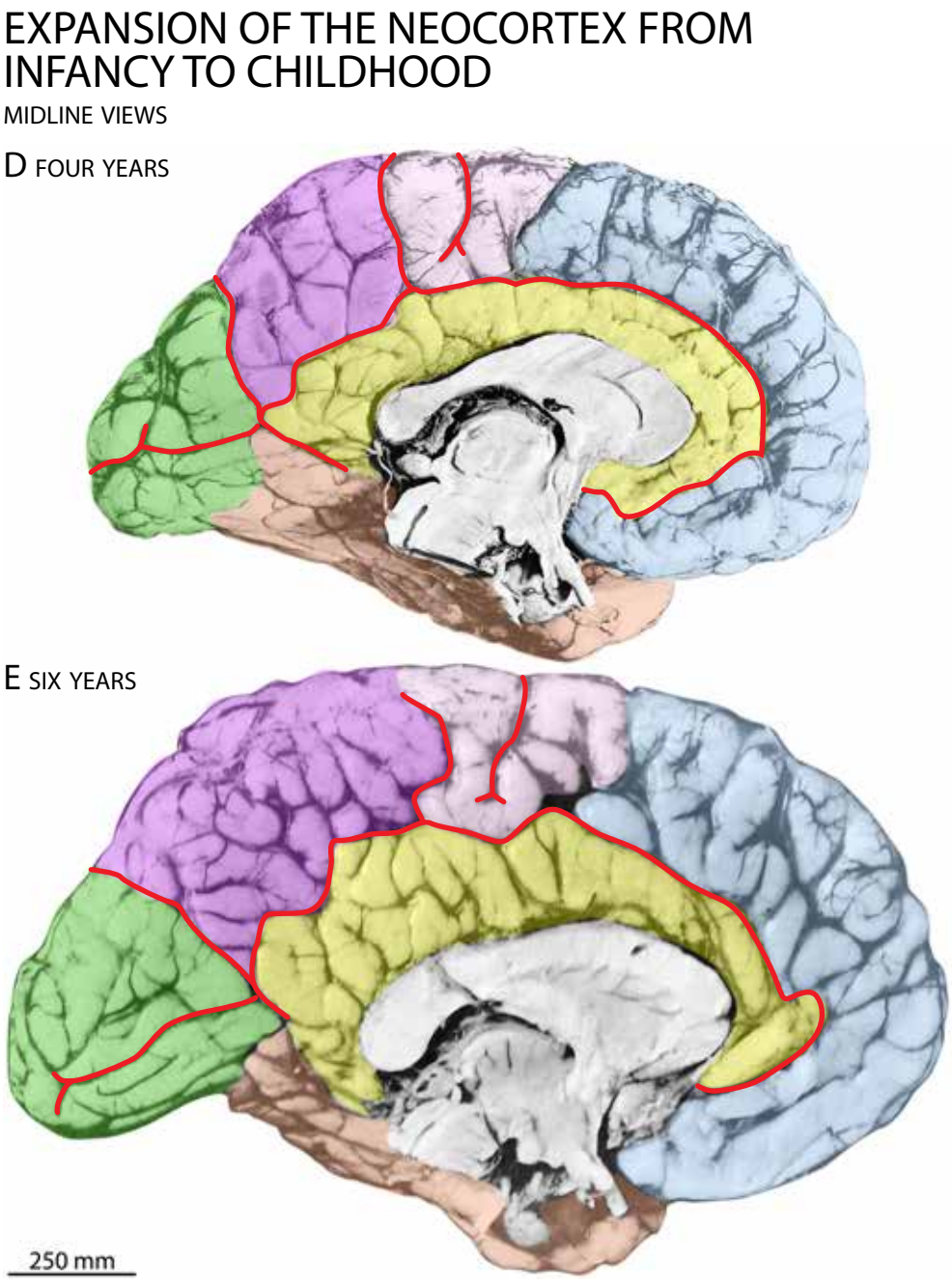

Fig. 42. Medial views of the postnatally expanding neocortex at the following postnatal ages: **A**, 1 month; **B**, 6 months; **C**, 2 years; **D**, 4 years; **E**, 6 years. (From Conel's Figure 4 in volumes 2, 3, 6, 7, and 8).
We colored Conel's photographs to delineate the different lobes: frontal lobe, *blue;* paracentral lobe, *pink*; parietal lobe, *violet*; occipital lobe, *green*; temporal lobe, *orange,* cingulate gyrus, *yellow*.
The delineation of the different lobes has been aided by the preservation of the surface blood vessels. The age-related expansion of the neocortex appears to be most pronounced in the association areas of the frontal and parietal lobes and the cingulate gyrus. Note the age-associated expansion of the corpus callosum.

Figures 43 through 60 (see list on page 108) show neocortical development in the brains of neonates, infants and children. The following text is an abstract of the major changes.

Associated with the expansion of the neocortex during infancy and early childhood is the increase in the number and size of sublobules. Among factors contributing to neocortical expansion are, first, the increase in the number of fibers in the lobes, as illustrated by Conel in material prepared with the Weigert's fiber stain in the auditory cortex (Fig. 43) and, second, the increase in short-distance arcuate fibers between the sublobules, as seen in the motor and somatosensory cortices of the paracentral lobe (Fig. 44). But several other changes also contribute to the expansion of the neocortex. As illustrated in the medial frontal gyrus in material stained to visualize neuronal cell bodies, there is an increase in perikaryal size between infancy and childhood and a decrease in their packing density (Fig. 45). The increase in the volume of the neuropil relative to perikaryal volume (fiber/cell ratio) is attributable to several factors: initially, an increase in the number, caliber and collateralization of cortical afferent and efferent axons; then the increase of association fibers; and finally the proliferation of dendrites, as illustrated in the material impregnated with the Golgi technique (Fig. 46). The apical and basal dendrites of pyramidal neurons are thin and have few branches in the medial frontal gyrus of the one month-old infant. Dendritic branching increases during the following months and reaches its peak at two years of age. A marked characteristic of the dendrites of young children is the immense concentration of small dendritic spines, the sites of axodendritic synapses. There may be a pruning of dendritic spines by 6 years of age.

Neocortical Myelination. Another important facet of neocortical expansion and maturation is myelination. The myelin sheath is a prerequisite for the rapid and coordinated transmission of neural information along axons through a process known as saltatory conduction. Myelination begins with the proliferation of supporting cells that stain for myelin (myelination gliosis); Schwann cells peripherally and oligodendroglia cells centrally. As illustrated in a GW20 fetus, the efferent fibers of the spinal motor neurons in the ventral root are myelinating or are myelinated by the middle of the second trimester, and the afferent fibers of the dorsal root display advanced reactive gliosis (Fig. 47). Myelination takes place earlier in much of the spinal cord and hindbrain and later in the forebrain. Most of the segmental and intersegmental fiber systems display reactive gliosis in the ventral quadrant of the spinal cord during the second trimester. However, the descending fibers of the ventral and lateral corticospinal tracts are free of reactive gliosis. In addition, advanced reactive gliosis is seen dorsally in the ascending afferents of the cuneate funiculus but not yet in the gracile funiculus. By the beginning of the third trimester, as seen in a GW26 fetus, much of the cuneate fasciculus is myelinated and reactive gliosis begins in the gracile funiculus. At the time of birth, as seen in a GW37 specimen, all dorsal column fibers are myelinated but most of the descending fibers of the lateral and ventral corticospinal tract are still unmyelinated. In the newborn (Fig. 48), fiber tracts in the core of the medulla, pons and cerebellum are myelinated but the white matter of the cerebral cortex and the corticospinal tract fibers traversing the pontine gray are still unmyelinated. The descending ventral corticospinal tract is beginning to myelinate in the 1-week-old infant and is myelinated in the 4-months-old infant, but the lateral corticospinal tract is

still unmyelinated (Fig. 49). Reactive gliosis of the lateral corticospinal tract begins during early infancy and its full myelination is not achieved until about 2 years of age.

In his pioneering study of the sequence of myelination in the human cerebral cortex, Paul Flechsig (1896) distinguished three regions: the early myelinating sensory and motor projection areas; the subsequently myelinating association areas; and the late-myelinating higher psychic areas (Fig. 50). Cecilie and Oscar Vogt (1902, 1904) offered a similar interpretation of the progress of neocortical myelination on the basis of their own preparations (Fig. 51). Our photomicrographs of brains in the Yakovlev Collection document the same sequence of myelination as proposed by Flechsig and the Vogts. In Figure 52, a "hot spot" of myelinated fibers in the internal capsule of a 4 week-old infant is associated with spreading myelination gliosis in the paracentral, somatomotor and somatosensory projection areas, while myelination gliosis is absent in the frontal and temporal lobes. In a 6 week-old infant (Fig. 53), myelination gliosis spreads from the internal capsule hot spot into the paracentral lobe dorsally and the occipital lobe posteriorly. Figures 54 through 57 feature the excellent histological material prepared by the Vogts. In a sagittaly-sectioned brain of a 2-months-old infant, the fibers in the thalamus, paracentral gyrus and occipital lobe are myelinating, and there is indication of the spread of myelination gliosis from the midline laterally (Fig. 54); however, the frontal and temporal lobes show little sign of reactive gliosis in this specimen. Figure 55 illustrates the outward spread of reactive gliosis and myelination in 13 coronal sections (anterior to posterior) from the brain of a 2.5-months-old infant. Figure 56 shows a series of 6 sagittal sections (medial to lateral) from the brain of a 3-months-old infant that show the advanced myelination of the white matter in the paracentral lobe and in the internal capsule, with two hot spots there, and the myelination of the visual radiation with a hot spot in the occipital lobe. While the spread of myelination gliosis is evident throughout the parietal lobe, it is only incipient in the frontal and temporal lobes with a medial-to-lateral gradient. The 12 dorsal-to-ventral horizontal sections in Figure 57 from the brain of a 4-months-old infant show that myelination appears to be fully developed in the somatomotor, somatosensory, visual, and auditory projection areas, with reactive gliosis spreading to the adjacent association areas. However, most gyri of the prefrontal cortex and the temporal cortex display only incipient reactive gliosis. In the brain of a 7-months-old child, myelination is far more advanced in the projection and association areas as well as in the posterior frontal lobe and parts of the temporal lobe (Fig. 58). The corpus callosum in this specimen displays reactive gliosis anteriorly, and myelination is in progress posteriorly at the level of the paracentral lobe. We complete this survey with two sagittal sections, one from an 11-months-old child, the other, from a 2-year-old child (Fig. 59). Much of the cortical white matter is myelinated in both specimens, including the corpus callosum, with the exception of the white matter in some of the frontal gyri. The last figure in this series highlights delayed myelination in the descending corticofugal fibers from the motor cortex. They are unmyelinated in the pontine gray in a newborn, which is in contrast to many of the ascending, regional, and descending fiber systems in the medulla and spinal cord (Fig. 60A). Some transpontine corticofugal fibers are myelinated in a 1.5 months-old infant (Fig. 60B), and the bulk of pontine corticofugal fibers are myelinated in an 8-months-old and a 2-years-old specimen (Fig. 60C,D)

ANNOTATED ILLUSTRATIONS OF NEONATE, INFANT, AND CHILDHOOD BRAINS

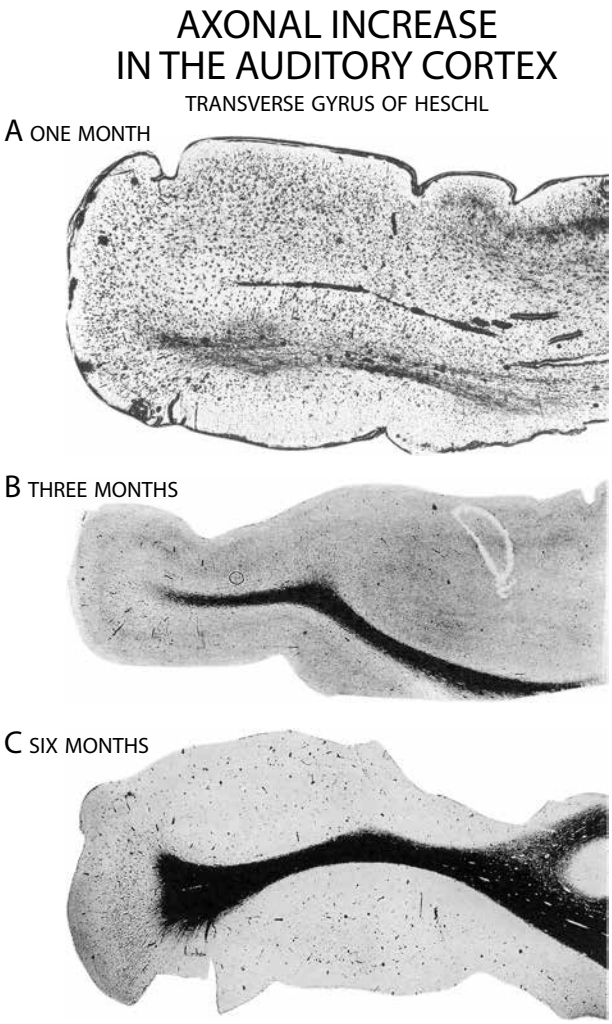

Fig. 43. Increase in the concentration of axons in the medullary layer of the primary auditory cortex in the transverse gyrus of Heschl, in infants aged 1 month (**A**), 3 months (**B**), and 6 months (**C**). Weigert fiber stain. (From Conel, Vol. 2, Fig. 210; Vol. 3, Fig. 219; Vol. 4, Fig. 224).

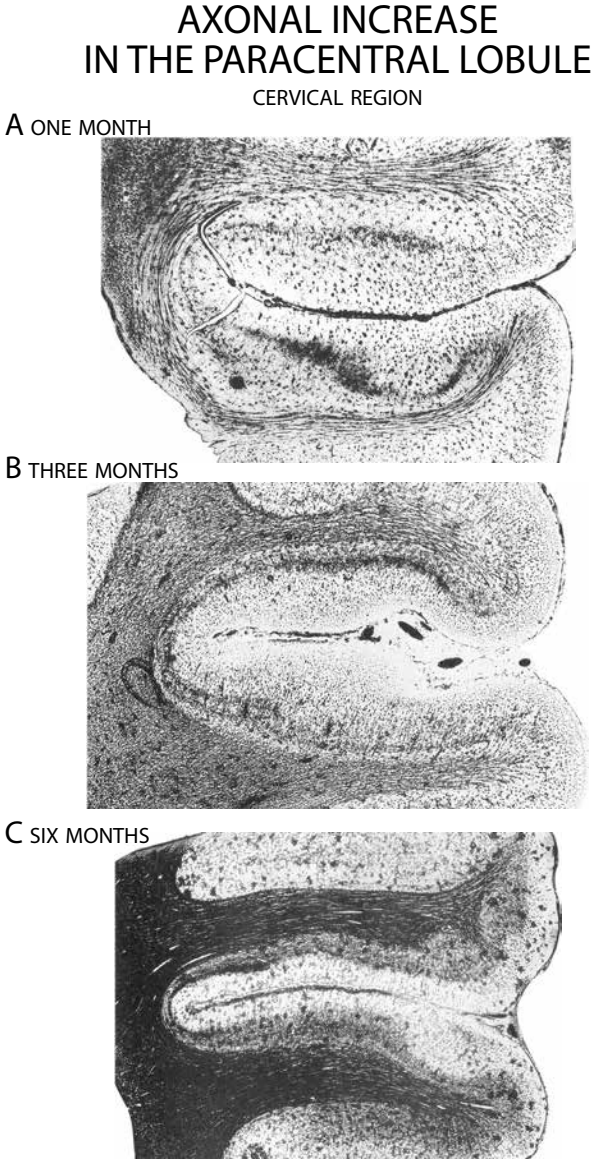

Fig. 44. Increase in the concentration of axons in the precentral and postcentral gyri (the somatomotor and somatosensory cortices) in infants aged 1 month (**A**), 3 months (**B**), 6 months (**C**). Weigert fiber stain. (From Conel, Vol. 2, Fig 206; Vol.3, Fig. 196; Vol. 4, Fig. 197).

Fig. 45 (on the following 3 pages). Photomicrographs of the cortical gray matter in the medial frontal gyrus stained for cell bodies (perikarya) at several postnatal ages. The neuronal cell bodies are relatively small in the early postnatal months but increase in size thereafter in association with a decrease in perikaryal packing density. The expansion of the neuropil is attributable to the space occupied by non-staining axons and dendrites.

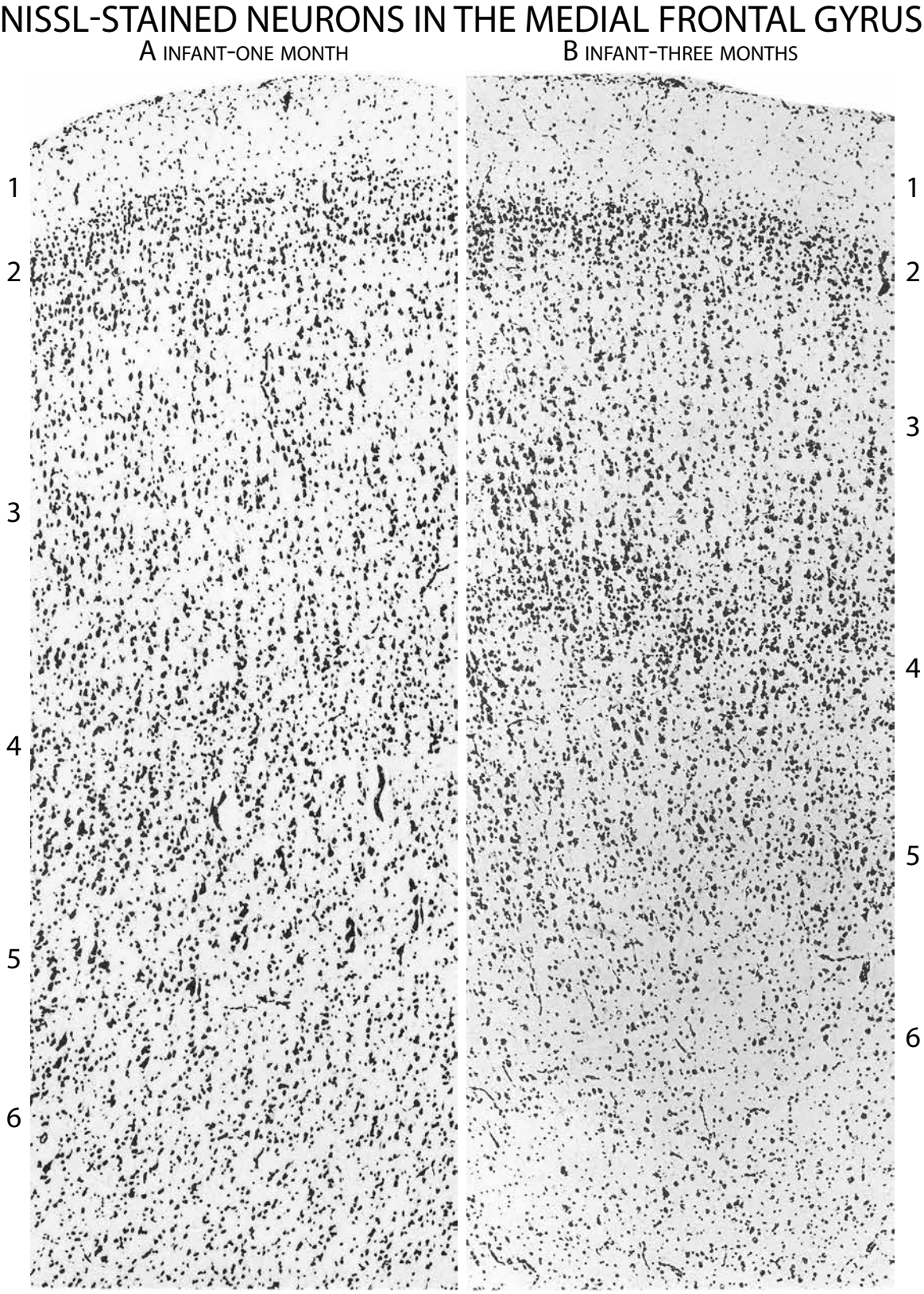

Fig. 45A. 1 month, (From Conel, Vol. 2, Fig. 59)

Fig. 45B. 3 months,. (From Conel, Vol. 3, Fig. 25)

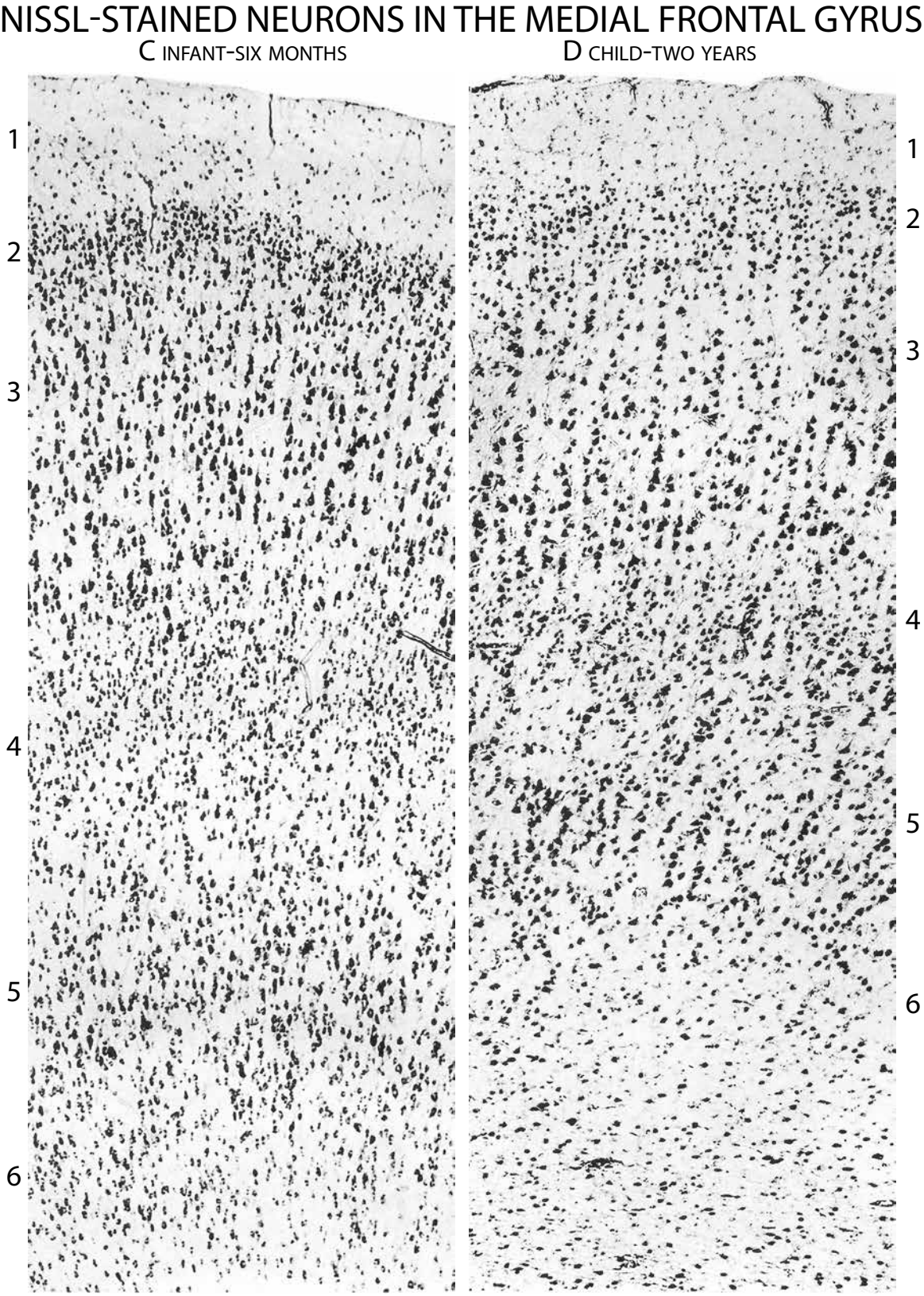

Fig. 45C. 6 months. (From Conel, Vol. 4, Fig. 49)

Fig. 45D. 2 years (From Conel, Vol. 6, Fig. 37)

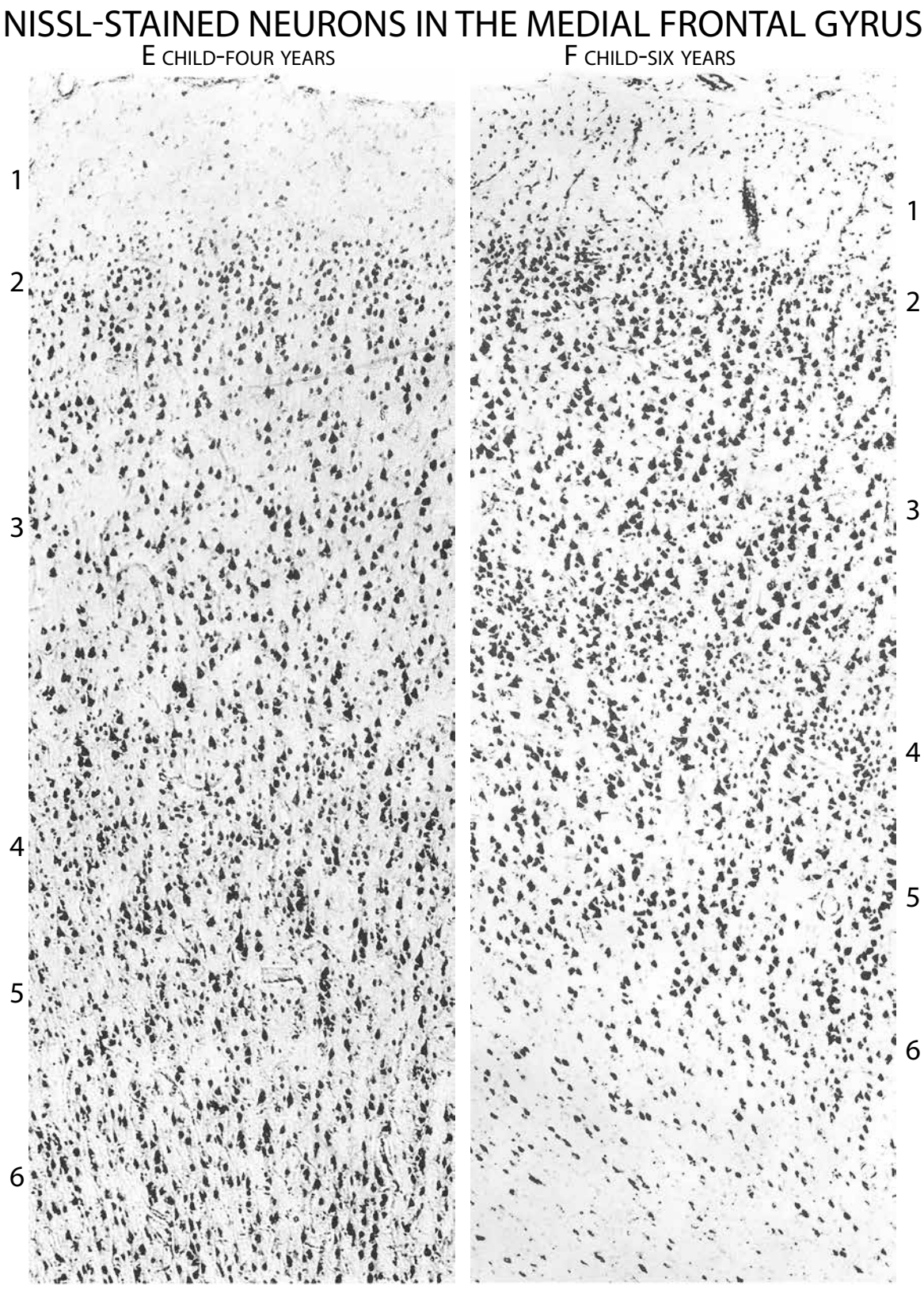

Fig. 45E. 4 years (From Conel, Vol. 7, Fig. 25).

Fig. 45F. 6 years (From Conel, Vol. 8, Fig. 25).

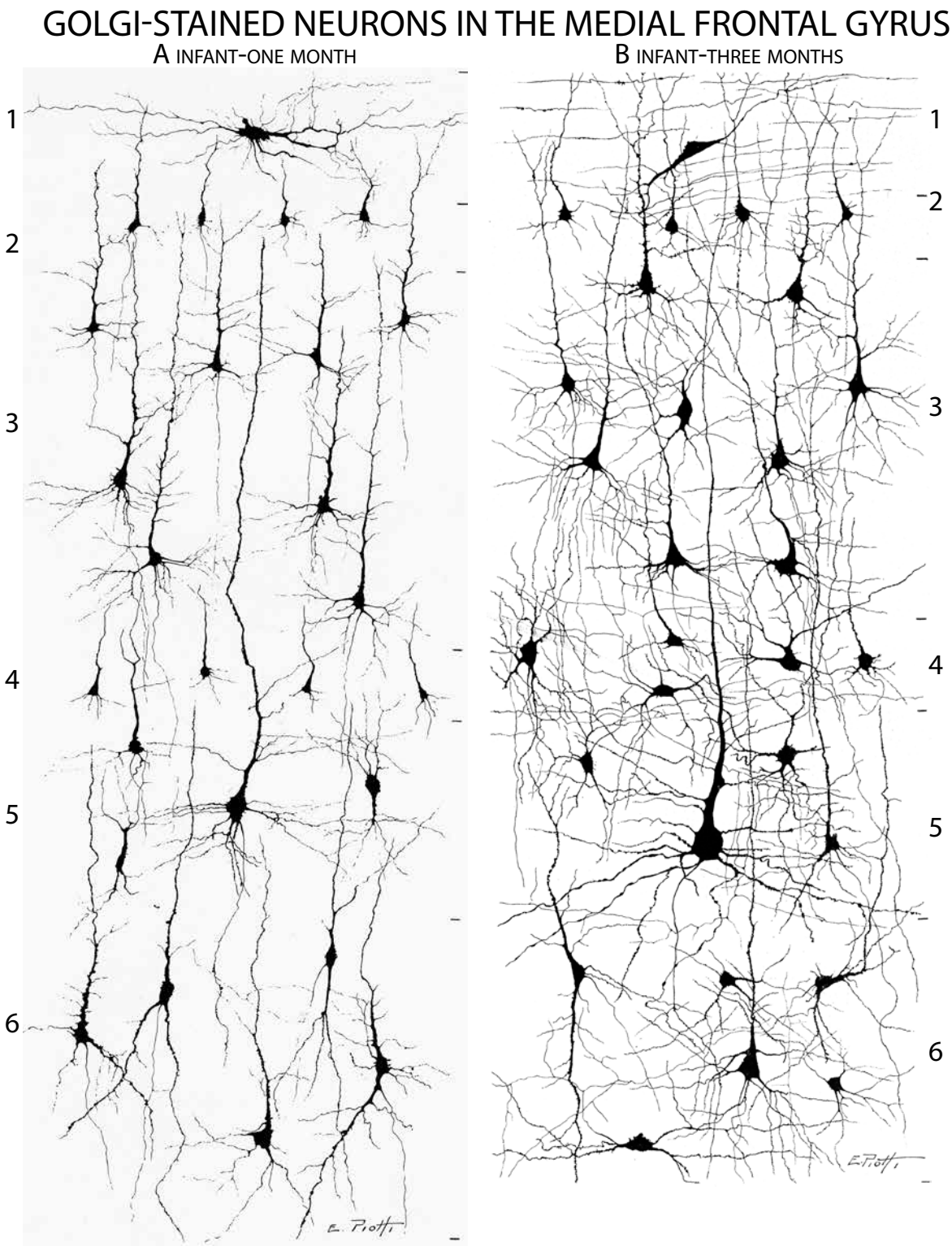

Fig. 46 (on this and the following 2 pages). Camera lucida drawings of Golgi-impregnated neurons and their processes in the medial frontal gyrus at several postnatal ages. There is a progressive increase in the branching and thickening of the apical and basal dendrites, and in the proliferation of dendritic spines, a site of axodendritic synapses, through infancy and early childhood. **A .** 1 month (From Conel, Vol. 2, Fig.62) **B.** 3 months (From Conel, Vol. 3, Fig. 28).

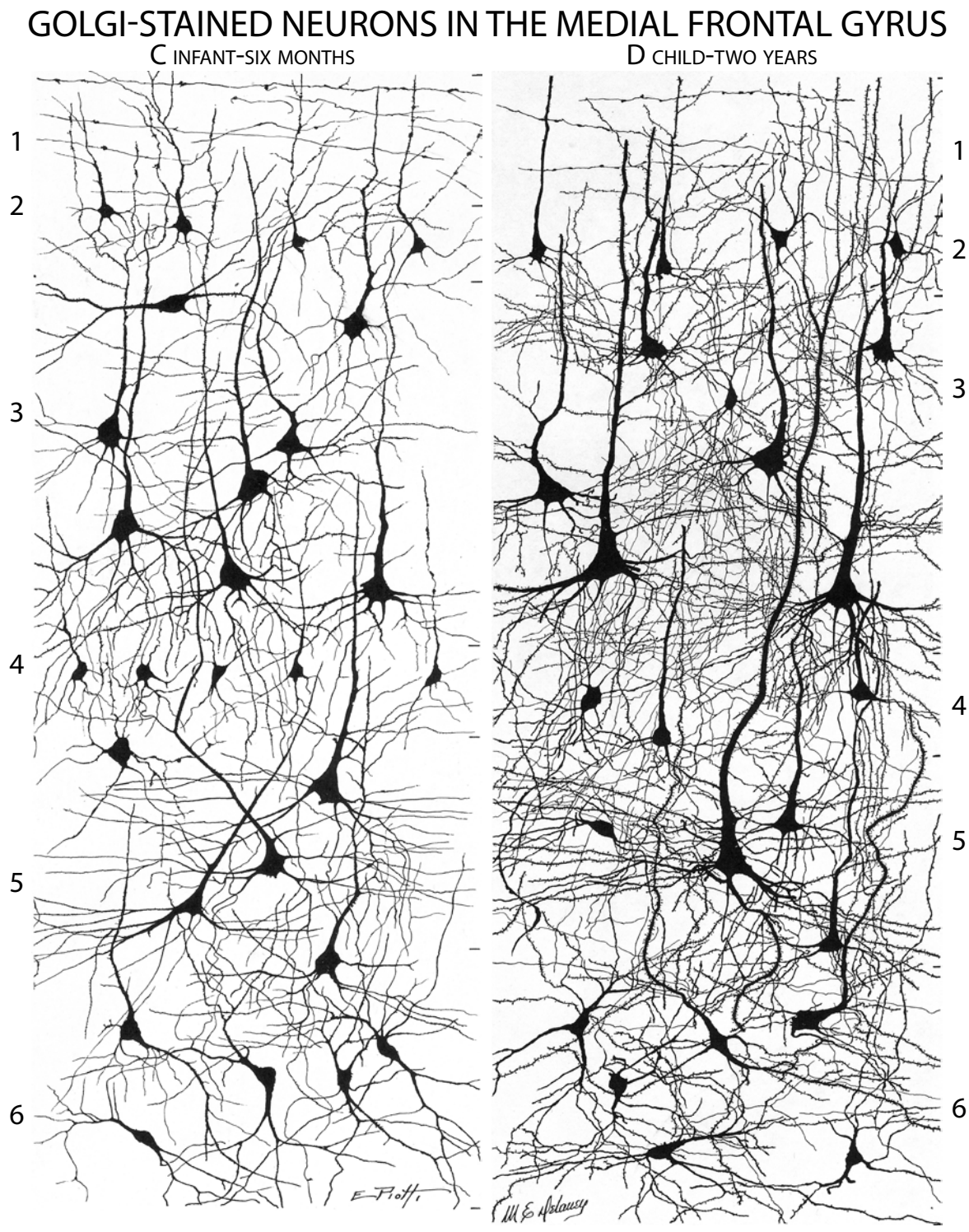

Fig. 46C. 6 months (From Conel, Vol. 4, Fig. 52).

Fig. 46D. 2 years (From Conel, Vol. 6, Fig. 40).

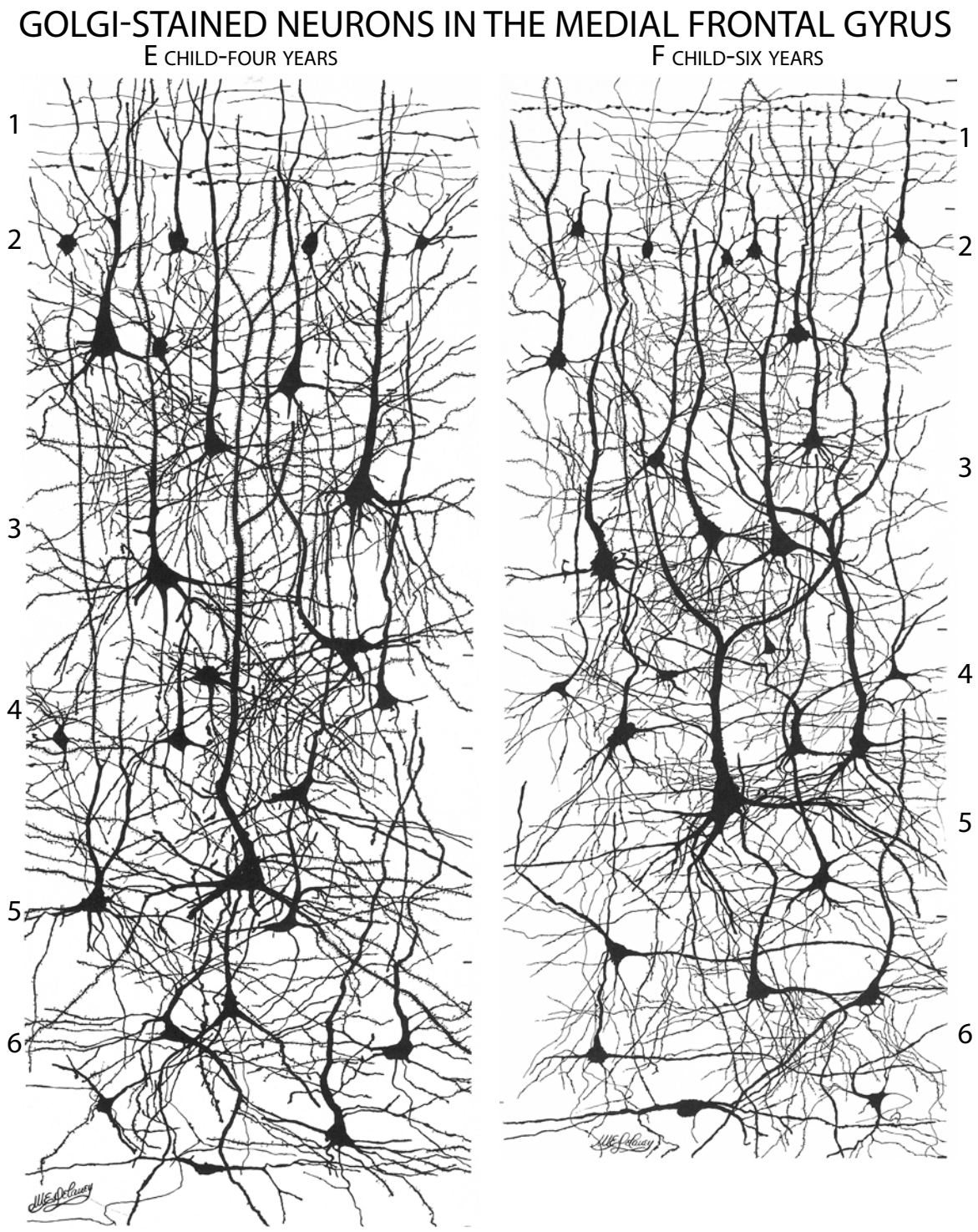

Fig. 46E. 4 years (From Conel, Vol. 7, Fig. 28).

Fig. 46F. 6 years (From Conel, Vol. 8, Fig. 28).

REACTIVE GLIOSIS AND MYELINATION IN THE SPINAL CORD

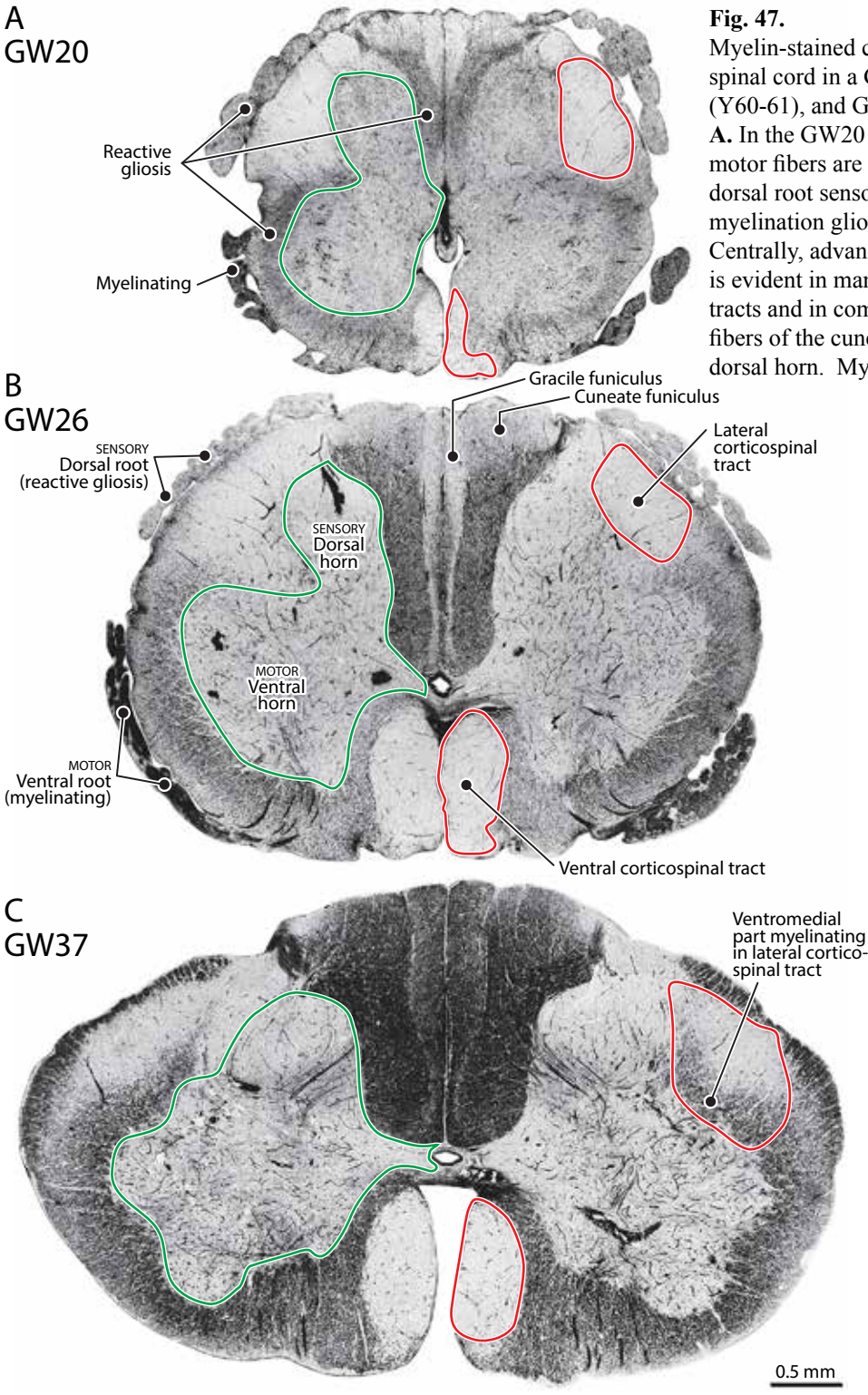

Fig. 47.
Myelin-stained coronal sections of the spinal cord in a GW20 (Y27-60), GW26 (Y60-61), and GW37 (Y117-61) fetuses. **A.** In the GW20 fetus, the ventral root motor fibers are myelinating and the dorsal root sensory fibers are undergoing myelination gliosis peripherally. Centrally, advanced myelination gliosis is evident in many of the ventral fiber tracts and in components of the ascending fibers of the cuneate funiculus in the dorsal horn. Myelination gliosis has not yet begun in the descending fibers of the lateral and ventral corticospinal tracts. **B**. In the GW26 fetus, the fibers of the cuneate funiculus are myelinating, as are components of the gracile funiculus, but myelination gliosis has not yet begun in the corticospinal tracts. **C**. In the GW37 fetus, virtually all components of the spinal cord white matter are myelinated, except for most of the fibers in the corticospinal tracts. The lateral corticospinal tract is beginning to myelinate in its ventromedial part.

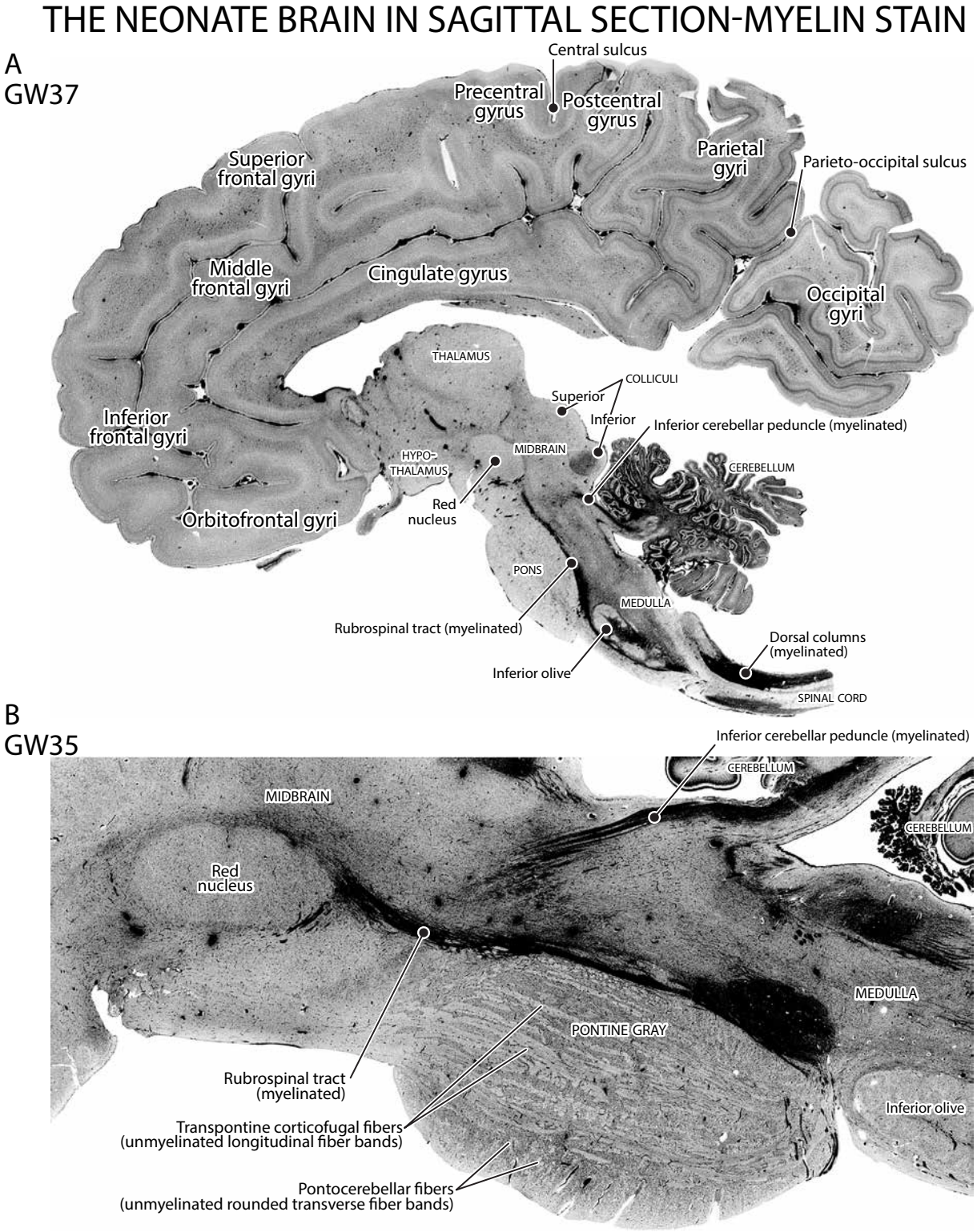

Fig. 48. A. Photomicrograph of a myelin-stained sagittal section of the brain of a neonate (Y62-61). Note the presence of myelin-stained (opaque) fibers in the cerebellum, medulla and spinal cord and their absence in the neocortex and the thalamus. **B**. The pontine region at higher magnification in another neonate (Y235-66). Unlike fibers of the inferior cerebellar peduncle and the rubrospinal tract, the descending corticospinal fibers traversing the pontine gray and the pontocerebellar fibers are unmyelinated.

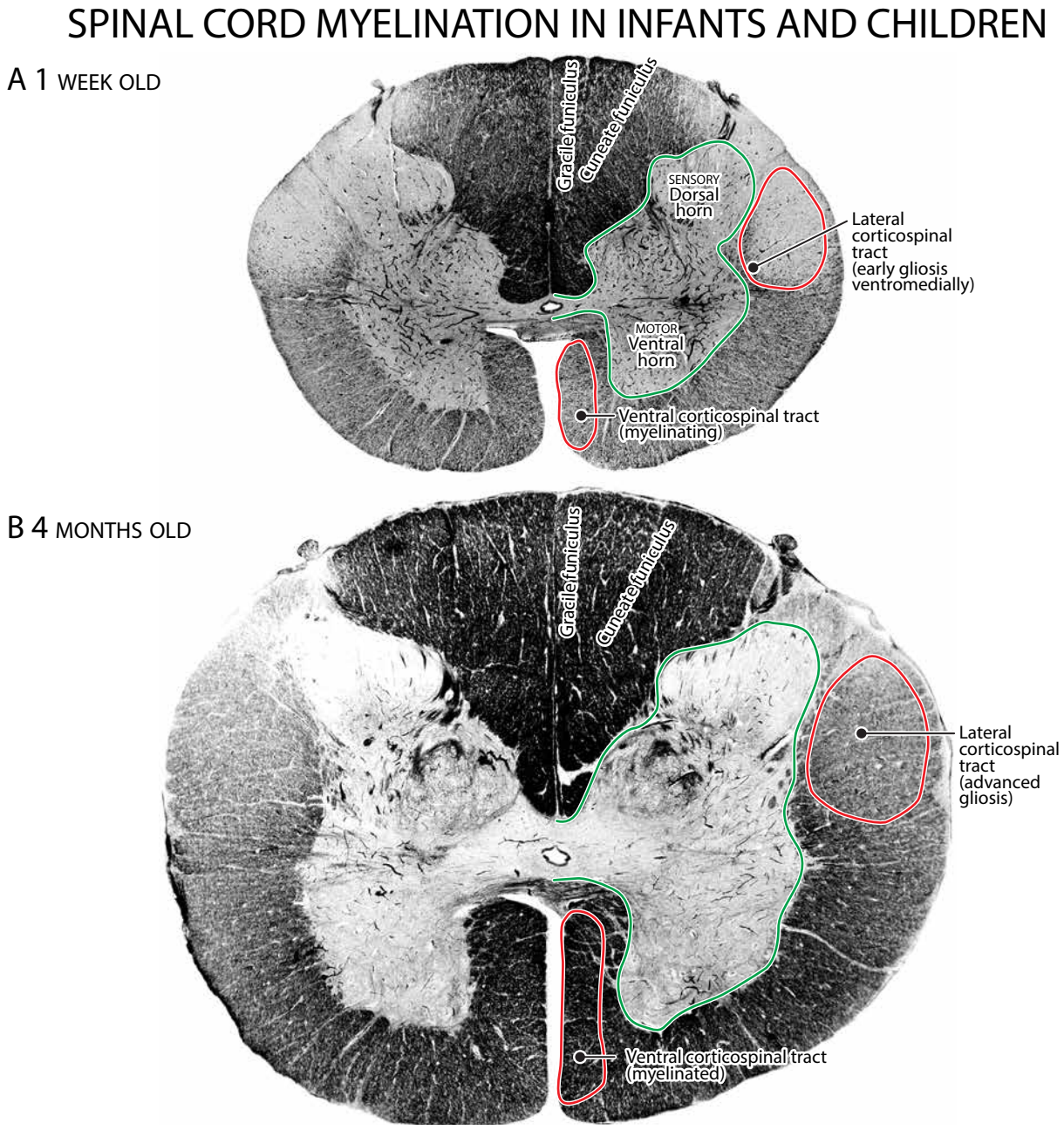

Fig. 49 (facing pages). Myelin-stained sections of the spinal cord. The fibers of the ipsilaterally projecting ventral corticospinal tract are myelinated in all these specimens. In contrast, the lateral corticospinal tract displays reactive gliosis in the infants, followed by its myelination in the toddler and young child.
A, a 1-week-old (Y23-60) infant;
B, a 4-months-old infant (Y286-62);
C, an 11-months-old (Y132-61) toddler;
D, a 2-year-old (Y425-63) child.

SPINAL CORD MYELINATION IN INFANTS AND CHILDREN

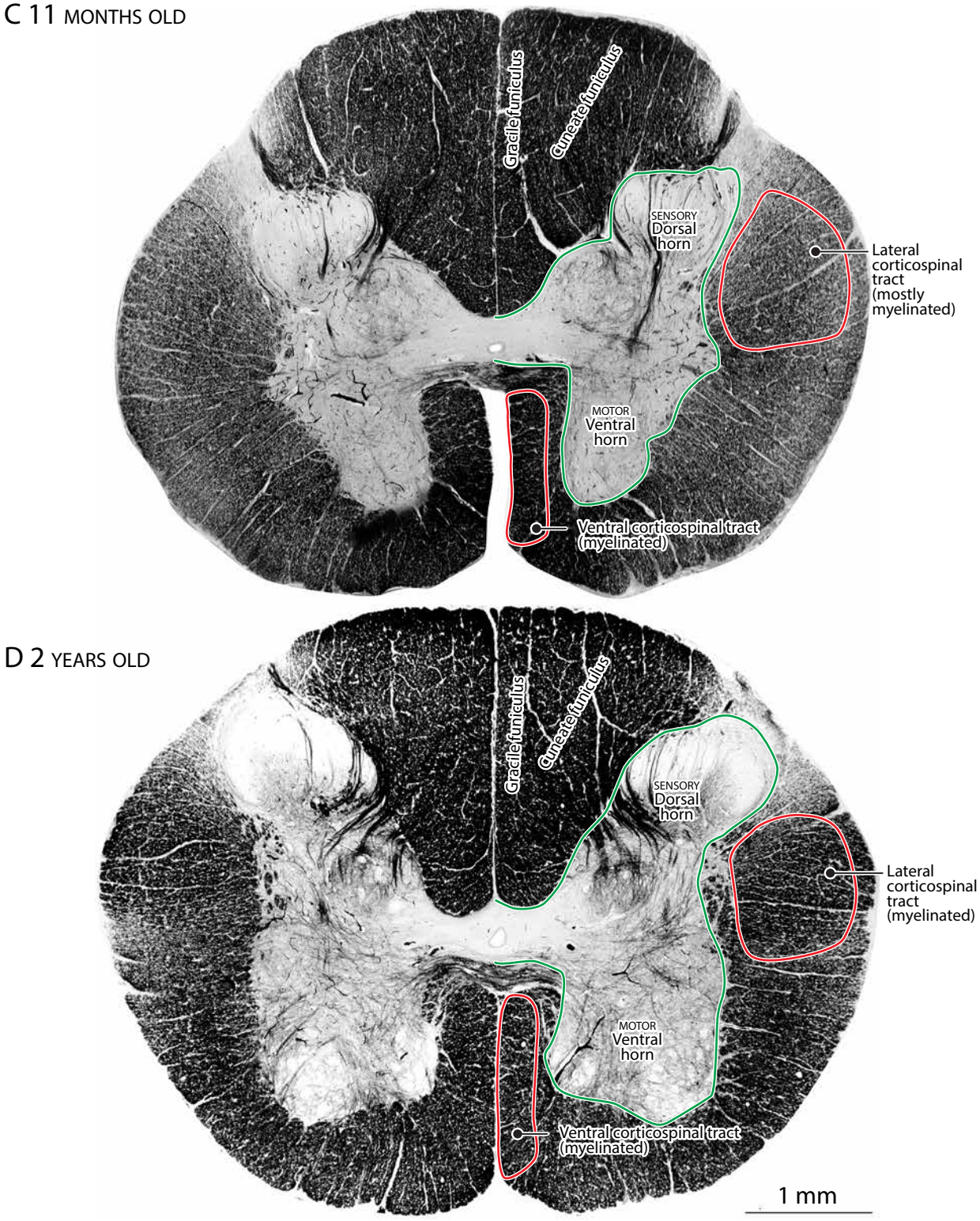

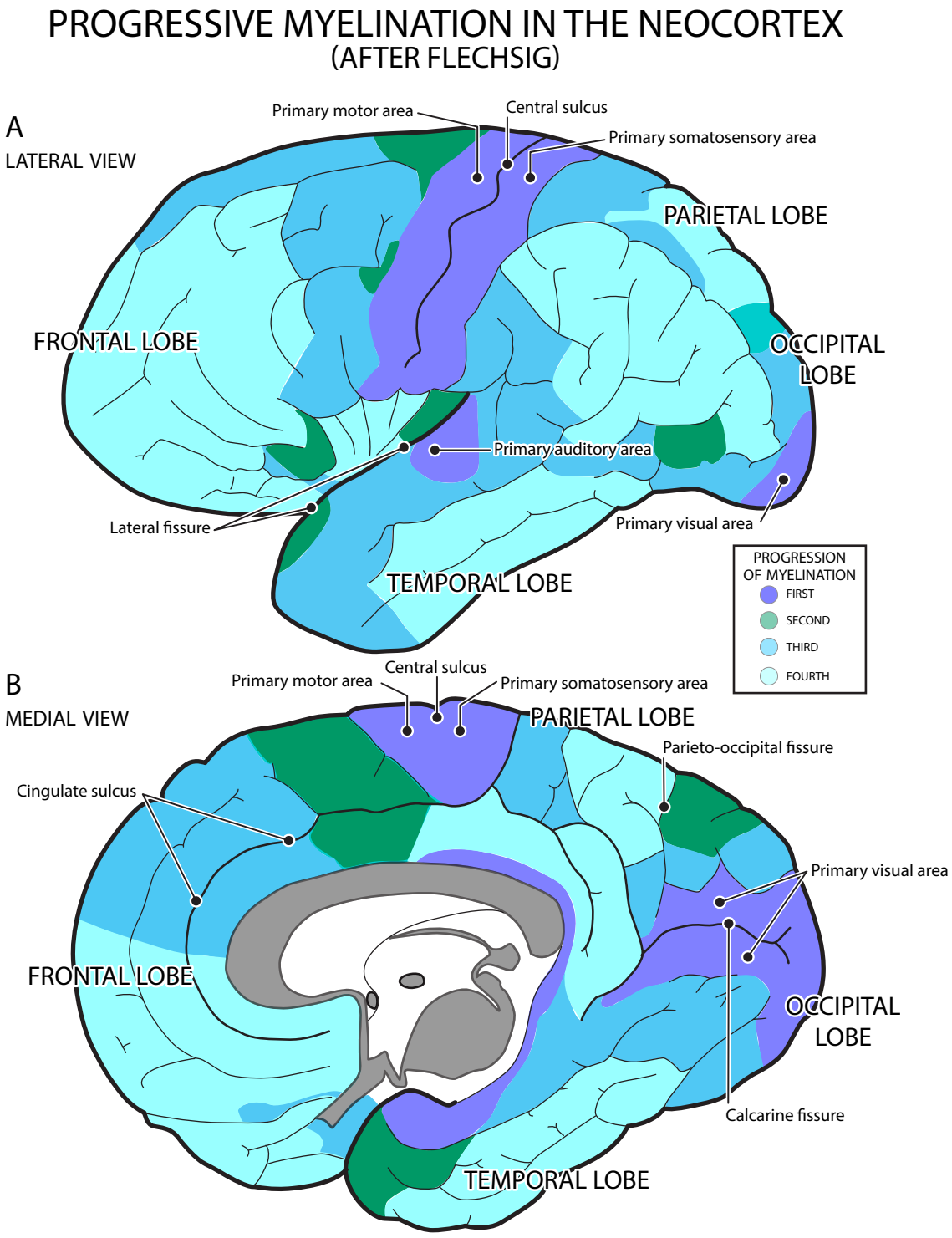

Fig. 50. The temporal sequence of myelination, according to Flechsig, in the lateral (**A**) and medial (**B**) aspect of the neocortex. *Purple*: primary projection areas. *Green and dark blue*: association areas. *Light blue*: higher-order integrative areas. Modified, after Ariëns Kappers et al. (1936).

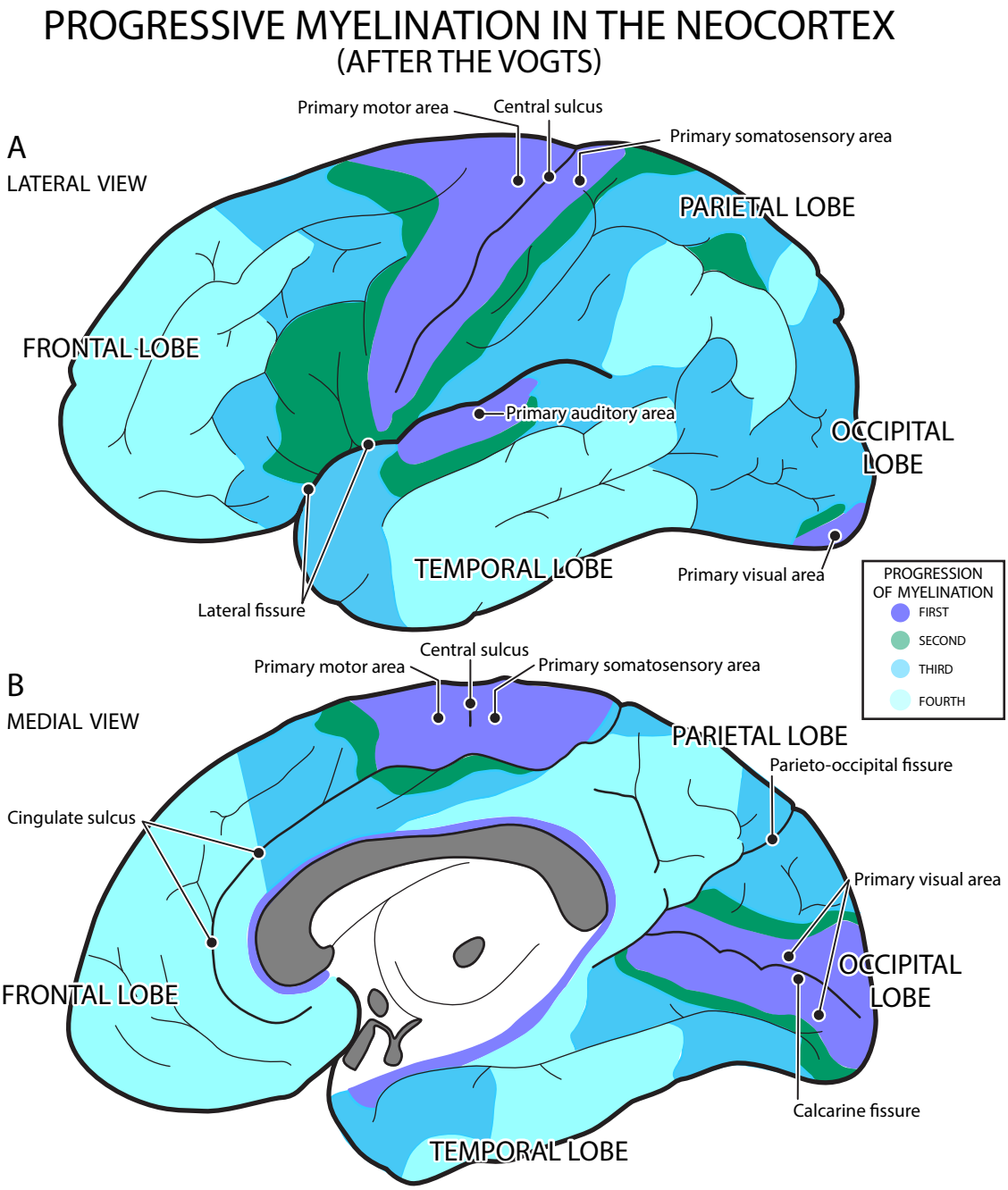

Fig. 51. The sequence of myelination, according to the Vogts, in the lateral (**A**) and medial (**B**) aspect of the neocortex. *Purple*: primary projection areas. *Green and dark blue*: association areas. *Light blue*: higher-order integrative areas. Modified, after Ariëns Kappers et al. (1936).

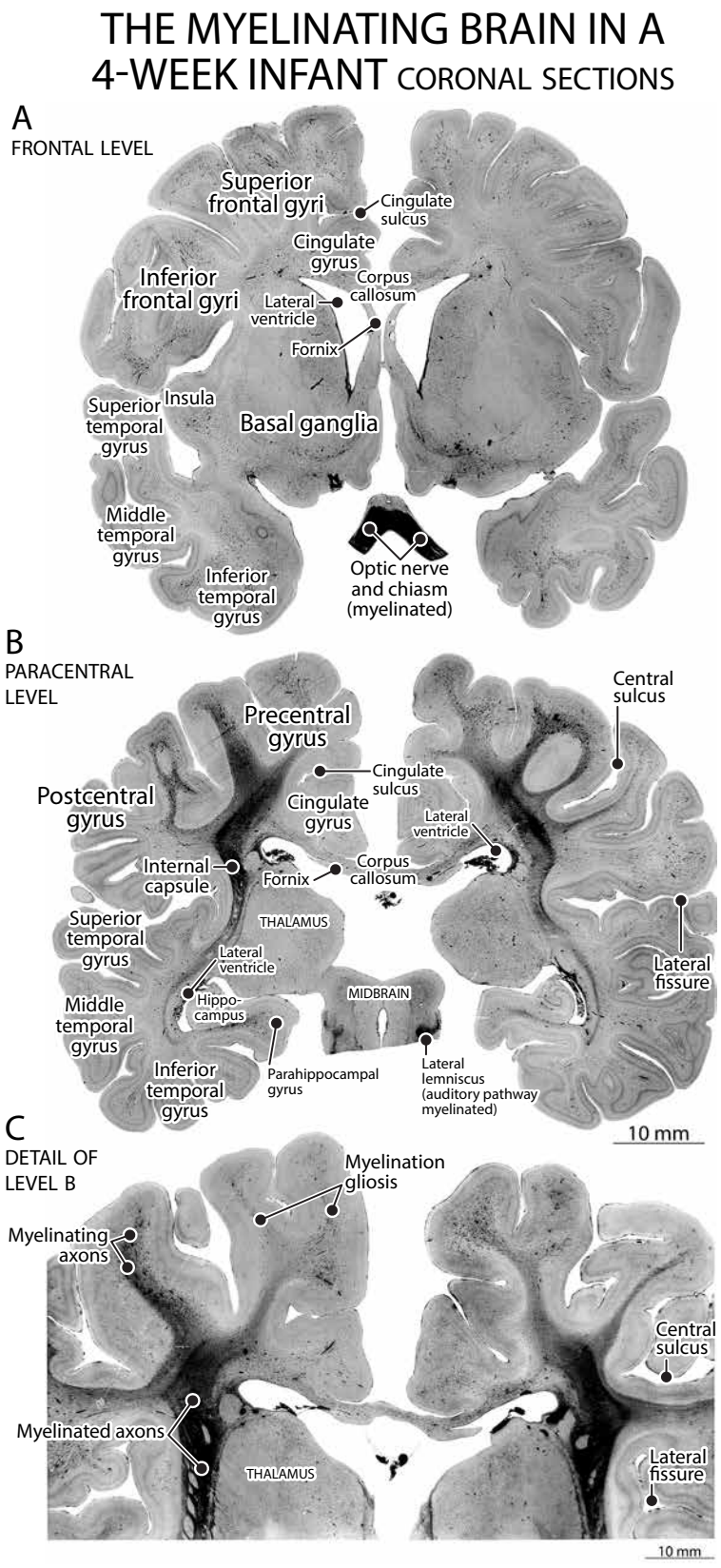

Fig. 52. Photomicrographs of myelin-stained coronal sections of the brain of a 4-weeks-old infant (Y28-60).
A. Anteriorly in a section through the frontal lobe and basal ganglia, the fibers of the optic nerve and chiasm (bottom) are myelinated. But corticofugal fibers traversing the basal ganglia and the fibers crossing in the corpus callosum are unmyelinated.
B. More posteriorly, at the level of the paracentral lobe and the thalamus, the fibers of the internal capsule are myelinated and lightly staining fibers spread from this "myelination hot spot" dorsally into the paracentral lobe and ventrally into the temporal lobe. More distally, the darkly stained specks are interpreted as indicative of myelination gliosis, a stage preceding the myelination of axons.
C. A higher magnification photo-micrograph showing the reactive specks and fragments preceding the spread of myelination from the hot spot.

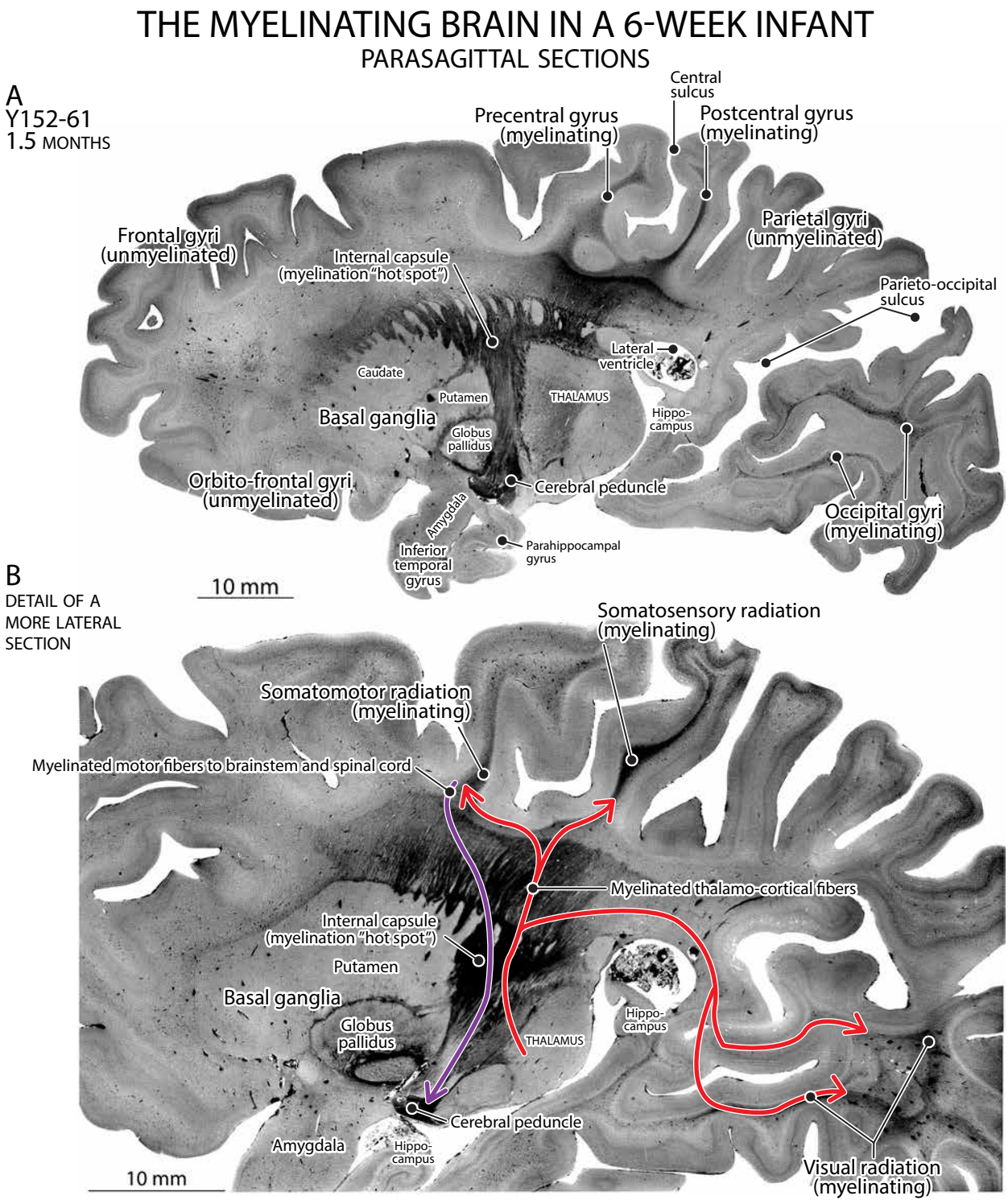

Fig. 53. Photomicrographs of myelin-stained parasagittal sections from the brain of a 6-weeks-old infant (Y152-61) at a lower (**A**) and a higher magnification (**B**), showing the spread of the "myelination hot spot" from the telencephalic-diencephalic junction to the corticofugal fibers traversing the basal ganglia, and to the somatomotor and somatosensory projection areas. Myelination is also spreading along the dorsal and ventral components of the optic radiation to the occipital lobe. Note the absence of myelination in the frontal and parietal lobes.

THE MYELINATING BRAIN IN A 2-MONTH INFANT

PARASAGITTAL SECTIONS

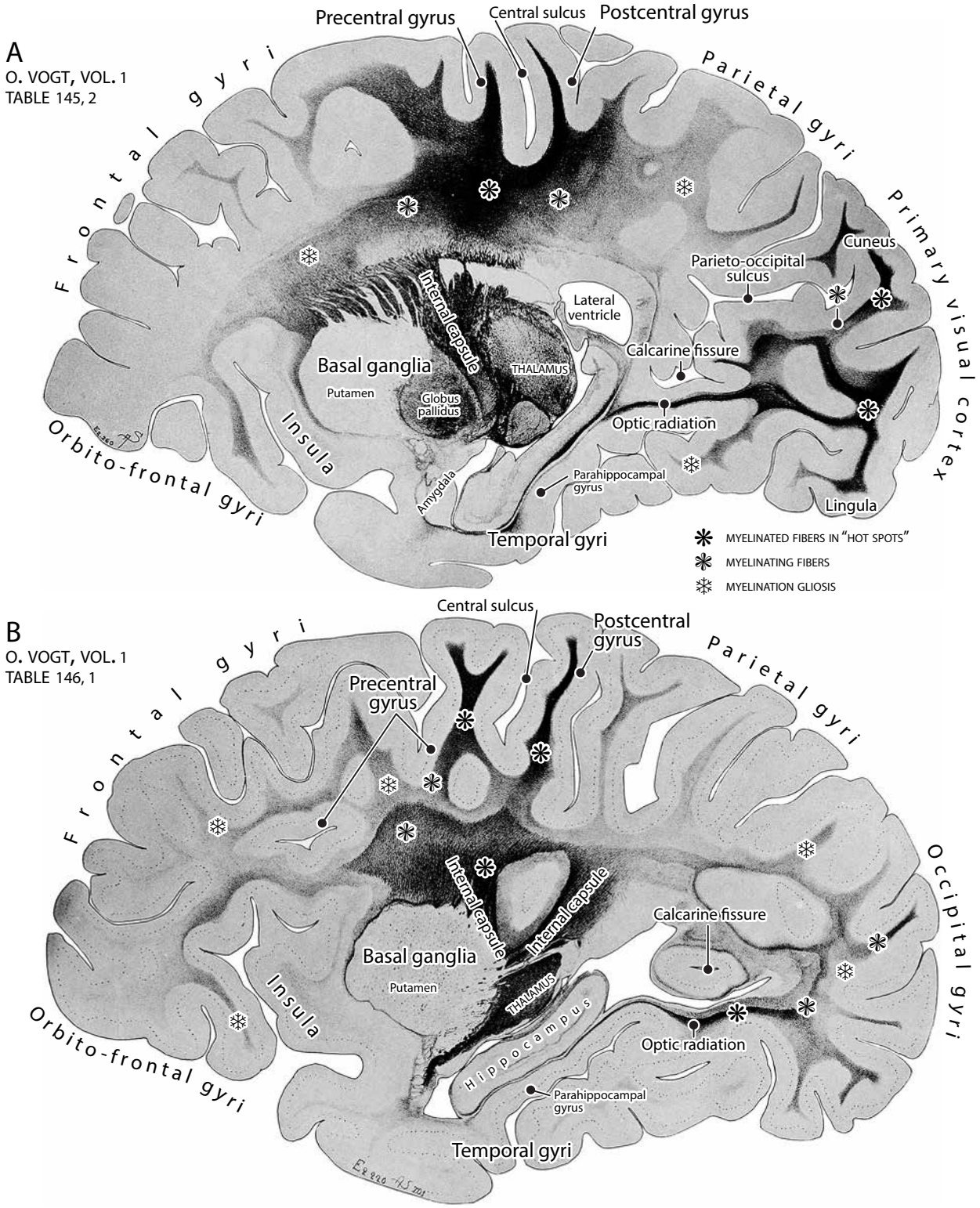

Fig. 54 (facing page). Myelin-stained parasagittal sections of the brain of a 2 months-old infant (brain E2, the Vogts' collection) from medial (**A**) to lateral (**B**). Three regions may be distinguished that are indicated by three different *asterisks*. (i) Opaque regions and those with recognizable myelinated axons cut longitudinally or transversely. These are spreading from "hot spots" (*first asterisk*) in the internal capsule at the telencephalic-diencephalic junction to myelinating fibers in the projection areas (*second asterisk*) of the motor, somatosensory and visual cortices, and to the basal ganglia and the thalamus. (ii) Speckled regions (*third asterisk*) in the proximal region of the frontal, parietal and temporal lobes, reflecting oligodendrocytes undergoing myelination gliosis. (iii) Regions devoid of stained cells (*no asterisks*) in the distal regions of the frontal and temporal lobes, interpreted as areas not yet mature enough to undergo myelination.

Fig. 55 (on the following 8 pages). 13 myelin-stained coronal sections from the brain of a 2.5 months-old infant (E13, Vogts' collection) from anterior to posterior. As in **Fig. 54**, various degrees of myelinatin are indicated by 3 different *asterisks*: myelinated axons (*asterisk 1*), myelinating axons (*asterisk 2*), myelination gliosis (*asterisk 3*). Unmyelinated fibers have *no asterisk* designation.

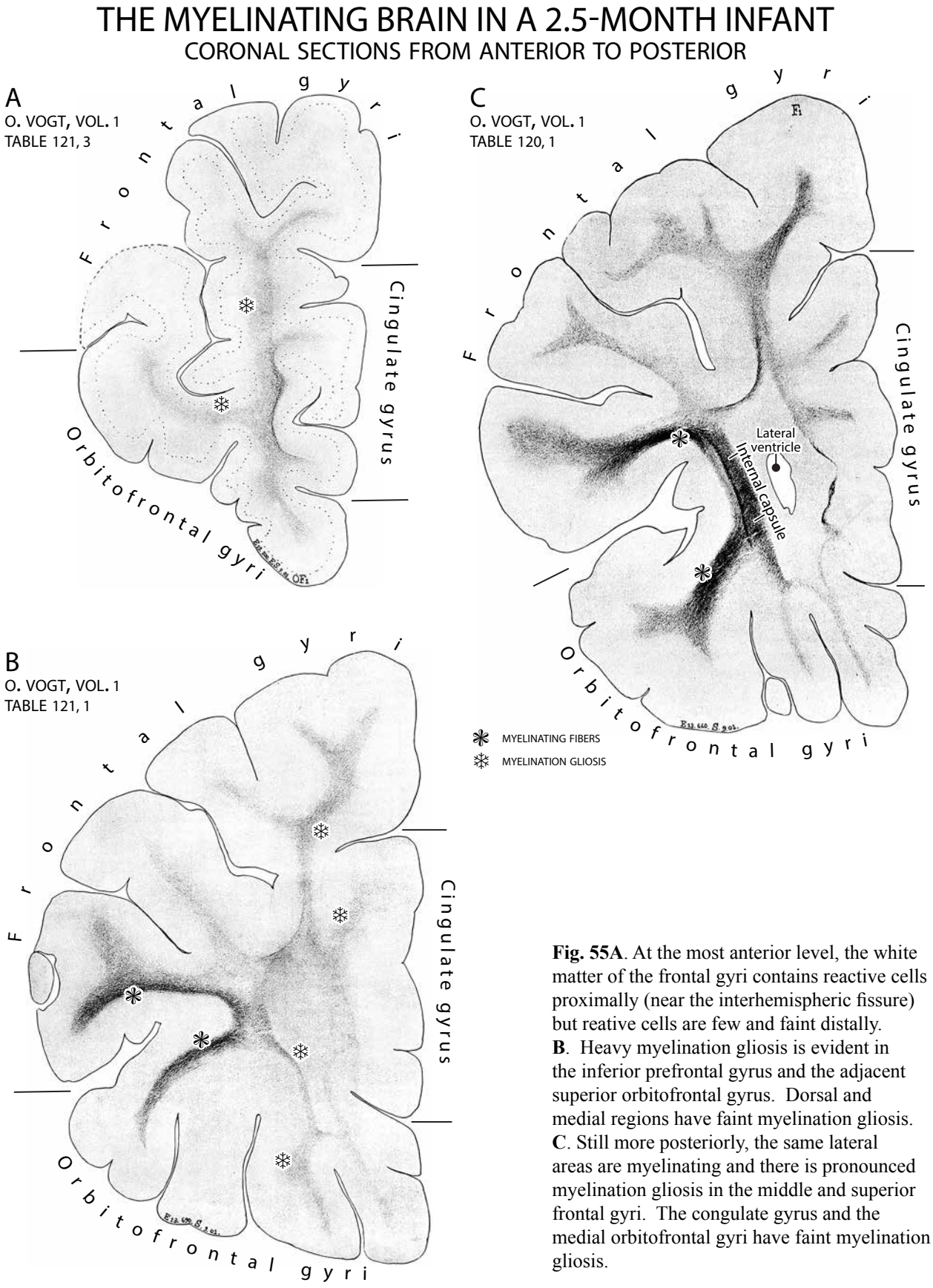

Fig. 55A. At the most anterior level, the white matter of the frontal gyri contains reactive cells proximally (near the interhemispheric fissure) but reative cells are few and faint distally. **B**. Heavy myelination gliosis is evident in the inferior prefrontal gyrus and the adjacent superior orbitofrontal gyrus. Dorsal and medial regions have faint myelination gliosis. **C**. Still more posteriorly, the same lateral areas are myelinating and there is pronounced myelination gliosis in the middle and superior frontal gyri. The congulate gyrus and the medial orbitofrontal gyri have faint myelination gliosis.

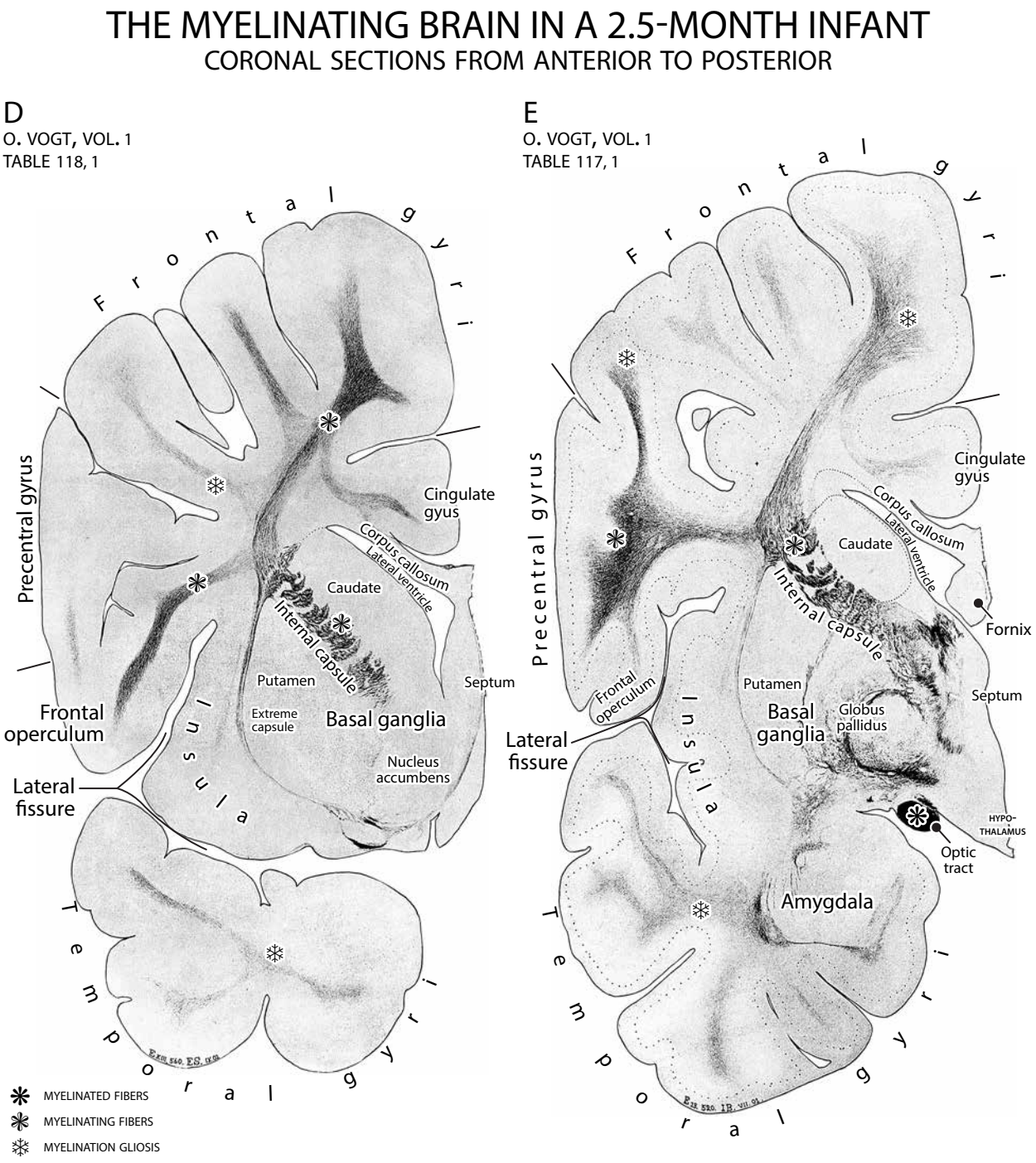

Fig. 55D and **E**. Proceeding back towards the paracentral region, myelination is in progress in the precentral somatomotor gyrus, in the superior frontal gyrus, and in the internal capsule. Note the myelinated fibers in the optic tract (**E**).

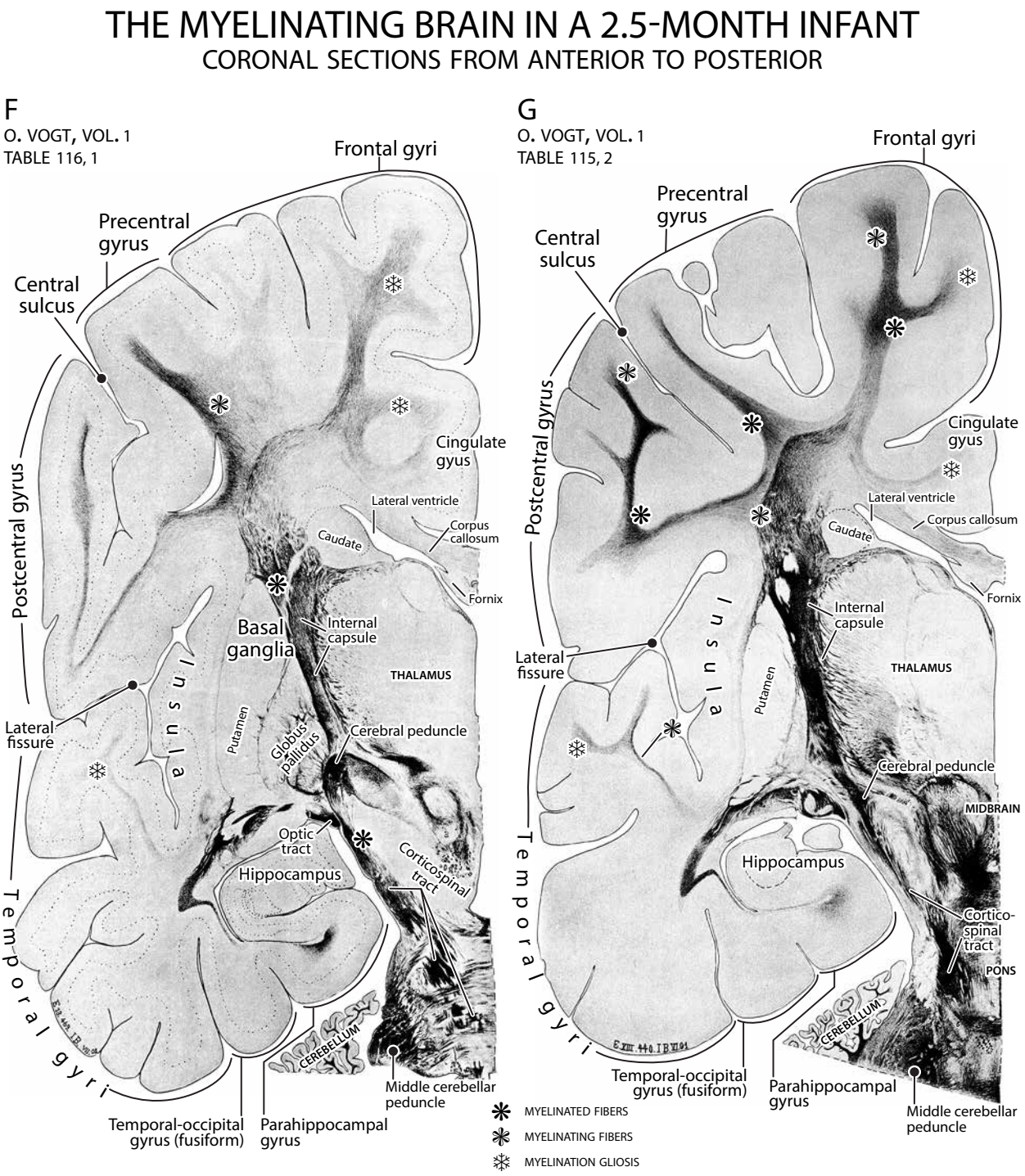

Fig. 55F and **G**. Myelinated fibers are in the somatomotor precentral gyrus and the somatosensory postcentral gyrus. Myelinated corticofugal fibers can be followed from the internal capsule to the cerebral peduncle and the corticospinal tract traversing the pons. Note the lack of myelination gliosis in the basolateral temporal lobe.

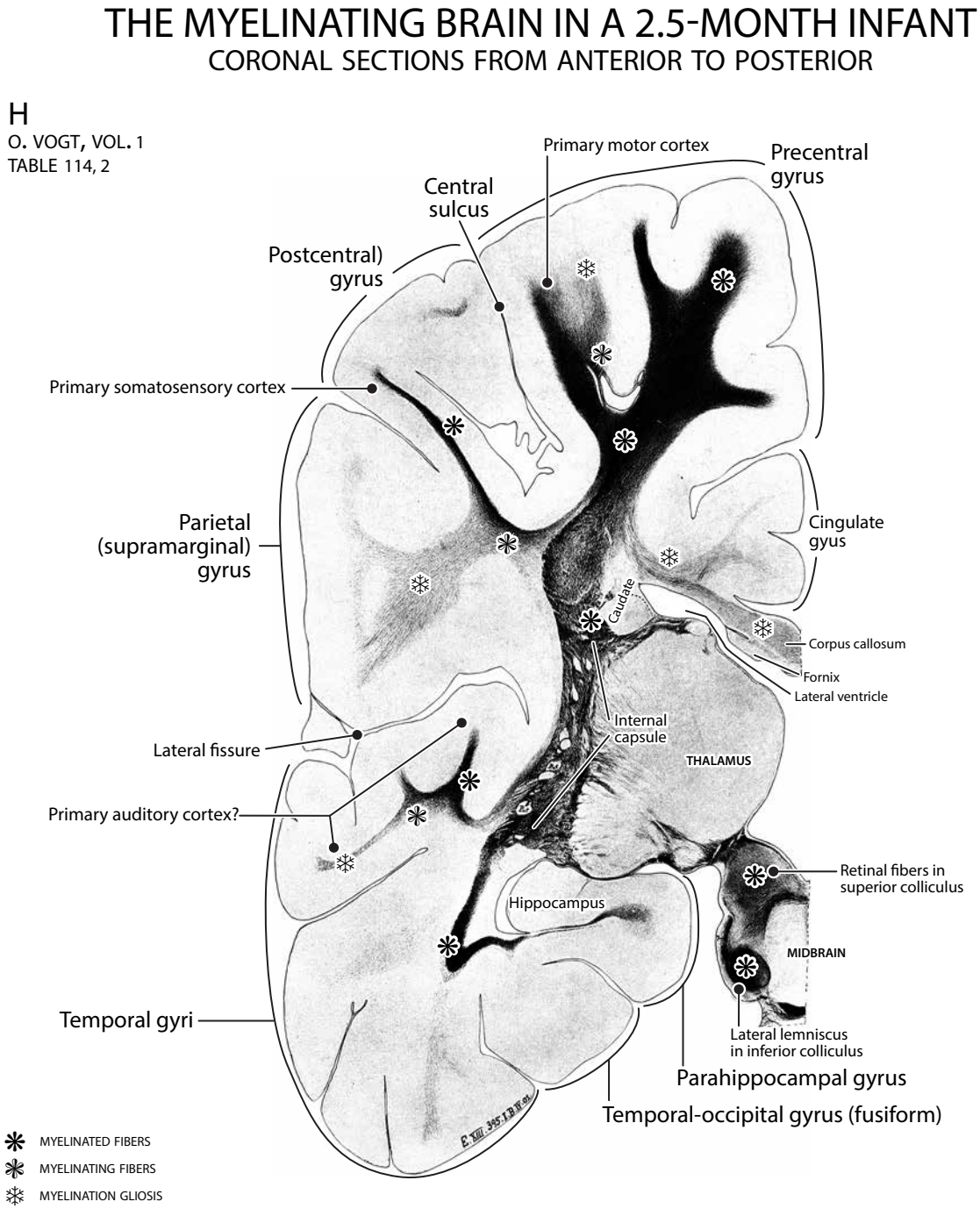

Fig. 55H. This section contains the most myelinated fibers. Hot spots in the internal capsule radiate into myelinated fibers in the precentral gyrus, postcentral gyrus, and the presumptive primary auditory cortex in the superior temporal gyrus. The myelinated fibers circumventing the hippocampus may be part of the visual radiation. Note that the superior colliculus is full of myelinated fibers (retinal fibers from the optic tract). The lateral lemniscus is heavily myelinated as it enters the inferior colliculus. Thus, all the primary sensory and primary motor areas are the first to be myelinated.

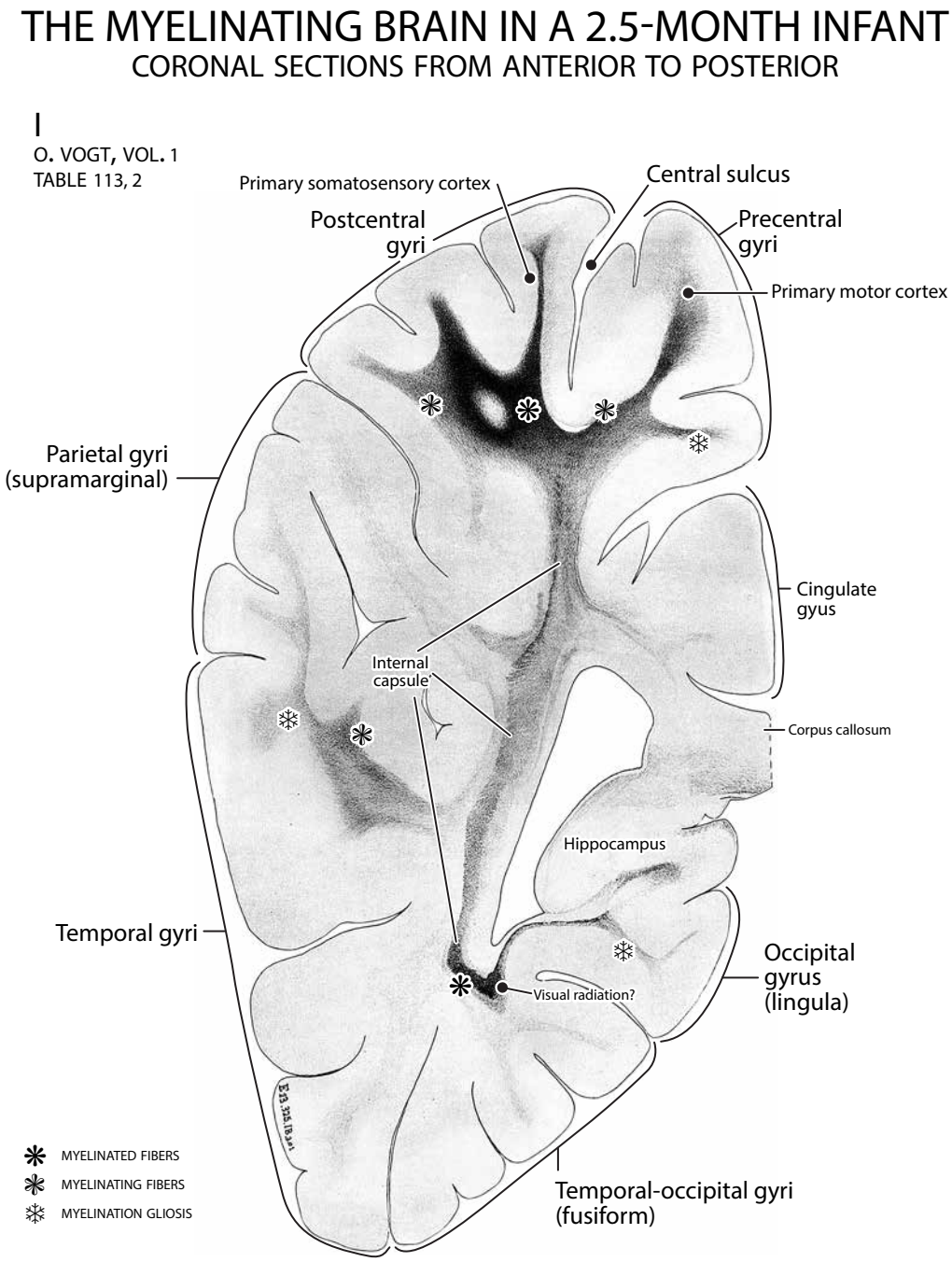

Fig. 55I. The only myelinated regions in this section are the primary somatosensory cortex in the postcentral gyrus and the myelinated fibers in the presumptive visual radiation. Most of the internal capsule at this level has only myelination gliosis. There is faint myelination gliosis in the parietal and temporal lobes and very faint gliosis in the cingulate gyrus.

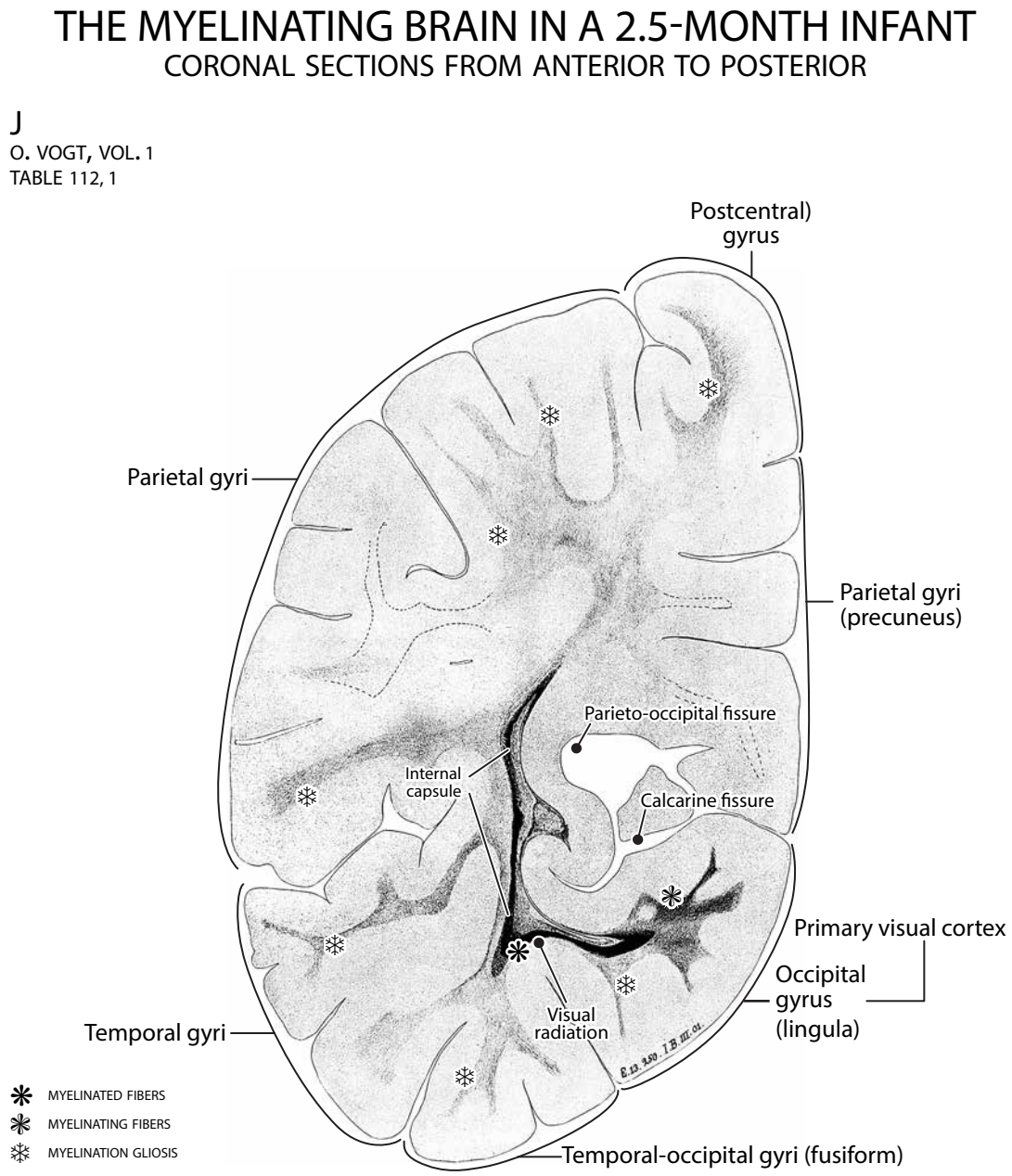

Fig. 55J. The visual radiation is myelinated and connects with a thin myelinated fiber bundle running through the internal capsule. The visual fibers spread into myelinating regions in the lingula of the primary visual cortex. All the other gyri have very faint myelination gliosis.

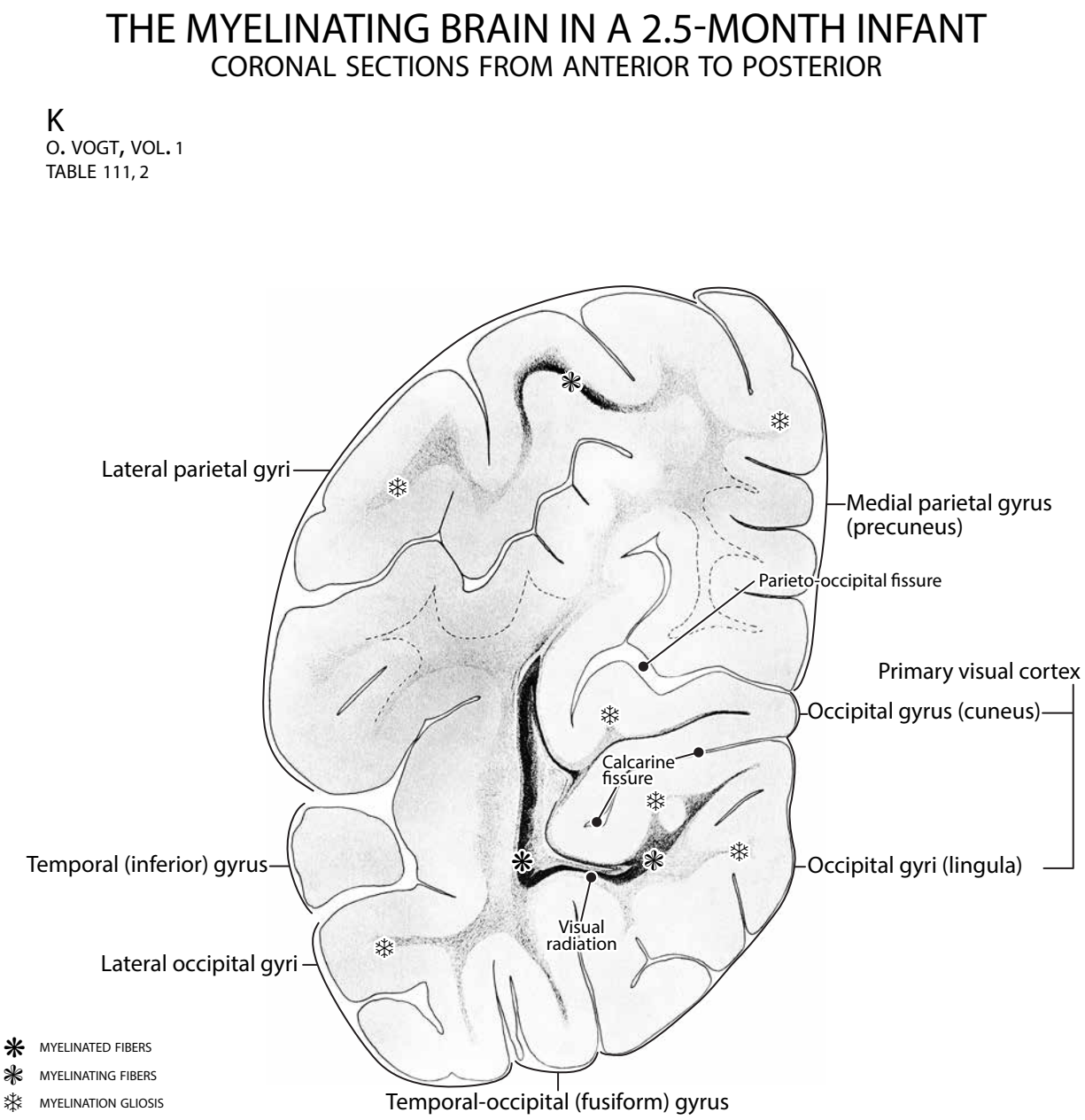

Fig. 55K. As in **Fig. 55J**, the visual radiation fibers are myelinated and fan out into myelinating fibers in the primary visual cortex that surrounds the calcarine fissure. There is only faint myelination gliosis in the parietal and temporal lobes, with the exception of a hook-like fiber bundle in one of the lateral parietal gyri.

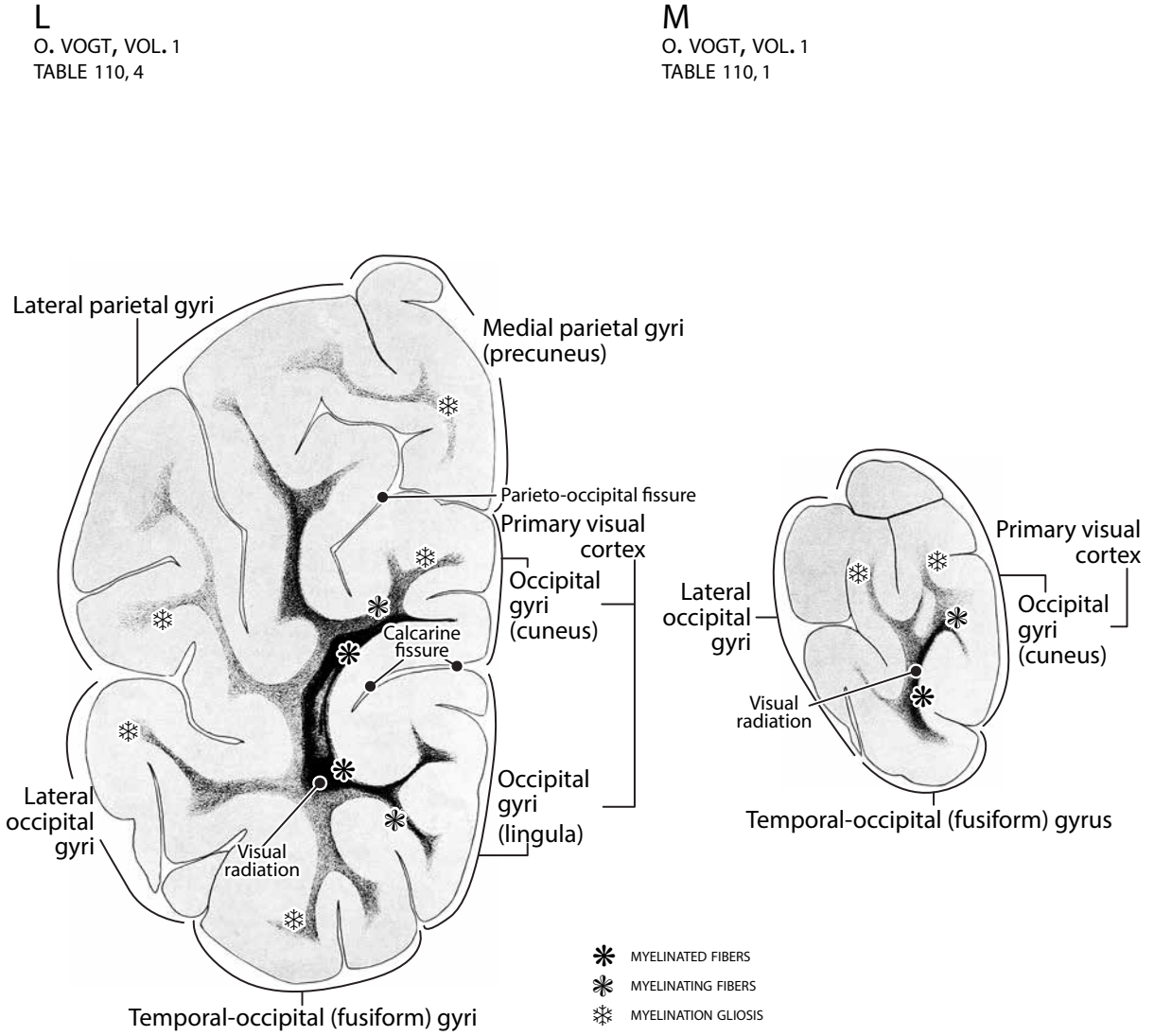

Fig. 55L and **M**. The only myelinated fibers in these two sections are in the visual radiation fanning out to the primary visual cortex surrounding the calcarine fissure in the occipital lobe. Note that the primary visual cortex is more heavily myelinated in **L** than in **Fig. 55J**. Myelinating fibers fan out to adjacent gyri in the parietal, temporal and the remaining gyri of the occipital lobe from a core area (**L**) in the primary visual cortex.

Fig. 56 (on the following 6 pages). Myelin-stained parasagittal sections of the brain of a 3 months-old infant (E1, Vogts' collection) from medial to lateral (**A** to **F**).

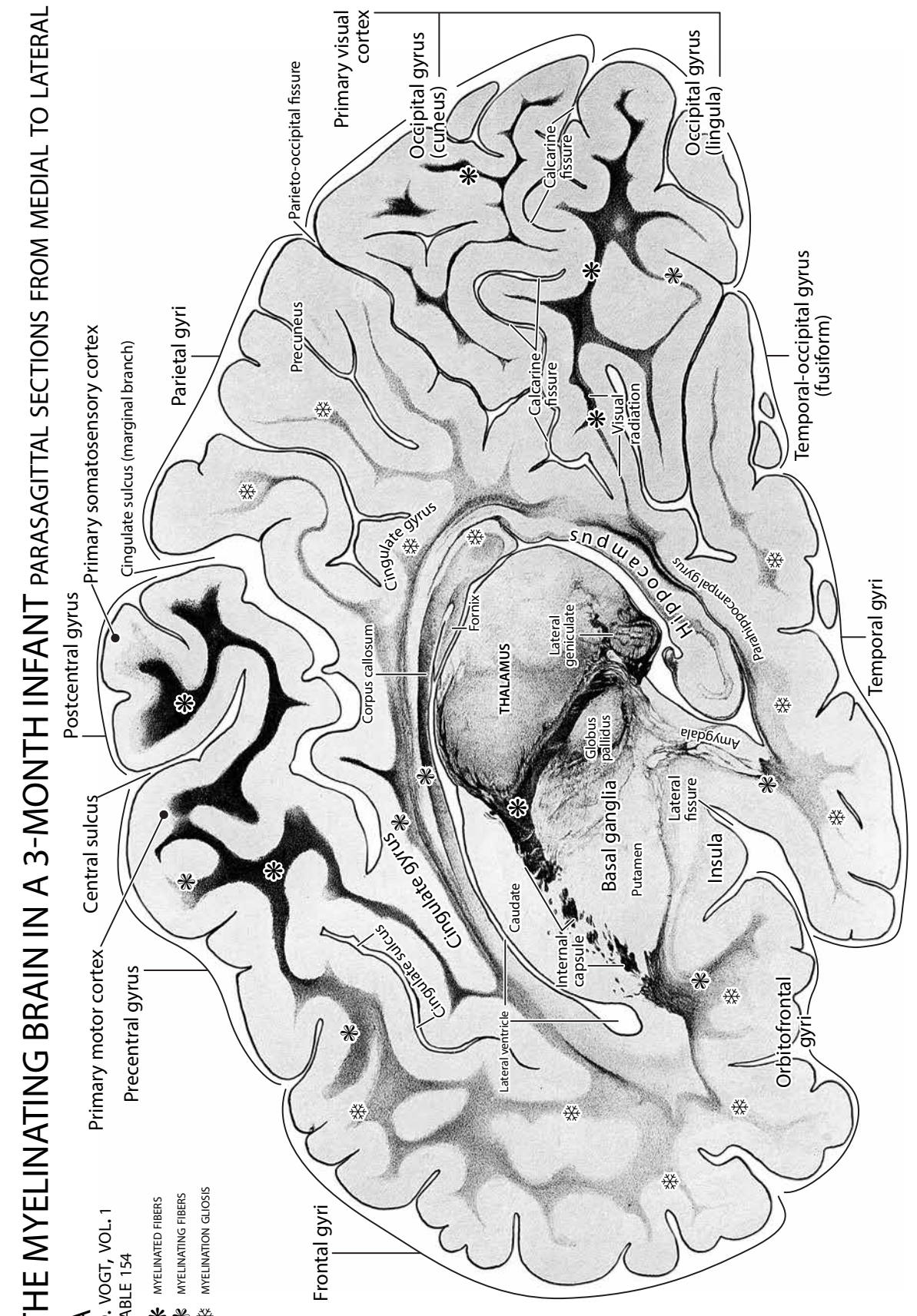

Fig. 56A and **B (facing pages)**. Advanced myelination is evident medially in the somatomotor and somatosensory projection areas of the paracentral lobe, the internal capsule is myelinated and so is the visual radiation to the occipital lobe.

THE MYELINATING BRAIN IN A 3-MONTH INFANT PARASAGITTAL SECTIONS FROM MEDIAL TO LATERAL

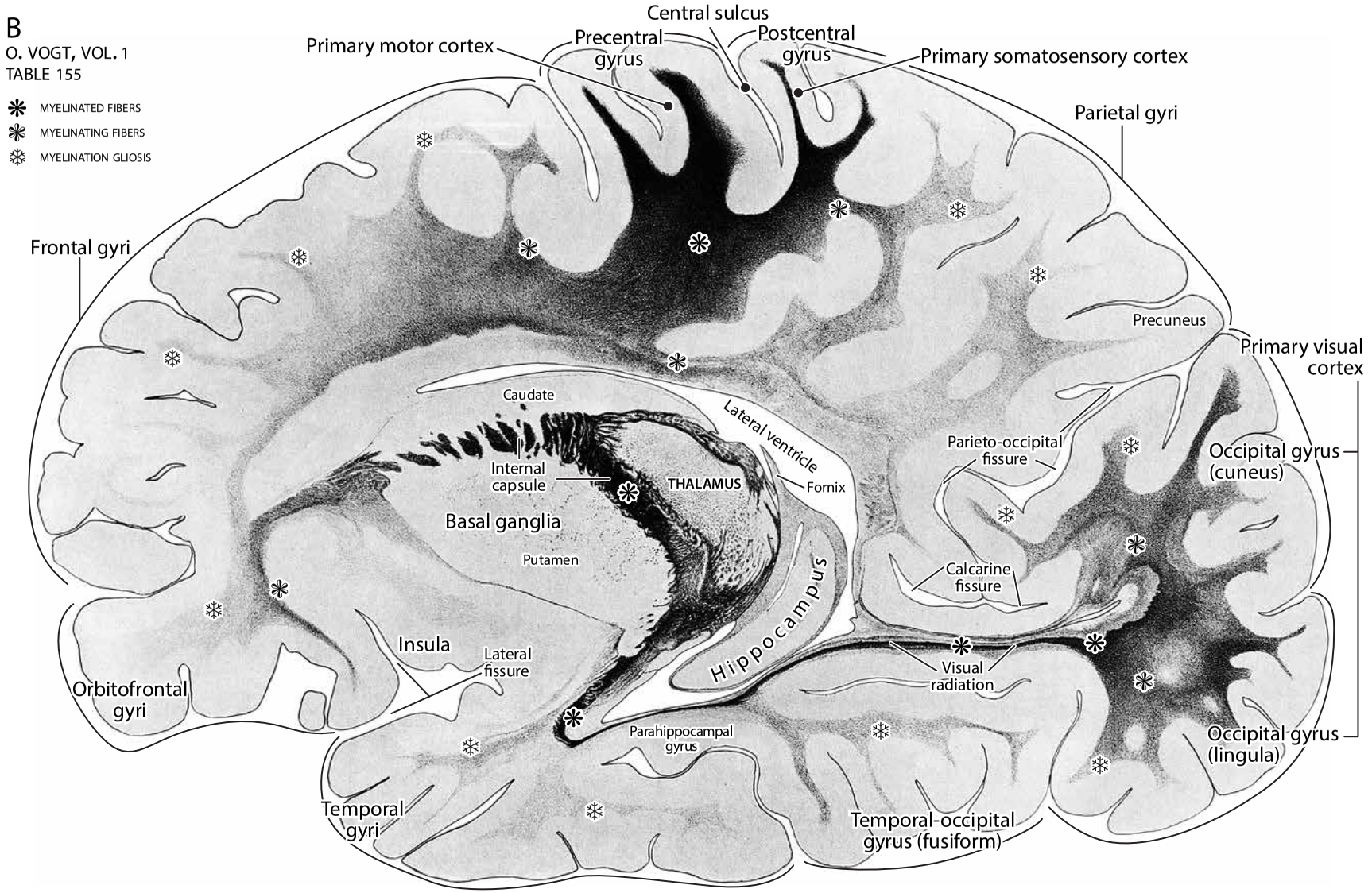

THE MYELINATING BRAIN IN A 3-MONTH INFANT PARASAGITTAL SECTIONS FROM MEDIAL TO LATERAL

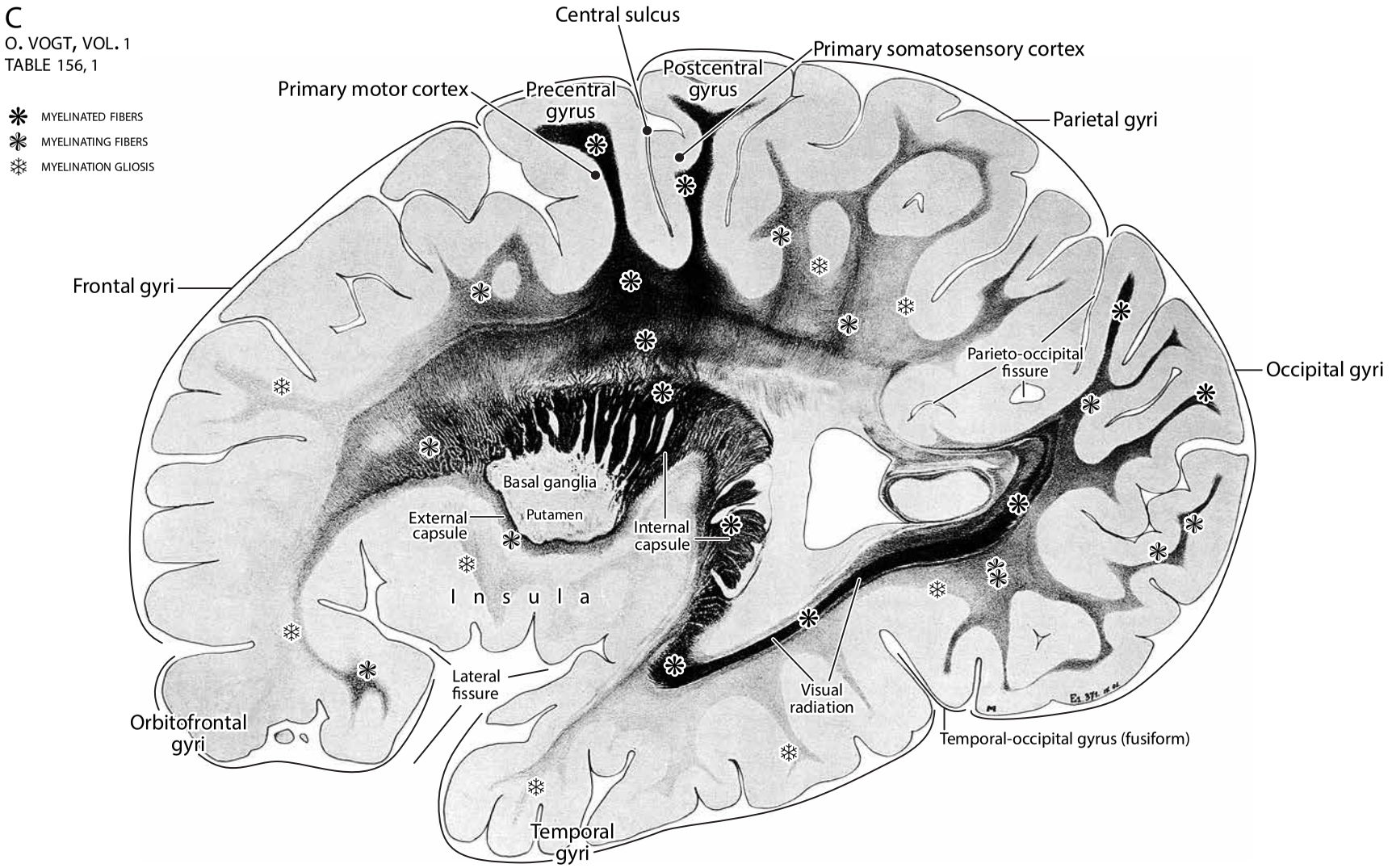

Fig. 56C and **D (facing pages)**. More laterally, myelination and myelination gliosis are in progress in the occipital lobe. Reactive gliosis is evident in some of the association areas abutting the projection areas but is still sparse in the frontal and temporal lobes and the insula.

THE MYELINATING BRAIN IN A 3-MONTH INFANT PARASAGITTAL SECTIONS FROM MEDIAL TO LATERAL

D

O. VOGT, VOL. 1
TABLE 156, 2

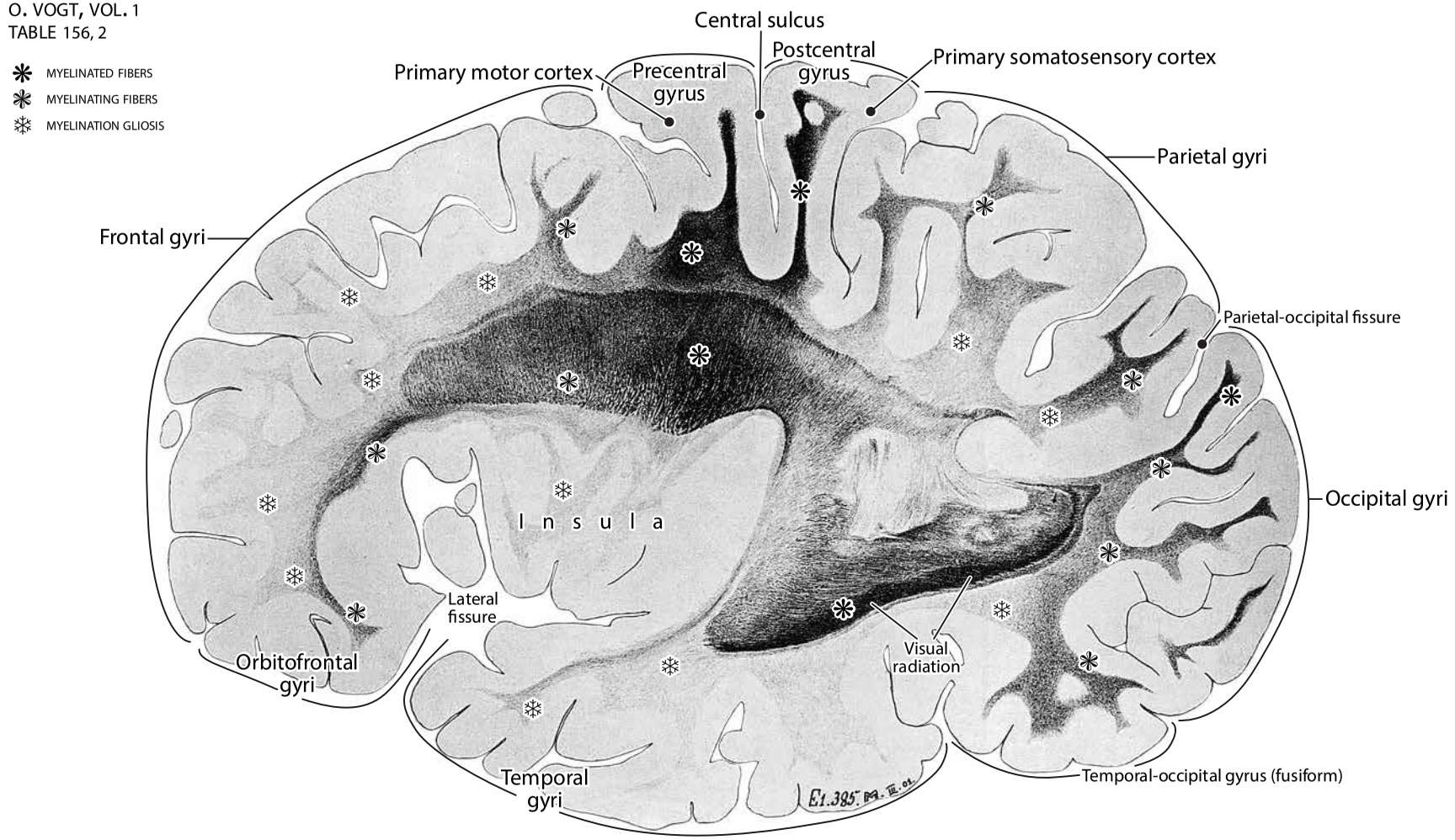

THE MYELINATING BRAIN IN A 3-MONTH INFANT PARASAGITTAL SECTIONS FROM MEDIAL TO LATERAL

E

O. VOGT, VOL. 1

TABLE 157, 1

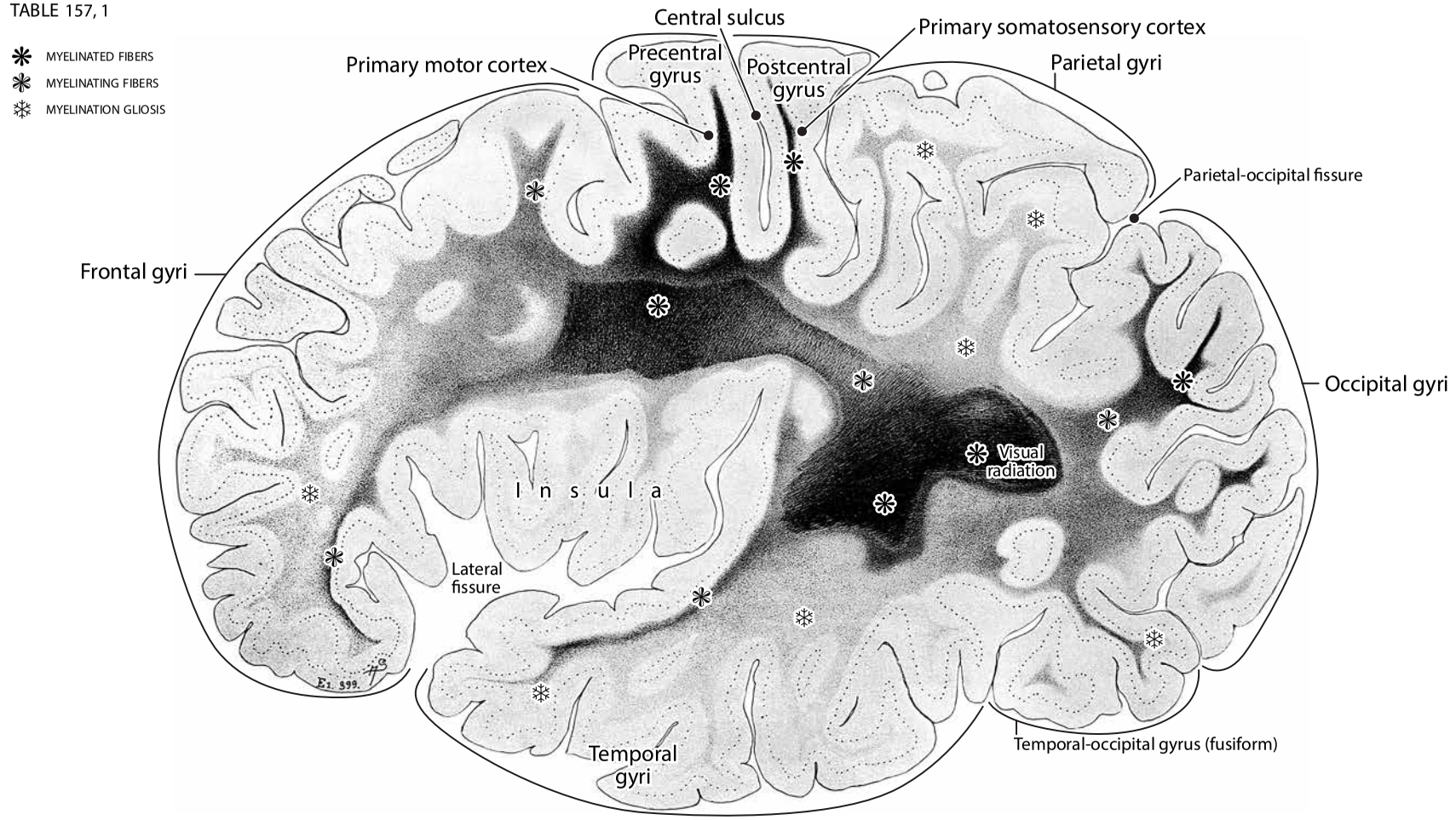

Fig. 56E and **F (facing pages)**. Farther laterally, there is an evident medial-to-lateral reduction in myelination from the "hot spot."

THE MYELINATING BRAIN IN A 3-MONTH INFANT PARASAGITTAL SECTIONS FROM MEDIAL TO LATERAL

F

O. VOGT, VOL. 1
TABLE 157, 2

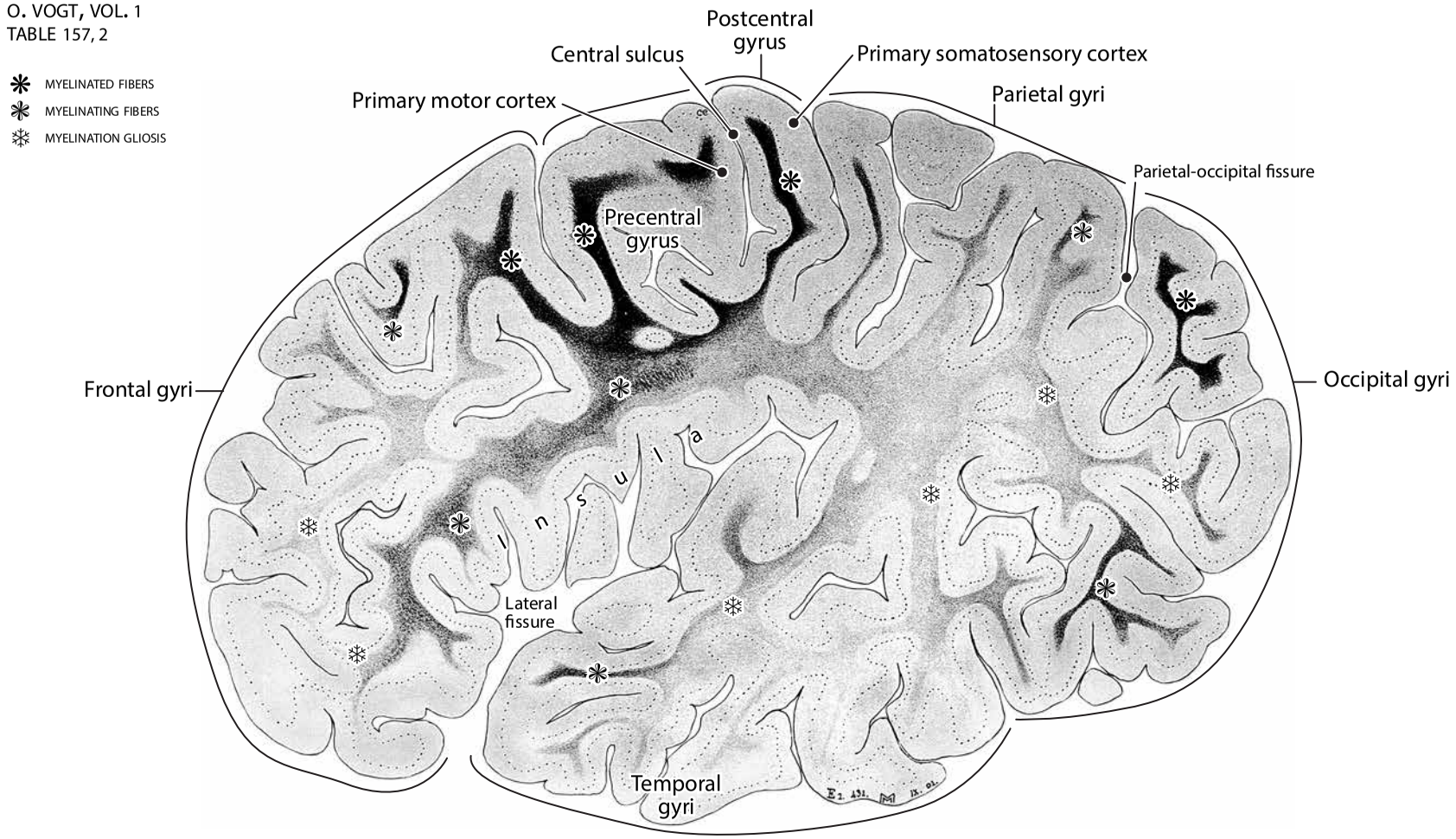

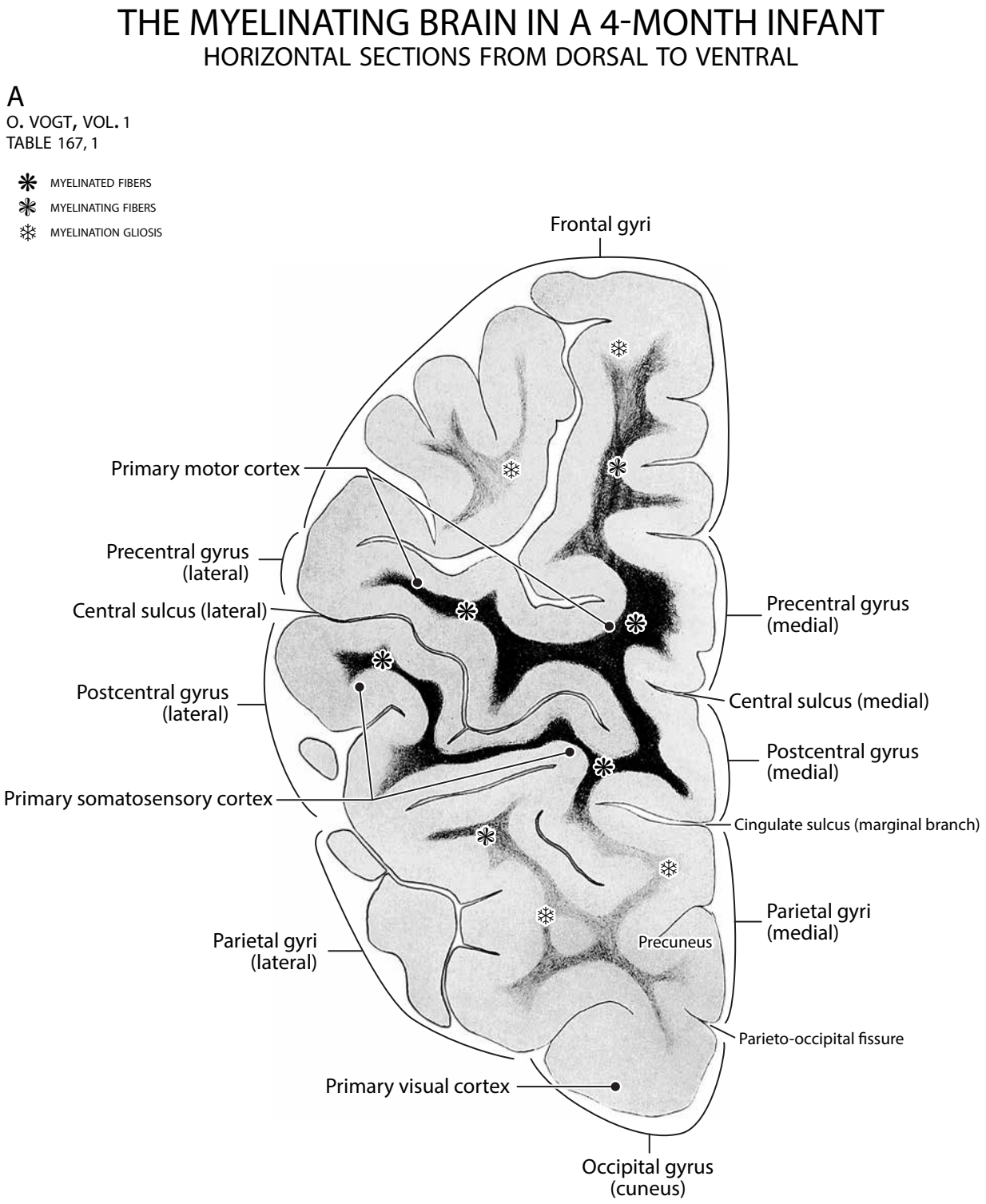

Fig. 57 (on this and the following 10 pages). 12 myelin-stained horizontal sections from the brain of a 4-months-old infant (brain E8, Vogts' collection) from dorsal to ventral. **A** and **B (facing pages).** Myelination is well advanced in the primary motor and primary somatosensory cortical areas, and reactive gliosis is spreading to gyri in the adjacent frontal and parietal lobes.

THE MYELINATING BRAIN IN A 4-MONTH INFANT

HORIZONTAL SECTIONS FROM DORSAL TO VENTRAL

B

O. VOGT, VOL. 1
TABLE 167, 2

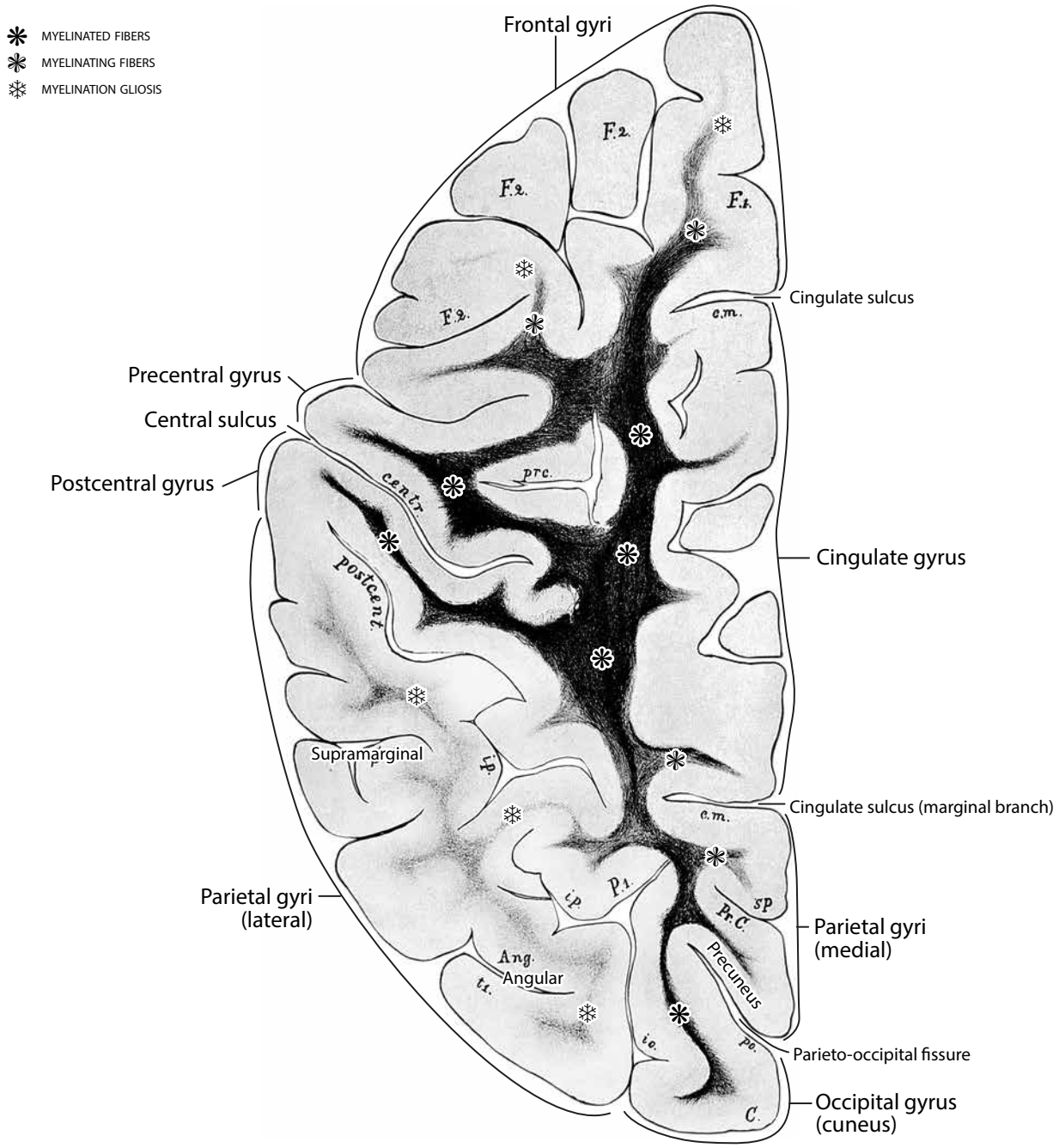

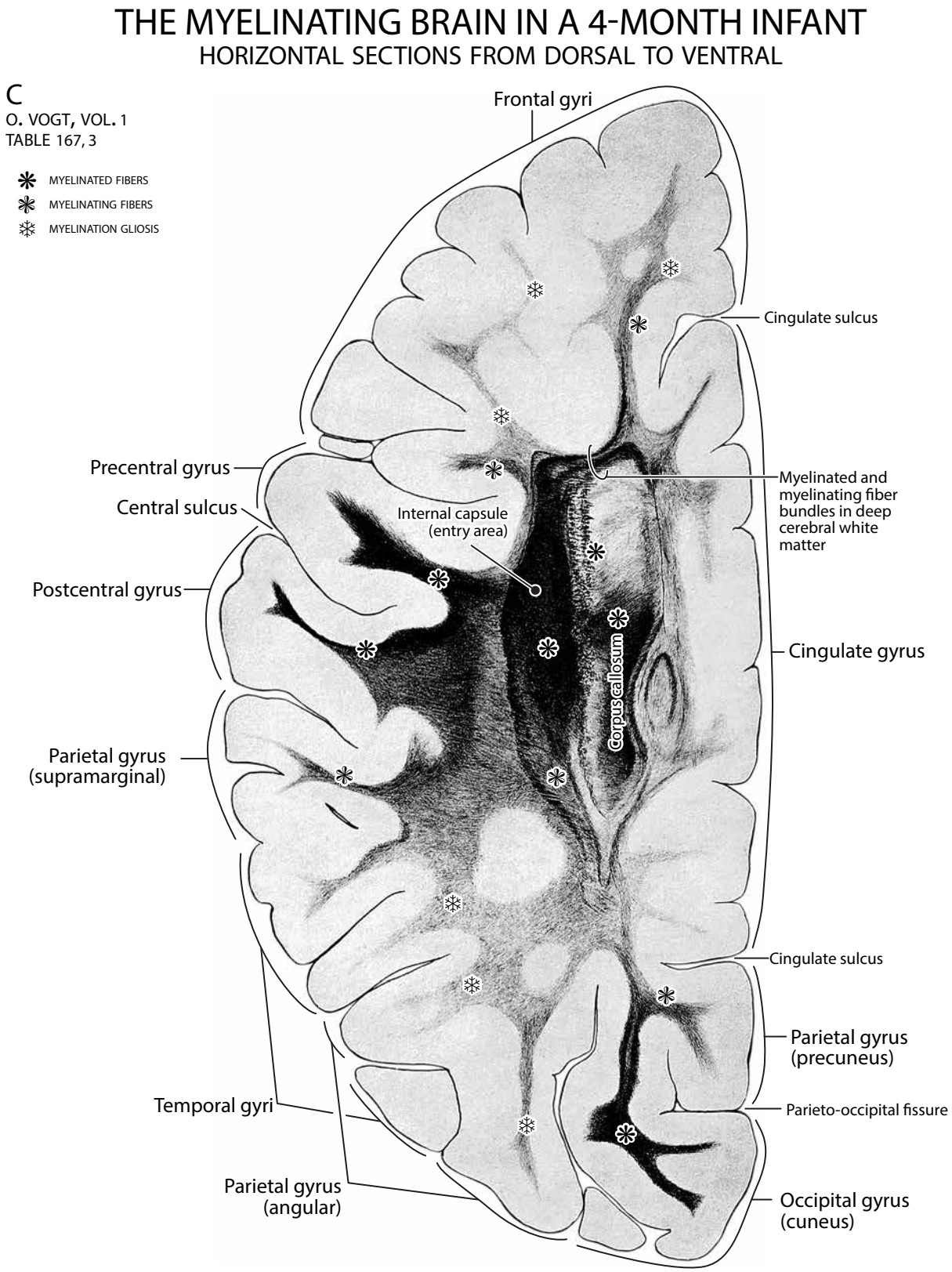

Fig. 57C and **D (facing pages)**. Myelination is advanced in the internal capsule where it enters the precentral and postcentral gyri. The corpus callosum myelinates only in a central part. The myelinated visual radiation extends into the cuneus of the occipital lobe.

THE MYELINATING BRAIN IN A 4-MONTH INFANT

HORIZONTAL SECTIONS FROM DORSAL TO VENTRAL

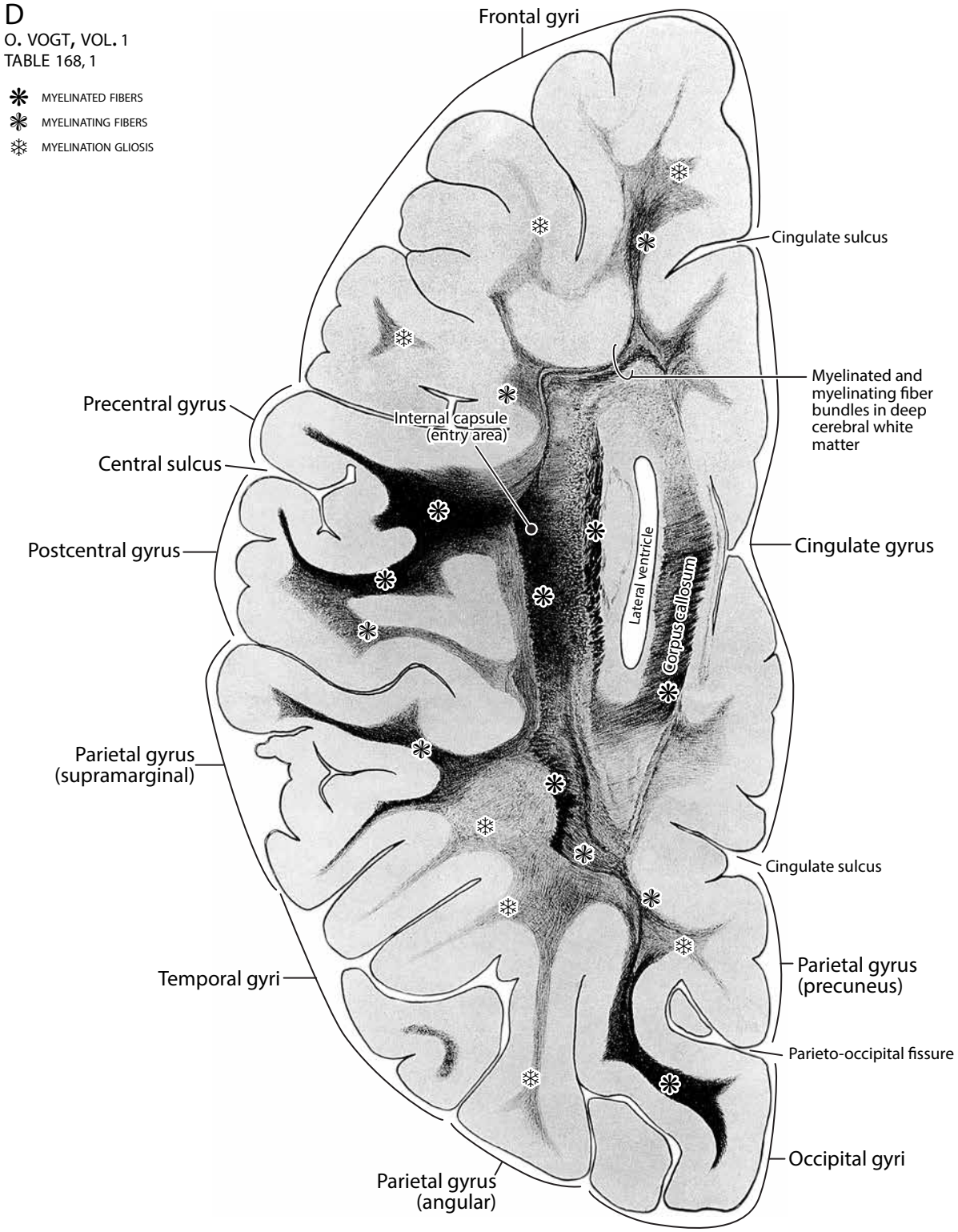

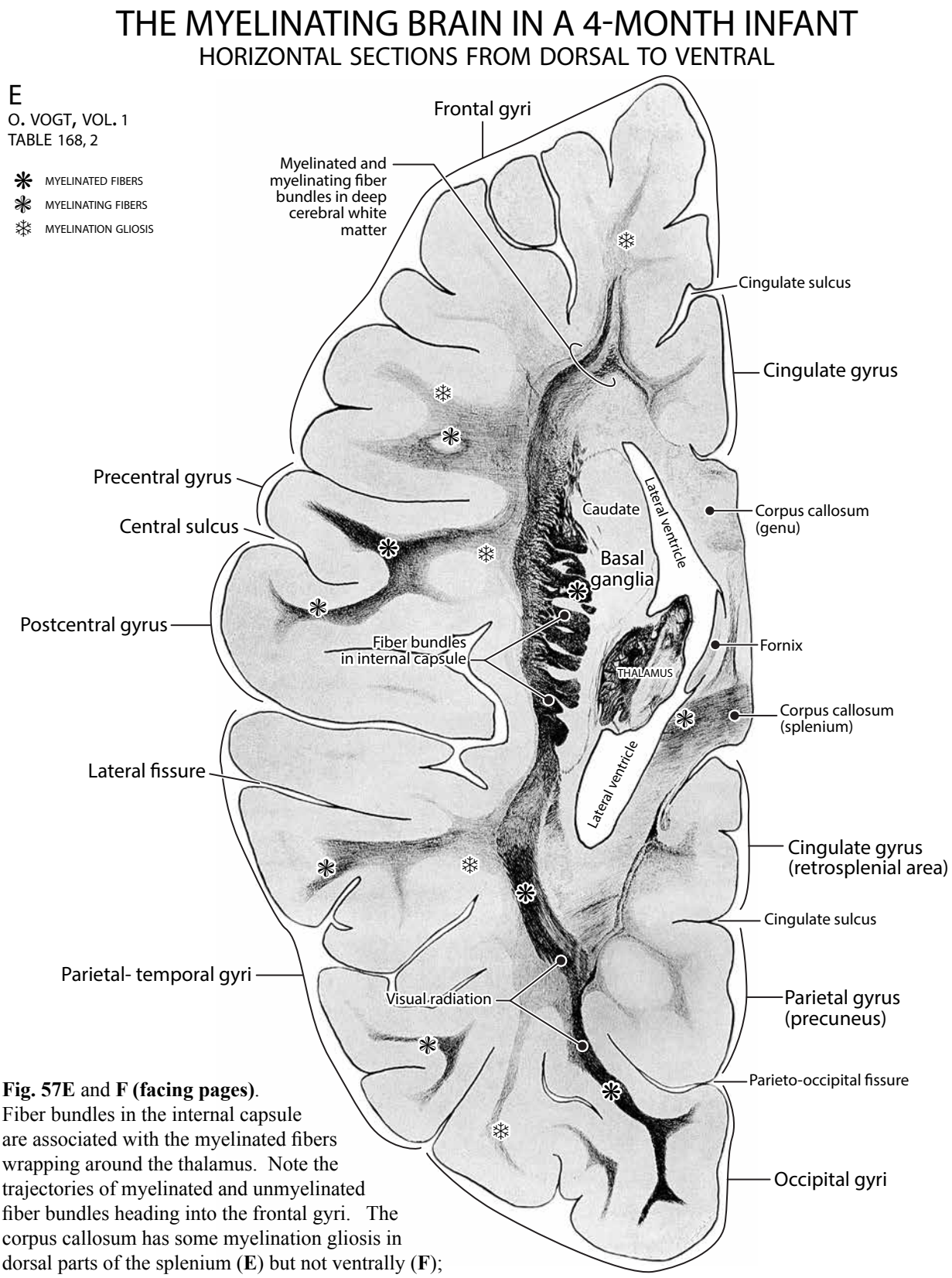

Fig. 57E and **F (facing pages)**.
Fiber bundles in the internal capsule are associated with the myelinated fibers wrapping around the thalamus. Note the trajectories of myelinated and unmyelinated fiber bundles heading into the frontal gyri. The corpus callosum has some myelination gliosis in dorsal parts of the splenium (**E**) but not ventrally (**F**); the genu has no gliosis. A more complete path of the myelinated visual radiation can be seen in these sections .

THE MYELINATING BRAIN IN A 4-MONTH INFANT

HORIZONTAL SECTIONS FROM DORSAL TO VENTRAL

F
O. VOGT, VOL. 1
TABLE 168, 3

✱ MYELINATED FIBERS
✱ MYELINATING FIBERS
❄ MYELINATION GLIOSIS

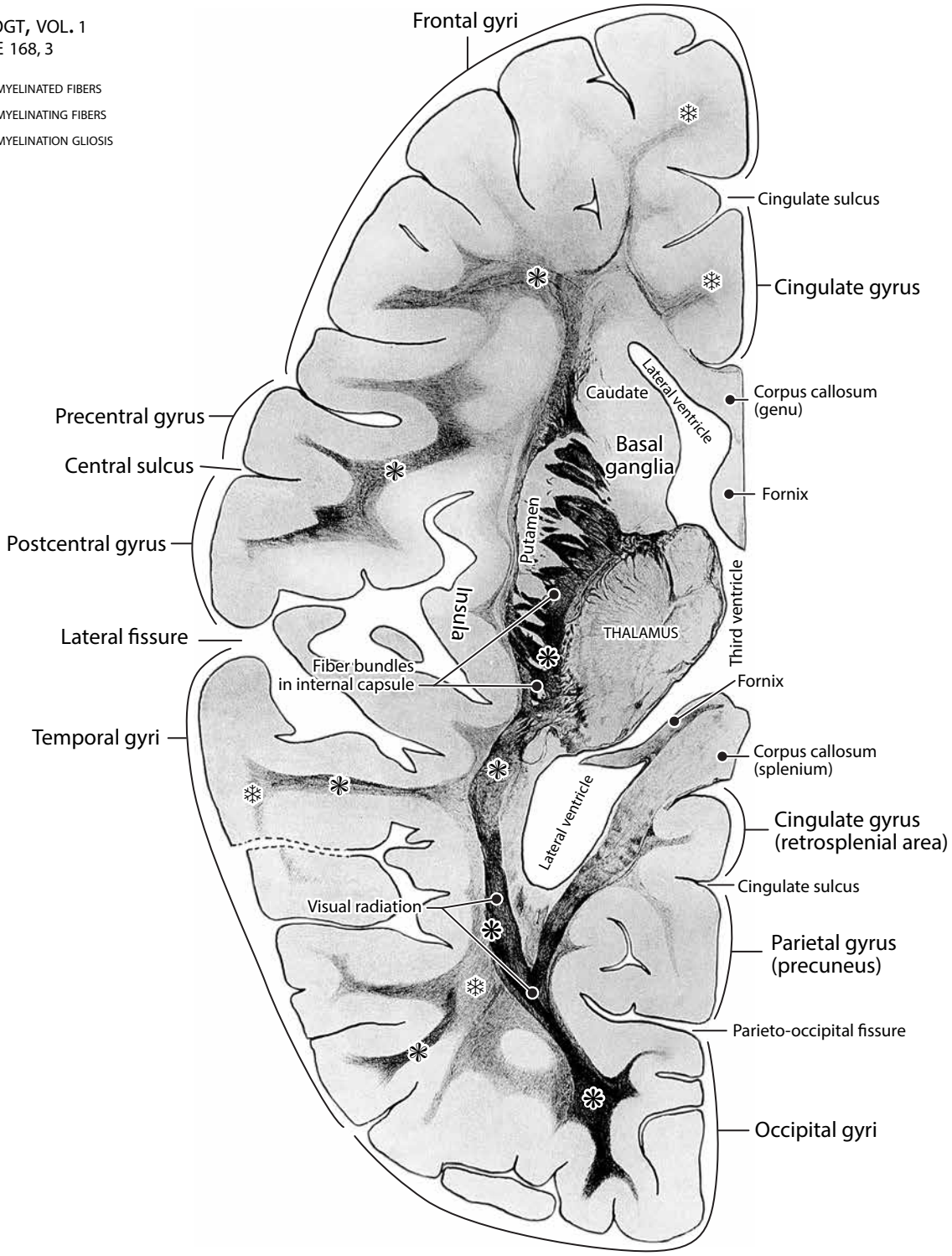

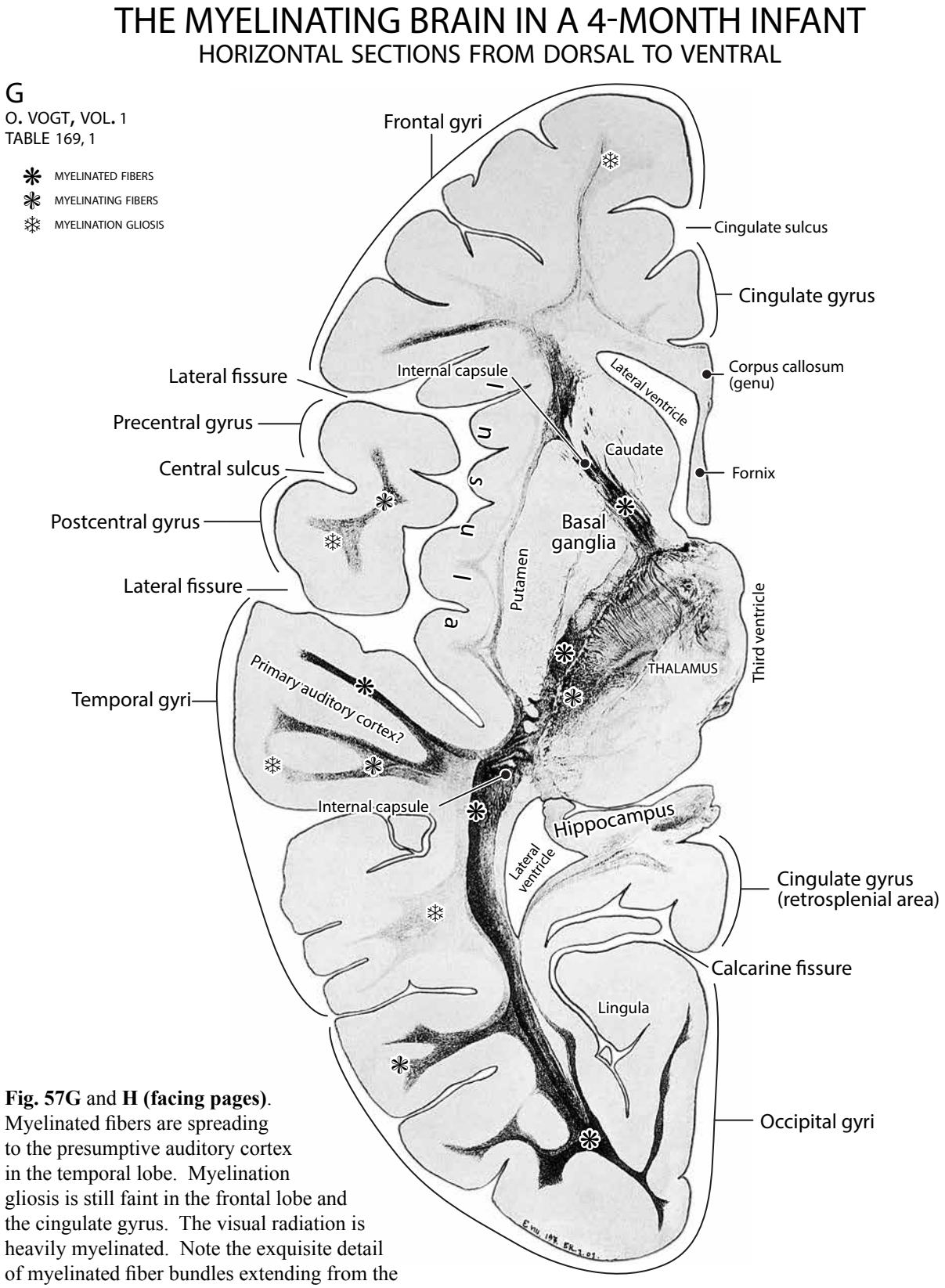

Fig. 57G and **H (facing pages)**. Myelinated fibers are spreading to the presumptive auditory cortex in the temporal lobe. Myelination gliosis is still faint in the frontal lobe and the cingulate gyrus. The visual radiation is heavily myelinated. Note the exquisite detail of myelinated fiber bundles extending from the anterolateral thalamus towrd the internal capsule.

THE MYELINATING BRAIN IN A 4-MONTH INFANT

HORIZONTAL SECTIONS FROM DORSAL TO VENTRAL

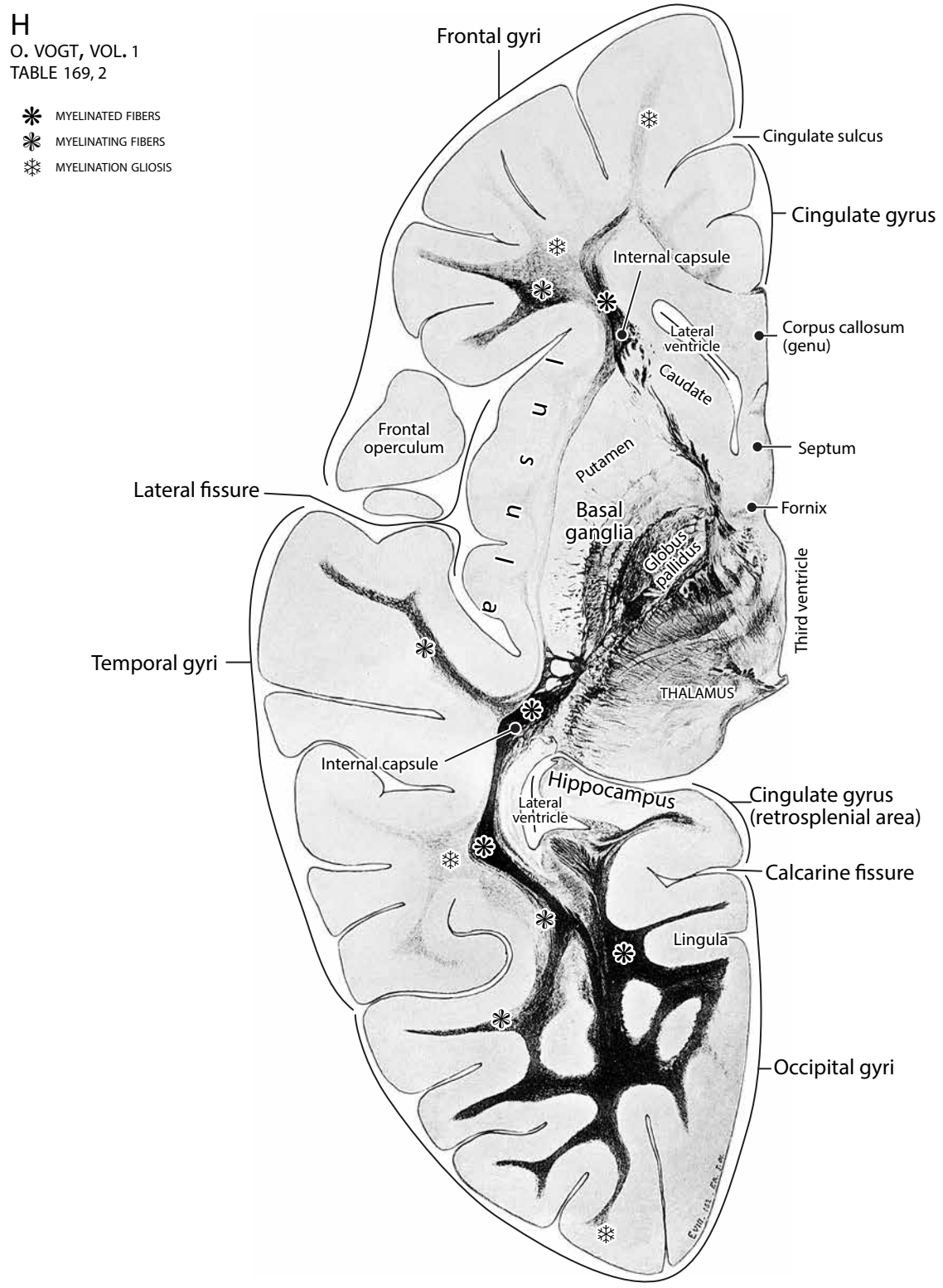

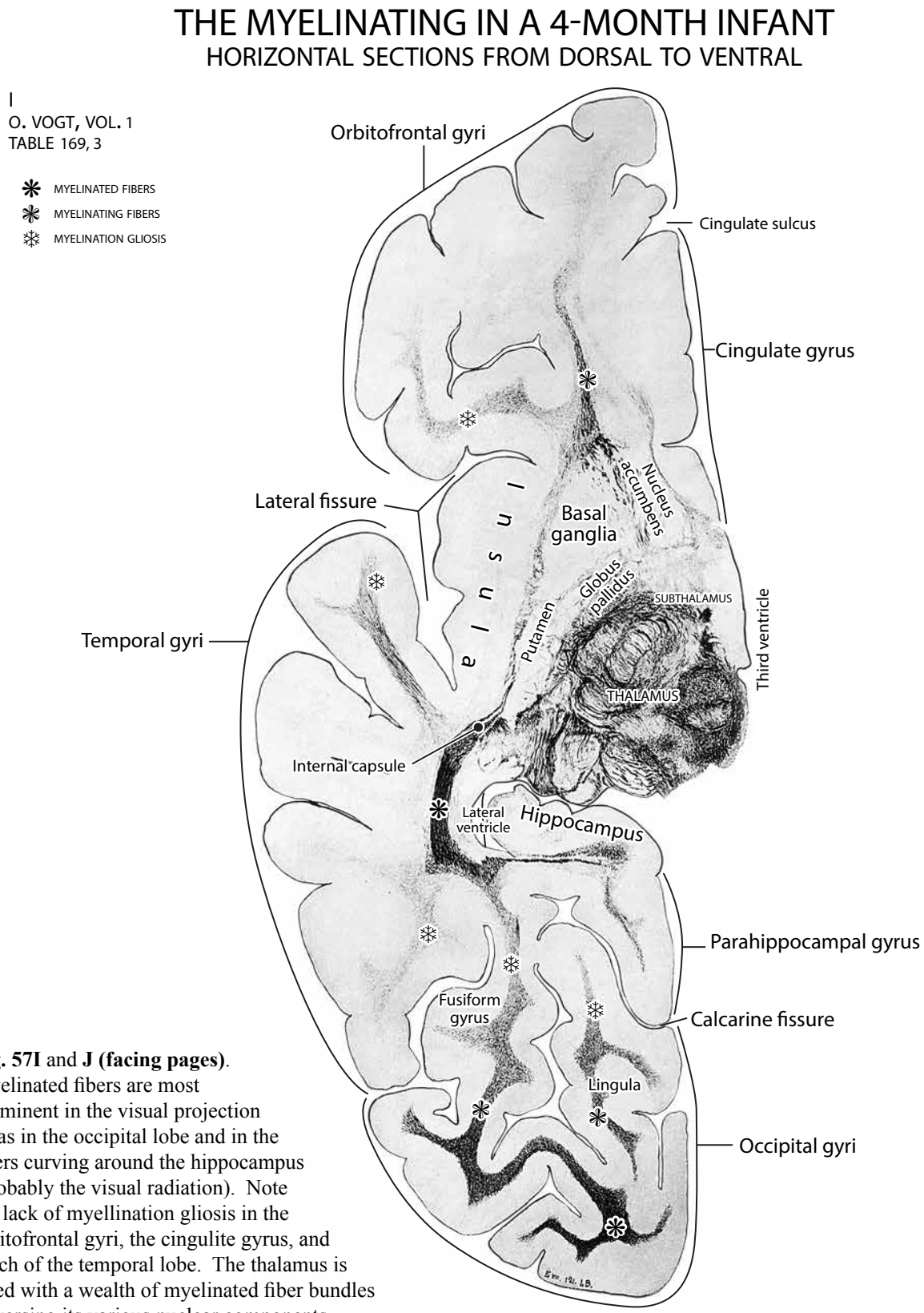

Fig. 57I and **J (facing pages)**. Myelinated fibers are most prominent in the visual projection areas in the occipital lobe and in the fibers curving around the hippocampus (probably the visual radiation). Note the lack of myellination gliosis in the orbitofrontal gyri, the cingulite gyrus, and much of the temporal lobe. The thalamus is filled with a wealth of myelinated fiber bundles traversing its various nuclear components.

THE MYELINATING BRAIN IN A 4-MONTH INFANT

HORIZONTAL SECTIONS FROM DORSAL TO VENTRAL

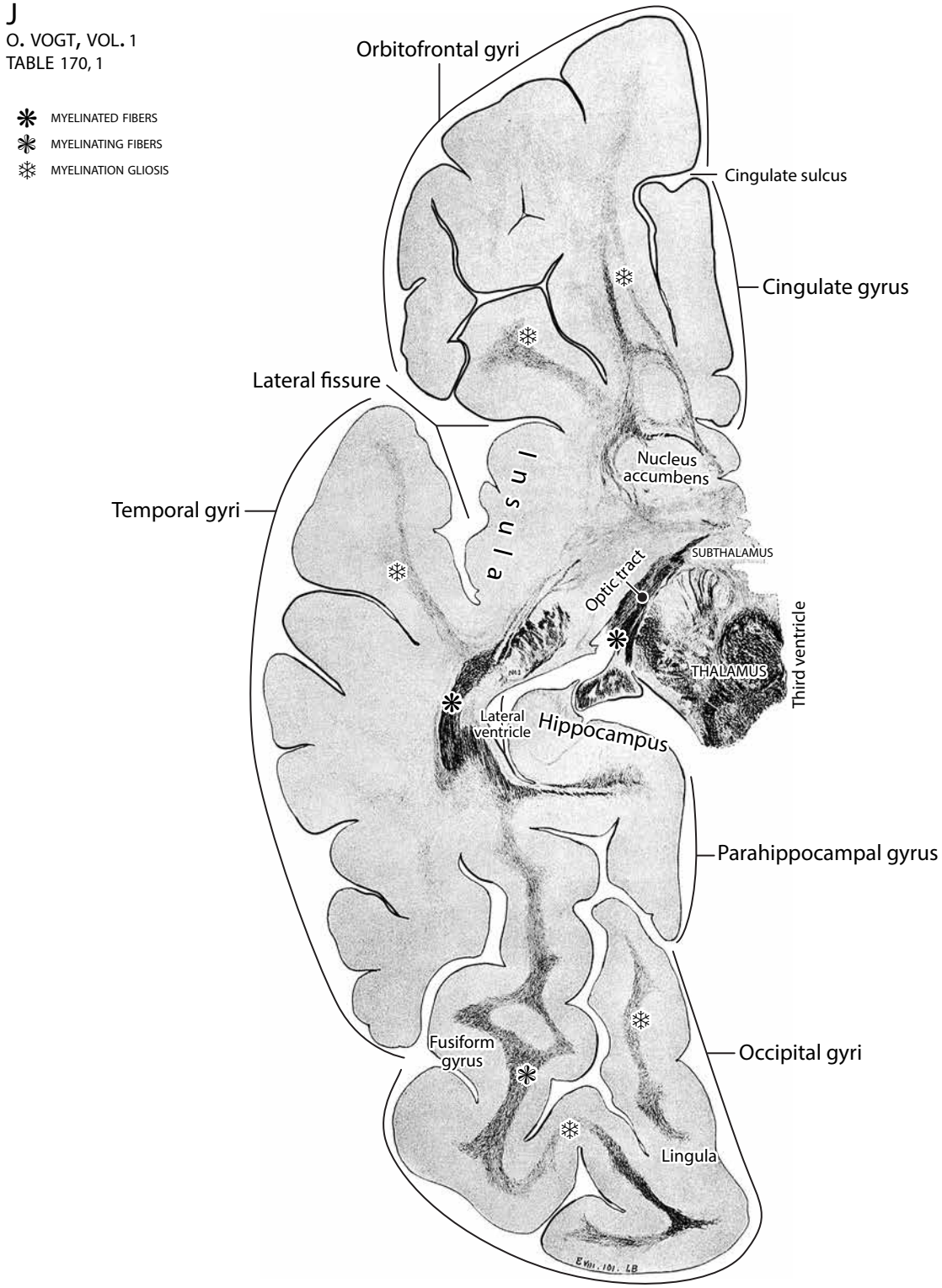

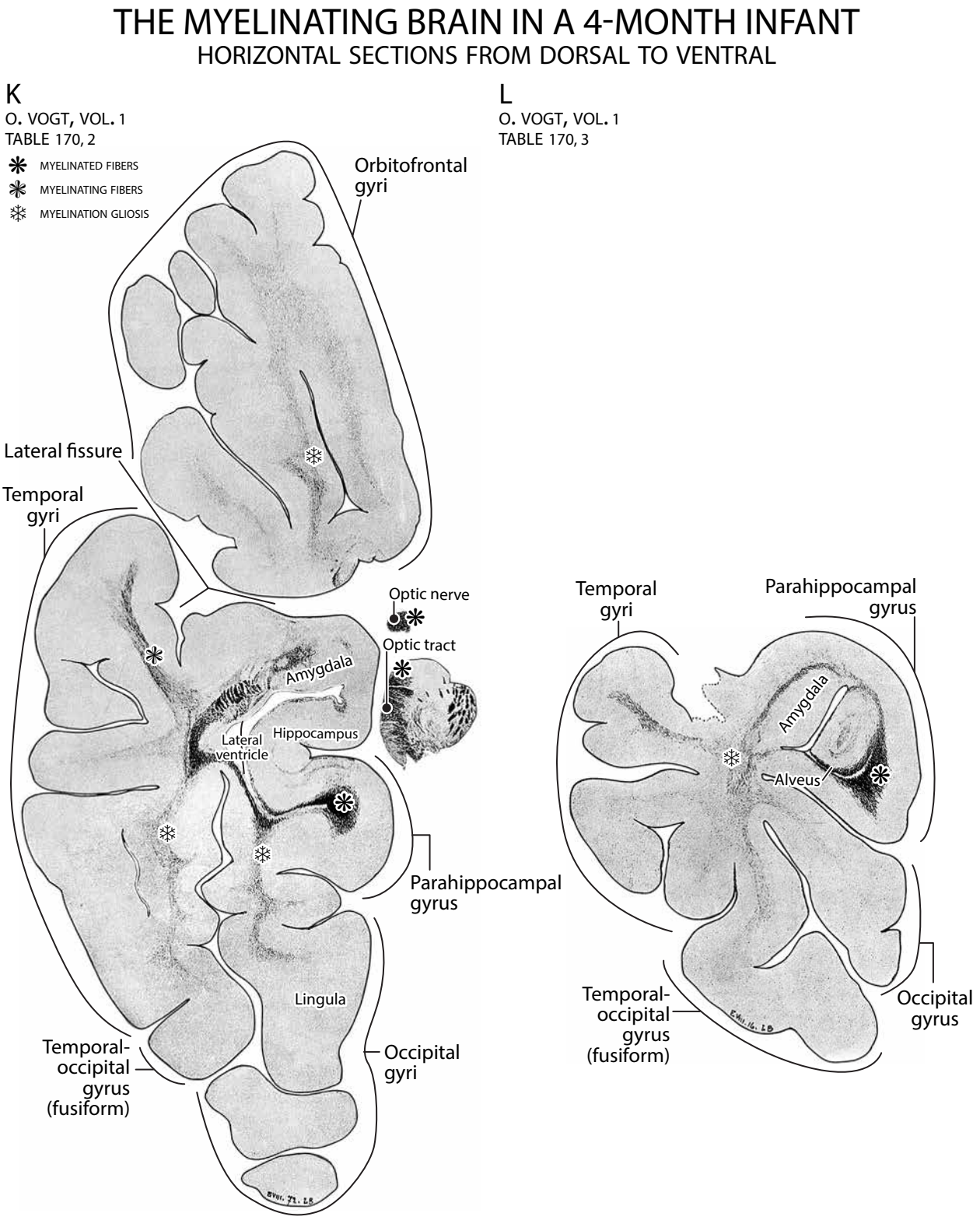

Fig. 57K and **L**. The only myelinated fibers at these ventral levels are those in the alveus surrounding the hippocampus itself and the deep parts of the parahippocampal gyrus. Myelinated fibers appear to be extending from the amygdala in a hook bundle that goes into the parahippocampal gyrus. Ventral parts of the orbitofrontal gyri, temporal gyri, and occipital gyri have only faint myelination gliosis.

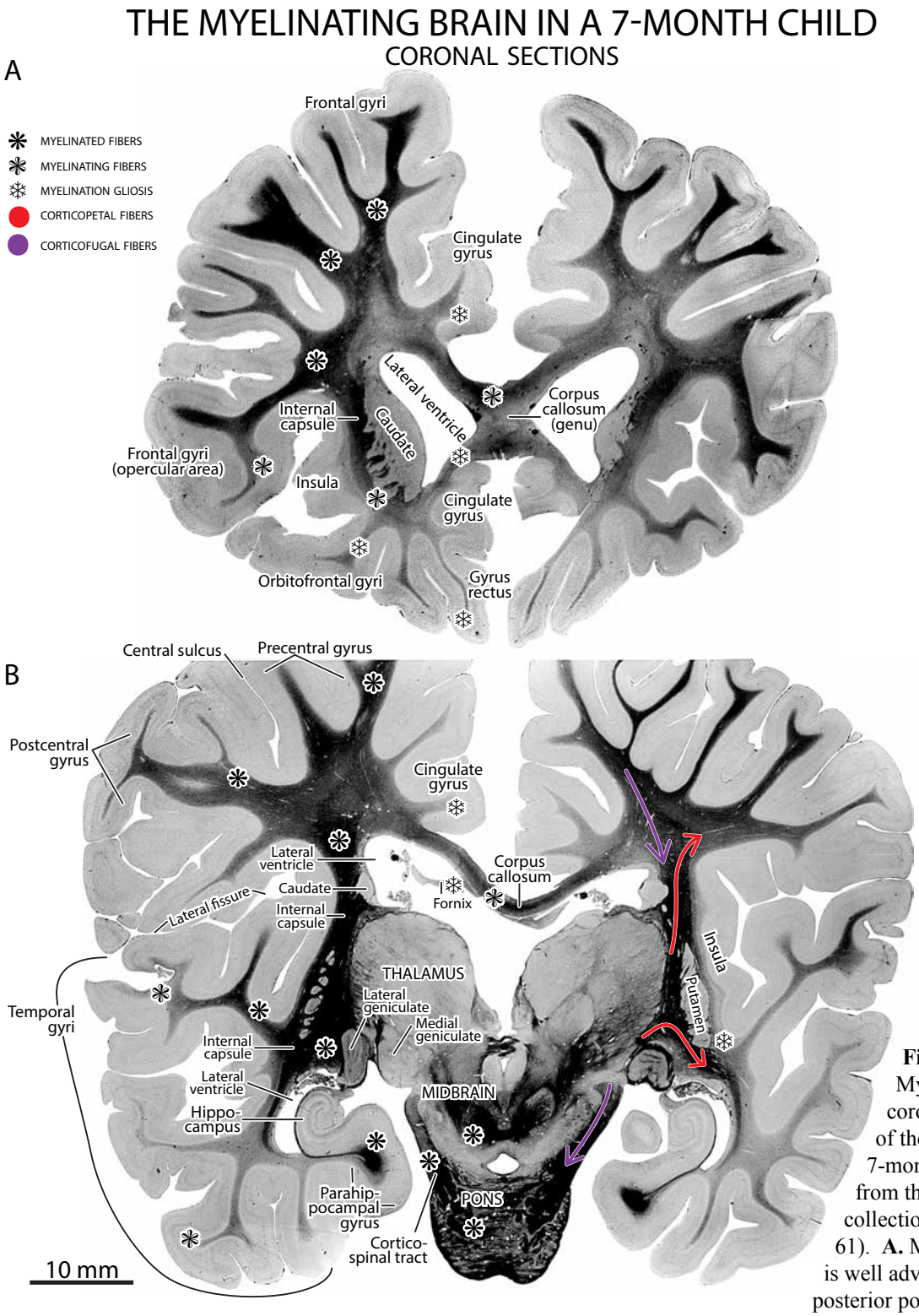

Fig. 58. Myelin-stained coronal sections of the brain of a 7-months-old child from the Yakovlev collection (Y123-61). **A.** Myelination is well advanced in the posterior portion of the frontal lobe but is still in an early stage in the inferior cingulate gyrus dorsally and in the orbitofrontal gyri ventrally. **B.** More posteriorly, the somatomotor and somatosensory paracentral gyri are well myelinated. On the input side to the neocortex, the somatosensory medial lemniscus and the capsule of the visual lateral geniculate nucleus are well myelinated. On the output side, the corticospinal fibers traversing the pontine gray are well myelinated. The temporal gyri, with the exception of the auditory cortex, are still in an early myelination stage.

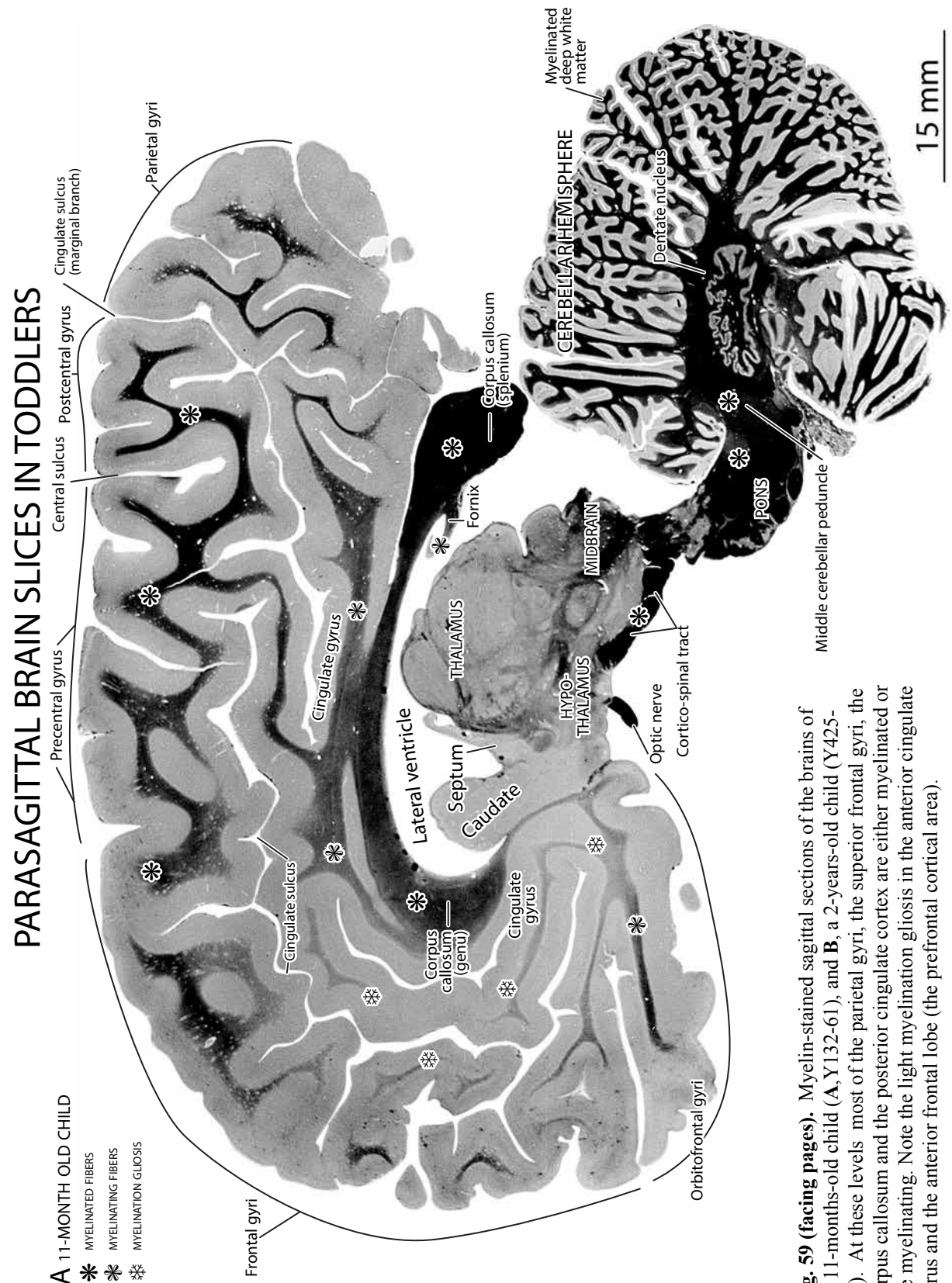

Fig. 59 (facing pages). Myelin-stained sagittal sections of the brains of an 11-months-old child (**A**, Y132-61), and **B**, a 2-years-old child (Y425-63). At these levels most of the parietal gyri, the superior frontal gyri, the corpus callosum and the posterior cingulate cortex are either myelinated or are myelinating. Note the light myelination gliosis in the anterior cingulate gyrus and the anterior frontal lobe (the prefrontal cortical area).

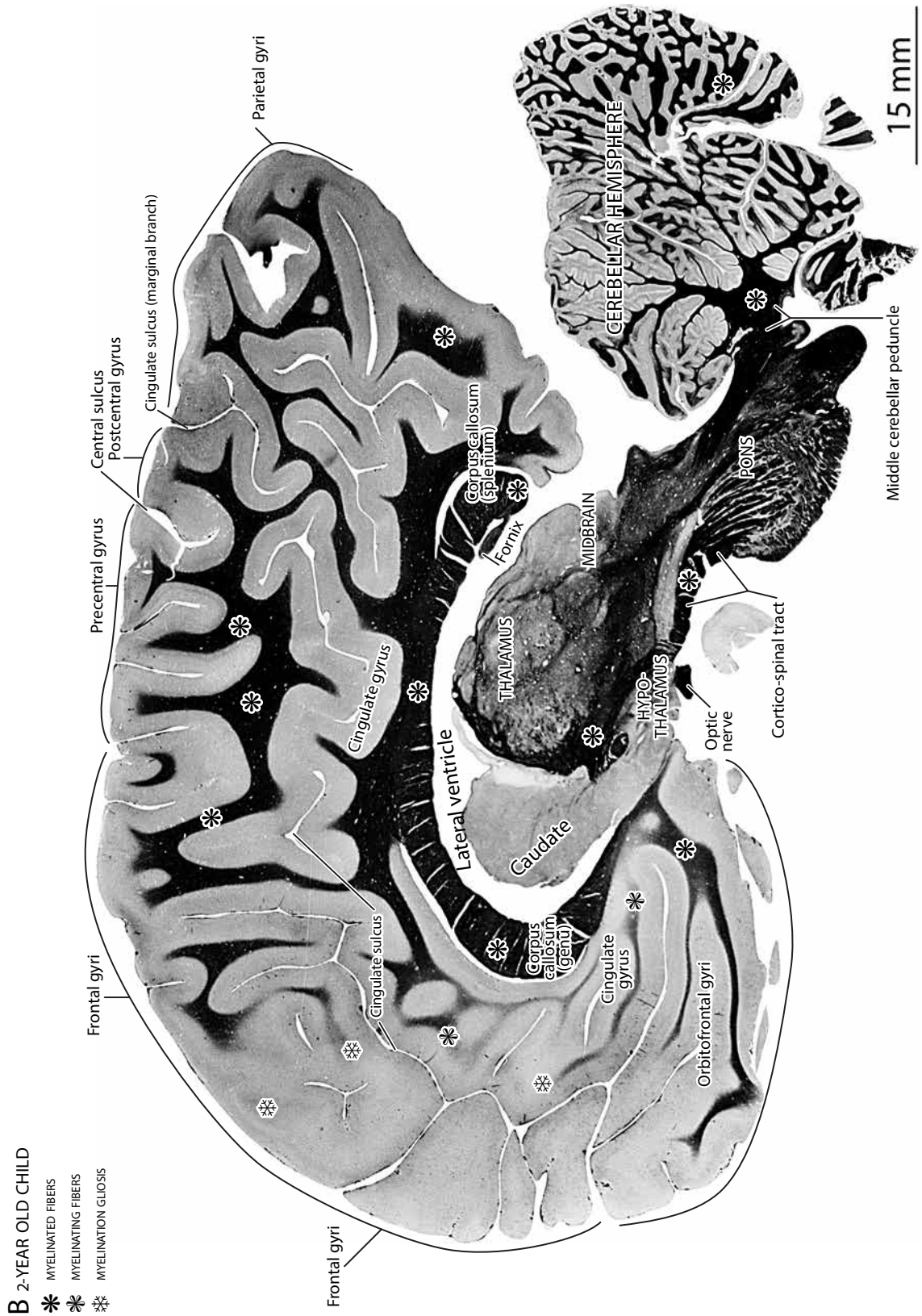
PARASAGITTAL BRAIN SLICES IN TODDLERS
B 2-YEAR OLD CHILD
MYELINATED FIBERS
MYELINATING FIBERS
MYELINATION GLIOSIS
Frontal gyri
Precentral gyrus
Central sulcus
Postcentral gyrus
Cingulate sulcus (marginal branch)
Parietal gyri
Cingulate sulcus
Cingulate gyrus
Lateral ventricle
Caudate
Corpus callosum (genu)
Cingulate gyrus
Orbitofrontal gyri
Frontal gyri
Corpus callosum (splenium)
Fornix
THALAMUS
MIDBRAIN
HYPO-THALAMUS
Optic nerve
PONS
Cortico-spinal tract
CEREBELLAR HEMISPHERE
Middle cerebellar peduncle
15 mm

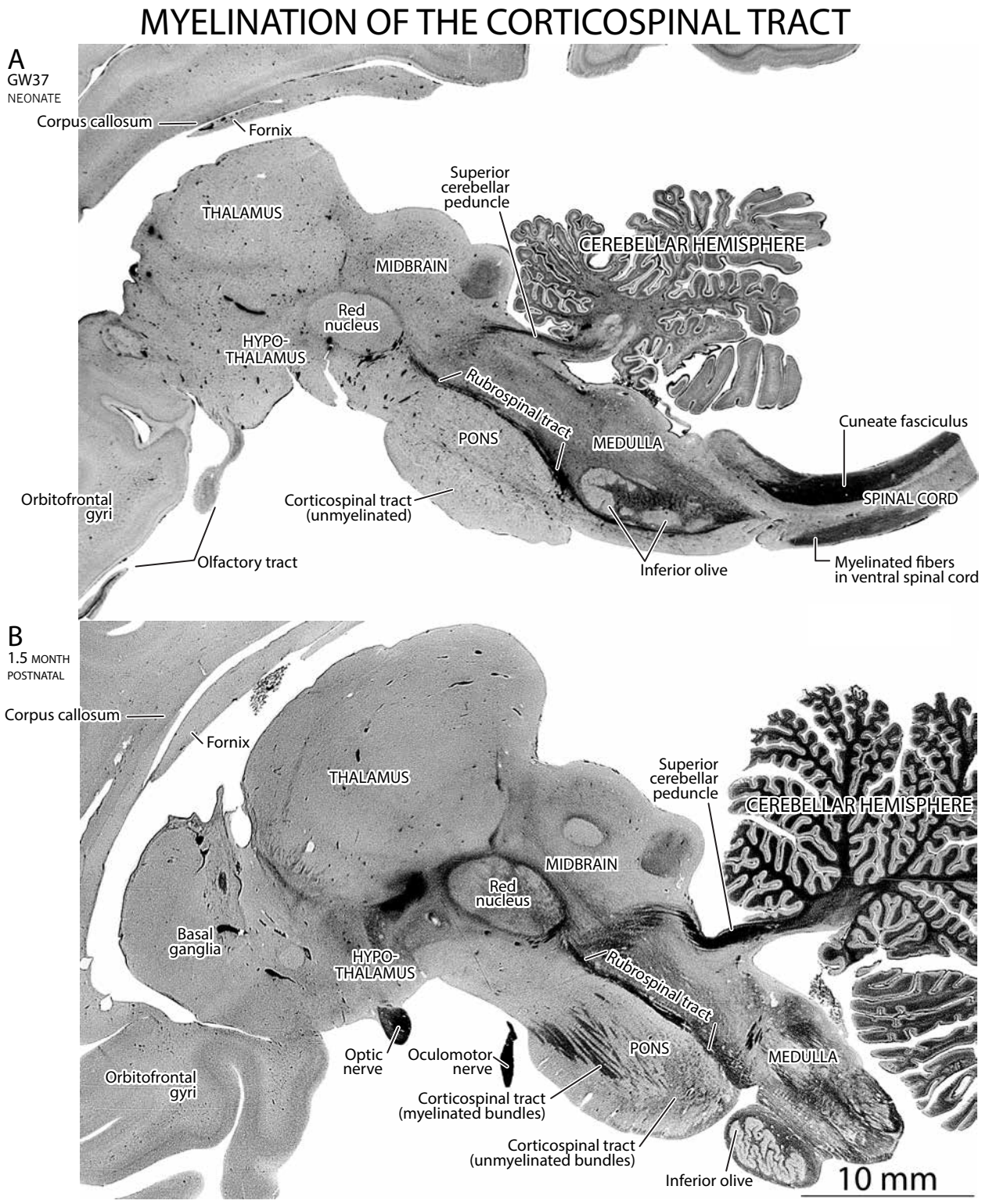

Fig. 60 (facing pages). The myelination of the descending transpontine corticospinal tract in sagittal sections.

A. The corticospinal tract fibers are unmyelinated in the brain of this neonate (Y62-61).
B. Some corticospinal tract fibers are myelinated, others are unmyelinated in this 1.5-months-old infant (Y152-61).

MYELINATION OF THE CORTICOSPINAL TRACT

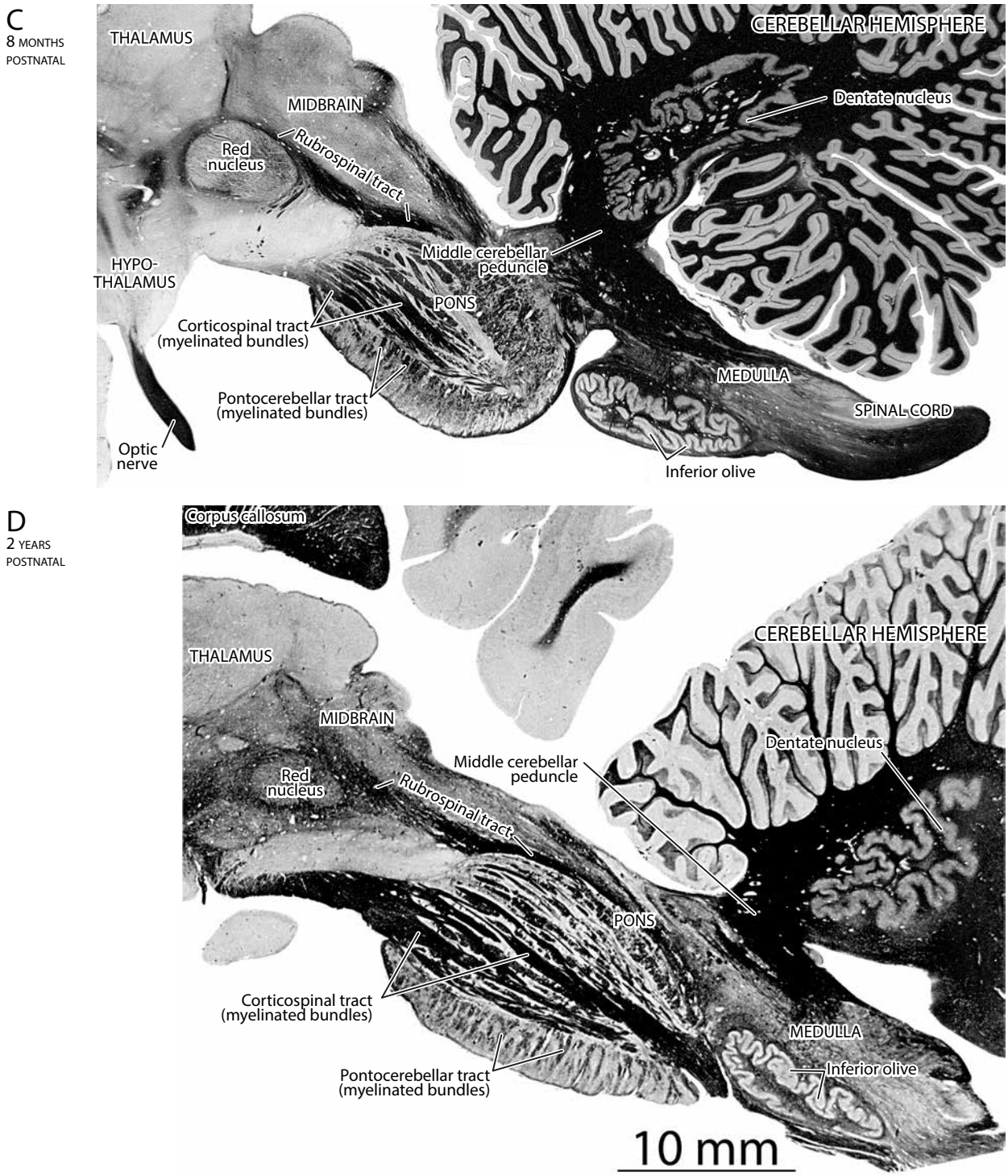

C. The myelination of the corticospinal tract is completed in this 8-months-old child and the myelination of the pontocerebellar fascicles is in progress.
D. The myelination of the pontocerebellar fascicles and of the middle cerebellar peduncle is well advanced in this 2-years-old child (Y425-63).

INTERPRETATIONS AND HYPOTHESES

D. THE FIRST STAGE OF HUMAN NEOCORTICAL DEVELOPMENT: THE PROLIFERATION AND STOCKPILING OF NEURONAL PRECURSOR CELLS

The Neuroepithelium. In vertebrates, early embryonic development is based on the formation of three germ layers, the endoderm, mesoderm and ectoderm. Proliferating endodermal cells give rise to the viscera: the linings of the stomach, intestines and colon, the pancreas, liver, and urinary bladder, the trachea and bronchi of the lungs, and most of the endocrine glands. Proliferating mesodermal cells form the smooth, skeletal and cardiac muscles; the vessels of the circulatory system; and the bones and cartilage. The proliferating cells of the ectoderm develop into such peripheral structures as the sense organs, and the peripheral and autonomic nervous systems. Notably, however, the neurons and neuroglia of the brain and spinal cord of vertebrates originate in a distinct proliferative derivative of the ectoderm, the neuroepithelium (NEP), a germinal matrix that becomes separated from the surface ectoderm early during embryonic development. We consider the vertebrate NEP a fourth germ layer that has properties fundamentally different from the other germ layers.

The NEP is identified in the early vertebrate embryo as a flat sheet of columnar ectodermal cells, known as the neural plate. At this stage, the proliferative cells of this *open NEP* are in contact with the fluid system of the embryonic sac, like the other germ layers. But then the neural plate bends and successively forms the neural groove, the neural folds, and the lateral edges of these folds that will fuse in the dorsal midline, forming a neural tube. This neural tube surrounds the *closed NEP*, a thin tube along the trunk (spinal cord and lower medulla) and enlarged brain vesicles in the head region. The columnar cells of the NEP become spindle shaped and form a widening pseudostratified germinal matrix, where the nuclei of dividing cells shuttle inward to the core cerebrospinal fluid pool when they undergo mitosis, and outward as they prepare to divide again (Sauer, 1936). Henceforth, with one exception, the NEP cells proliferate along the shoreline of a single, compartmentalized *midline* cerebrospinal fluid pool along the neuraxis: the spinal canal caudally, and the medullary, pontine, cerebellar, mesencephalic, diencephalic and telencephalic ventricles rostrally (Fig. 61). The exception is the late-forming telencephalic NEP, which in mammals lines two separate spherical compartments, the right and left *lateral ventricles*. The telencephalic NEP that forms around the lateral ventricles is the proliferative source of neurons of three large brain systems: the basal ganglia (caudate, putamen, globus pallidus), several midline ganglionic (septum) and paleocortical structures (primary olfactory cortex, hippocampus), and the large convexity of the cerebral hemispheres, the neocortex.

The Human Telencephalic Neuroepithelium. Human central nervous system development is initially very similar to that of other mammals, with the elongated NEP of the spinal cord forming along the trunk, and the NEP of the medulla, cerebellum, mesencephalon, diencephalon and telencephalon forming in the head region. There are similarities in the early development of the telencephalic NEP in all mammals, particularly primates and man, but a major difference emerges between lower and higher primates and between apes and man. The neocortex of higher primates and man is greatly enlarged and far more convoluted than those of lower primates, and that is linked with the lengthened period of cortical development. The functional significance of the development of

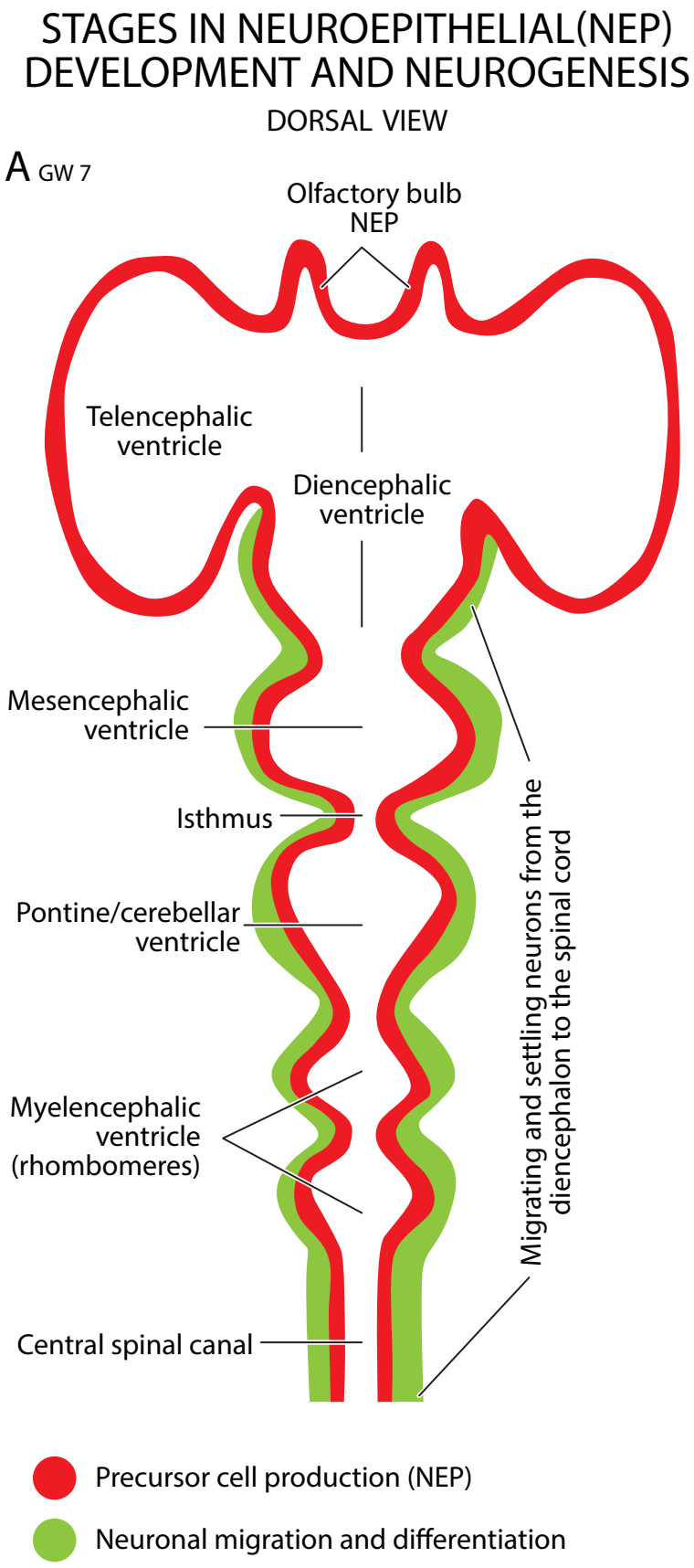

Fig. 61 (on this and the next 2 pages). Schematic diagrams of stages of early human neocortical development in comparison with the rest of the central nervous system (CNS), in a flattened dorsal diagrammatic view.
A. During the first stage, at about GW7, the different subcortical NEP divisions of the CNS (*red*), which surround a series of *midline* fluid compartments, are already flanked by early differentiating neurons (*green*). In contrast, the later developing neocortical NEP (also *red*) around the *paired* lateral ventricles has no surrounding zone of differentiating and migrating neurons.

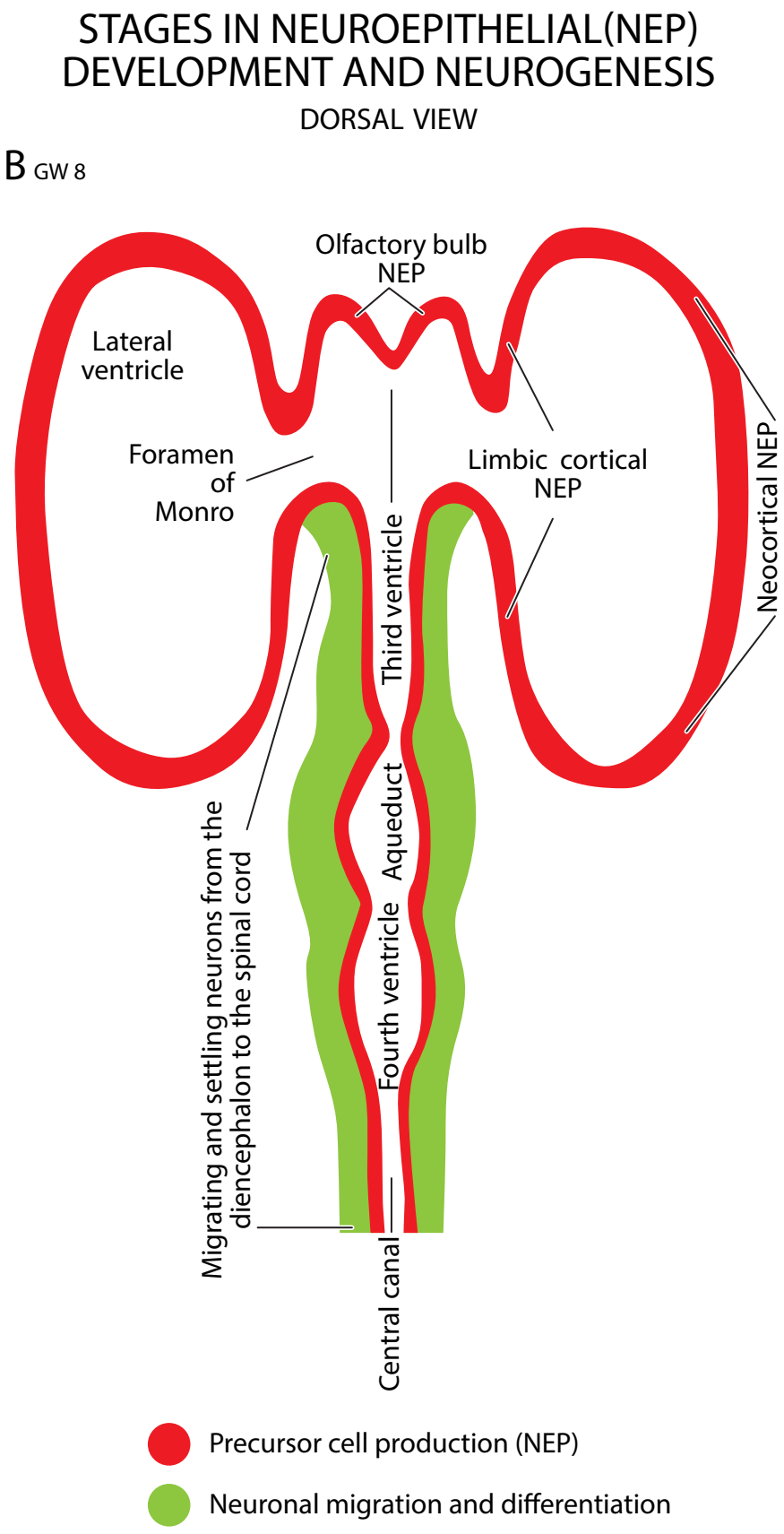

Fig 61B. In the second stage, at about GW8, the subcortical fluid compartments begin to shrink from the third ventricle to the central canal of the spinal cord with a corresponding thinning of the NEP (*red*) in these structures. The early neurons of the spinal cord, medulla, pons, cerebellum, midbrain, hypothalamus, and thalamus are migrating and differentiating, expanding the parenchyma of these structures (*green*). In contrast, there is still no zone of migrating and differentiating neurons around the neocortical and limbic cortical NEPs. Instead, the NEP in the cortical areas of the forebrain continues to grow and surround the expanding lateral ventricles.

Fig. 61C. In the third stage, at about GW9, differentiating neurons have left the NEP of the paired lateral ventricles in large numbers to form, in this plane of sectioning, the cortical plate of the medial limbic cortex and the lateral neocortex. There are many fiber bundles in the deep white matter below the cortical plate, and many fibers are crossing the midline in the corpus callosum.

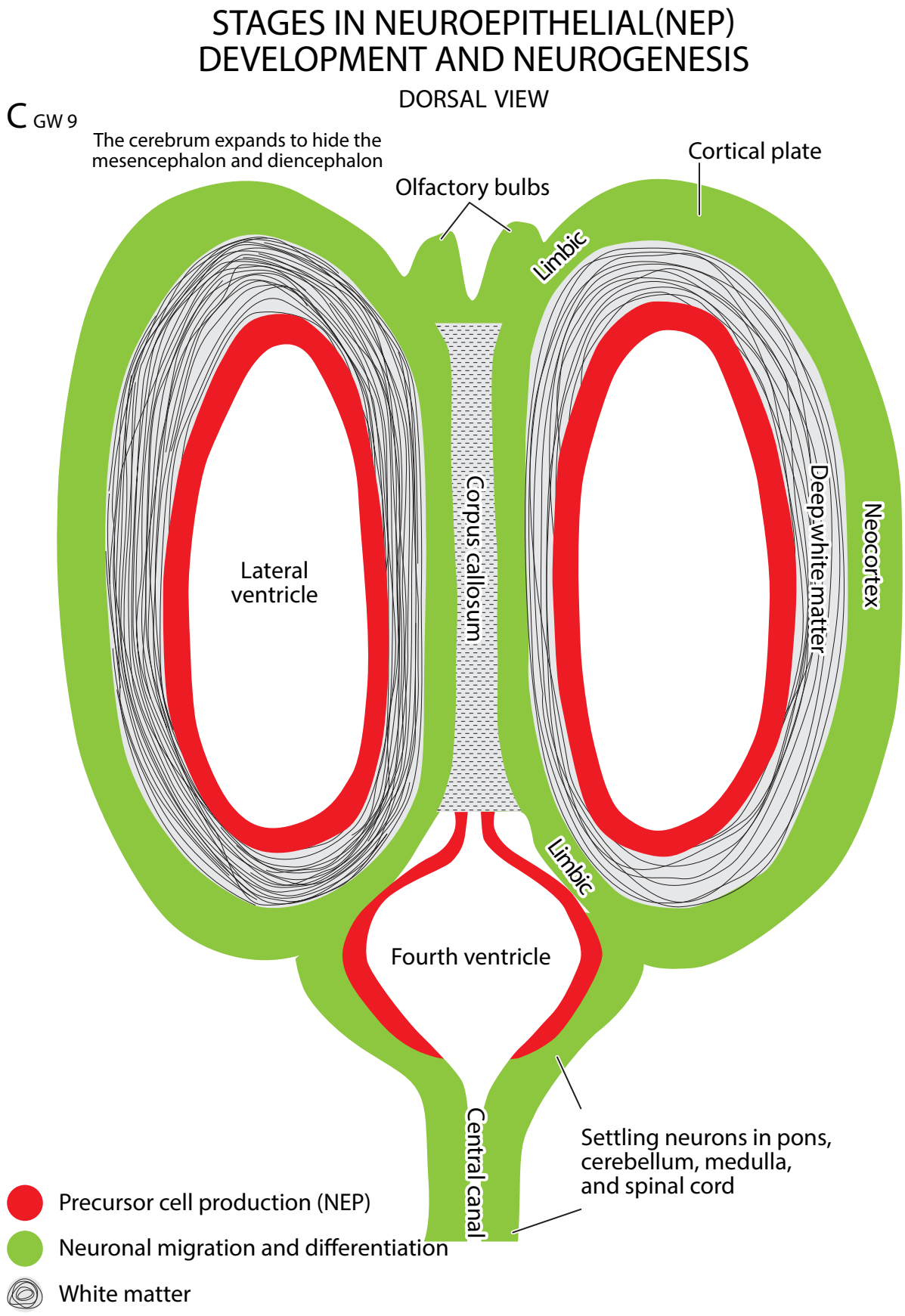
STAGES IN NEUROEPITHELIAL(NEP)
DEVELOPMENT AND NEUROGENESIS
DORSAL VIEW
C GW 9
The cerebrum expands to hide the mesencephalon and diencephalon
Cortical plate
Olfactory bulbs
Limbic
Lateral ventricle
Corpus callosum
Deep white matter
Neocortex
Limbic
Fourth ventricle
Central canal
Settling neurons in pons, cerebellum, medulla, and spinal cord
Precursor cell production (NEP)
Neuronal migration and differentiation
White matter

the large and highly foliated cerebral cortex is obvious: more neurons and interconnections provide humans not only with greater information processing power and storage capacity but also with a large reservoir of spare neurons. These uncommitted neurons can be recruited to mediate novel behavioral and mental functions, such as linguistic communication, tool fabrication, reading and writing, and, more generally, the complex demands of becoming members of a civilized society. However, the immense enlargement of the human neocortex has produced the vital problem how to allow a fetus with such a large brain to pass through the birth canal. The evolutionary solution has been to delay much neocortical maturation until after birth and to package the neocortical gray matter and white matter as compactly as possible within the protective braincase.

The Time Course of Early Telencephalic NEP Development. NEP closure in the human fetus is completed before GW4 (O'Rahilly and Müller, 1987;1994; Bayer and Altman, 2002-2008) but the paired telencephalic NEP that will envelope the lateral ventricles is absent in the GW4, GW5 and GW6 fetuses (Figs. 5, 6). The bicameral telencephalic NEP, divided by the interhemispheric fissure, forms during GW7 as two evaginations from the unicameral prosencephalon (Fig. 7). By the end of GW7, two telencephalic NEP regions can be distinguished: the alar or roof division dorsally and the basal or floor division ventrally. The boundary of the dorsal and ventral divisions of the telencephalic NEP is indicated in the GW8 fetus (Fig. 8H), and is clearly delineated in the GW9 fetuses by the wedge that we refer to as the alar-basal junction (Figs. 9B, 9C, 10C). Very few differentiating cells are seen during this period outside the expanding NEP dorsally (Figs. 17A and 17B), but differentiating cells are accumulating ventrally in the primordium of the basal ganglia, signaling the onset of neuronal differentiation (Fig. 7F). Differentiating cells are still scarce in the roof division by GW8, but cells surrounding the NEP of the floor division have increased greatly in the ventral telencephalon (Fig. 8).

By GW9, two components may be distinguished in the dorsal telencephalic NEP: the continuous dome-like thicker lateral one, and the discontinuous thinner midline one, which is separated into a dorsal and ventral component by non-neural tissue that will produce the choroid plexus. The continuous lateral NEP consists of the proliferative precursor cells of neocortical neurons that by this age begin to migrate outward to form a thin but compact layer composed of young neurons, known as the cortical plate (Figs. 9-11, 62). The discontinuous medial NEP contains precursor cells that will become (i) neurons of the limbic system, such as the septum and the hippocampus; (ii) a bridge that will form the choroid plexus; and (iii) a ventral component that will give rise to such ganglionic structures as the amygdala. On the basis of the histological evidence presented, we conclude that between GW7 and GW8—for about two weeks during the first trimester—neocortical development consists mainly of increasing the stock of the proliferating precursors of neurons and other neural elements in the greatly expanding neocortical NEP, with minimal or no concurrent neuronal production. From GW9 on, new neurons migrate to the cortical plate as it slowly thickens, with a gradient from lateral to dorsal, and central to frontal, during the following weeks (Figs. 13, 14, 15).

Fig. 62. Stages in the early development of the dorsal neocortex in relation to the basal telencephalon, shown in a schematic lateral view. **A.** By about GW7, the NEP (*red*) of the basal telencephalon is surrounded by differentiating neurons (*green*) but the dorsal telencephalic NEP, the primordium of the neocortex, consists only of proliferative

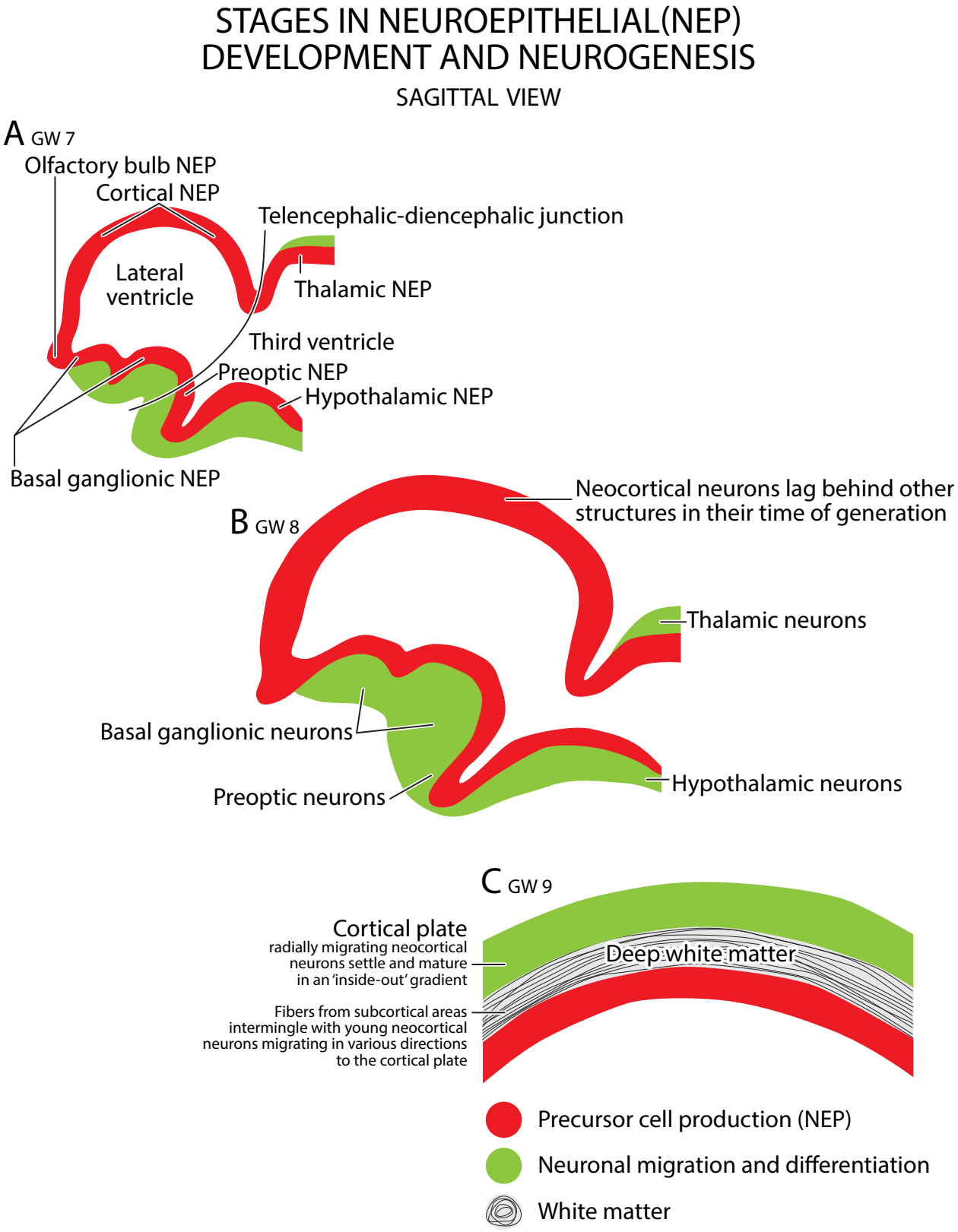

precursor cells. **B**. By GW8, the NEP has expanded both ventrally and dorsally but there are still few differentiating neurons in the neocortex. **C**. By GW9, a contingent of migrating young neurons have begun to form the cortical plate, the primordium of the cortical gray matter, which is separated from the NEP by the formative white matter.

The Role of the Embryonic Meninges and the Hypertrophied Choroid Plexus. The nuclei of proliferative NEP cells have to shuttle to the shoreline of the ventricular fluid space to undergo mitotic division (Fig. 17). The size of any neuronal population is dependent on the size of that shoreline occupied by its precursors and their endurance over time. The immense number of neurons in the human neocortex can be directly attributed to the enormous volume of the embryonic human lateral ventricles surrounded by the neocortical NEP and their endurance through the first and second trimesters, before the ventricles begin to shrink and in some regions disappear altogether. The expansion and maintenance of that large ventricular space requires the production of cerebrospinal fluid with adequate pressure, and that appears to be initially dependent, before the vascular system develops (Padget, 1957), on the greatly enlarged meninges and the hypertrophied choroid plexus (Fig. 63). Both of these structures differ during the embryonic period from what they become later during the fetal period. Little is known of the properties of the hypertrophied, fluid-filled embryonic meninges (Sturrock, 1990; Kamiryo et al., 1990). It is notable that the embryonic choroid plexus has a cell-sparse and spongy morphology (Fig. 63D), while the fetal and mature choroid plexus is a distinctive frond-like tissue, composed of a monolayer of cuboidal cells that surround a capillary core. It is known from studies in animals that the early choroid plexus contains glycogen granules, suggesting a role in energy metabolism (Tennyson and Pappas, 1964; Dohrmann, 1970; Dziegielewska et al, 2001; Saunders et al., 2015), and there is evidence that it contains factors that promote NEP cell proliferation (Gato et al., 2005; Johansson et al., 2005; Martin et al., 2006; Parada et al., 2006; Mashayekhi and Salehi, 2006; Lehtinen et al., 2011).

Aspects of Early Neocortical NEP Development. The first step in the prolonged process of human neocortical development, antedating the differentiation of neurons, is the generation of a large population of self-replicating precursor cells by a dedicated germinal matrix, the NEP. In the histological specimens that we have examined, the NEP cells of the neocortex look uniform. But considering the fact that these precursors cells will generate not only *neurons*, and different classes of neurons, but also other *neural* elements, such as cells of the choroid plexus, astroglia cells, oligondendrocyes, and ultimately ependymal cells, the question is: are these NEP cells "indifferent" pluripotent cells whose differentiation is due to extrinsic influences at a later stage of development or are they already "specified" before leaving the NEP? Our normative material cannot answer this question. But emerging evidence from genetic studies, mostly carried out in mutant or "knockout" mice, indicate that the neocortical NEP itself contains different types of precursor cells whose fate is already specified by intrinsic factors before leaving the NEP. The histological evidence indicates that some NEP cells undergo symmetrical division within the NEP, parallel to the lining of the ventricle, giving rise to two progeny with mitotic potential, while other cells undergo asymmetric division, cleaving at a right angle to the ventricular lining and giving rise to one stock-building progeny, which stays in the NEP, and another that is ready to leave the NEP (e.g., Bayer and Altman, 1991). The exiting cells may have different fates: determined to differentiate as a postmitotic neuron, or as a neural precursor cell that moves to a secondary germinal matrix (such as the subventricular zone), or a particular type of glia cell.

We assume that initially the majority of NEP cells undergo symmetrical division to build the stock of neural precursor cells but later more and more of them undergo asymmetrical division. The

Fig. 63. The expansion of the developing telencephalon and the formation of the cortical plate are associated with the development of the choroid plexus, as seen in sagittal sections. **A**. The choroid plexus is absent in this

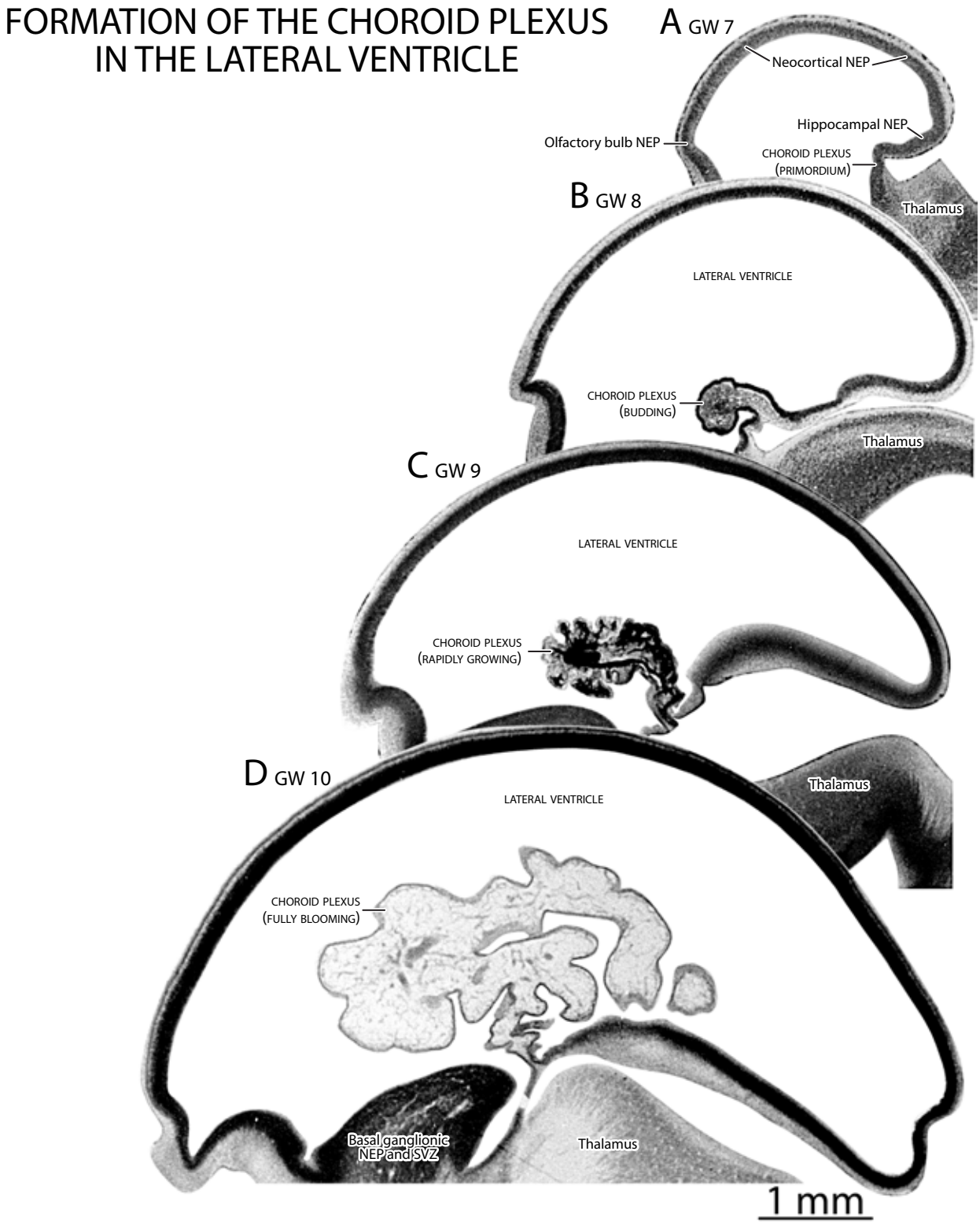

GW7, CR 15 mm fetus (C927). **B**. The stalk of the choroid plexus is beginning to produce the rudiment of the choroid plexus in this GW8, CR 21 mm fetus (C6202). **C.** The developing choroid plexus in a GW9, CR 24.7 mm fetus (C632). **D.** The blooming of the choroid plexus in the expanded lateral ventricle in this GW10, 33 mm fetus (C145).

progression of cortical NEP cells from symmetrical to asymmetrical division has been attributed to the influence of Pax6, a transcription factor that regulates the development of the eye, nostrils, and the CNS (Estivill-Torrus et al., 2002; Quinn et al., 2007; Walcher et al., 2013). Pax6 plays a role in the interkinetic nuclear shuttling of NEP cells (Tamai et al., 2007). Decreasing Pax6 levels facilitates precursor cell self-renewal; increasing Pax6 levels facilitates neurogenesis (Sansom et al., 2009). Pax6 also plays a role in the dorsoventral patterning of the mouse telencephalon by persisting in the dorsal telencephalic NEP that produces neocortical neurons and disappearing in the ventral telencephalic NEP that generates basal ganglia neurons (Stoykova et al., 2000). Studies indicate that Pax6 interacts with other transcription factors, such as Gsh2 (Torreson et al., 2000; Yun et al., 2001), Tbr2 and Tbr1 (Englund et al., 2005), Neurog 2, Asc1 and Hes 1 (Sansom et al., 2009), and Emx1 and Emx2 (Bishop et al, 2003), and that, together with the BAF transcription factors, Pax6 directs the development of neuronal rather than glial differentiation (Ninkovic et al., 2013). However, complicating this picture, it has been reported that that Pax6 is expressed by the prosencephalic neural plate of mice before it folds and fuses (Inoue et al., 2000), that is, before the telencepalon forms, and that Pax6, Tbr2 and Tbr1 are expressed not only by progenitor cells but also by postmitotic neurons in the developing neocortex (Englund et al., 2005).

In humans, Pax6 is uniformly expressed by NEP cells in early fetuses and in neural cells developing in vitro (Zhang et al., 2010). According to the same study, overexpression of Pax6 in vitro turns pluripotent NEP cells into a committed neuronal lineage and the cells form rosettes as they settle. This happens during the early phase of development; at a later phase, another transcription factor, Sox 1, is expressed. An interesting observation is that the expression of Pax6 is more pronounced and protracted in monkeys and humans than in mice, which may be a mechanism for assembling a much larger stock of precursor cells prior to their differentiation (Zhang et al., 2010). Finally, loss of Pax6 results in microcephaly and the loss of late-generated, upper layer cortical neurons (Quinn et al., 2007). Several gene mutations have been linked to microcephaly. One of them, MCPH1, encodes the protein microcephalin (Woods et al., 2005; Pulvers et al., 2015). In MCPH1 knockout mice, the proportion of asymmetric divisions of NEP cells is reduced and the mice become microcephalic. Proliferating precursors of neurons are extremely radiosensitive and microcephaly was reported to be the only proven malformation in children born to mothers who were near the epicenter of the nuclear bomb explosions in Hiroshima and Nagasaki (Plummer, 1952; Yamazaki, 1954; Miller and Blot, 1972).

From Neocortical NEP Uniformity to Heterogeneity. During its early development, the embryonic human CNS consists of a continuous sheet of NEP cells along the entire length of the neuraxis from rostral to caudal (Figs. 61, 62, 63). There is no obvious discontinuity in that germinal matrix in relation to the different divisions of the CNS, such as the mesencephalon, diencephalon or telencephalon, or in relation to the different future components of these divisions, such as the thalamus, subthalamus or hypothalamus. But as development proceeds, two kinds of regional differences emerge: one is the transient appearance of protuberances, invaginations and evaginations, foci of high rate of NEP cell proliferation that produce a variegated ventricular shoreline; the other is the subsequent thinning and eventual disappearance of the NEP at sites where precursor cell production slows down or ceases altogether. Most conspicuous of the former are the transient rhombomeres in the medulla, which are targets of fibers of the different cranial nerve

ganglia (Bayer and Altman, 2002-2008), and the transient evaginations and invaginations along the third ventricle, which are sources of the neurons destined to form the different components (nuclei) of the thalamus and hypothalamus (Altman and Bayer, 1988). We have suggested that these transient proliferative foci reflect NEP "mosaicism," regional differences in the rate of cell division in relation to the precise timetable in the production of different classes of neurons along the neuraxis (Bayer et al., 1993).

In sharp contrast to the subcortical regions manifesting visible NEP mosaicism, the early neocortical NEP and the the cortical plate, appear to be uniform throughout, with no visible indications of cellular differences in relation to the later developing different lobes and of areal differences within the lobes. Does that mean that unlike the "specified" NEP of most subcortical structures that display mosaicism, the entire neocortical NEP is initially "plastic?" If so, the neocortical NEP would have to become specified at a later stage, perhaps some time after the arrival of the visual, somatosensory and auditory radiation fibers from the thalamus. But if so, what signaling mechanisms make visual system fibers target the occipital lobe and create a retinotopic map there; what makes somatosensory fibers target the paracentral lobe and create a somatotopic map there; and what makes auditory system fibers target the temporal lobe and create a cochleotopic map there? Instructive in this regard is the evidence that optic fibers from the lateral geniculate nucleus do not initially grow in the direction of the occipital lobe but, rather, first grow anteriorly and then, taking a detour around the caudate nucleus, turn around (known as Meyer's loop) and grow caudally in the direction of the occipital lobe (Fig. 16). The simplest explanation would be that the occipital lobe neurons do possess some specificity and emanate signals to attract optic fibers but repel fibers of other sensory modalities.

Formation of the Fronto-Temporal Cleavage. A morphogenetic change that begins early in the development of the neocortex, and appears anomalous, is its change from its regular ovoid shape by assuming a folded crescent form as the result of the formation of the fronto-temporal dimple (Fig. 13A) that later turns into the fronto-temporal cleavage. We cannot attribute any functional utility to this change from the perspective of cortical organization because that chasm hinders rather than facilitates communication between the frontal and the temporal cortices as the circuitry of the cortex develops. However, we can offer a two-stage developmental interpretation. As seen in sagittal sections, the expanding neocortical NEP retains its smooth, dome-like configuration in the GW7 (Fig. 63A), GW8 (Fig. 63B) and most GW9 embryos (Figs. 9, 10), but a dimple appears at the base of the neocortical surface by about GW10 and GW11 (Fig. 13), and turns into a cleavage by the end of the first trimester and early in the second trimester (Fig. 19). That dimple is apparently produced by pressure exerted by the hypertrophied meninges of the developing neocortex—in particular, the hypertrophied superarachnoid reticulum that we have described earlier. That dimple widens and deepens in the subsequent months of cortical development, as the vascular system develops, as seen in lateral views of the brains of an early 4 months-old fetus (Fig. 64A), a late 4 months-old fetus (Fig. 64B), and 5 months-old fetus (Fig. 64C). As a result, the convex lateral surface of the neocortex splits into two parts, with the fronto-temporal cleavage separating the pole of the temporal cortex from the rear of the frontal cortex. That cleavage comes to serve as the entry sites for the elaborate branches of the medially situated arteries that supply with oxygenated blood the expanding gray matter of the lateral neocortical convexity (Fig. 65A).

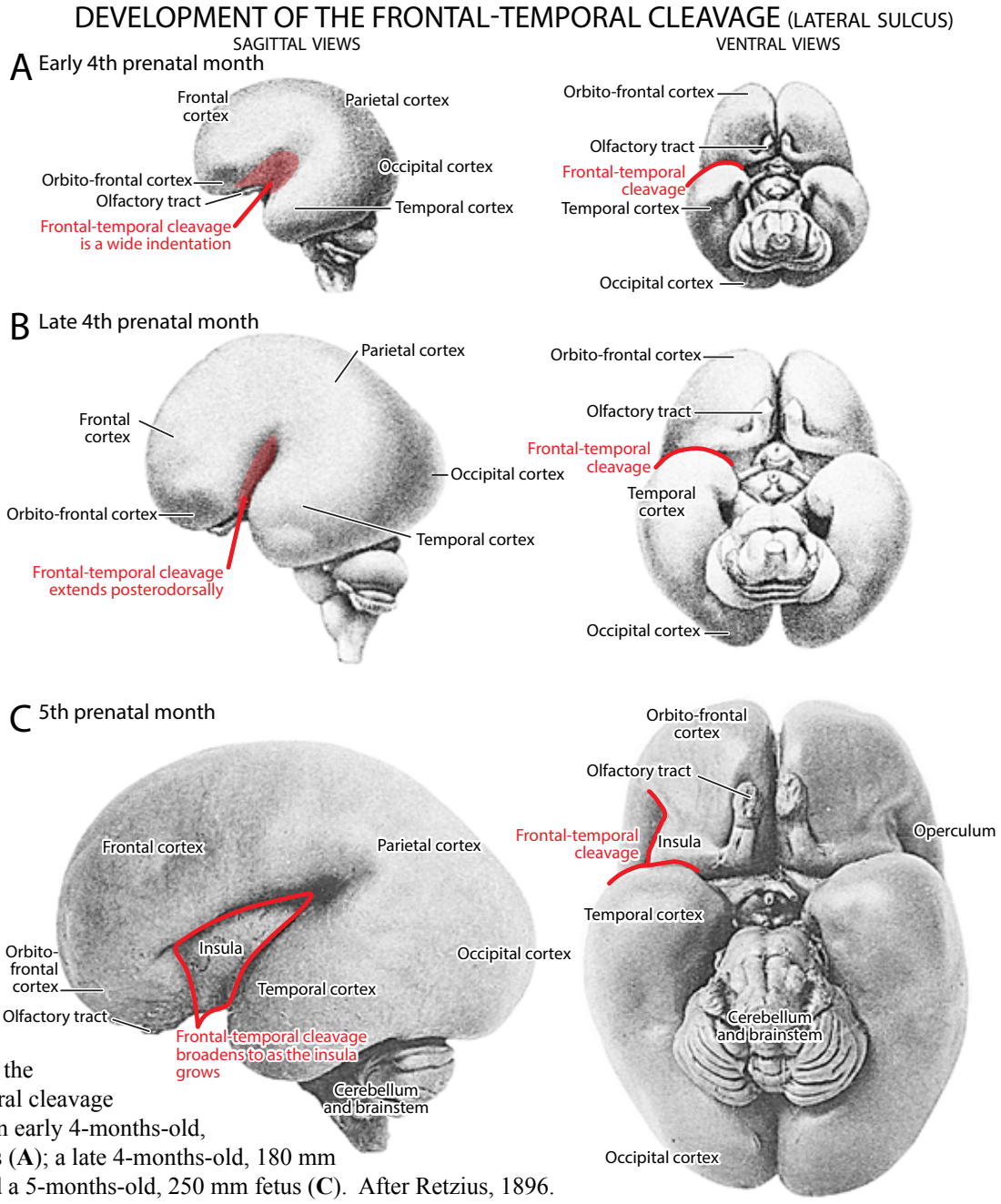

Fig. 64. Expansion of the fronto-temporal cleavage in the brain an early 4-months-old, 120 mm fetus (**A**); a late 4-months-old, 180 mm fetus (**B**); and a 5-months-old, 250 mm fetus (**C**). After Retzius, 1896.

The gray matter of the expanding neocortex is supplied with oxygenated blood by three medially situated large vessels: the ascending basilar artery, which branches into the paired posterior cerebral arteries; the paired internal carotid arteries, which form the middle cerebral arteries; and the paired anterior cerebral arteries (Fig. 65B). (Communicating arteries that form the circle of Willis interconnect these three systems.) As seen from the base of a mature brain, the branches of the posterior cerebral arteries vascularize the convexity of the posterior neocortex, including the occipital lobe (Fig. 65C). As seen in a sagittally transected brain, branches of the anterior cerebral artery vascularize the midline cortex (Fig. 65E). And as seen in a coronally transected brain (Fig.

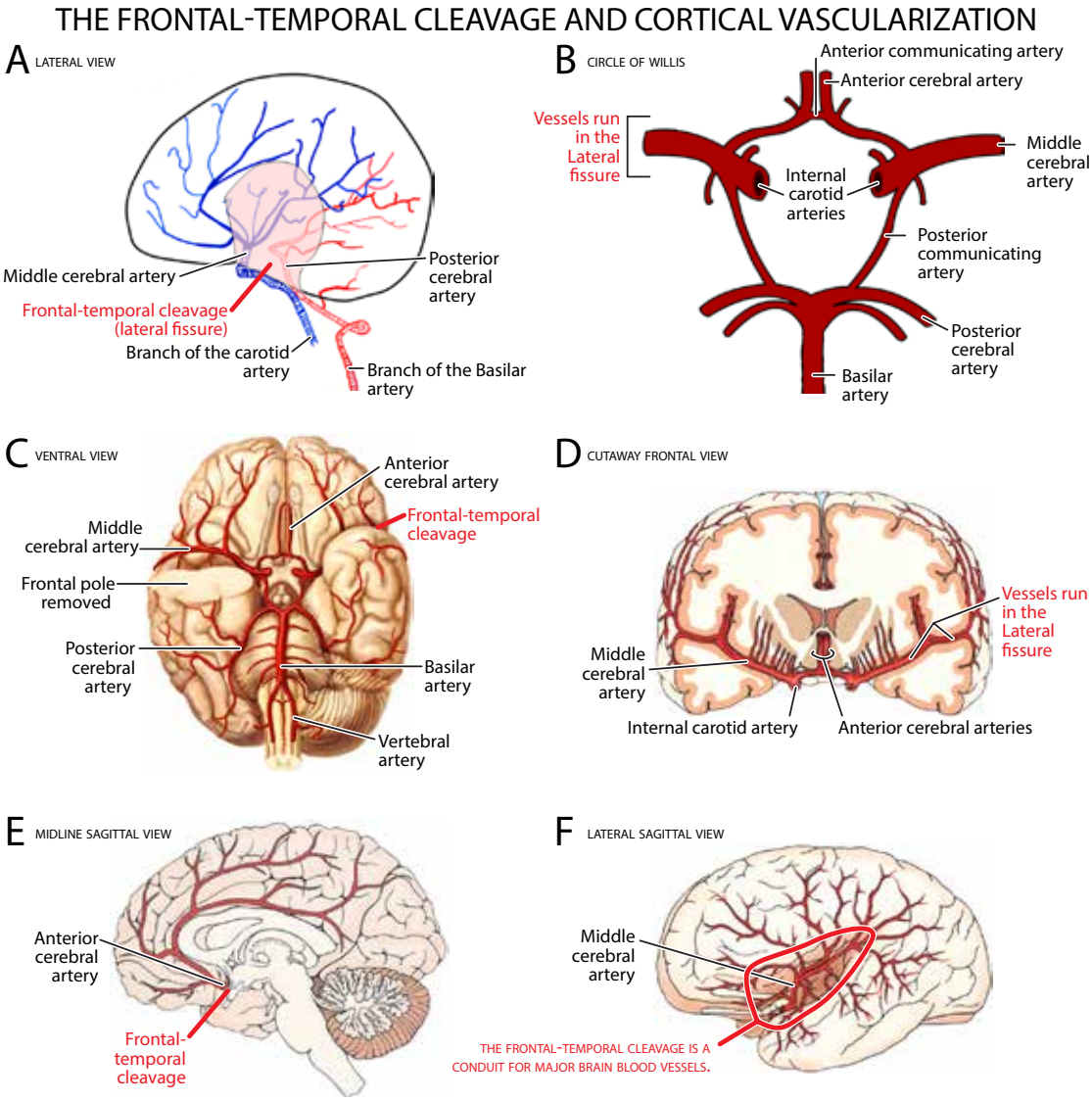

Fig. 65. A. The middle cerebral artery (*blue*) and the midline posterior cerebral artery (*red*) in early second trimester fetuses. Branches from the two pass from the midline laterally over the neocortical convexity by way of the frontal-temporal cleavage. **B**. Simplified diagram of the arterial system of the mature cerebral cortex. The internal carotid arteries and the basilar artery, in combination with the communicating arteries of the Circle of Willis, are the source of the blood supply of the anterior and posterior neocortex, respectively. **C**. Ventral view of the branching pattern of the basilar artery and the middle cerebral artery in the mature brain. Note the middle cerebral artery passes laterally above the frontal-temporal cleavage. **D**. Coronal view of the distribution of branches of the anterior cerebral artery. **E**. The distribution of branches of the anterior cerebral artery as seen in the midline. **F.** View of the course of the middle cerebral artery as seen in a brain with the frontal lobe and the temporal lobe pulled apart. Based on Retzius (1896), Padget (1948), Jaworski, StudyBlue, Internet), and other sources.

65D) and from its lateral aspect (Fig. 65F) the middle cerebral arteries vascularize much of the lateral convexity of the neocortex. We conclude that the fronto-temporal cleavage serves as the gateway for the branches of the middle and anterior cerebral arteries, originating medially, over to the lateral convexity of the neocortex.

E. THE SECOND STAGE OF HUMAN NEOCORTICAL DEVELOPMENT: NEURONAL DIFFERENTIATION, MIGRATION, AND SETTLEMENT

Formation of the Cortical Plate. Neocortical neuronal differentiation and migration begins about GW9 as postmitotic cells exit the NEP and form a compact superficial band of young neurons, known as the cortical plate (Figs. 9,10, 11, 17D). These settling neurons are the earliest components of the presumptive neocortical gray matter. In younger GW9 fetuses, the cortical plate emerges laterally in the central portion of the neocortex (Figs. 9B, 9C); it is still absent in the future frontal lobe anteriorly (Fig. 9A) and in the future occipital lobe posteriorly (Fig. 9D). In older GW9 fetuses, the cortical plate is better developed and has become more extensive (Figs. 10, 11). There is a gradient in the formation of the cortical plate, starting laterally in the presumptive paracentral/ insular region, spreading from there dorsally and ventrally, and anteriorly and posteriorly.

In addition to the development of the cortical plate, a notable development during GW9 is the assembly of a unique set of horizontally-oriented neurons, the Cajal-Retzius cells, in the superficial fibrous layer I between the cortical plate and the pia (Fig. 17D). It has been hypothesized that the earliest settled neurons in the cortical plate will form the base of the gray matter, the subplate (layer VII); settling neurons later come to be sandwiched between it and the superficial layer I containing the Cajal-Retzius cells (Marin-Padilla, 1988, 1992; Bayer and Altman, 1991). The Cajal-Retzius cells are a unique class of neural elements with two features: they have a rich arbor of horizontally-oriented fibers beneath the pia, and they secrete a glycoprotein, reelin. Cajal-Retzius cells are transient elements and they have been shown in mutant rodents to be essential for the normal development of the cytoarchitecture of the neocortical gray matter (Caviness, 1976; Ogawa et al., 1995; Meyer and Goffinet, 1998). Less is known about the fate of the early cortical plate neurons of layer VII; early on, they delaminate from the cortical plate and form a more diffuse layer beneath it (Bayer and Altman, 1991). They, too, may be structural rather than functional elements, serving as the scaffolding for the proper assembly of the permanent neuronal population of the laminated cortical gray matter that will settle above them.

Early neocortical neuronal differentiation and migration is associated with several other developments. The first of these, as noted before, is the rapid expansion of the choroid plexus of the lateral ventricles between GW8 and GW 10 (Figs. 63B-D). We assume that the growth of the choroid plexus plays a pivotal role in the great expansion and persistence of the fluid compartment of the human lateral ventricles, which supports the extensive and prolonged proliferation of neocortical NEP cells. The second developmental phenomenon, as seen in older first trimester fetuses, is the hypertrophy of the meninges that encase the neocortex—the mesenchymal tissues of the dura, arachnoid, and pia (Figs. 14 and 16). The enlargement of these meningeal constituents is most pronounced in the midrib of the neocortex, where their transient hypertrophy leads, as noted before, to the mid-cephalic constriction of the cerebrum (the frontal-temporal dimple and the invaginating insula) and the partition of the lateral ventricles into an anterior and a posterior component (Fig. 16). We proposed earlier that that these fluid-filled spongy tissues support neocortical development metabolically and hydrodynamically prior to the onset of neocortical vascularization. But as the vascularization of the expanding neocortex begins (Fig. 18), that dimple turns into the widening frontal-temporal cleavage and is the site for branches of the medially situated cerebral arteries to expand over the lateral surface of the neocortex (Fig. 65). The persistence of this cleavage has

consequences as to how connections between the frontal and temporal lobes form, as the fibers have to make a detour around the chasm created, such as is the case with the uncinate fasciculus.

The third developmental event, which starts in early GW9 fetuses and continues in older ones, is the sprouting of thalamocortical fibers and their ascent towards and penetration of the formative neocortex, and the concurrent sprouting and descent of corticofugal fibers (Figs. 12, 13 and 16). In the older first trimester fetuses the corticofugal axons are seen to penetrate the basal ganglia (Fig. 16D), giving rise to a fibrous aggregate known as the internal capsule (Figs. 15 and 16). With regard to the thalamocortical fibers, one set of axons are seen to make a loop around the basal ganglia, these are optic fibers from the lateral geniculate nucleus growing toward the occipital lobe (Fig. 16E); another set of fibers appears to target the paracentral lobule (Fig. 16E).

Formation of the Stratified Transitional Field: The First Step in Areal Diversification. Casting new light on the issue of neuronal differentiation and the development of neocortical areal specificity (what traditionally is known as "brain localization") is the histological evidence that beginning towards the end of the first trimester, following the settling of the *first migratory wave* of early-generated neurons from the NEP in the cortical plate (the neurons in the future subplate), a *second migratory wave* of neurons displays a different pattern of migration (Figs. 19, 20 and 21). These migratory neurons will settle in layers VI to II, but they all stop (sojourn) in the intermediate zone between the NEP and the cortical plate and form a series of discrete cellular and fibrous bands, what we have called the stratified transitional field, or STF (Bayer and Altman, 1991; Altman and Bayer, 2002; Bayer and Altman, 2002-2008;). The STF persists throughout the second trimester (Figs. 25, 26, 27, 28) but disappears by the early third trimester as the cortical plate is transformed into the differentiating areas of the gray matter (Fig. 30). We postulated that this second wave of sojourning neocortical neurons establishes intimate relationships with incoming thalamocortical afferents before they penetrate the cortical plate. Apparently, the STF is a staging area where different classes of sojourning cortical neurons and afferent fibers interact with one another before they proceed to their targets. The implication of this hypothesis is that the areal and topographic specificity of differentiating neocortical neurons is a product of some sort of transaction between the sojourning neuron and the topographically organized ingrowing thalamocortical fibers. Then, by the end of the second trimester, the STF is beginning to disappear (Fig. 28) and it is gone by the third trimester (Figs. 30-31). With all the migrating and sojourning neurons settling in the expanded cortical gray matter, the STF is replaced by the cortical white matter.

There are notable differences in STF layering in the presumptive orbitofrontal, frontal, motor, somatosensory, parietal, occipital, and temporal cortical areas, and we assume that there is a direct relationship between banding patterns in the STF and unique lamination patterns in different cortical areas (Figs. 19-21, 25-27). Much research will need to be done to establish the identity of the neurons forming STF2, STF3 and STF5, and to identity the fibers forming STF1, STF4 and STF6. The available evidence suggests the following tentative identification. The fibrous STF1 band beneath the cortical plate, which progressively expands during the second and third trimesters, will evidently become the deep white matter. The cellular STF2, which is prominent in the future anterior premotor and motor areas but virtually absent in the posterior visual cortex, contains the differentiating large pyramidal neurons of layer VI and V. These neurons sprout long-distance efferent axons, including the corticofugal fibers that traverse the basal ganglia and descend to the

brain stem and spinal cord. The cellular STF3, which is most prominent and elaborate in the future visual c ortex but is absent in the frontal cortex, contains the layer IV neurons that will differentiate as granule cells and are the main target of thalamocortical afferents. There are apparent differences in STF3 configuration in the different presumptive sensory projection areas and association areas of the neocortex. An important STF3 feature is the multitude of minicolumns aligned at a right angle to the cortical surface. That pattern suggests a topographic segregation of incoming afferents at this site (the "honeycomb matrix") as presumably they establish connections with and specify the neurons that will later ascend and penetrate the cortical plate (Fig. 23). The fibrous STF4, which is present in both the anterior and posterior cortical areas, may contain descending corticofugal efferents and thalamocortical afferents, respectively. The cellular STF5 may differentiate as the small pyramidal neurons of the supragranular layers III and II. Finally, STF6 appears to contain the fibers of the corpus callosum. Once all the neurons of the cellular bands have migrated to the cortical plate, the fibrous bands become part of the expanding white matter.

Neuronal Migration and Axonogenesis. To reach their targets, the early corticofugal and corticopetal axons must navigate through different regions as exemplified, for instance, by the visual fibers that first grow rostrally toward the internal capsule, then turn caudally to approach the occipital lobe (Fig. 16E). However, we have practically no information available in the developing human neocortex regarding how afferent axons are guided towards specific cortical targets. Experimental studies carried out mostly in rodents suggest that growth cones and filopodia of axons respond to diffusible molecular guidance signals by moving forward, retracting or changing direction. Among these navigational signals are netrins (Métin et al., 1997), ephrins (Castellani et al., 1998; Mann et al., 2002; Dufour et al., 2003; Bolz et al., 2004), N-cadherin (Huntley and Benson, 1999; Poskanzer et al., 2003), Tbr1 and Gbx2 (Hevner et al., 2002), Fez (Chen et al., 2005; Molyneaux et al., 2005; Kwan et al., 2012; de la Rosa et al., 2013), and semaphorins (Pasterkamp, 2012). Axon branching and arborization at particular target locations by budding filopodia has been associated with neurotrophins, such as fibroblast and nerve growth factors (Gallo and Letourneau, 2000; Szebenyi et al., 2001; Kalil and Dent, 2014).

F. THE THIRD STAGE OF HUMAN NEOCORTICAL DEVELOPMENT: AREAL DIFFERENTIATION AND PROGRESSIVE GYRIFICATION

Areal Differentiation of the Neocortical Gray Matter. As seen in the sagittal plane in the GW7 (Fig. 7A) and GW8 (Fig. 8D) fetuses, the cortical plate is relatively uniform in terms of its cell packing density and depth. The same uniformity is suggested in the coronally and horizontally sectioned brains of GW9 embryos (Figs. 9D, 10B). That uniformity persists into the early second trimester, as shown in a GW14 embryo (Fig. 19A-D). However, by the mid-second trimester, as seen in a GW20 embryo (Figs. 20A-D, 22), the thickness of the cortical plate begins to differ from anterior to posterior, in parallel with differences in the organization of the STF in the two regions. And in the GW23 fetus, a difference is also becoming evident in the lamination pattern of the frontal, paracentral, and posterior cortical plates (Fig. 28). As development proceeds, the relatively homogeneous neocortical plate is transformed into the neocortical gray matter, a composite tissue of neuronal cell bodies, dendrites, and axon terminal branches. The human neocortex features many different areas, each having a unique organization of cells and fibers (cytoarchitectonics) different connections, and different functions.

That areal differentiation of the neocortical gray matter is a gradual and prolonged process. For instance, there is little difference in the cell-packing density and cell-depth of the presumptive motor and visual cortices in a 4-months-old fetus (Fig. 32). In 5-months-old fetuses differences emerge between the two regions: cell-packing density and cell depth are lower in the visual cortex than in the motor cortex (Figs. 33, 34A,C). In the visual cortex, the development of gray matter lamination is associated with the dissolution of the STF (compare Figs. 34A and 34B). The sojourning neurons have resumed their migration and became aligned in the gray matter as vertical minicolumns separated from each other by vertical fiber bands (Fig. 35). By the 7th fetal month, areal differences are also marked throughout the neocortex by differences in the predominance of different types of neurons in the horizontal layers of the frontal lobe, the premotor and motor cortices, the parietal lobe, and the occipital lobe (Fig. 36). By the time of birth, the cellular lamination pattern of different cortical areas is similar to that seen in the maturing postnatal neocortex (Fig. 37). The presumed outcome of this neocortical areal differentiation is that by birth the projection areas receive detailed somatotopic, retinotopic and cochleotopic information about features and changes in the outside world.

The Phenomenon of Neocortical Gyrification: Formation of Lobules and Sublobules. In the first trimester embryo, the neocortex has a smooth surface (Figs. 7, 9, 15, 16) but during the second trimester, the neocortex begins to fold, forming gyri and sulci (Figs. 19E-F, 25, 26, 27, 28). This change begins as the white matter composed of the growing afferent, efferent, and commissural fibers begins to expand in 4-months-old fetuses, concurrently with shrinkage of the fluid space in the lateral ventricles (Figs. 66B, C). The first site of that gyrification takes place in the occipital lobe, where the parieto-occipial and calcarine fissures begin to form (Fig. 66B). (See also the onset of calcarine fissure formation in Fig, 19E, F.) These two fissures have become deeper in 5 months-old fetuses, as a result of which the occipital lobe becomes separated from the parietal lobe, and the calcarine fissure divides the occipital lobe into two primary gyri, the dorsal cuneus and the ventral lingula (Fig. 66C).

PROGRESSIVE GYRIFICATION. We have followed the onset of gyrification in the rest of the neocortex in the sagittal plane in a young 6 months-old fetus (Fig. 26), and the ongoing subsequent gyrification by comparing the neocortex of a 5-months-old fetus with that of a 7-months-old fetus in the horizontal plane (Fig. 28). Fig. 67 illustrates progressive neocortical gyrification in three fetuses aged GW24, GW29, and G34 at matched coronal levels. The comparison suggests that increased gyrification is associated with four ongoing morphogenetic processes: (i) a reduced NEP around (ii) a shrinking lateral ventricle; (iii) expansion of the white matter; and (iv) expansion of the surface area of the cortical plate. NEP reduction signals the diminution and ultimate cessation of neocortical neurogenesis. Henceforth, differentiated ependymal cells will line the shrunken lateral ventricle. The expansion of the white matter is attributable to increasing numbers of afferent axons, the immense growth in the number and lengths of axons and collaterals of the differentiating cortical neurons, such as long-distance and short-distance association fibers, and commissural fibers of the corpus callosum. Finally, the expansion of the surface area of the neocortex is associated with the disappearance of the stratified transitional field, as the sojourning neurons resume their migration and settle in the cortical plate. The settled neurons, particularly pyramidal cells, grow laterally spreading dendrites causing a widening of the neuropil between the cellular minicolumns. Significantly, the great expansion of the gray matter and the white matter is associated with

increased gyrification. Instead of ballooning, the cortical gray matter gets distributed over the increasing number of buds, swellings and branches of the partitioning white matter. As a result, a high proportion of the neurons of the cortical gray matter become distributed along the banks (sulci) of the lobules and sublobules formed (Fig. 67C).

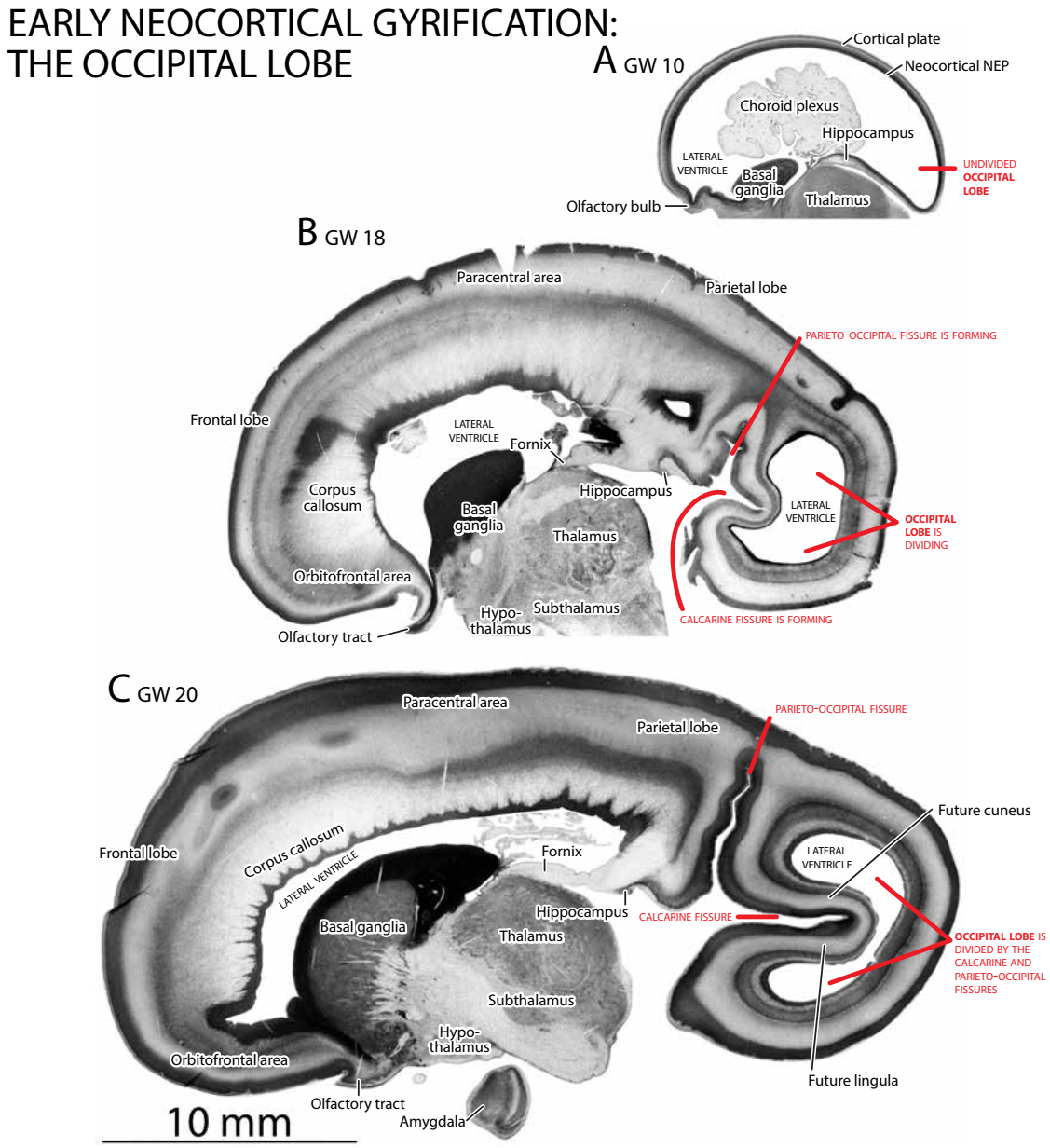

Fig. 66. The beginning of neocortical gyrification, illustrated in matched sagittal brain sections. **A**. In this GW10, 40 mm embryo (C6658), the neocortical NEP and the formative cortical plate that surrounds the expanded lateral ventricle have a smooth surface. **B.** The neocortex is still smooth over much of its extent in this GW18, 145 mm fetus (Y37-63), in which the cortical plate has become thicker and the white matter growing inward begins to fill the space vacated by the shrinking lateral ventricle. The exception is the formation of the parieto-occipital and calcarine fissures in the posterior neocortex. **C**. In this GW20, 160 mm fetus (Y27-60), the deepened parieto-occipital fissure separates the occipital lobe from the parietal lobe, and the calcarine fissure divides the occipital lobe into two primary lobules, the dorsal cuneus and the ventral lingula.

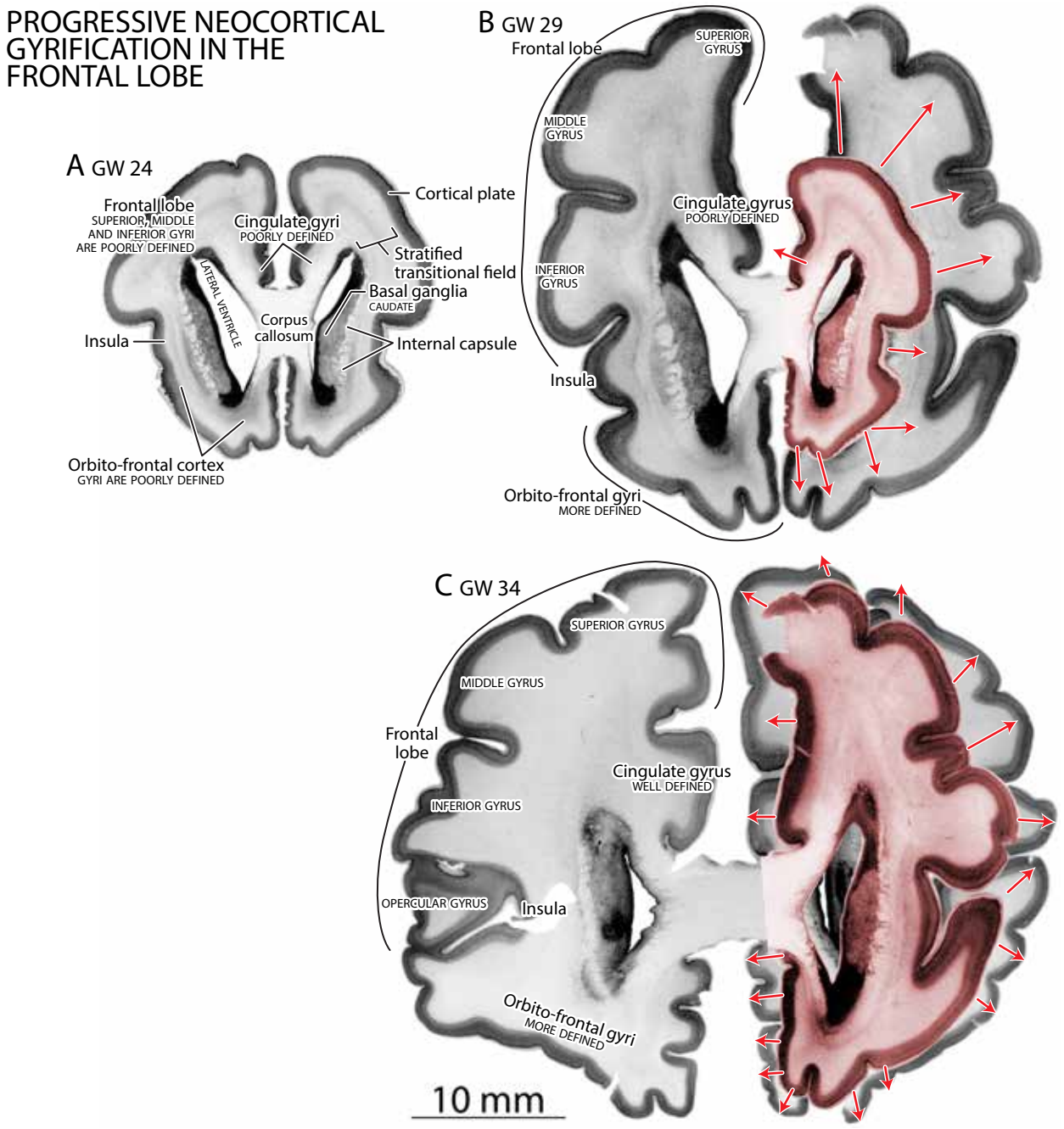

Fig. 67. Ongoing neocortical gyrification in fetuses of increasing age, illustrated in the coronal plane at matched anterior levels. **A**. In this GW24, 210 mm fetus (Y94-62), the shallow lateral fissure separates the prefrontal lobe from the orbitofrontal lobe but there are only hints of the onset of lobules in these two lobes. **B**. In this GW29, 260 mm fetus (Y14-59), the ongoing gyrification is evident in both the prefrontal and orbitofrontal cortices. The inset on the right in this section is a copy of the same region in the GW24 fetus to indicate that the ongoing gyrification is due to the partitioning of the expanding white matter by budding and swelling (red arrows). **C**. There is an increase in the number of gyri in those two regions in this GW34, 295 mm fetus (Y232-66). The inset on the right in this section is a copy of the same region in the GW29 fetus.

THE DISTINCTION BETWEEN LOBES, LOBULES, AND SUBLOBULES. The conventional division of the mature human cerebral cortex into *lobes*—frontal, parietal, occipital and temporal—has a long history, even though the boundaries of some of these lobes are uncertain or arbitrary. Thus the posterior boundary of the frontal lobe is problematic, with some authorities including in it the frontal eye field and the premotor cortex. Similarly, while the posterior boundary of the parietal lobe with the occipital lobe is well delineated by the parieto-occipital fissure, its boundaries with the temporal cortex are uncertain. The same applies to the uncertain boundaries between the occipital lobe and the temporal lobe. In contrast, because the precentral gyri and the postcentral gyri are easy to delineate both morphologically and physiologically, and the two are related as the primary somatomotor and somatosensory projection areas, some authorities designate them as the "paracentral lobe." Similarly, while the delineation of some of the *lobules*—such as the superior, middle and inferior temporal gyri—is relatively easy, subdivision of lobules in other regions, such as the frontal lobe, is problematic. The difficulty with these delineations is mostly due to the increased gyrification during development, as lobes become subdivided into lobules. Besides that, there are many individual differences in the pattern of ongoing higher-order gyrification. The ontogenetic approach we take here, and supplement below with a phylogenetic approach, is useful because it allows us to follow the gradual elaboration of primary lobes into higher order *lobules* and *sublobules*, making the basic gyral pattern difficult to discern in the mature human neocortex.

On the facing page is a list of annotated illustrations on the next 4 pages that show progressive gyrification. We first summarize the process in the human neocortex with illustrations selected from Retzius' (1896) monograph showing specimens in the second trimester of fetal life up to birth, in lateral and medial views (Fig. 69, left and right columns). We next follow the continuing gyrification of the neocortex in infants and children by illustrations taken from Conel's books (1939-1967). In the lateral view of a 5-months-old fetus, the surface of the cortex is smooth, with the exception of the fronto-temporal cleavage. In the medial view, the commencement of gyrification is indicated by the formation of the calcarine fissure in the occipital lobe and the onset of the formation of the parieto-occipital fissure (Fig. 68A, right). These primary fissures of the visual cortex expand in the older 6- and 7-months old fetuses, with the result that the occipital lobe becomes partitioned into the cuneus and lingula, or dorsal and ventral occipital *lobules* (Figs. 68B, C, D, E, right). Then, in the 8- and 9-months-old fetal brains the lobules become partitioned into higher older *sublobules* (Fig. 68F, G). The partitioning of lobules into higher order sublobules continues postnatally, together with an expansion of the sublobules in the growing neocortex, as seen in specimens aged from 6 months to six years (Fig. 69). As a consequence of sublobulation, the boundaries of many lobules become less and less distinct.

ANNOTATED ILLUSTRATIONS OF PROGRESSIVE GYRIFICATION DURING HUMAN BRAIN DEVELOPMENT

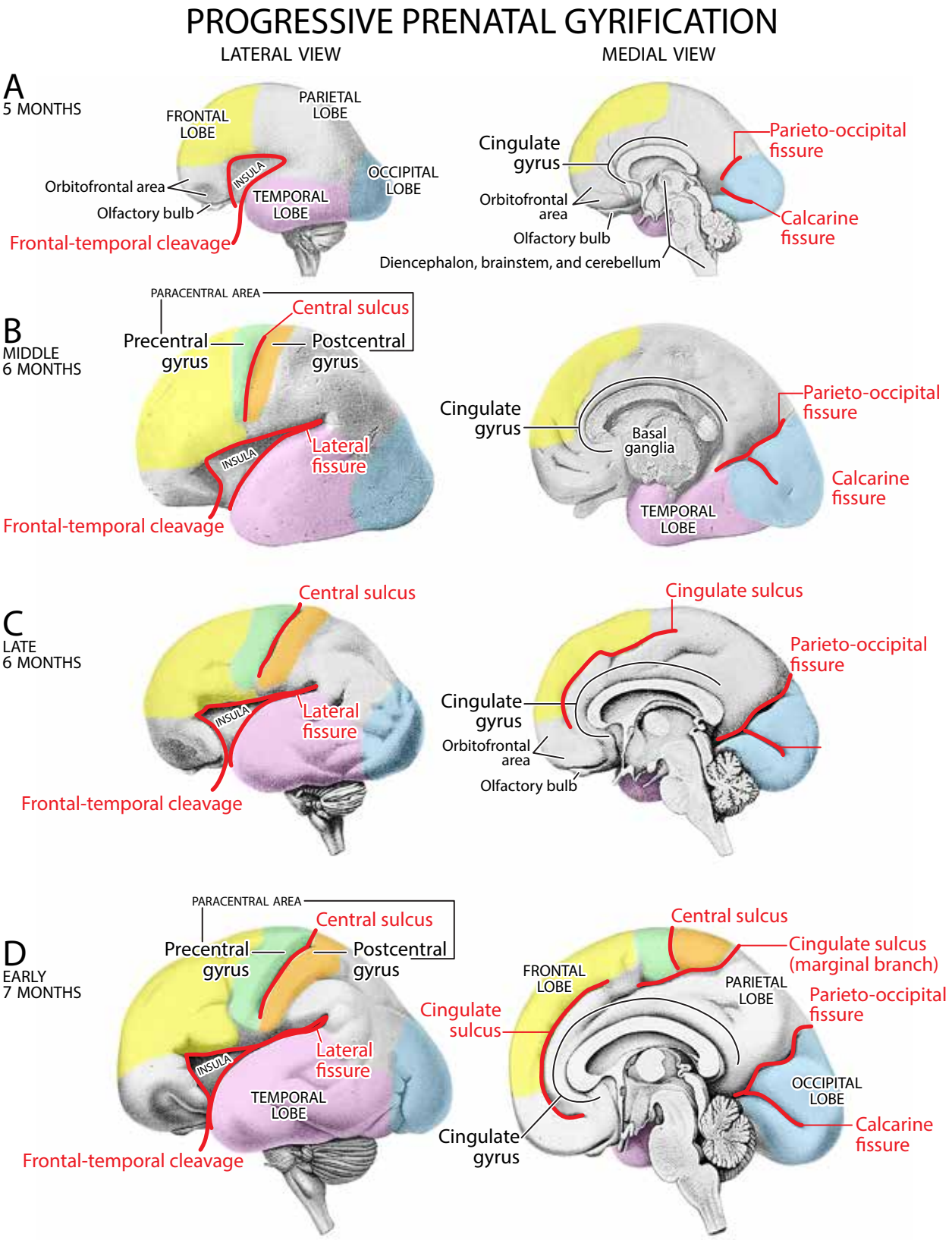
PROGRESSIVE PRENATAL GYRIFICATION
LATERAL VIEW
MEDIAL VIEW
A
5 MONTHS
FRONTAL LOBE
PARIETAL LOBE
OCCIPITAL LOBE
TEMPORAL LOBE
INSULA
Orbitofrontal area
Olfactory bulb
Frontal-temporal cleavage
Cingulate gyrus
Parieto-occipital fissure
Orbitofrontal area
Olfactory bulb
Calcarine fissure
Diencephalon, brainstem, and cerebellum
B
MIDDLE
6 MONTHS
PARACENTRAL AREA
Central sulcus
Precentral gyrus
Postcentral gyrus
Lateral fissure
INSULA
Frontal-temporal cleavage
Cingulate gyrus
Basal ganglia
Parieto-occipital fissure
Calcarine fissure
TEMPORAL LOBE
C
LATE
6 MONTHS
Central sulcus
Lateral fissure
INSULA
Frontal-temporal cleavage
Cingulate sulcus
Parieto-occipital fissure
Cingulate gyrus
Orbitofrontal area
Olfactory bulb
D
EARLY
7 MONTHS
PARACENTRAL AREA
Central sulcus
Precentral gyrus
Postcentral gyrus
Lateral fissure
INSULA
TEMPORAL LOBE
Frontal-temporal cleavage
Central sulcus
Cingulate sulcus (marginal branch)
FRONTAL LOBE
PARIETAL LOBE
Parieto-occipital fissure
Cingulate sulcus
OCCIPITAL LOBE
Calcarine fissure
Cingulate gyrus

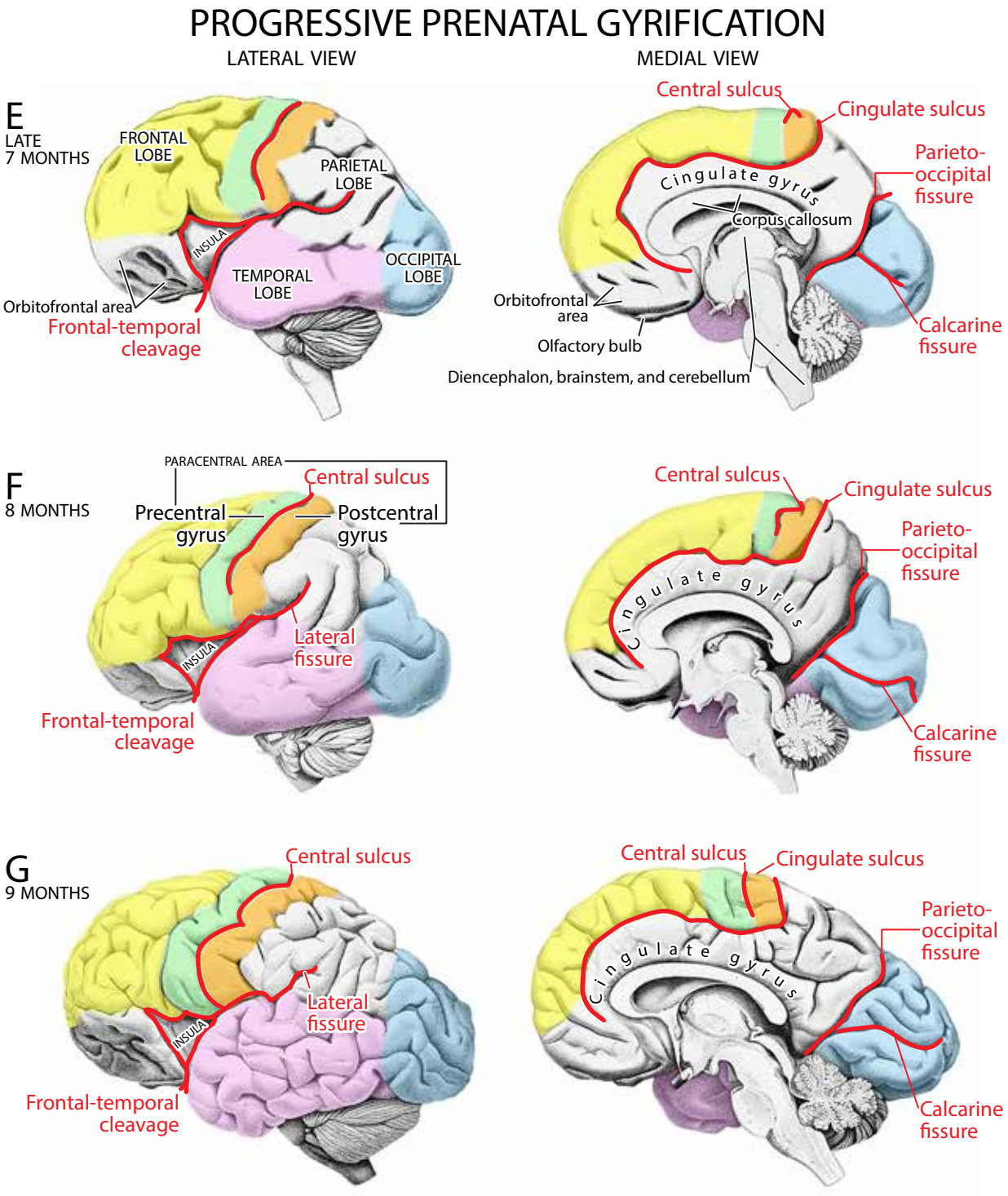

Fig. 68 (on facing pages). Prenatal gyrification of the neocortex, as seen in selected photomicrographs of the brain ranging in fetal age from 5 months (**A**) to 9 months (**G**). From Retzius' *Das Menschenhirn* (1896). Lateral view on the *left*; medial view on the *right*. See text for the distinction between the early formation of smooth primary lobules in some regions and the later formation of secondary sublobules. Color coding of the presumptive lobes is inferential. Dorsal frontal lobe, *yellow*; precentral lobule, *green*; postcentral lobule, *orange*; temporal lobe, *pink*; occipital lobe, *blue*. The orbitofrontal area, insula, parietal lobe, and cingulate gyrus are not colored.

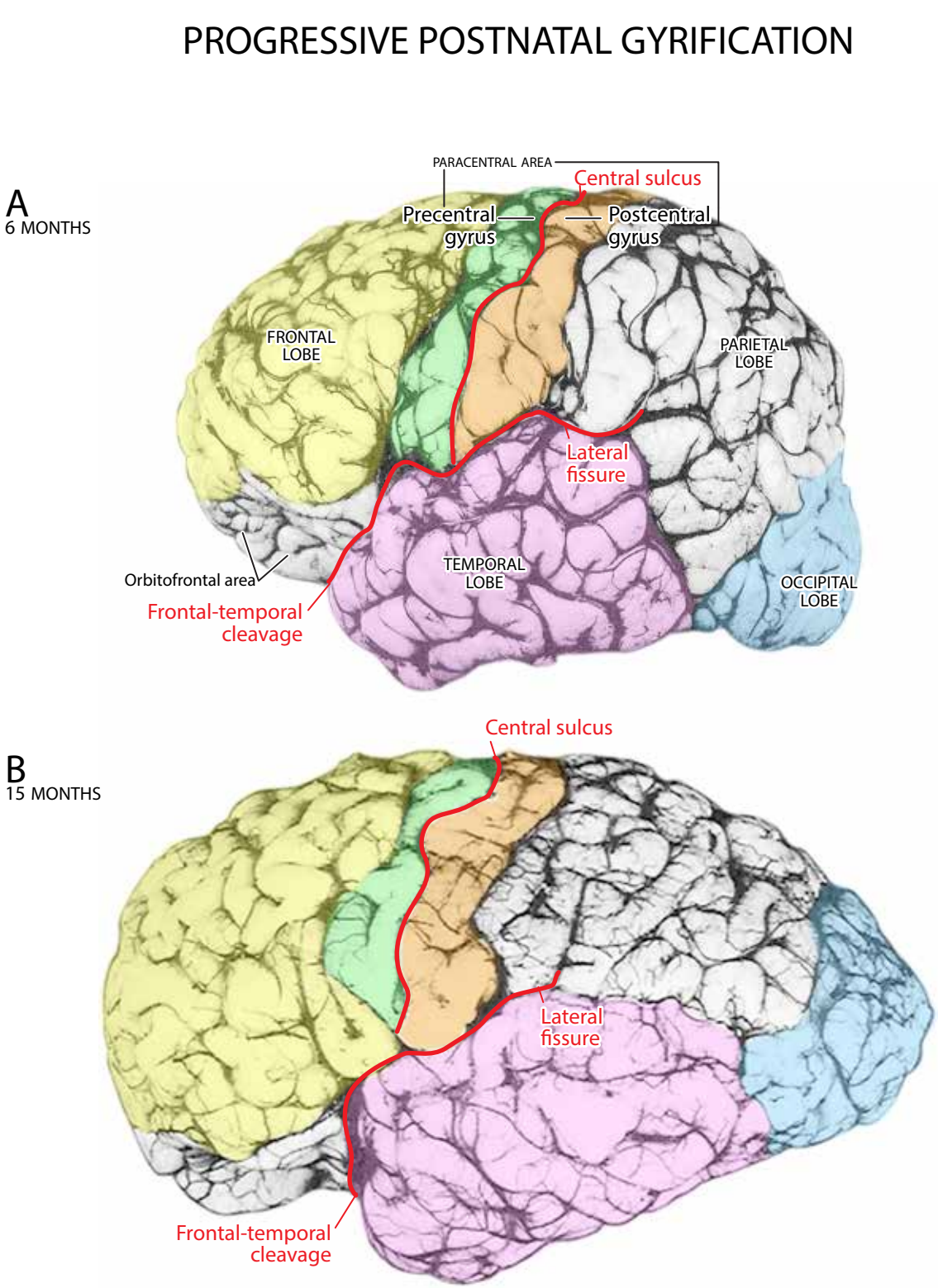

Fig. 69 (facing pages). Postnatal expansion of the neocortex at (**A**) 6 months. (**B**) 15 months, (**C**) 2 years, and (**D**) 6 years. After Conel (1939-1967). Color coding: Dorsal frontal lobe, *yellow*; precentral lobule, *green*; postcentral lobule, *orange*; parietal lobe, *white*; occipital lobe, *blue*; temporal lobe, *pink*. The expansion and sublobulation of the frontal. temporal and parietal association areas appear to be far more pronounced during this period than the somatomotor and somatosensory projection areas.

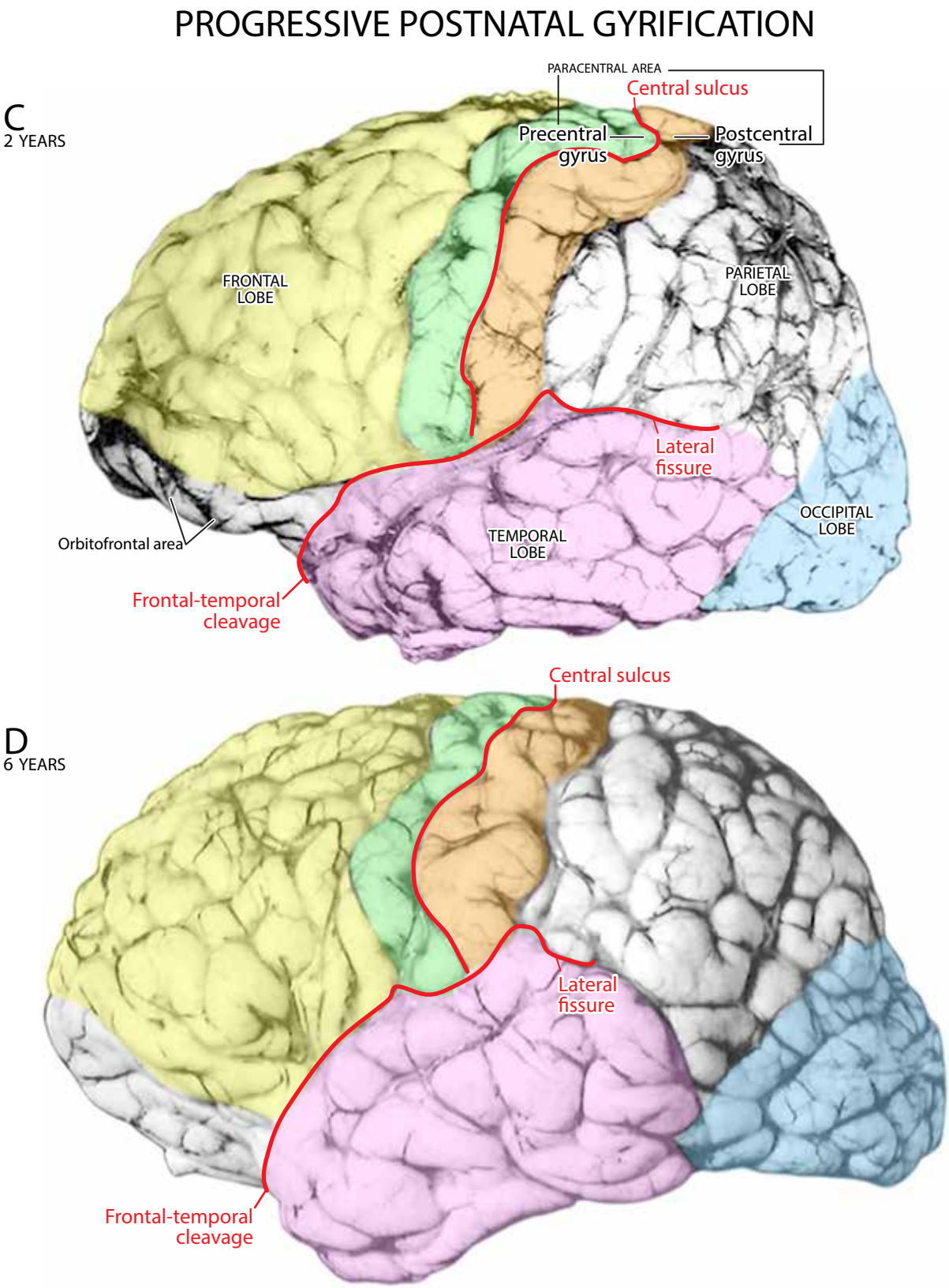
PROGRESSIVE POSTNATAL GYRIFICATION
C
2 YEARS
PARACENTRAL AREA
Central sulcus
Precentral gyrus
Postcentral gyrus
FRONTAL LOBE
PARIETAL LOBE
Lateral fissure
OCCIPITAL LOBE
TEMPORAL LOBE
Orbitofrontal area
Frontal-temporal cleavage
D
6 YEARS
Central sulcus
Lateral fissure
Frontal-temporal cleavage

THE PHYLOGENY OF LOBULATION. Progressive lobulation—starting with a smooth surfaced neocortex, followed by the formation of primary lobules, and ending with the formation of higher order sublobules—has its parallel in mammalian phylogeny (Figs. 70-74). For instance, paleoneurological evidence has been obtained that the neocortex has not only become greatly enlarged but also more convoluted in the evolution of Equidae from the small four-toed, ancient browser *Eohippus* to the large one-toed, grazing modern *Equus* (Edinger, 1948). Because the width the pelvic girdle is limited by the requirement that the hind limbs be close together for rapid locomotion, there was evolutionary pressure to package the enlarged brains of large-bodied animals as compactly as possible so that the head of the newborn can pass through the narrow birth canal. We illustrate that relationship between body and brain size and increased gyrification in two felines, the small domestic cat and the large lion (Fig. 70).

Progressive gyrification is more pronounced in the ascending line of primates than in other mammalian orders. We illustrate that by comparing the neocortex in several species of prosimians (Fig. 71), monkeys (Fig. 72), and a chimpanzee and human (Fig. 73). The neocortex of a very small prosimian, the tarsier, is virtually without fissures (Fig. 71A). The small bushbaby has a lateral fissure, which separates the smooth-surfaced frontal lobe from the smooth-surfaced temporal lobe (Fig. 71B). In the larger greater galago, a fissure separates the temporal lobe into two lobules (Fig. 71C), and that fissure is better developed in the much larger ring-tailed lemur (Fig. 71D). Lobulation is also evident in the frontal lobe but not in the occipital lobe. There is little indication of the formation of sublobules Among monkeys, the small marmoset, the lateral fissure separates the frontal lobe from the neocortex, and an incipient fissure is present in the temporal lobe (Fig. 72A). In the larger squirrel monkey (Fig. 72B) the temporal lobe is divided into lobules, and howler monkey into three (Fig. 72C). Gyrification is quite advanced in the spider monkey (Fig. 72 D) and the large guinea baboon (Fig. 72 E) with the presence of some sublobules. Lobule and subslobue formation is more advanced in the hominid ape, the chimpanzee (Fig. 73A) and reaches its peak in humans (Fig. 73B). It has been reported that the surface area of the human neocortex is nearly three times as large as it would be in the absence of convolutions (Van Essen, 1997).

The increase in neocortical gyrification in the ascending scale of prosimians, monkeys, ape, and man is attributable to a great increase in the white matter of the cerebrum and the expansion of the surface area of the cortical gray matter. This is illustrated in histological sections of the frontal lobe in the squirrel monkey (Fig. 74A), the rhesus monkey (Fig. 74B), the mandrill (Fig. 74C), the chimpanzee (Fig. 74D), and man (Fig. 74E). Inspection of these sections suggests two features that underlie this progressive gyrification. The one is the branching or partitioning of the smooth surfaced white matter, seen in the squirrel monkey, into an increasing number of protruding fiber branches in larger primates; the other is the crowning of these branches by cortical gray matter with a similar width. We will return later to these two features in our attempt to explain the mechanisms underlying cortical gyrification.

The Functional Necessity of Increased Gyrification. Mammals with a large neocortex have a selective advantage over those with a smaller neocortex because they have more neurons with synapses (processing units) in their gray matter to process information that is conveyed by more fibers (transmission lines) in their expanded white matter. Previously we have argued that gyrification in animals with a large neocortex is a reproductive necessity because that prevents enlargement of the

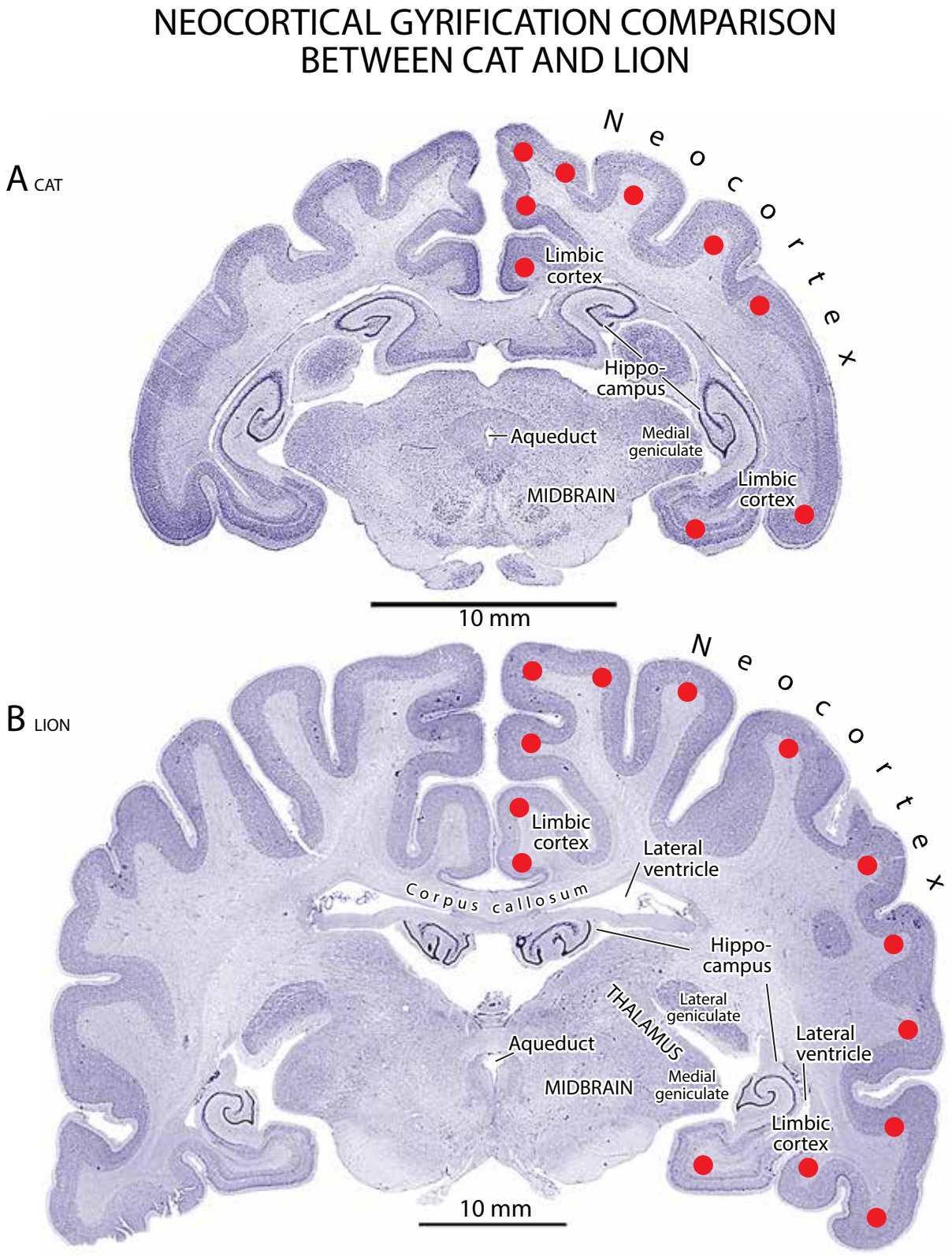

Fig. 70. Matched coronal sections of the brain in the small domestic cat (**A**) and the big African lion (**B**), illustrating the great increase in the number and depth of the gyri in the larger neocortex of the latter. Dots highlight the well-developed gyri. (Photomicrographs from the collection of the BrainMuseum.org)

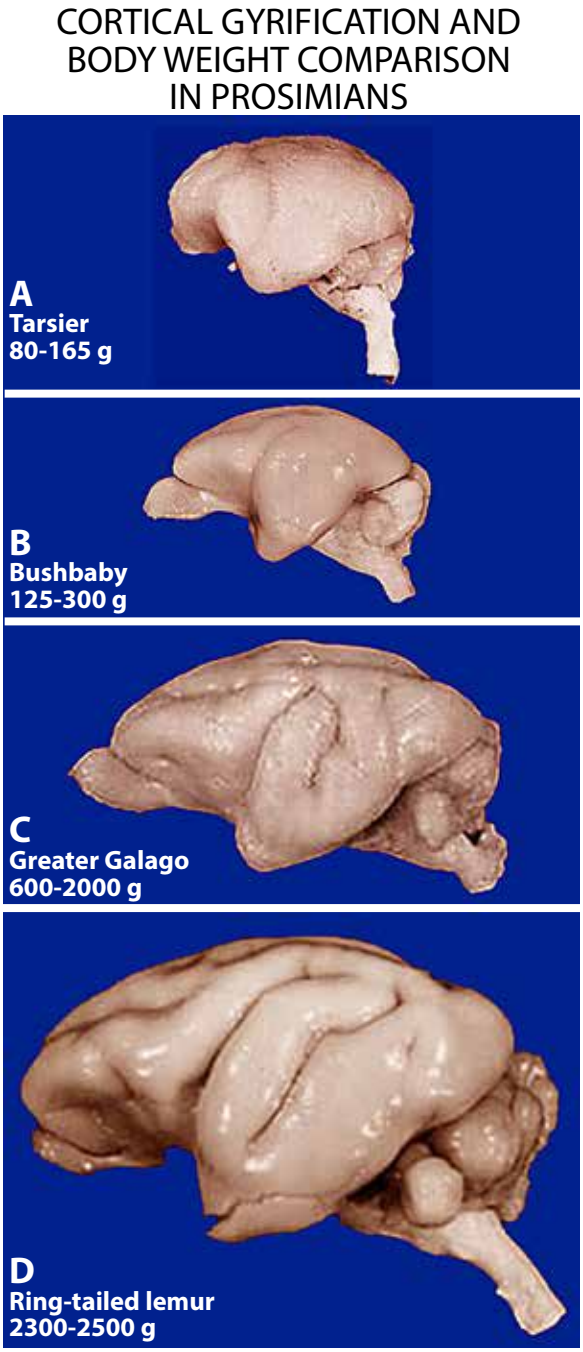

Fig. 71. The smooth-surfaced neocortex of *Tarsius syrichta* (**A**) and *Galago senegalensis* (**B**), and the lobulated neocortex of *Otolemur crassicaudatus* (**C**) and *Lemur catta* (**D**), in lateral view. A correlation is indicated between body weight (in grams) and degree of gyrification. (Photographs from the collection of the BrainMuseum.org)

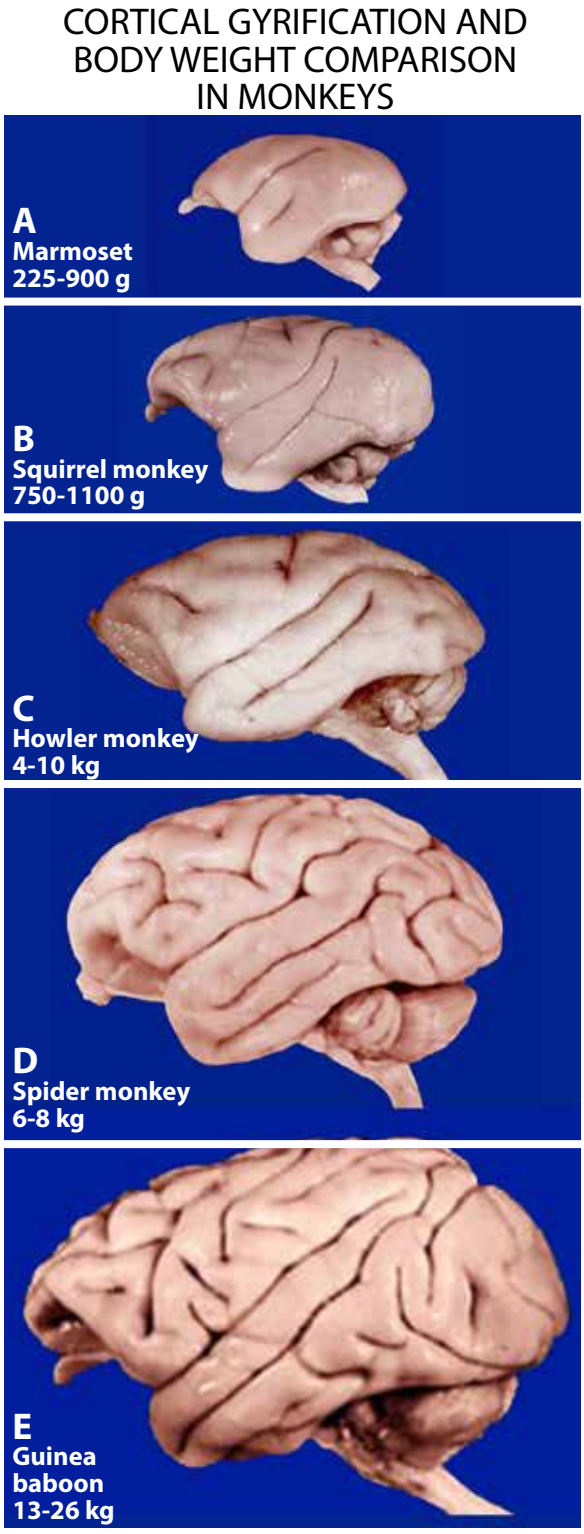

Fig. 72. Increase in gyrification in five monkey species with increasing body weight: *Callithrix jacchus* (**A**), *Saimiri sciureus* (**B**), *Alouatta palliate* (**C**), *Ateles geoffroyi* (**D**) and *Papio papio* (**E**). (Photographs from the collection of the BrainMuseum.org)

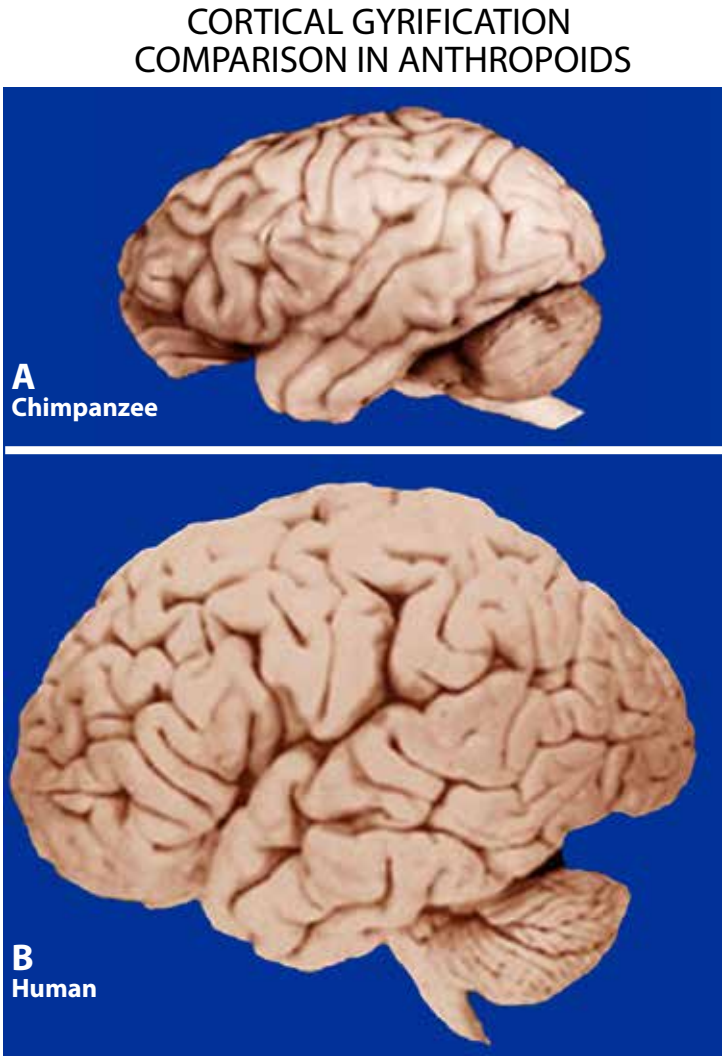

Fig. 73. The great increase in the size of the neocortex and its gyrification in chimpanzee (**A**) and man (**B**). (Photographs from the collection of the BrainMuseum.org)

FRONTAL LOBE GYRIFICATION IN MONKEYS

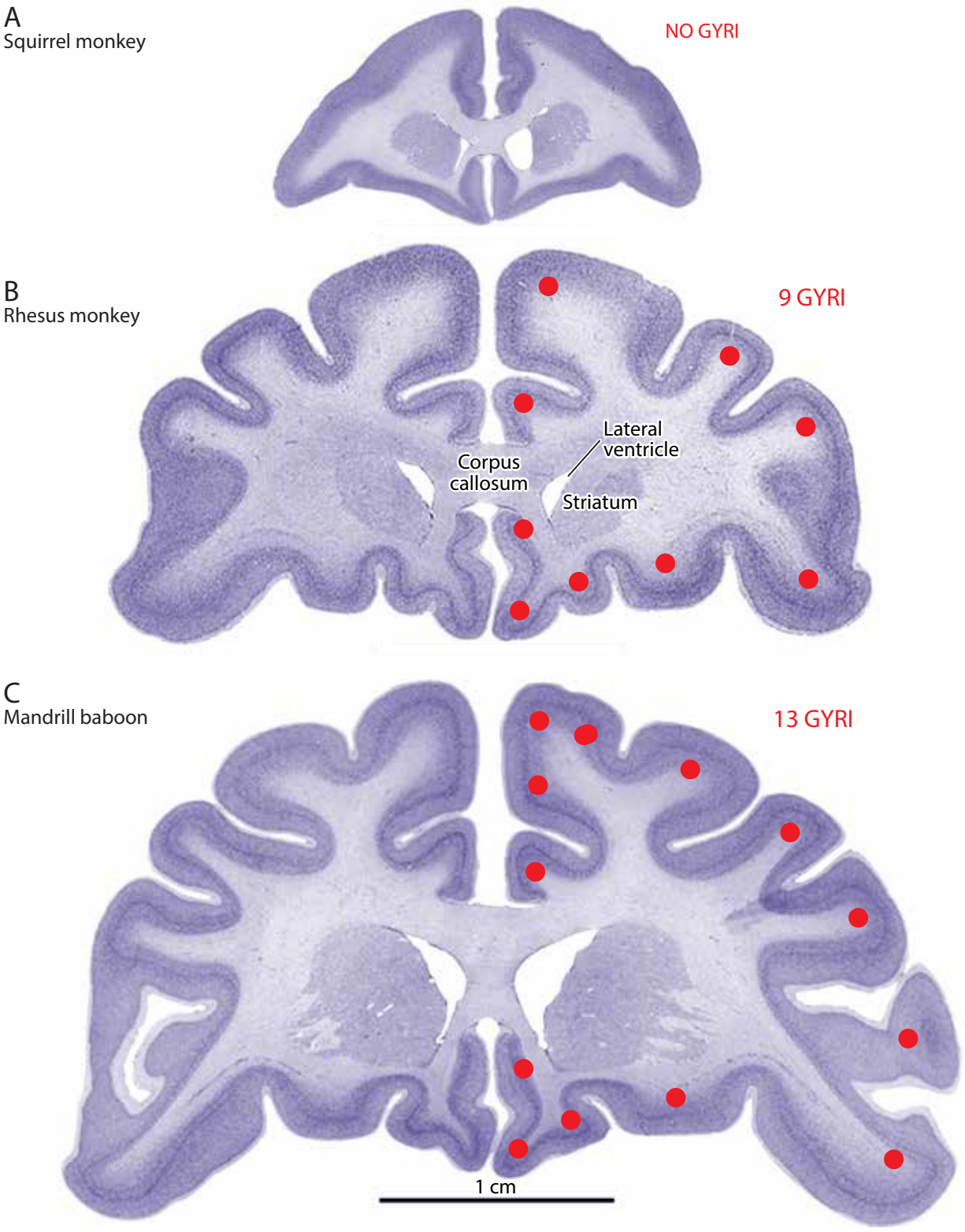

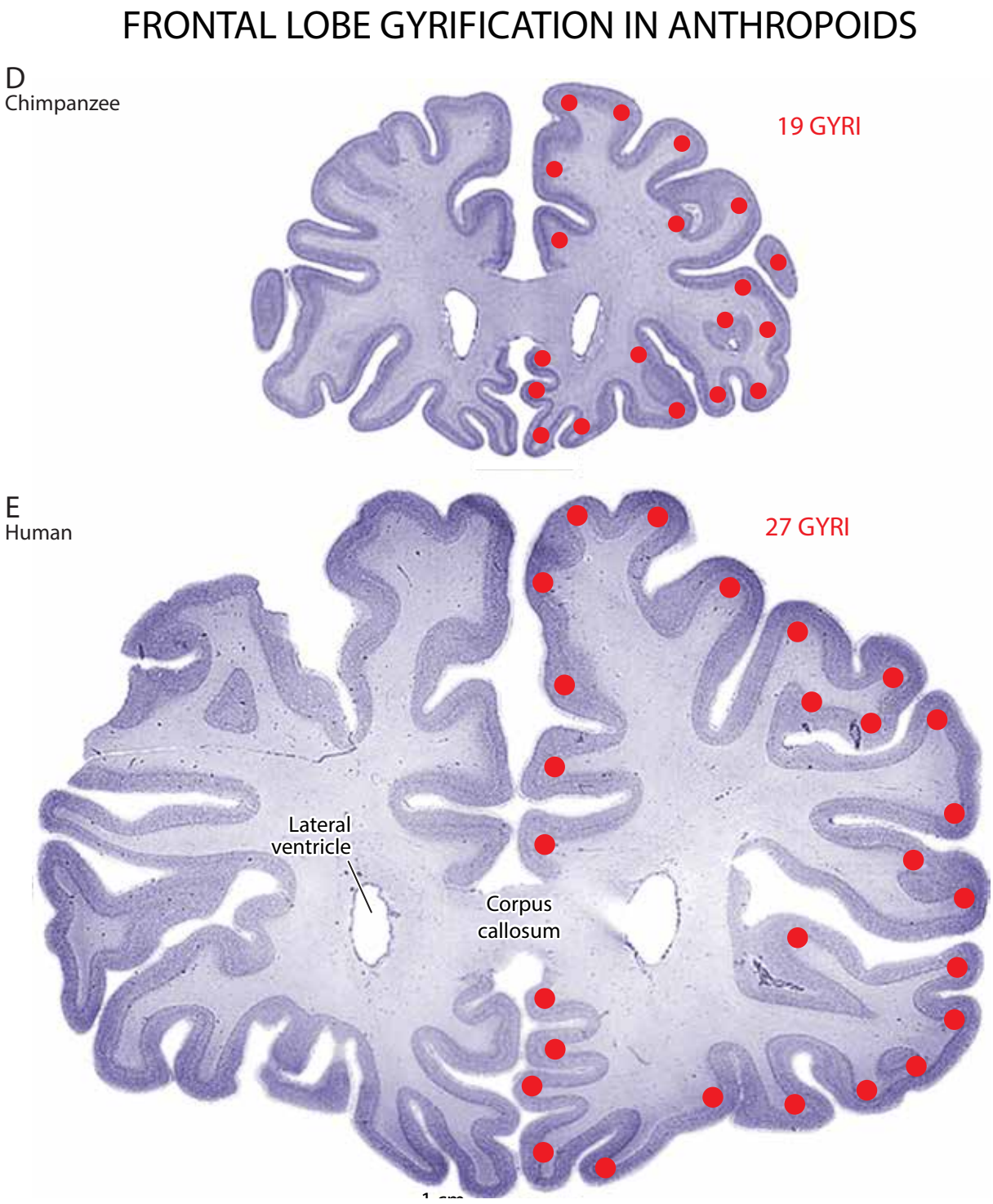

Fig. 74 (on facing pages). Coronal sections of the frontal lobe in squirrel monkey (**A**), rhesus monkey (**B**), mandrill (**C**), chimpanzee (**D**), and human (**E**). The progressive gyrification is associated with increased branching (partitioning) of the flat core of the white matter and of the cortical gray forming a shell around these protrusions. The increased number of gyri formed are indicated by red dots. (Photomicrographs from the collection of the BrainMuseum.org.)

head by the time of delivery to such an extent that the neonate cannot pass through the birth canal. Here we shall argue that the formation of neocortical lobules and sublobules through gyrification is also of great functional significance.

The task of the central nervous system is to process salient sensory information and generate a behavioral response to that stimulus that is as rapid and effective as possible. Information processing can be simple or complex, stereotyped or discriminative. Evidently, simple stimulus processing requires fewer neurons and brain circuits than does complex processing. The function of the neocortex of mammals is to produce responses to stimuli that are based not on simple, readymade mechanisms but on tailor-made learning and cognition-based processing mechanisms. However, increased processing creates the problem of making the reaction time to a stimulus become so protracted that the response fails to benefit the organism. That problem is due to the fact that nerve impulse propagation and chemical transmission across synapses are extremely slow processes when compared with the speed of signal transmission in inanimate systems by conducting wires or wirelessly by electromagnetic radiation. That slowness of sensory-motor processing is exacerbated once distances between different brain areas increase as the brain becomes larger, and as processing becomes dependent on more and more brain regions. As the neocortex has expanded in mammalian phylogeny, two trends evolved to deal with these predicaments: (i) Neurons performing related functions settle close together in integrated wiring circuits that are topographically organized maps (retinotopic, somatotopic, cochleotopic) of the sensory system in lobules and sublobules. (ii) More and more stations are created that parallel process different features of the available information. The ontogeny of lobulation in the human neocortex reflects that phylogeny, as seen in the gyrification of the occipital lobe.

LOBULATION IN THE OCCIPITAL LOBE. The presumptive occipital NEP and cortical plate is smooth in the GW10 embryo (Fig 66A). At this age there is as yet no evidence for visual radiation fibers growing from the thalamus towards the neocortex. That growth begins about the end of the first trimester when a small complement of fibers leaves the lateral geniculate nucleus, enters the internal capsule, loops around the basal ganglia and turns posteriorly (Fig. 16E). The occipital lobe still has a smooth surface for several weeks, but then, in combination with the formation of the stratified transitional field, two small cleavages appear in the cortex of a GW18 fetus, the parieto-occipital fissure and the calcarine fissure (Fig. 66B). Both fissures are greatly enlarged in the GW20 fetus (Fig. 66C), which leads to the partitioning of the occipital lobe into two lobules, the cuneus and the lingula. As we illustrated earlier in a GW23 fetus (Figs. 26 and 27), this partitioning of the occipital lobe by the calcarine fissure begins with the arrival of visual radiation fibers and continues in fetuses ranging in age from 5 to 9 months. It is about the time of birth that sublobules begin to form in the cuneus and lingula (Fig. 68F,G) and that lobulation continues at a modest rate in infants and young children (Fig. 69). What is the functional significance of this partitioning? We offer here an evolutionary explanation, which postulates that the visual cortex has two separate functions in primates and anthropoids.

THE TWO VISUAL FUNCTIONS OF THE OCCIPITAL LOBE. The function of the laterally situated eyes in lower vertebrates is vigilance, orientation and navigation. Lateral eyes scan the visual field (the horizon) for friend or foe, explore the environment to discriminate among objects and events that are beneficial or harmful, and construct route maps to locate feeding sites, escape avenues

and migratory routes. The principal central nervous mechanism that coordinates these visual functions in lower vertebrates lacking a neocortex is the midbrain tectum. In mammals with medially placed eyes and dexterous fingers, such as monkeys and apes, vision has an additional function, that of palpation and manipulation, using hand-eye coordination. Sight directed towards the upper visual field retains the function of vigilance and exploration of the environment. But sight directed towards lower visual field is used to closely inspect the properties of objects. That visual information aids in coordinating arm reaching, hand grasping, and fingers palpating and manipulating objects. During such object inspection, the individual tends to be stationary in its personal space. In contrast, exploration of the surrounding environment involves turning the entire body in a particular direction, to climb, run, or jump from one place to another. Both functions involve perception, attention and action, but one is self-centered or egocentric, the other world-directed or allocentric. In higher primates different lobules of the striate cortex regulate these two functions. As illustrated in the monkey brain, the lower visual field is mapped in the cuneus, the dorsal occipital lobule, whereas the upper visual field is mapped in the lingula, the ventral occipital lobule (van Heuven, after Fulton, 1943; Fig. 75). About a century ago, Inouye (1909), and Holmes and Lister (1916) arrived at a corresponding conclusion of occipital localization in clinical studies of humans suffering the effects of war-related selective gunshot wounds.

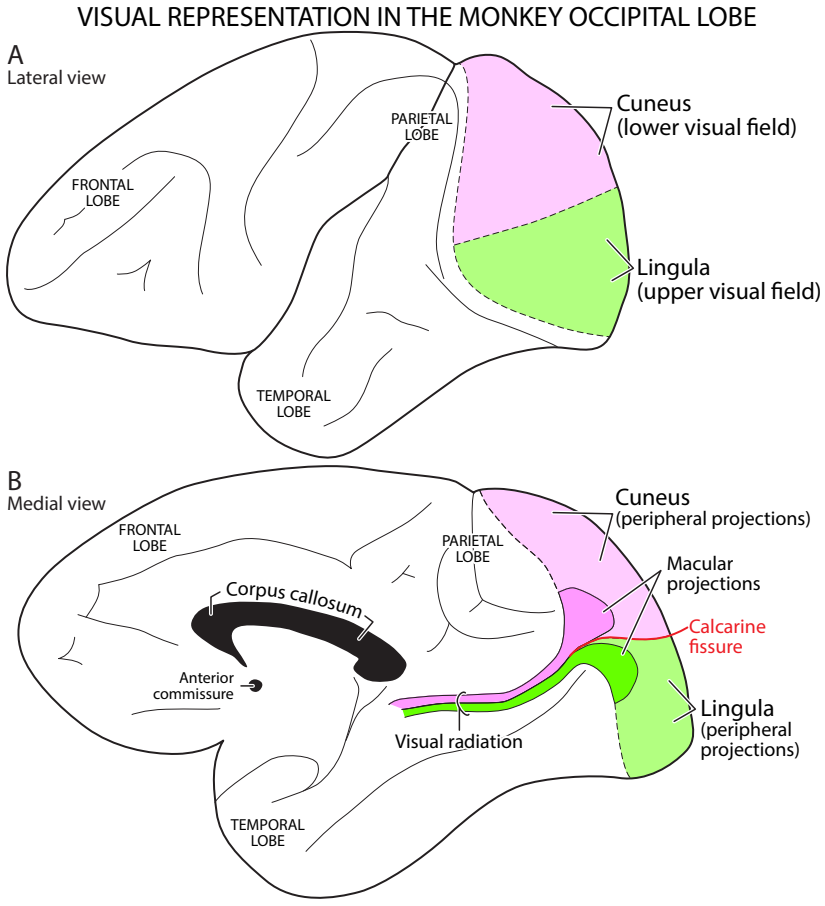

Fig. 75. Projection of the lower half of the visual field via a lateral geniculate relay to the cuneus (*pink*) and another projection of the upper half of the visual field via a lateral geniculate relay to the lingula (*green*), two major sublobules in the primary visual cortex. (After G. J. van Heuven, in Fulton, 1943.)

We illustrate the trajectory of the two components of the visual radiation fibers in the human brain (Fig. 76), as seen in dissections where the soft cortical tissue was meticulously scraped away in selected regions to show the distribution of the underlying tough fiber fascicles (Ludwig and Klingler, 1956). That technique allows the visualization of large fiber tracts, such as the descending corticospinal tract traversing the basal ganglia, and the ascending thalamocortical fibers coursing toward the neocortex (Fig. 76A). In Fig. 76B, the large visual radiation from the lateral geniculate nucleus to the occipital lobe is visualized and shown to terminate in two compartments, the dorsal complement in the cuneus (l*ower set of red arrows*) and the ventral complement in the lingula (*upper set of red arrows*). The vental radiation forms a wide fan that first courses rostrally and then takes a caudal turn (Meyer's loop).

Contemporary clinical studies have confirmed these gross anatomical fiber dissections. Separated by the calcarine fissure that bisects the primary visual cortex, the cuneus and the lingula receive topographically organized input from the retina via a relay in the lateral geniculate nucleus so that the lower half of the visual field maps dorsally, and the upper half of the visual field maps ventrally (e.g., Horton, 2006; Wandell et al., 2007; Sherbondy et al., 2008; Schira et al., 2009). That pattern of projection is summarized diagrammatically in Figure 77. As we have argued, the principal function of input from the upper visual field in higher primates and humans is scanning the distant environment with an upward gaze to detect friends and foes (approach them, fight them, or flee from them) and construct maps for orientation and navigation. We call that the allocentric visual projection which targets the lingula. The principal function of input from the lower visual field is object inspection with a gaze directed downward that gathers information about the properties of the objects reached for, grasped, palpated and manipulated. That egocentric visual projection targets the upper occipital lobule.

THE TWO NEOCORTICAL VISUAL SYSTEMS ARE WIDELY DISTRIBUTED. The bisected upper vs. lower visual field representation extends beyond the primary visual cortex (V1d and V1v, Fig. 78) so that higher order dorsal and ventral visual association areas are also separated (Van Essen and Zeki, 1978; Gattass et al., 1988; Felleman et al., 1997a). Outflows from the dorsal projection and association areas, referred to as the "dorsal stream," target adjacent multimodal visual and haptic (touch) areas in the parietal cortex, whereas outflows from the dorsal projection and association areas, the "ventral stream," target adjacent multimodal visual areas in the temporal cortex. According to an early hypothesis (Ungerleider and Mishkin, 1982), the dorsal stream is concerned with spatial vision (the "where" pathway) whereas the ventral stream deals with object vision (the "what" pathway). The accumulating evidence also suggests that a developmental sequence brings about the bisected visual pathways.

SOME CORREPSONDENCE BETWEEN VISUAL PROCESSING AND NEOCORTICAL DEVELOPMENT. Visual processing and feature extraction in primates and man begins in the retina, continues in segregated layers of the lateral geniculate nucleus, and is greatly elaborated in the striate cortex, peristriate areas and several extrastriate visual areas (Hubel, 1988). The first stage in that processing occurs in first-order neurons in the striate cortex to register elementary features of the retinotopic input from the lateral geniculate nucleus. The second stage is the extraction of more information by second-order neurons in the peristriate cortex. The third stage is the conveyance of the extracted information to third-order multimodal neurons in distributed loci in the parietal and temporal

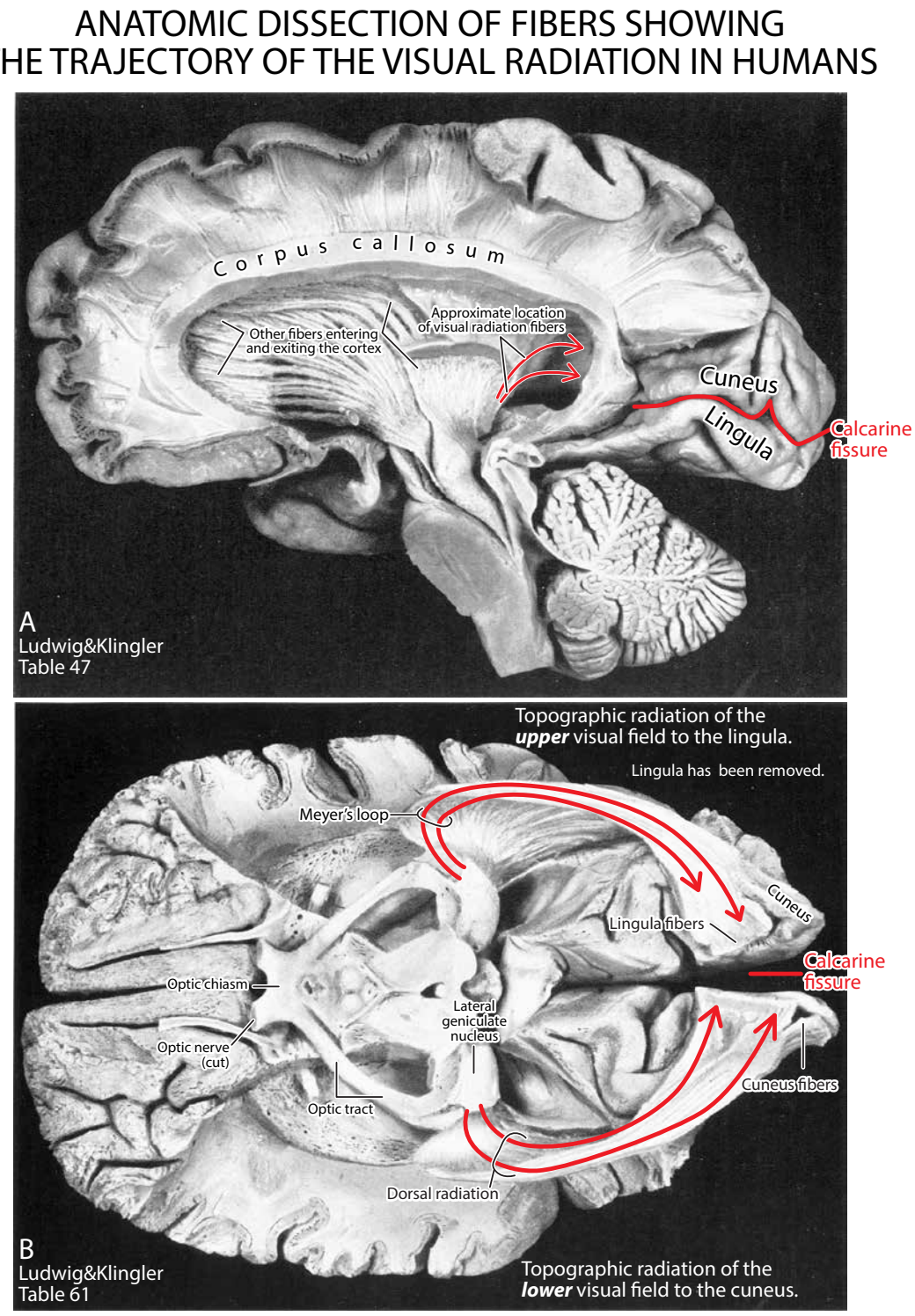

Fig. 76. In these dissections of the mature brain, using a special technique by Ludwig and Klingler's (1956), the soft gray matter was scraped away in selected regions to show the tough fiber tracts in the white matter. **A**. In this specimen, seen in the midsagittal view, the cuneus and lingula of the occipital lobe have been preserved but the white matter fiber tracts are not visible (*red outlines* the calcarine fissure). **B**. In this horizontal preparation, shown in ventral view, we can follow the course of the optic tract to the lateral geniculate nucleus, and the course of the dorsal visual radiation to the cuneus (*bottom red arrows*) and the ventral radiation to the lingula (*top red arrows*).

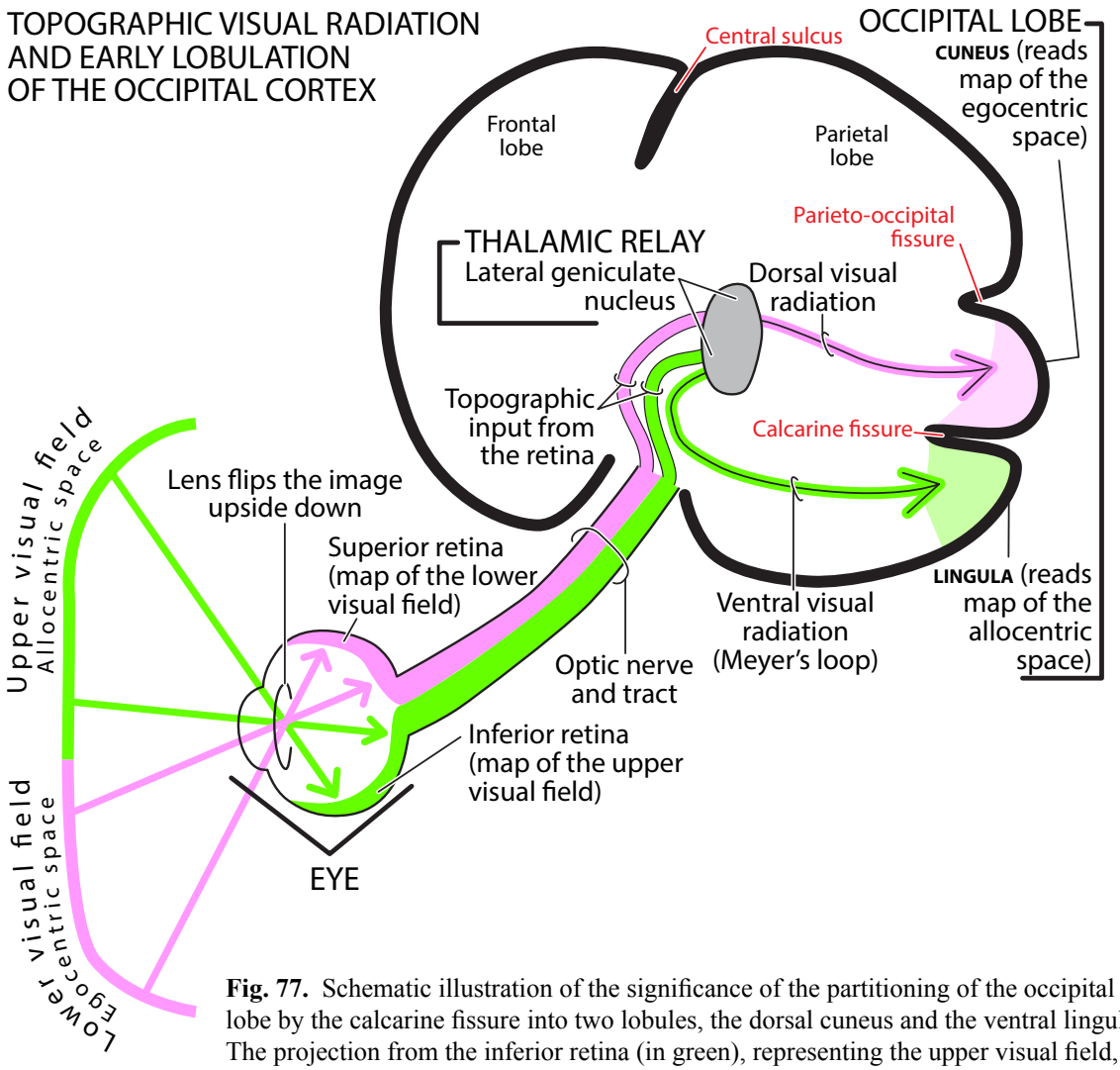

Fig. 77. Schematic illustration of the significance of the partitioning of the occipital lobe by the calcarine fissure into two lobules, the dorsal cuneus and the ventral lingula. The projection from the inferior retina (in green), representing the upper visual field, terminates through a relay in the lateral geniculate nucleus in the ventral occipital lobule. The projection from the superior retina (in red), representing the lower visual field, terminates in the dorsal occipital lobule. The dorsal visual radiation and the cuneus map the individual's self-centered (egocentric) space; the ventral visual radiation and the lingula map the individual's world-centered (allocentric) space.

cortex, and beyond. It is probable that the initial steps are mainly sequential and hierarchic, while the later steps proceed in parallel more or less simultaneously and are greatly modulated by higher-level mnemonic and cognitive contributions. Of interest from a developmental perspective is the correspondence between the stages in the functional processing of visual information and the stages in the development of the neocortical visual system. Retinal cells and the optic tract develop quite early, and as we know from animal studies, the lateral geniculate nucleus is an early forming brain structure. Pioneering visual radiation fibers that form Meyer's loop are already present in the late first trimester embryos prior to the formation of the distinctive STF of the occipital lobe and before the smooth occipital lobe has become partitioned into two lobules by the calcarine fissure (Fig. 16). Occipital STF stratification and the partitioning of the occipital lobe take place during the second

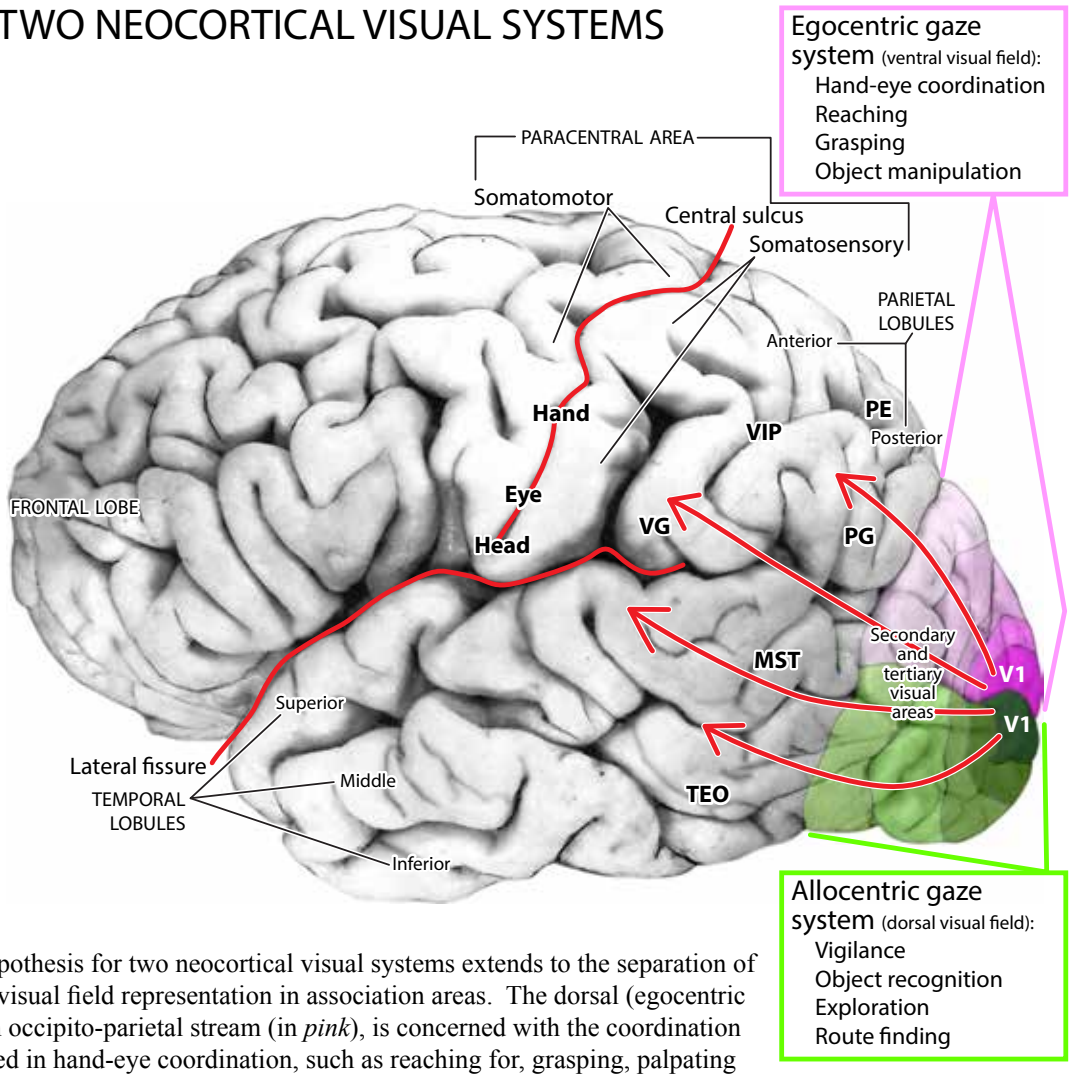

Fig. 78. The hypothesis for two neocortical visual systems extends to the separation of upper vs. lower visual field representation in association areas. The dorsal (egocentric gaze system), an occipito-parietal stream (in *pink*), is concerned with the coordination of vision involved in hand-eye coordination, such as reaching for, grasping, palpating and manipulating objects. The ventral (allocentric gaze system), an occipito-temporal stream (in *green*), is concerned with object recognition, vigilance, exploration and orientation in the wide world. The identification of the occipital, parietal and temporal components of these two systems in the human neocortex is inferential, based mainly on research in monkeys.

trimester (Figs. 19, 20, 66B,C) and it is later, during the middle and end of the third trimester, that the partitioning of the two occipital lobules into sublobules commences (Figs. 68F, G). By this time the occipital STF has disappeared, indicating that all the sojourning neurons have settled in the cortical gray matter. We assume that the early partitioning of the occipital lobe into dorsal and ventral lobules reflects the onset of the structural maturation of the striate and nearby parastriate areas, the initial centers of visual information processing. The later development of sublobules in the occipital lobe and adjacent parietal and temporal lobules suggest that the maturation of cortical areas responsible for higher-order multimodal information processing also develop later. That interpretation is strongly supported by well-documented studies of myelination progression from the visual radiation, to the striate cortex, to the parastriate areas, and finally to the considerably delayed myelinating areas in parietal and temporal association areas (Figs. 53, 54, 56, 57).

The Mechanisms of Neocortical Gyrification. While the functional utility of increased gyrification is obvious—it expands the area of the cortical gray matter without increasing the circumference of the cranium—the question remains what morphogenetic mechanisms are involved in the formation of gyri. Can the histological evidence of neocortical development that we have reviewed here throw any light on this question? To answer that affirmatively, we briefly review here what we have learned nearly two decades ago about the foliation of the developing rat cerebellar cortex (Altman and Bayer, 1997) and will examine what the two processes have in common and how they differ from one another.

THE LESSON LEARNED FROM THE STUDY OF CEREBELLAR FOLIATION. The embryonic rat cerebellum is initially an ovoid mass (Fig. 79A). The foliation of the smooth-surfaced cerebellar cortex begins a few days before birth (about embryonic day 21, E21), and over a postnatal period of about 20 days (when the young are ready to be weaned), the fasciculating white matter sprouts radiating trunks, branches, and branchlets that are enveloped by a continuous canopy of the expanding cerebellar cortex, its lobes, lobules and sublobules. As seen in midline sagittal plane tracings of the vermis (the part of the cortex that spans the midline), 4 fissures divide the smooth cerebellar cortex into 5 lobes by E21 (Fig. 79B). Lobule formation begins on postnatal day 1 (P1; Fig. 79C) and by P10, most of the lobes have become partitioned into lobules (Fig. 79D).

The great areal expansion of the cerebellar cortex in young rats and its lobulation are due to several interrelated developmental processes: formation of the external germinal layer; growth and alignment of the densely packed small Purkinje cells with their expanding dendritic arbor into a monolayer; the accumulation of the immense number of postnatally forming small neurons (granule cells) in the expanding internal granular layer; and the expansion of the molecular layer composed of the axons of the granule cells (the parallel fibers), the arborizing dendrites of Purkinje cells, and other cellular and fibrous elements. The composition of the cerebellar white matter is known and relatively simple. There are two afferent systems, the early arriving climbing fibers from the inferior olive and the later arriving mossy fibers. Initially, the climbing fibers make contact with the early-maturing deep nuclear neurons and secondarily with the later-maturing Purkinje cells. The mossy fibers come from multiple sources, including a large complement from the late-developing deep pontine gray nucleus (via the pontocerebellar tract) that relays input from the neocortex to the late descending granule cells. There are two efferent systems: (i) an intrinsic one, the axons of the Purkinje cells to the deep nuclei, and (ii) an extrinsic one, the axons leaving the deep nuclei and targeting extracerebellar structures. In seeking to explain the mechanisms involved in cerebellar foliation, we postulated that the earliest fasciculating white matter fibers serve as guy wires that *anchor* the expanding cortex at their point of contact and prevent cortical expansion at those points but allowing expansion around those points (Fig. 79E). The result is that the fiber trunks and branches covered by the expanding cortex bulge into expanding *lobes*, and *sublobules* (Fig. 79F). We could not exactly specify the anchoring elements involved, but the early climbing fibers that contact both the deep nuclei and the cerebellar cortex may serve as the guy wires that tie the depths of the primary fissures as the lobes form, while the mossy fibers to the internal granular layer may be involved in anchoring the secondary and tertiary fissures as the lobules and sublobules form.

Fig. 79 (facing page). **A**. The smooth-surfaced cerebellar cortex in an 18 day (E18) rat embryo. **B**. Formation of five lobes by 4 early fissures (*F1-F4*) in an E21 rat embryo as the white matter expands and fasciculates.

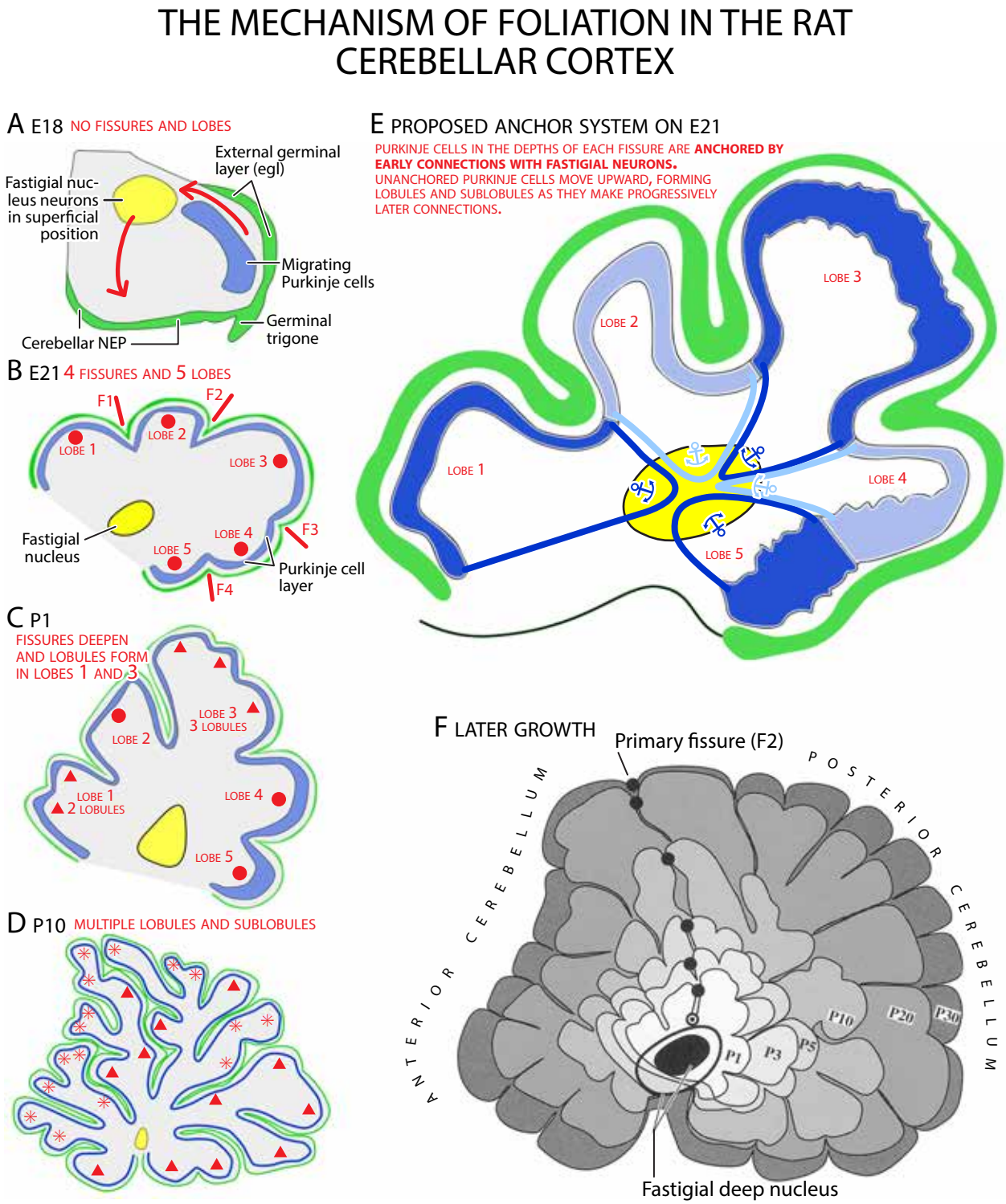

C. Formation of the first lobules in a postnatal day 1 (P1) neonate. **D**. Formation of sublobules in a P10 rat infant. (Tracings shown at decreased magnification.) **E**. Hypothesis of anchoring of the cerebellar cortex (anchors in the deep nucleus) by fibers acting as "guy wires" at points that become the depth of the fissures and the cerebellar cortex expanding around them, forming the initial lobes. **F**. Six superimposed tracings of the midline vermis to show expansion of the cerebellar cortex and increase in the depth of fissures and in the number of sublobules between P1 and P30. The tracings were centered by using the fastigial nucleus as the fulcrum, and having the primary fissure form a straight line to the surface of the expanding cerebellar cortex. (Modified after Atman and Bayer, 1997.)

EARLY GYRIFICATION IN THE NEOCORTEX. There are similarities between cerebellar-cortical and cerebral-cortical lobulation as well as major differences. To begin with, the embryonic cerebellum consists initially of two separate far-lateral structures that form along the upper rhombic lip, which later spread medially and fuse to form a single structure, the midline vermis (Altman and Bayer, 1997). In contrast, the embryonic cerebrum starts as a single midline structure (the unicameral telencephalon) but soon becomes divided into two separate hemispheres that remain disconnected until the corpus callosum develops. But there are also more important structural differences. Included among them, first, is that unlike the cerebellum, the neocortex receives well-segregated, direct input from the various sensory systems by way of relay nuclei in the thalamus. Second, the cytoarchitectonics of the neocortex is far more complex and far less understood than that of the cerebellar cortex. Third, the foliation of the neocortex is far more varied from individual to individual than is the regular foliation patterns in the cerebellar cortex. Hence, to explain neocortical foliation, or gyrification, we offer the following modification of the mechanisms involved.

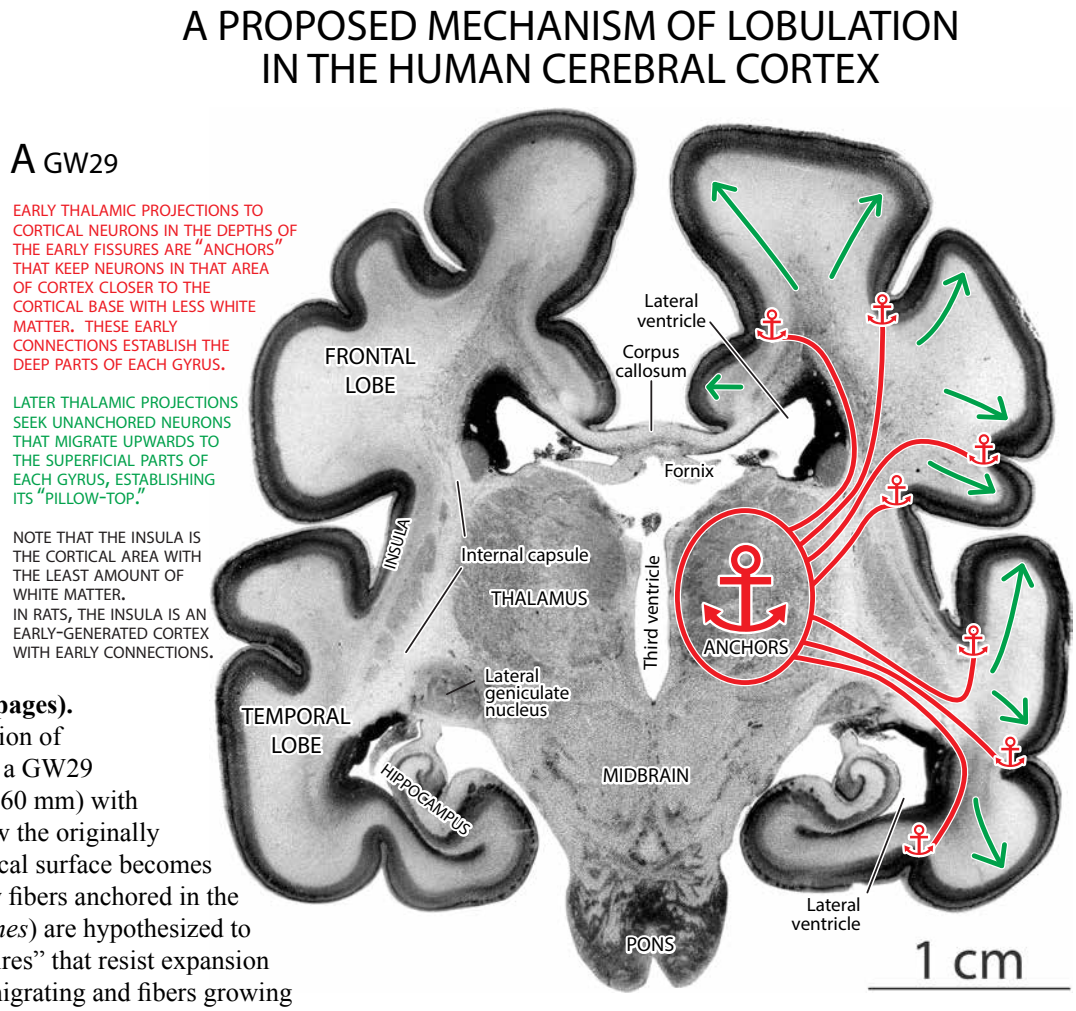

Fig. 80 (facing pages). **A.** Coronal section of the neocortex in a GW29 fetus (Y14-59, 260 mm) with a suggestion how the originally smooth neocortical surface becomes lobulated. Early fibers anchored in the thalamus (*red lines*) are hypothesized to serve as "guy wires" that resist expansion while neurons migrating and fibers growing towards the neocortex (*green arrows*) elevate the expanding cortex at the unanchored sites. Note that at the presumed anchored sites the white matter tends to remain narrow. **B (facing page).** The smooth cortical surface before gyrification. In the region where thalamic fibers arrive early, the cortical surface becomes anchored. That region becomes the depth of the future fissure. **C (facing page)**. As later arriving fibers and neurons reach the adjacent areas, the pressure exerted causes the cortical surface to bulge at adjacent unanchored sites.

Figure 80A illustrates the initial gyrification of the neocortex in a coronal section at the level of the thalamus. We hypothesize that, as in the case of the cerebellum, three processes—(i) neuronal proliferation, (ii) fiber increase and fasciculation, and (iii) anchoring of the cortex at certain points of early contact—are major factors that bring about lobulation. Gyrification begins after a complement of early thalamocortical radiation fibers contact the earliest differentiating neurons of the cortical plate and serve as anchoring "guy wires" that resist expansion of the growing cortical surface at that site (Fig. 80A). Elevation of the cortical surface commences in the surrounding areas as later-forming fibers and migrating neurons from the STF reach the cortical plate (Fig. 80B). The early fixation sites become the depths of the sulci. As new neurons and fibers arrive the banks of the gyri become elevated (Fig 80C). We illustrate this process in the paracentral lobe and the occipital lobe in Fig. 81. Early arriving somatosensory fibers from the thalamus to the somatosensory and somatomotor cortices act as guy wires to anchor the deepest part of the central sulcus; the banks of the precentral and postcentral gyri appear as the neocortex expands. Similarly, early fibers of the two components of the visual radiation from the lateral geniculate nucleus serve as guy wires in the calcarine fissure that separate the occipital lobe into the dorsal cuneus and the ventral lingula. The depth of the parieto-occipital fissure may be formed by early forming fibers from the pulvinar to the parietal lobe (Gamberini et al., 2015).

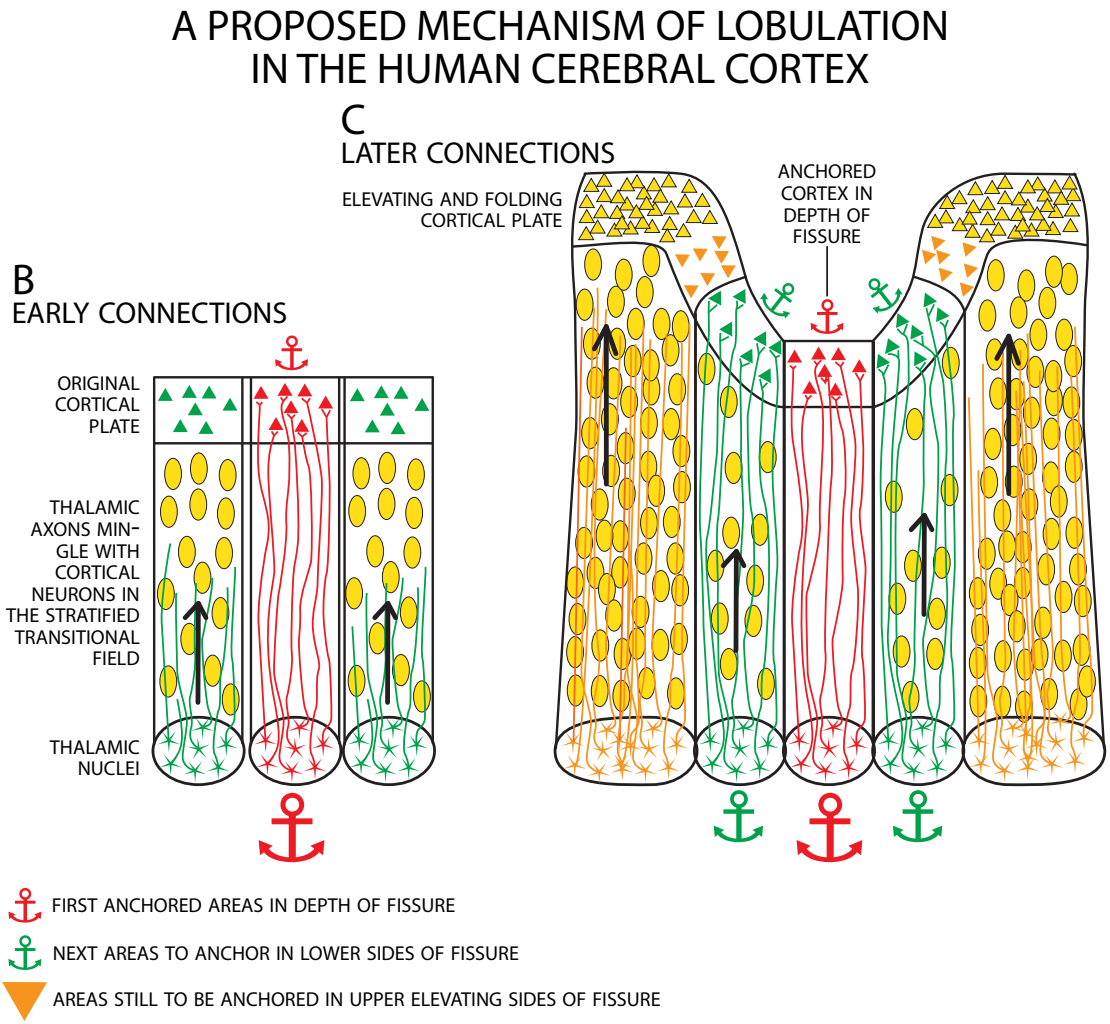

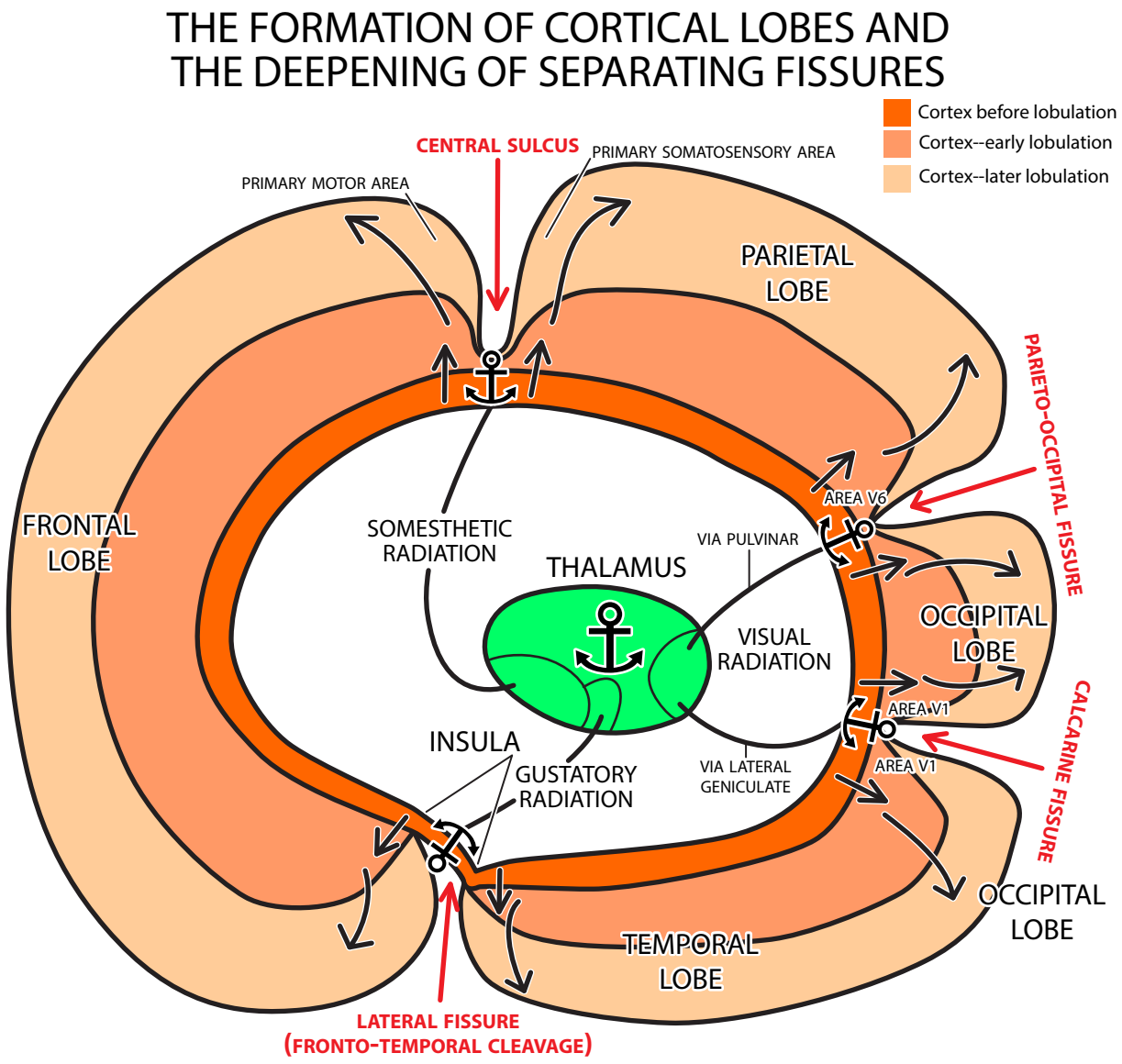

Fig. 81. Hypothesis of the formation and elevation of the precentral and postcentral gyri around the central fissure, and of the dorsal and ventral occipital gyri around the calcarine fissure. Early radiation fibers from the thalamic relay nuclei and the pulvinar anchor the expanding neocortex, deepening of the sulci and elevating the bank of these gyri (*arrows*) as the neocortex expands.

The subsequent process of lobular growth and sublobule formation we attribute, likewise, to progressive fasciculation of the white matter in conjunction with the expansion of the gray matter, but anchoring now shifts from the thalamus to the white matter itself. This is illustrated in a comparison of matched coronal sections in GW24 (Fig. 82A) and a GW37 (Fig. 82B) fetuses. The white matter of the frontal lobe and temporal lobe are relatively smooth in the younger fetus (*red line*) but the older fetus shows radiating branches of white matter (*green arrow*s) forming sublobules, all covered by the expanding cortical plate. We assume that white matter branching is associated with two types of functional fasciculation, unimodal articulation and multimodal integration.

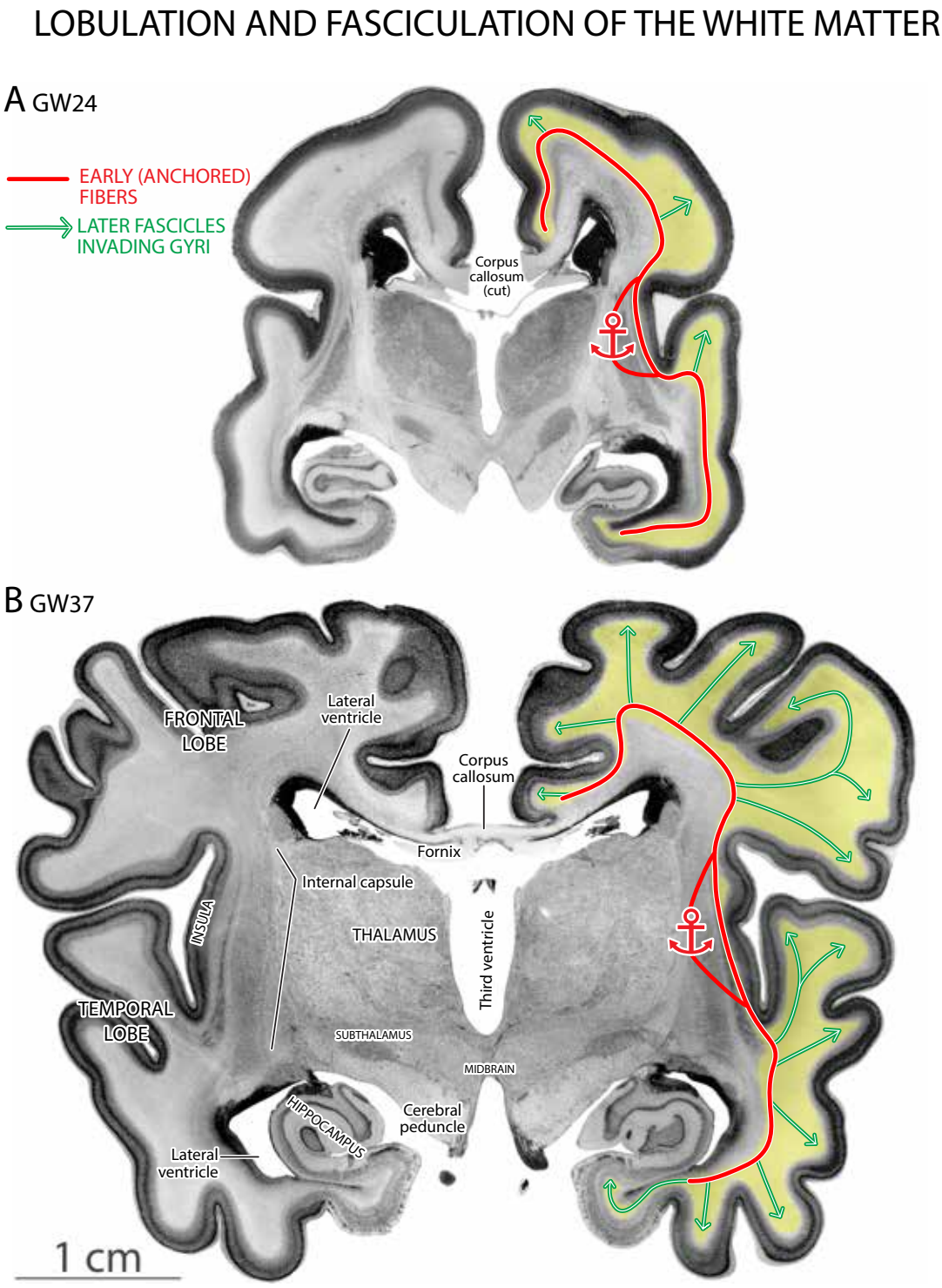

Fig. 82. **A.** The smooth configuration of the white matter in a coronal section of the midportion of the neocortex in a GW24 fetus (Y994-62, 210 mm). **B.** The many radiating branches of the white matter (green arrows) in both the frontal lobe and the temporal lobe in a GW37 neonate (Y217-65, 350 mm) are anchored to the earlier formed white matter (red anchor). Sublobule formation is interpreted to be the outcome of the expanding gray matter forming a canopy over the fiber swellings of the white matter.

GYRIFICATION IN RELATION TO UNIMODAL ARTICULATION AND TO MULTIMODAL INTEGRATION. Human neocortical expansion is associated with the formation of more and more functional modules for better processing of the available information and the generation of more refined responses. These modules are of two kinds: (i) those responsible for articulation of a single sense modality, and (ii) those responsible for integration from different sense modalities.

In detail, *unimodal articulation*, allows the advance from perceiving only global features of an object (size, shape, color) to perceiving other features based on fine configurational and textural differences. This is an important perceptual advance because it allows discrimination of the multiplicity of things and events in the environment and generates more selective behavioral responses. That analytic function has been made possible, we postulate, by partitioning single afferent fiber tracts of the CNS into separate fascicles, each of them conveying information about different facets of the available information and mapping them separately onto distinct neocortical modules (sublobules or their components) for *parallel processing* (Figure 83). In the visual system of higher primates for instance, that partitioning of perception has made it possible to process unique facial features of different individuals, the configurations of their eyes and mouths, their different bodily postures, and the like at separate sites in a greatly expanded neocortex with multiple gyri.

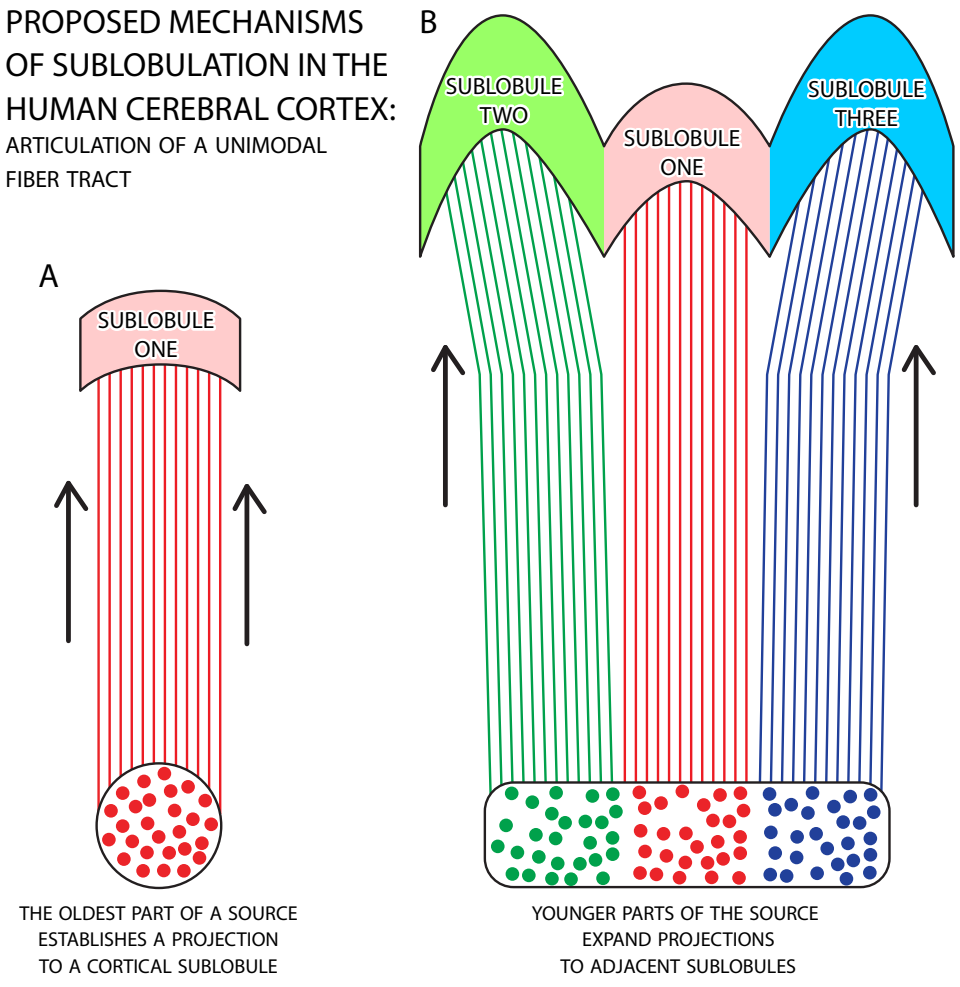

Fig. 83. Schematic diagram of the postulated mechanism of increasing functional articulation from a single source. **A.** The pioneer fibers in the tract terminate in a single sublobule, but that provides limited functional articulation and analytic power. **B.** Addition of younger fibers fasciculate around the pioneers, still from the same source, terminate in different sublobules, allowing for the parallel processing of different facets of the available information.

That articulation in the somatosensory and the somatomotor systems involves separate fascicles and cortical foci devoted to the tongue and mouth to allow articulated vocalization in language use, and extensive finger representation that permits the advance from the ability to paw an object in a clumsy fashion to handle it with dexterity.

The other process serving improved perception and action is *multimodal integration*, the use of several sense modalities for a better appreciation of the different features of the same object. The prime example of multimodal integration is hand-eye coordination, focusing the eyes on what the hands and fingers are doing when skillfully manipulating and constructing objects. That is made possible by integrative sublobules in the parietal lobe that receive both haptic (touch) input from the somatosensory cortex and visual input from the occipital lobe. Multimodal integration also includes the conveyance and processing of salient input from other sources, such as relevant past experience, the object's affective value, cognitive cost and benefit assessment, norms and value judgments, and so forth. Multimodal integration has been made possible, we postulate, by the convergence of fascicles from different association areas, limbic system affective structures, mnemonic and computing mechanisms, and other sources to expanding sublobules that are dedicated to a particular function (Fig. 84).

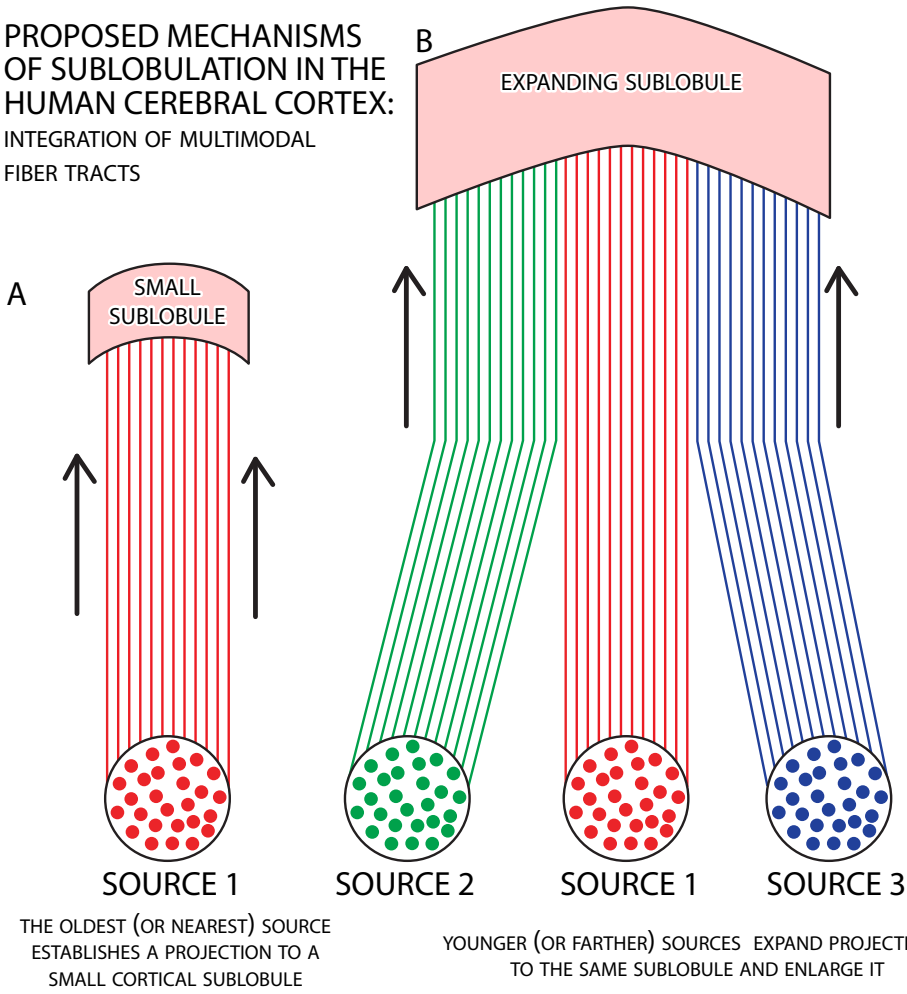

Fig. 84. Schematic diagram of the postulated mechanism of increasing functional integration from more than one source. **A**. A small sublobule first receives input from a single early developing source. (**B**) Expansion of that same sublobule as fibers from other, later developing sources, come to target it. This allows for the integration of information by serial processing from several sources at once.

LATE GYRIFICATION OF THE NEOCORTEX. The sublobulation of the neocortex begins during the third trimester, after neuron production is finished in nearly all areas, as manifested by the diminution or disappearance of the NEP. At the same time neuronal migration is waning, as manifested by the disappearance of the STF and the decerased number of migrating neurons in the white matter (Fig. 67). Hence, we have to find different mechanisms to account for the subdivision of major cortical gyri into subgyri. That does not depend on the increased number of neurons because most are already in the cortical plate. Early thalamic fibers have already played their role in anchoring the anatomical features of lobes and major gyri . We postulate instead the involvement of three new processes. (i) The growth of long and short distance association and commissural axons within and between different cortical areas increases during gyrification. (ii) As these association fibers fasciculate and branch to other cortical areas, they accumulate on the stabilized early core of white matter, adding to its volume by projecting upward into the newly appearing subgyri. (iii) The gray matter of the cortical plate increases its linear extent and depth during dendritic maturation and the expansion of ingrowing axonal terminal branching. That growth over the expanding white matter, further increases forces that cause more folding (gyrification) in the cortical sheet (Fig. 85).

Late gyrification is a complex dynamic process, which may explain why their formation tends to be irregular with great individual variability in their configuration. Presumably, each fiber bundle seeks to make maximal contact with most of the neurons in an initially flat patch of the cortical gray forming a spherical bulge. But because so many fascicles compete with one another for connections in the same cortical area, a tug-of-war results in the formation of distorted semi-spherical configurations of different sizes (green arrows, Fig. 85A). This complexity would explain why cerebellar foliation is much more regular, brought about by a limited set of fiber projections (see above), compared to the neocortex. The variability of regional gyrification in the human neocortex, with its far more heterogeneous inputs, displays much more regional and individual variability than the cerebellum. Notwithstanding that complexity, however, the width of the cortical gray matter remains relatively uniform during this growth stage. We may recall in this context Marin-Padilla's (1992) hypothesis of stratification of the six-layered cortical gray matter. He proposed that cortical lamination develops as the apical dendrites of early generated pyramidal cells become locked in place by attaching to cells in superficial layer I (the "primordial plexiform layer") that contains the horizontally oriented fibers of the Cajal-Retzius cells. As new neurons arrive in the cortical plate, the apical dendrites of the pyramidal cells in layers VI and V elongate as successive waves of younger neurons settle above them. The larger and sturdier older pyramidal cells with their basal dendrites already anchored in the deep cortical layers may resist stretching as more and more younger neurons settle above them (especially in layers IV, III, and II) along the banks and crowns of subgyri.

→

Fig. 85 (facing page). A. Parasagittal section of a cerebral cortex of a GW35 fetus (Y37-60, 300 mm.) with our hypothesis of the two mechanisms of "anchoring" that bring about late gyrification. Early lobe and gyral formation is due to the anchoring of cortical gray expansion where contact has been made with early fibers coming mainly from extracortical sources, i.e., thalamus (*red anchor and red lines with dots*). These contacts create the depths of the primary fissures and early gyri with typically thin white matter beneath the cortical plate. Later subgyrification is due to the invasion of fascicles (*green lines with arrows*) that add thickness to the already stabilized core of the white matter. These new fascicles cause the white matter to project up into the later subgyri.
B. High magnification photomicrograph of another GW35 fetus (Y133-61, 330 mm) showing the different thicknesses of the white matter in the ridges and depths of area V1 (striate projection area) and area V2 (visual association area) in the occipital lobe.

A PROPOSED MECHANISM OF HIGHER-ORDER LOBULATION IN THE HUMAN CEREBRAL CORTEX

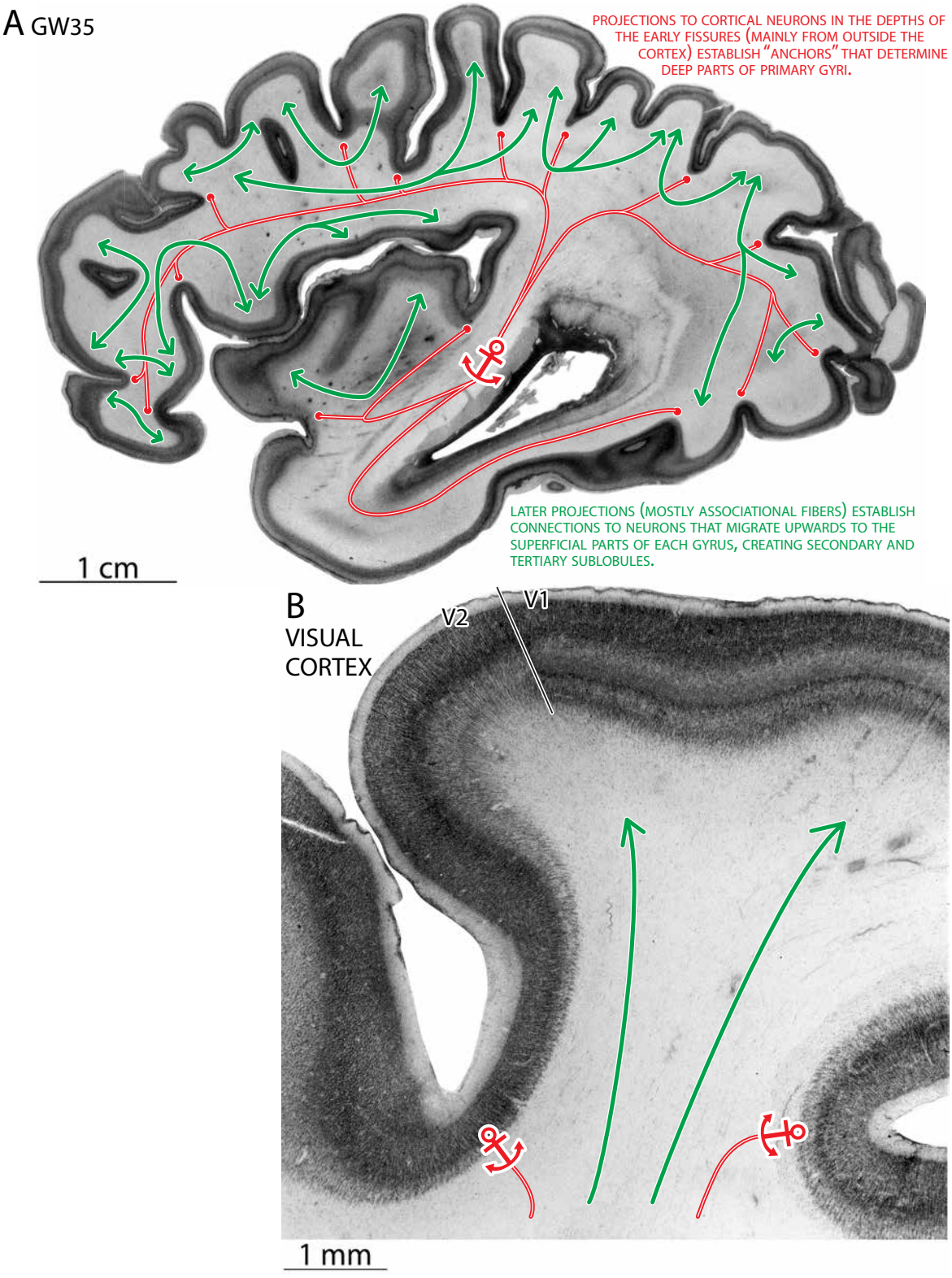

G. THE FOURTH STAGE OF HUMAN NEOCORTICAL DEVELOPMENT: FINE CIRCUITRY FORMATION, SYNAPTOGENESIS, AND MYELOGENESIS

Postnatal Growth of the Neocortex. The stages of neocortical development described—the stockpiling of proliferating precursor cells, the migration and settling of differentiating postmitotic neurons, and the areal differentiation and progressive gyrification of gray matter—are prenatal events. Building the stock of precursor cells and the migration and settling of differentiating neurons are major factors in determining the total number of neocortical neurons that will be available to the individual. Neocortical areal differentiation may be a factor in determining the considerable individual differences in behavioral and mental abilities. Gyrification supports optimal packaging of the expanding gray matter, a necessity that permits the passage of the large head of the human neonate through the birth canal. That packaging, however, has not allowed the newborn head of *Homo sapiens* to emerge with a mature brain, and much of neocortical development takes place after birth.

The newborn's skull consists of bones with wider, unfused sutures that allow movement during parturition and growth during early infancy through childhood. Head circumference increases from about 34 cm at birth to a median (50th percentile) of about 51 cm at 5 years of age, with the increase being most rapid during the first year of life and declining after the third year (Fig. 86). Brain weight quadruples between birth and the end of the third year (Fig. 39). Similar increases were reported for the weight of the "forebrain" (still not an exact measure of the weight of the neocortex and neocortical white matter) from birth to adulthood (Dobbing and Sands, 1973). According to

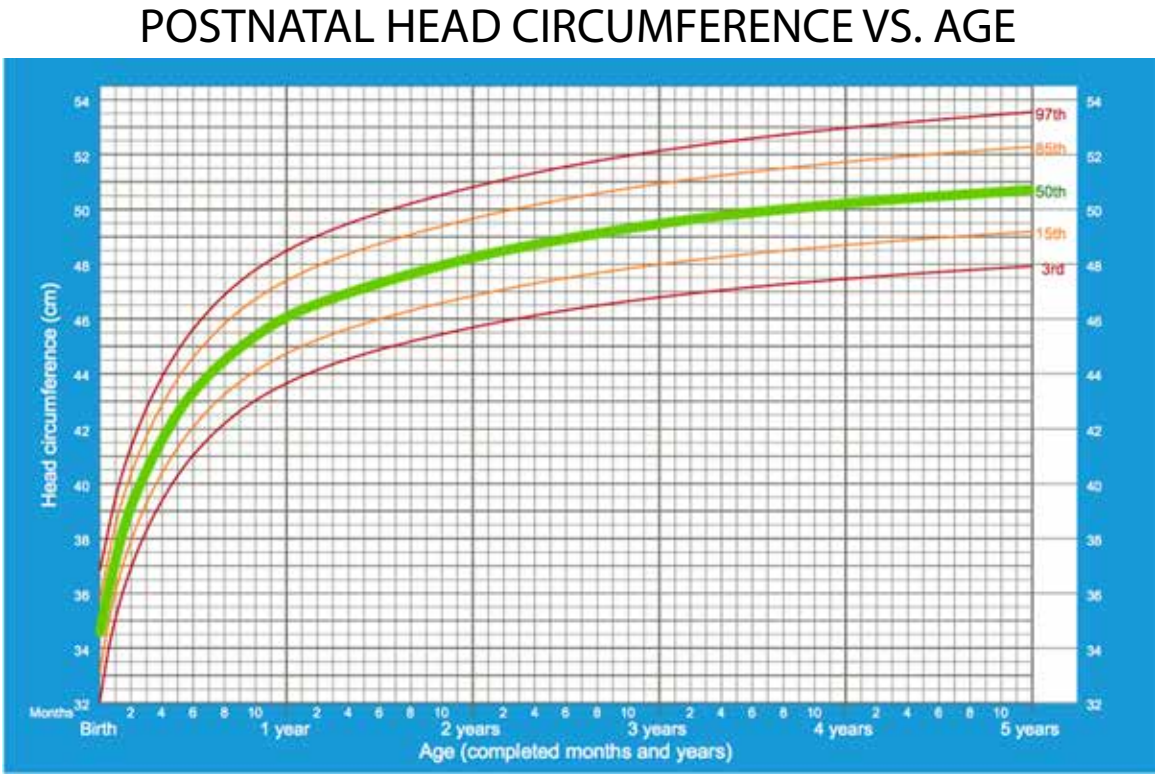

Fig. 86. Median (green curve) and percentile rankings of head circumference growth in boys from birth to 5 years of age. (World Health Organization.)

recent studies based on MRI scanning of a large sample of live subjects, brain volume at birth is about 380-420 cm^3, one-third of the adult volume (Huppi et al. 1998), and cerebral volume is about 36% of the adult value at 2-4 weeks and 72% at 12 months (Knickmeyer et al. 2008). Cerebral volume reaches about 80% of adults at 3 years, and about 90% by 9 years of age (Caviness et al., 1996). However, according to another MRI study, the global increase of neocortical surface area is much smaller during the first two years of life (Li et al., 2013). According to a recent MRI study with a large sample of subjects, cortical surface area expansion is the greatest during adulthood (Schnack et al., 2015). In terms of regional differences in the expansion of the neocortical surface area from birth to adulthood, we plotted earlier Blinkov and Glezer's (1968) data, according to which the occipital lobe expands 5-times, the temporal lobe 8-times, and the frontal lobe expands 9-times from birth to adulthood (Fig. 40). In contrast to Blinkov and Glezer's report of great areal increase in the temporal and frontal cortices during the first two years of life, Li et al. (2015) report only a modest increase from about 350 cm^2 at birth to 650 cm^2 at 1 year, and to about 750 cm^2 at 2 years, with the high-growth regions being located in the association cortices, and the low-growth regions located in the projection areas. The discrepancy between Glazer and Blinkov's data, based on a small sample using microsocopic histology, and Li's data with a larger sample using low-resolution MRI remains to be clarified.

Fine Circuitry Formation: Dendrogenesis and Synaptogenesis. Because the production of neurons ceases after birth (with the hippocampus and olfactory bulb excepted; Altman and Bayer 2015), the postnatal growth of the cerebral cortex must be due to other factors than neurogenesis. Much of the expansion of the white matter can be attributed to the growth of long- and short-distance associational and commissural fibers and their collaterals, but we have currently little information about the specifics of that process. More is known about the progressive increase in neocortical gray matter volume during infancy and early childhood, and that can be broken down into several contributing factors: (i) increase in the size of neuronal cell bodies (perikarya); (ii) expansion of the neuropil, the unstained background in Nissl-stained preparations of such constituents as locally ramifying axons, dendrites, and dendritic spines (Fig. 45); and (iii) increase in the number of glial cells and their processes, growth of capillaries, and myelin formation. The combined outcomeof these factors is a decrease in the packing density of neuronal perikarya stained with the Nissl method between birth and early childhood. Known as the gray-cell coefficient (Haug, 1956), this development reflects in a nonspecific way the postnatal establishment of the fine circuitry of the neocortex. The growth of dendrites in the early maturing motor cortex begins during the third trimester (Mrzljak et al., 1992) but their rapid expansion occurs after birth. Using the Golgi technique and camera lucida drawings from birth to 6 years of age, Conel (1939-1967) illustrated the time course of pyramidal cell perikaryal growth and increases in the number of spines on their dendrites in several regions of the neocortex, (Figs. 46A-D). Schadé and van Groningen (1961) quantified volumetric growth of pyramidal cell perikarya and concurrent decreases in their packing density between birth and adulthood in the frontal lobe. According to that study, the increase in perikaryal expansion and the changes in the gray-cell coefficient with age is most pronounced in the pyramidal cells of layer V, and least so in cells of granular layer IV (Fig. 87). In a more recent MRI study with a large sample of subjects, Li et al. (2015) reported an increase in neocortical thickness in the first year of postnatal life and little change during the second year. The postnatal three-dimensional expansion of the dendrites of pyramidal cells in layer III and layer V of the prefrontal cortex has been quantified by Koenderink et al. (1994, 1995). The specimens ranged

from 7.5 months to adulthood. There was a rapid phase of expansion during the first year, a slower phase up to 5 years. Thereafter, dendritic growth became stable at least up to 27 years. According to Travis et al. (2005), the dendritic length of basal dendrites of pyramidal neurons in layer V of neonates was higher in Brodmann's area 4 (primary motor cortex) than in frontal area 10, and there was an inverse relationship in adults with greatest dendritic complexity observed in area 10. Much has yet to be learned about the time course of and regional differences in the cytological development of the human neocortical gray matter.

PYRAMIDAL CELL BODY VOLUME AND THEIR PACKING DENSITY VERSUS AGE IN THE MIDDLE FRONTAL GYRUS

A PYRAMIDAL CELL BODY VOLUME

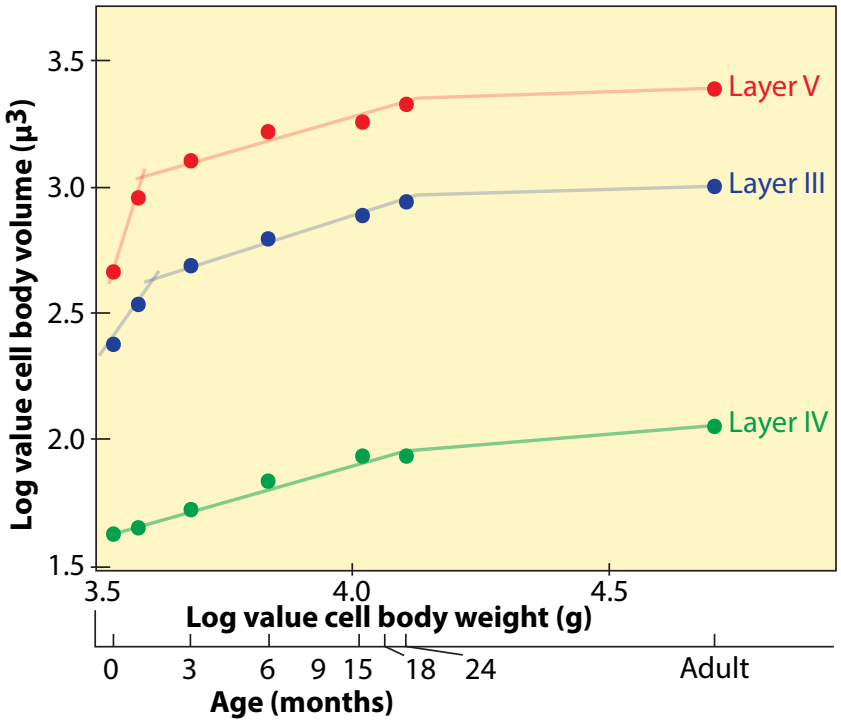

B PYRAMIDAL CELL PACKING DENSITY (PD) AND GRAY CELL COEFFICIENT (GCC)

	Newborn	6 Months	24 Months	Adult
LAYER III				
PD (x 10^3/mm^3)	99.0	30.5	20.1	12.5
GCC*	41	53	55	77
LAYER IV				
PD (x 10^3/mm^3)	444.1	151.0	59.8	35.0
GCC*	55	95	180	250
LAYER V				
PD (x 10^3/mm^3)	60.5	16.1	8.9	6.0
GCC*	36	37	52	66

$$*GCC = \frac{\text{volume of griseum}}{\text{volume of nerve cells contained in it}}$$ (only calculated for pyramidal cells)

Fig. 87. A. Growth in volume (log value in μ^3) of pyramidal cells in layers III, IV and V of the middle frontal gyrus, in relation to age and body weight from birth to adulthood. **B.** Packing density (PD) and gray-cell coefficient (GCC) of pyramidal cells in the same three layers of the middle frontal gyrus at three ages. (From Schadé and van Groningen, 1961.)

Even less is known about neocortical synaptogenesis in humans. According an initial report by Huttenlocher (1979), using electron microscopy, synaptic concentration increases in the middle frontal gyrus (prefrontal cortex) during the first two years of life and then declines between 2 and 16 years in relation to the decrease in perikaryal density. In a later report, Huttenlocher and Dabholkar (1997) compared synaptogenesis in the middle frontal gyrus and Heschl's gyrus (the primary auditory cortex). In both regions synapse formation begins at GW27 and increases rapidly thereafter in the auditory cortex, with maximum attained at 3 months postnatal, while in the prefrontal cortex synaptogenesis is more protracted and maximum synaptic density is reached at 15 months. This is followed by synapse pruning during childhood, which ends at 12 years of age in the auditory cortex and in late adolescence in the prefrontal cortex. (Pruning in monkeys has recently been reviewed by Elston and Fujita, 2014). An indirect method of studying synaptogenesis in humans has been the quantification of dendritic spine concentration in Golgi preparations. In a recent study, Petanjek et al. (2011) found that dendritic spine density in the prefrontal cortex of human children exceeds adult values two- to three-fold, and that the elimination of dendritic spines continues beyond adolescence but becomes stabilized during adulthood. In the context of these studies it must be noted that data about the time course of dendritic branching and spine proliferation and pruning provide little information about the identity of the fibers tracts that establish synaptic connections in the different areas of the neocortex and to what extent the connections made are genetically determined and modulated by epigenetic factors, such as nutrition, health, and mental facilitation through training and education.

Myelogenesis. Axons become fully functional when they become myelinated. Due to the process known as saltatory conduction—the propagation of the action potential from one node of Ranvier to the next by physical rather than bioelectric current spread—myelinated fibers conduct impulses faster and more reliably than do unmyelinated fibers. In the CNS, myelination is produced by oligodendroglia cells, which have cytoplasmic processes that wrap around the axon by forming spiral lamellae. Myelination is preceded by the proliferation of oligodendroglia cells, known as myelination gliosis (Roback and Scherer, 1935; Fleischauer and Hillebrand, 1968), which produce myelin basic proteins and associated glycoproteins in abundance (Gilles et al, 1983; Barkovich et al. 1988; Poduslo and Jang, 1988). This stage becomes manifest in myelin-stained tissues as fine dots or small fragments (Figs. 47-57). Next, select fiber tracts become lightly stained, we referred to that stage as "myelinating," and when that is succeeded by the tract becoming opaque, as "myelinated." As we saw, myelination of the thalamocortical and corticospinal tract fibers is principally a postnatal event (Figs. 48, 52-60), much delayed relative to the myelination of afferent and efferent fibers of subcortical structures, including the cuneate and gracile fasciculi (Fig. 47).

The material prepared by Yakovlev and photographed and digitized by us confirms the early findings of Flechsig (Fig. 50) and the Vogts (Fig. 51)) that the first fiber tracts to myelinate in the cerebral cortex are the thalamocortical projection fibers of the precentral somatomotor cortex, the postcentral somatosensory cortex, and the visual fibers targeting the occipital cortex. That myelination takes place in infants between the postnatal ages of 1.5 to 2.5 months, but the myelination of axons, as seen both in the Yakovlev and the Vogts material (Figs. 53, 54, 55D) has not yet spread into the cortical gray matter. Apparently, myelination starts in "hot spots" in the core of white matter, and spreads from there outward into the white matter of the neocortical lobules and sublobules *en masse*. Following that myelination in the projection areas, proliferation gliosis commences in the

association areas of the frontal, parietal and occipital cortex in 2.5-months- (Fig. 55), 3-months- (Fig. 56) and 4-months-old infants (Fig. 57). The white matter is fully myelinated in most lobules throughout the neocortex in the 7-months-old infant, except in the temporal lobe (Fig. 58), and many of the frontal sublobules are still in the stage of myelination gliosis in the 11 months-old infant (Fig. 59). Recent MRI sutdies, which provide lower resolution but in living subjects, indicate a similar trend (Deoni et al., 2011). Paralleling the onset of myelination in the somatomotor cortex at the age of 1.5 months, the first fibers of the descending corticospinal tract reach and penetrate the pontine gray nucleus at about the same age (Fig. 60B). By 8 months, all the longitudinal transpontine corticospinal fibers, as well as transverse pontocerebellar fibers, appear to be fully myelinated (Fig. 60). Myelination spreads into the cortical gray matter at a later age. Myelination probably contributes to the progressive expansion of the white matter through childhood and into adolescence, as indicated by the MRI scanning technique (reviewed by Giedd and Rapaport, 2010, and Dubois et al. 2014). An interesting, paradoxical finding has been the phenomenon of "cortical thinning" or "gray matter loss" that begins in late childhood and adolescence, and proceeds from projection areas to higher order association areas (reviewed by Toga et al. 2006). However, that interpretation of thinning based on MRI scans may be an erroneous one, ignoring the fact that an aspect of neocortical development is the spread of myelination from the white matter into the lower layers of the cortical gray matter (Miller er al., 2010), endowing the latter at low resolution with density characteristics of the white matter (Fig. 88).

Behavioral Correlations. Taking into consideration the upside-down map of the body ("homunculus") in the somatomotor and somatosensory cortices (Penfield and Rasmussen, 1950) and the spread of myelination in the same areas from bottom to top, as here documented, we conclude that the myelination of corticospinal tract fibers representing the head region takes place before those of the arm and the hands, which are followed by the trunk and the legs. This sequence also holds for the myelination of the corticospinal tract in the spinal cord, where fibers controlling upper body regions run medially and those controlling lower body regions run laterally (Foerster, 1936); the myelination gradient in the lateral corticospinal tract exactly follows that sequence (Altman and Bayer, 2001). There is a good correlation between that sequence of myelination and the development of voluntary control of behavior (Halverson, 1937; McGraw, 1943; Gesell, 1954; Forssberg, 1985) as we summarized and illustrated earlier in our book on the development of the human spinal cord (Altman and Bayer, 2001). Infants begin to lift and rotate their head when in a supine position at about 3-4 months. That is followed at about 4-6 months by the ability to use arms and hands to reach for and play with accessible objects when securely seated in a chair. Babies lift their trunks off the ground with extended arms by about 8 months; crawl by using arms and legs by 10 months; and walk upright with support at about 1 year, and without support by 1.5 years of age.

A somewhat different developmental brain-behavior correlation holds for the acquisition of language through the control of the vocal cords, tongue, and lips. Language learning may be dependent on the maturation, including myelination, of Broca's and Wernicke's areas in the frontal and temporal lobe association areas, respectively. Speech begins when infants about 6 months of age begin to babble, learning the voluntary control of the vocal tract to produce monosyllables with consonants, such as "ba," "ma," "da," "ga" (Lenneberg, 1967; Oller, 1980). This is done without any referential meaning, as the infants babble as much when alone as when others are around. This

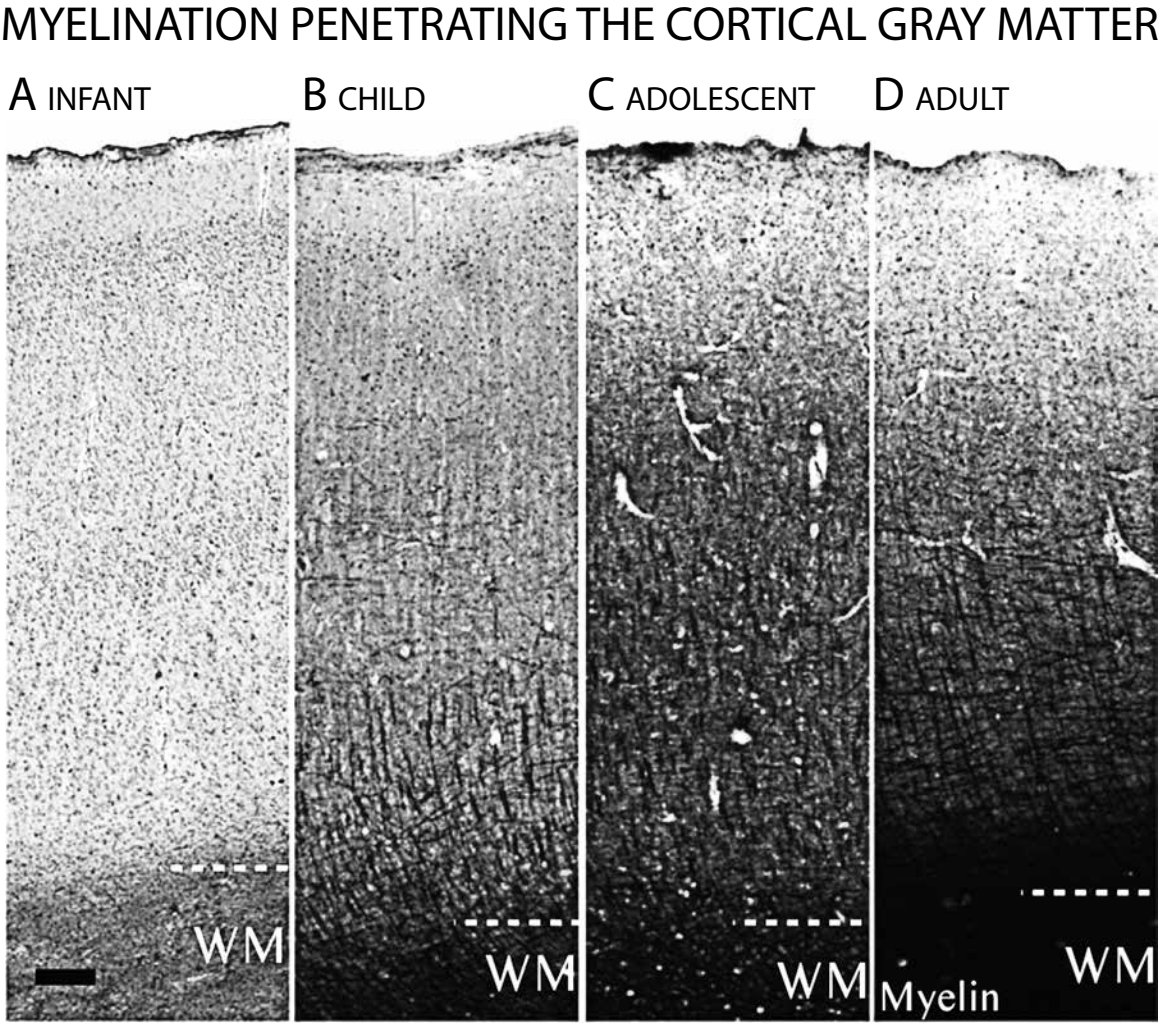

Fig. 88. Spread of myelination from the white matter into layers of the gray matter as a function of age. Sections representative of the motor cortex of 0-1 years infants (**A**); 3-9 years-old children and juveniles (**B**); 13-23 years-old adolescents and young adults (**C**); and adults 28 years or older (**D**). After Miller et al., 2012.

stage is followed by producing polysyllables like "baba," "mama," "dadada," "gagaga," and by 7-8 months the infant's utterances begin to resemble phonologically the words their caretakers are using. Infants begin to use single words by imitation and as a means of communication at about 12 months of age but with unclear message. The word "cookie" may mean, "I see a cookie," "I want a cookie," or "the dog eats a cookie." By about 14 months, the toddler may combine several words to deliver a message or describe an observed event, "Susie want cookie" or "mommie eat cookie." By about 2 years of age, as an aspect of cognitive development, the child has learned that every object, event or action has a word assigned to it and that multiple words have to be combined grammatically to make one's speech unambiguous (Baldwin, 1993; Preissler and Carey, 2004; Plunkett et al., 2008). Recent studies based on MRI technology suggest that word understanding and word speaking in toddlers are correlated with tissue changes (Aeby et al., 2013; Travis et al., 2013) and increased myelination (Pujol et al., 2006) in language-related areas of the neocortex.

Confirmation of a maturational and a myelination gradient from the projection areas to the association areas of the neocortex, and in particular the protracted development of the prefrontal cortex provides support for the role of genetically- and epigenetically-based neural factors in the later development of individual differences in intelligence and executive functions (Erlenmeyer-Kimling and Janek, 1963; Vernon, 1979). Current studies using structural and functional mapping techniques (MRI, fMRI, PET scans) have implicated the prefrontal cortex in expressive and receptive language development (O'Muircheartaigh et al., 2014), individual differences in children's IQ (Wilke et al., 2003), and in the fluid intelligence, speed of reasoning ability, and numerical performance of adults (e.g., Duncan et al., 2000; Geake and Hansen, 2005; Jung and Haier, 2007; Tang et al., 2010; Colom et al., 2013). This relationship has been confirmed recently by a meta-analysis of 12 structural and 16 functional brain-imaging studies (Basten et al., 2015). There is an association between individual differences in intelligence, as assessed by established psychometric tests, and either activation of the frontal lobe when engaged in a cognitive task or cortical gray matter thickness.

REFERENCES

Aeby, A., X. De Tiege, M. Creuzil, et al. 2013. Language development at 2 years is correlated to brain microstructure in the left superior temporal gyrus at term equivalent age: A diffusion tensor imaging study. *Neuroimage*, 78:145-151.

Altman, J. 2012-2014. *Neural and Mental Evolution: Origins of the Human Body, Brain, Behavior, Consciousness, and Culture.* www.brainmindevolution.org.

Altman, J. and S. A. Bayer. 1988. Development of the rat thalamus. I. Mosaic organization of the thalamic neuroepithelium. *Journal of Comparative Neurology*, 275:346-377.

Altman, J. and S. A. Bayer. 1997. *Development of the Cerebellar System in Relation to its Evolution, Structure, and Functions*. Boca Raton, FL: CRC Press.

Altman, J. and S. A. Bayer. 2001. *Development of the Human Spinal Cord: An Interpretation Based on Experimental Studies in Animals.* New York: Oxford University Press.

Altman, J. and S. A. Bayer. 2002. Regional differences in the stratified transitional field and the honeycomb matrix of the developing human cerebral cortex. *Journal of Neurocytology*, 31:613-632.

Altman, J. and S. A. Bayer. 2014. *Brief Communications.* No 1: Hippocampal neurogenesis in children. The Laboratory of Developmental Neurobiology. www.neurondevelopment.org.

Ariëns Kappers, C. U., G. C. Huber and E. C. Crosby. 1936. *The Comparative Anatomy of the Nervous System of Vertebrates, Including Man*. 2 volumes. New York: Macmillan. (Reprinted in 3 volumes, New York: Hafner, 1960).

Baker, C. I., M. Behrmann and C. R. Olson. 2002. Impact of learning on representation of parts and whole in monkey inferotemporal cortex. *Nature Neuroscience*, 5:1210-1216.

Baldwin, D. A. 1993. Early referential understanding: Infant's ability to recognize planned movement in a sequential reach task. *Journal of Neurophysiology*, 85:539-544.

Barkovich, A. J., B. O. Kjos, D. E. Jackson and D. Norman. 1988. Normal maturation of the neonatal and infant brain: MR imaging at 15 T. *Radiology*, 166:173-180.

Basten, U., K. Hilger and C. J. Fiebach. 2015. Where smart brains are different: A quantitative meta-analysis of functional and structural brain imaging studies on intelligence. *Intelligence*, 51:10-27.

Batista, A. P. and R. A. Andersen. 2001. The parietal reach region codes for the next referential acts for what they are. *Developmental Psychology*, 29:832-843.

Bayer, S. A. and J. Altman. 1991. *Neocortical Development.* New York: Raven Press.

Bayer, S. A., J. Altman, R. J. Russo and X. Zhang. 1993. Timetables of neurogenesis in the human brain based on experimentally determined patterns in the rat. *Neurotoxicology*, 14:83-144.

Bayer, S. A. and J. Altman. 2002-2008. *Atlas of Human Central Nervous System Development*. 5 volumes. Boca Raton, FL: CRC Press.

Baylis, G. C., E. T. Rolls and C. M. Leonard. 1987. Functional subdivisions of the temporal lobe neocortex. *Journal of Neuroscience*, 7:330-342.

Binkofski, F., G. Buccino, K. M. Stephan, et al. 1999. A parieto-premotor network for object manipulation: Evidence from neuroimaging. *Experimental Brain Research*, 128:210-213.

Bishop, K. M., G. Goudreau and D. D. O'Leary. 2000. Regulation of area identity in the mammalian neocortex by Emx2 and Pax2. *Science*, 288:344-349.

Blinkov, S. M. and I. I. Glezer. 1968. *The Human Brain in Figures and Tables: A Quantitative Handbook.* (Translated by B. Haigh). New York: Plenum Press.

Bolz, J., D. Uziel, S. Muhlfriedel, et al. 2004. Multiple roles of ephrins during the formation of thalamocortical projections: Maps and more. *Journal of Neurobiology*, 59:82-94.

Bosco, A., R. Breveglieri, D. Reser, et al. 2015. Multiple representation of reaching space in the medial posterior parietal area V6A. *Cerebral Cortex*, 25:1654-1667.

Bruce, C., R. Desimone and C. G. Gross. 1981. Visual properties of neurons in a polysensory area in superior temporal sulcus of the macaque. *Journal of Neurophysiology*, 46:369-384.

Castellani, V., Y. Yue, P. P. Gao, et al. 1998. Dual action of ligand for Eph receptor tyrosine kinase on specific populations of axons during the development of cortical circuits. *Journal of Neuroscience*, 18:4663-4672.

Caviness, V. S. 1976. Patterns of cell and fiber distribution in the neocortex of the reeler mutant mouse. *Journal of Comparative Neurology*, 170:435-447.

Caviness, V. S., D. N. Kenney, J. F. Bates and N. Makris. 1996. The developing brain: A morphometric profile. In R. W. Thatcher et al. (eds.), *Developmental Neuroimaging: Mapping the Development of Brain and Behavior*, pp. 3-14. New York: Academic Press.

Chen, B., L. R. Schaevitz and S. K. McConnell. 2005 Fez1 regulates the differentiation and axon targeting of layer 5 subcortical projection neurons in cerebral cortex. *Proceedings of the National Academy of Sciences, USA,* 102, 17184-17189.

Cole, M. W., T. Yarkoni, G. Repovš, et al. 2012. Global connectivity of prefrontal cortex predicts cognitive control and intelligence. *Journal of Neuroscience*, 32:8988-8999.

Colom, R., M. Burgaleta, F. J. Román, et al. 2013. Neuroanatomic overlap between intelligence and cognitive factors: Morphometry methods provide support for the key role of the frontal lobes. *NeuroImage*, 72:143-152.

Conel, J. L. 1939-1967. *The Postnatal Development of the Human Cerebral Cortex*. 8 volumes. Cambridge, MA: Harvard University Press.

Connolly, J. D., R. A. Andersen and M. A. Goodale. 2003. FMRI evidence for a 'parietal reach region' in the human brain. *Experimental Brain Research*, 153:140-145.

Debowy, D. J., S. Ghosh, J. Y. Ro and E. P. Gardner. 2001. Comparison of neuronal firing rates in somatosensory and posterior parietal cortex during prehension. *Experimental Brain Research*, 137:269-291.

DeKaban, A S. and D. Sadowsky. 1978. Changes in brain weights during the span of human life: Relation of brain weights to body heights and body weights. *Annals of Neurology*, 4:345-356.

De la Rossa, A., C. Bellone, B. Golding et al. 2013. In vivo reprogramming of circuit connectivity in postmitotic neocortical neurons. *Nature Neuroscience*, 16:193-200.

Deoni. S. C. L., E. Mercure, A. Blasi, et al. Mapping infant brain myelination with magnetic resonance imaging. *Journal of Neuroscience,* 31:784-791.

Desimone, R., T. D. Albright, C. G. Gross and C. Bruce. 1984. Stimulus-selective properties of inferior temporal neurons in the macaque. *Journal of Neuroscience*, 4:2051-2062.

Desimone, R. and C. G. Gross. 1979. Visual areas in the temporal cortex of the macaque. *Brain Research*, 178:363-380.

DeSouza, J. F. X., S. P. Dukelow, J. S. Gati, et al. 2000. Eye position signal modulates a human parietal pointing region during memory-guided movements. *Journal of Neuroscience*, 20:5835-5840.

Dobbing. J. and J. Sands. 1973. Quantitative growth and development of human brain. *Archives of Diseases in Childhood*, 48:757-767.

Dohrmann, G. J. 1970. The choroid plexus: A historical review. *Brain Research*, 18:197-218.

Dubois, J., G. Dehaene-Lambertz, S. Kulikova et al. 2014. The early development of brain white matter: A review of imaging studies in fetuses, newborns, and infants. *Neuroscience*, 276:48-71.

Duffy, C. J. and R. H. Wurtz. 1991. Sensitivity of MST neurons to optic flow stimuli. I. A continuum of response selectivity to large-field stimuli. *Journal of Neurophysiology*, 65:1329-1345.

DufourA., J. Seibt, L. Passante, et al. 2003. Area specificity and topography of thalamocortical projections are controlled by ephrin/Eph genes. *Neuron*, 39:453-465.

Duhamel, J. R., C. Colby and M. Goldberg. 1998. Ventral intraparietal area of the macaque: Congruent visual and somatic response properties. *Journal of Neurophysiology*, 79:126-136.

Duncan, J., R. J. Seitz, J. Kolodny et al. 2000. A neural basis for general intelligence. *Science*, 289:457-460.

Dziegielewska, K. M., J. Ek, M.D. Habgood and N. R. Saunders. 2001. Development of the choroid plexus. *Microscopic Research Techniques*, 52:5-20.

Edinger, T. 1948. Evolution of the horse brain. *Memoirs of the Geological Society of America*, 25:1-177.

Elston, G. N. and I. Fujita. 2014. Pyramidal cell development: Postnatal spinogenesis, dendritic growth, axon growth, and electrophysiology. *Frontiers in Neuroanatomy*, 8 (78):1-20.

Englund, C., A. Fink, C. Lau, et al. 2005. Pax6, Tbr2, and Tbr1 are expressed sequentially by radial glia, intermediate progenitor cells, and postmitotic neurons in developing neocortex. *Journal of Neuroscience*, 25:247-251.

Erlenmeyer-Kimmling, L. and L. F. Janek. 1963. Genetics and intelligence: A review. *Science*, 142:1477-1479.,

Estivill-Torrus, G., H. Pearson, V. van Heyningen, et al. 2002. Pax6 is required to regulate the cell cycle and the rate of progression from symmetrical to asymmetrical division in mammalian cortical progenitors. *Development*, 129:455-466.

Faugier-Grimaud, S., C. Frenois and D. G. Stein. 1978. Effects of posterior parietal lesions on visually guided behavior in monkeys. *Neuropsychologia*, 16:151-168.

Fattori, P., V. Raos, R. Breveglieri et al. 2010. The dorsomedial pathway is not just for reaching: Grasping neurons in the medial parieto-occipital cortex of the macaque monkey. *Journal of Neuroscience*, 30:342-349.

Felleman, V. J., A. Burkhalter and D. C. Van Essen. 1997a. Cortical connections of area V3 and VP of macaque monkey extrastriate visual cortex. *Journal of Comparative Neurology*, 379:21-47.

Felleman, D. J., Y. Xiao and E. McClendon. 1997b. Modular organization of occipito-temporal pathways: Cortical connections between visual area 4 and visual area 2 and posterior inferotemporal ventral area in macaque monkeys. 17:3185-3200.

Felleman, D. J. and D. C. Van Essen. 1991. Distributed hierarchical processing in the primate cerebral cortex. *Cerebral Cortex*, 1:1-47.

Ferrera, V. P., K. K. Rudolph and J. H. Maunsell. 1994. Responses of neurons in the parietal and temporal visual pathways during a motion task. *Journal of Neuroscience*, 14:6171-6186.

Flechsig, P. 1896. *Gehirn und Seele.* Leipzig: Veit.

Fleischauer, K. and H. Hillebrand. 1966. Über die Vermehrung der Gliazellen bei der Markscheidenbildung. *Zeitschrift für Zellforschung*, 69:61-68.

Foerster, O. 1936. Motorische Felder und Bahnen. In: O. Bumke and O. Foerster (eds.), *Handbuch der Neurologie*, vol. 5, pp. 1-357. Berlin: Springer.

Forssberg, H. 1985. Ontogeny of human locomotor control. I. Infant stepping, supported locomotion and transition to independent locomotion. *Experimental Brain Research*, 57:480-493.

Fulton, J. F. 1943. *Physiology of the Nervous System.* 2nd ed. London: Oxford University Press.

Galletti, C., D. F. Kutz, M. Gamberini et al. 2003. Role of the medial parieto-occipital cortex in the control of reaching and grasping movements. *Experimental Brain Research*, 153:158-170.

Gallo, G. and P. C. Letourneau. 2000. Neurotrophins and the dynamic regulation of the neuronal cytoskeleton. *Journal of Neurobiology*, 44:159-173.

Gamberini, M., S. Bakola, L. Passarelli , et al. 2015. Thalamic projections to visual and visuomotor areas (V6 and V6A) in the rostral bank of the parieto-occipital sulcus of the macaque. *Brain Structure and Function*, DOI 10.1007/s00429-015-0990-2.

Gardner, E. P., K. S. Babu, S. D. Reitzen et al. 2007. Neurophysiology of prehension. I. Posterior parietal cortex and object-oriented hand behaviors. *Journal of Neurophysiology*, 97:387-406.

Gato, A., J. A. Moro, M. I. Alonso, et al. 2005. Embryonic cerebrospinal fluid regulates neuroepithelial survival, proliferation, and neurogenesis in chick embryos. *Anatomical Record*, A284:475-484.

Gattass, R., A. P. B. Sousa and C. G. Gross. 1988. Visuotopic organization and extent of V3 and V4 of the macaque. *Journal of Neuroscience*, 8:1831-1845.

Geake, J. G. and P. C. Hansen. 2005. Neural correlates of intelligence as revealed by fMRI of fluid analogies. *NeuroImage,* 26:555-564.

Gesell, A. 1954. The ontogenesis of infant behavior. In: L. Carmichael (ed.), *Manual of Child Psychology*, pp. 335-373. 2nd ed. New York: Wiley.

Giedd, J. N. and J. L. Rapoport. 2010. Structural MRI of pediatric brain development: What have we learned and where are we going? *Neuron*, 67:728-734.

Gilles, F. H., W. Shankle and E. C. Dooling. 1983. Myelinated tracts: Growth patterns. In: F. H. Gilles et al. (eds.), *The Developing Human Brain*, pp. 117-183. Boston: Wright.

Hagler, D. J., L. Riecke and M. I. Sereno. 2007. Parietal and superior frontal visuospatial maps activated by pointing and saccades. *Neuroimage*, 35:1562-1577.

Haleem, M. 1990. *Diagnostic Categories of the Yakovlev Collection of Normal and Pathological Anatomy and Development of the Brain*. Washington, DC: Armed Forces Institute of Pathology.

Halverson, H. M. 1937. Studies of grasping responses of early infancy. *Journal of Genetic Psychology*, 51:371-449.

Hanazawa, A. and H. Komatsu. 2001. Influence of the direction of elemental luminance gradients on the responses of V4 cells to textured surfaces. *Journal of Neuroscience*, 21:4490-4497.

Haug, H. 1956. Remarks on the determination and significance of the gray cell coefficient. *Journal of Comparative Neurology*, 104:473-492.

Hevner, R. F., E. Miyashita-Lin and J. L Rubenstein. 2002. Cortical and thalamic pathfinding defects of Tbr1, Gbx2 and Pax6 mutant mice: Evidence that cortical and thalamic axons interact and guide one another. *Journal of Comparative Neurology*, 447:8-17.

Hochstetter, F. 1919. *Beiträge zur Entwicklungsgeschichte des menschlichen Gehirns*. I. Teil. Mit 18 Abbildungen im Text und 25 Tafeln. Wien und Leipzig: Franz Deuticke.

Holmes, G. and W. T. Lister. 1916. Disturbances of vision from cerebral lesions, with special reference to representation of the macula. *Brain*, 39:34-73.

Horton, J. C. 2006. Ocular integration in human visual cortex. *Canadian Journal of Ophthalmology*, 41:584-593.

Hubel, D. H. 1988. *Eye, Brain, and Vision*. New York: Scientific American Library.

Huntley, G. W. and D. L. Benson. 1999. N-cadherin at developing thalamocortical synapses provides an adhesion mechanism for the formation of somatotopically organized connections. *Journal of Comparative Neurology*, 407:453-471.

Huppi, P. S., S. Warfield, R. Kikinis, et al. 1998. Quantitative magnetic resonance imaging of brain development in premature and mature newborns. *Annals of Neurology*, 43:224-235.

Huttenlocher, P. R. 1979. Synaptic density in human prefrontal cortex: Developmental changes and effects of aging. *Brain Research*, 163:195-205.

Huttenlocher, P. R. and A. S. Dabholkar. 1997. Regional differences in synaptogenesis in human cerebral cortex. *Journal of Comparative Neurology*, 387:167-178.

Inoue, T., S. Nakamura and N. Osumi. 2000. Fate mapping of the mouse prosencephalic neural plate. *Developmental Biology*, 219:373-383.

Inouye, T. 1909. *Die Sehstörungen bei Schussverletzungen der kortikalen Sehsphäre.* Leipzig: Engelmann.

Johansson, P. A., K. M. Dziegielewska, C. J. Ek, et al. 2005. Aquaporin-1 in the choroid plexuses of developing mammalian brain. *Cell and Tissue Research*, 322:353-364.

Jung, R. E. and R. J. Haier. 2007. The parieto-frontal integration theory (P-FIT) of intelligence: Converging neuroimaging evidence. *The Behavioral and Brain Sciences*, 30:135-154 (Discussion, 154-187).

Kalil, K. and E. W. Dent 2014. Branch managemnt: Mechanisms of axon branching in the developing vertebrate CNS. *Nature Reviews Neuroscience*, 15:7-18.

Kamiryo, T., T. Orita, T. Nishizaki and H. Aoki. 1990. Development of the rat meninx: Experimental study using bromodeoxyuridine. *Anatomical Record*, 27:207-210.

Kawano, K., M. Shidara, T. Watanabe and S. Yamane. 1994. Neural activity in cortical area MST of alert monkey during ocular following responses. *Journal of Neurophysiology*, 71:2305-2324.

Kawashima, R., E. Naitoh, M. Matsumura, et al. 1996. Topographic representation in human intraparietal sulcus of reaching and saccade. *NeuroReport*, 17:1253-1256.

Knickmeyer, R. C., S. Gouttard, C. Kang, et al. 2008. A structural MRI study of human brain development from birth to 2 years. *Journal of Neuroscience*, 28:12176-12182.

Kobatake, E., G. Wang and K. Tanaka. 1998. Effects of shape-discrimination training on the selectivity of inferotemporal cells in adult monkeys. *Journal of Neurophysiology*, 80:324-330.

Koenderink, M. J., H. B. Uylings and L. Mrzljak. 1994. Postnatal maturation of the layer III pyramidal neurons in the human prefrontal cortex: A quantitative Golgi analysis. *Brain Research*, 653:173-182.

Koenderink, M. J. and H. B. Uylings. 1995. Postnatal maturation of layer III pyramidal neurons in the human prefrontal cortex: A quantitative Golgi analysis. *Brain Research*, 678:233-243.

Kwan, K. Y., N. Sestan and E. S. Anton. 2012. Transcriptional co-regulation of neuronal migration and laminar identity in the neocortex. *Development*, 139: 1535-1546.

Lagae, L., H. Maes, S. Raiguel, D. K. Xiao and G. A. Orban. 1994. Responses of macaque STS neurons to optic flow components: A comparison of MT and MST. *Journal of Neurophysiology*, 71:1597-1626.

Lamotte, R. H. and C. Acuña. 1978. Defects in accuracy of reaching after removal of posterior parietal cortex in monkeys. *Brain Research*, 139:309-326.

Larroche, J.-C. 1966. Development of the central nervous system during intrauterine life. In: F. Falkner (ed.), *Human Development*, p. 258. Philadelphia: Saunders.

Lenneberg, E. H. 1967. *Biological Foundations of Language*. New York: Wiley.

Lehtinen, M. K., M. W. Zappaterra, X. Chen, et al. 2011. The cerebrospinal fluid provides a proliferative niche for neural progenitor cells. *Neuron*, 69:893-905.

Li, G., L. W., J. H. Gilmore et al. 2015. Spatial patterns, longitudinal development, and hemispheric assymetries of cortical thickness in infants from birth to 2 years of age. *Journal of Neuroscience*, 35:9150-9162.

Li, G., Nie, J., Wang, L. et al. 2013. Mapping region-specific longitudinal cortical surface expansion from birth to 2 years of age. *Journal of Neuroscience*, 34:4226-4238.

Loughna, P., L. Citty, T. Evans and T. Chudleigh. 2009. Fetal size and dating: Charts recommended for clinical obstetric practice. *Ultrasound*, 17:161-167.

Luck, S. J., L. Chelazzi, S. A. Hillyard and R. Desimone. 1997. Neural mechanisms of spatial selective attention in areas V1, V2, and V4 of macaque visual cortex. *Journal of Neurophysiology*, 77:24-42.

Ludwig, K. and J. Klingler. 1956. *Atlas Cerebri Humani*. Basle: Karger.

Mann, F., C. Peuckert, F. Dehner, et al. 2002. Ephrins regulate the formation of terminal axonal arbors during the development of thalamocortical projections. *Development*, 129:3945-3955.

Marin-Padilla, M. 1988. Early ontogenesis of the human cerebral cortex. In: A. Peters and E. D. Jones (eds.) *Cerebral Cortex*, vol. 7, *Development and Maturation*, pp. 1-34. New York, Plenum Press.

Marin-Padilla, M. 1992. Ontogenesis of the pyramidal cells of the mammalian neocortex and developmental cytoarchitectonics. *Journal of Comparative Neurology*, 321:223-240.

Martin, C., D. Bueno, M. I. Alonso, et al. 2006. FGF2 plays a key role in embryonic cerebrospinal fluid trophic properties over chick embryo neuroepithelial stem cells. *Developmental Biology*, 297:402-416.

Mashayekhi F. and Z. Salehi. 2006. The importance of cerebrospinal fluid on neural cell proliferation in developing chick cerebral cortex. *European Journal of Neurology*, 13:166-172.

McGraw, M. B. 1943. *The Neuromuscular Maturation of the Human Infant.* New York: Columbia University Press.

Medendorp, W. P., H. C. Goltz, T. Vilis and J. D. Crawford. 2003. Gaze-centered updating of visual space in human parietal cortex. *Journal of Neuroscience*, 23:6209-6214.

Métin, C., D. Deléglise, T. Serafini, et al. 1997. A role of netrin-1 in the guidance of cortical efferents. *Development*, 124:5063-5074.

Miller, D. J., T. Duka, C. D. Stimpson et al. 2010. Prolonged myelination in human neocortical evolution. *Proceedings of the National Academy of Sciences USA*, 109:16480-16485.

Miller, R. W. and W. J. Blot. 1972. Small had size after in-utero exposure to atomic radiation. *Lancet*, October 14 issue: 784787.

Miyashita, Y. 1988. Neuronal correlate of visual associative long-term memory in the primate temporal cortex. *Nature*, 335:817-820.

Miyashita, Y., A. Date and H. Okuno. 1993. Configurational encoding of complex visual forms by single neurons of monkey temporal cortex. *Neuropsychologia*, 31:1119-1131.

Meyer, G. and A. M. Goffinet. 1998. Prenatal development of reelin-immunoreactive neurons in the human neocortex. *Journal of Comparative Neurology*, 397:29-40.

Molyneaux, B. J., P. Arlotta , T. Hirata et al. 2005. Fez1 is required for the birth and specification of corticospinal motor neurons. *Neuron*, 47:817–831.

Mrzljak, L., H. B. Uylings, I. Kostovic and C. G. van Eden. 1992. Prenatal development of neurons in the human prefrontal cortex. II. A quantitative Golgi study. *Journal of Comparative Neurology*, 316:485-496.

Ninkovic, J. A., A. Steiner-Mezzadri, M. Jawerka. et al. 2013. The BAF complex interacts with Pax6 in adult neural progenitors to establish a neurogenic cross-regulatory transcriptional network. *Cell, Stem Cell*, 13:403-418.

Ogawa, M., T. Miyata, K. Nakajima, et al. 1995. The reeler gene-associated antigen on Cajal-Retzius neurons is a crucial molecule for laminar organization. *Neuron*, 14:899-912.

Oller, D. K. 1980. The emergence of the sounds of speech in infancy. In: G. H. Yeni-Komshian, J. F. Kavanagh and C. A. Ferguson (eds.), *Child Phonology*, vol. 1, pp. 93-112. New York: Academic Press.

O'Muircheartaigh, J., D. C. Dean, C. E. Ginestet, et al. 2014. White matter development and early cognition in babies and toddlers. *Human Brain Mapping*, 35:4475-4487.

O'Rahilly, R. and F. Müller. 1987. *Developmental Stages in Human Embryos*. Carnegie Institution of Washington Publication 637.

O'Rahilly, R. and F. Müller. 1994. *The Embryonic Human Brain: An Atlas of Developmental Stages.* New York: Wiley-Liss.

Padget, D. H. 1957. The development of the cranial venous system from a viewpoint of comparative anatomy. *Carnegie Institution Contributions to Embryology*, 247:79-140.

Page, W. K. and C. J. Duffy. 1999. MST neuronal responses to heading direction during pursuit eye movements. *Journal of Neurophysiology*, 81:596-610.

Palmer, A. and R. Klein. 2003. Multiple roles of ephrins in morphogenesis, neuronal networking, and brain function. *Genes and Development*, 17:1429-1450.

Paolini, M., C. Distler, F. Bremmer, M. Lappe and K. P. Hoffmann. 2000. Responses to continuously changing optic flow in area MST. *Journal of Neurophysiology*, 84:730-743.

Parada, C., A. Gato, M. Aparicio and D. Bueno. 2006. Proteome analysis of chick embryonic choroid plexus. *Proteomics*, 6:312-320.

Pasterkamp, R. J. 2012. Getting neural circuits into shape with semaphorins. *Nature Review Neuroscience*, 13:605-618.

Pasternak, T., J. W. Bisley and D. Calkins. 2003. Visual processing in the primate brain. In: M. Gallagher and R. J. Nelson (eds.), *Handbook of Psychology*, vol. 3, *Biological Psychology*, pp. 139- 185. New York: Wiley.

Penfield, W. and T. Rasmussen, 1950. *The Cerebral Cortex of Man: A Clinical Study of Localization of Function.* New York: Macmillan.

Petanjek, Z., M. Judaš, G. Šimic, et al. 2011. Extraordinary neoteny of synaptic sites in the human prefrontal corotex. *Proceedings of the National Academy of Sciences, USA*, 108:13281-13286.

Plummer, G. 1952. Anomalies occurring in children exposed in utero to the atomic bomb in Hiroshima. *Pediatrics*, 10:687-693.

Plunkett, K., J.-F. Hu and L. B. Cohen. 2008. Labels can override perceptual categories in early infancy. *Cognition*, 106:665-681.

Poduslo, S. E. and Y. Jang. 11984. Myelin development in infant brain. *Neurochemical Research*, 9:1615-1626.

Poskanzer, K., L. A. Needleman, O. Bozdagi and G. W. Huntley. 2003. N-cadherin regulates ingrowth and laminar targeting of thalamocortical axons. *Journal of Neuroscience,* 23:2294-2305.

Preissler, M. A. and S. Carey. 2004. Do both pictures and words function as symbols for 18- and 24-month-old children? *Journal of Cognition and Development*, 5:185-212.

Pujol, J., C. Soriano-Mas, H.Oriz, et al. 2006. Myelination of language-related areas in the developing brain. *Neurology*, 66:339-343.

Pulvers, J. N., N. Journiac, Y. Arai and J. Nardelli. 2015. MCPH1: A window into brain development and evolution. *Frontiers in Cellular Neuroscience*, 9:92.

Quinn, J. C., M. Molinek, B. S. Martynoga, et al. 2007. Pax6 controls cerebral cortical cell number by regulating exit from the cell cycle and specifies cortical cell identity by a cell autonomous mechanism. *Developmental Biology*, 302:50-65.

Randolph, M. and J. Semmes. 1974. Behavioral consequences of selective subtotal ablations in the postcentral gyrus of *Macaca mulatta*. *Brain Research*, 70:55-70.

Retzius, G. 1896. *Das Menschenhirn: Studien in der makroskopischen Morphologie.* Stockholm: Königliche Buchdruckerei.

Roback, H. N. and H. J. Scherer. 1935. Über die feinere Morphologie des frühkindlichen Hirnes under besondere Berücksichtingung der Glia Entwicklung. *Virchov's Archiv für pathologische Anatomie*, 294:365-413.

Rolls, E. T. 1984. Neurons in the cortex of the temporal lobe and in the amygdala of the monkey with responses selective for faces. *Human Neurobiology*, 3:209-222.

Rushworth, M. F., P. D. Nixon and R. E. Passingham. 1997. Parietal cortex and movement. I. Movement selection and reaching. *Experimental Brain Research*, 117:292-310.

Sakata, H., M. Taira, A. Murata and S. Mine. 1995. Neural mechanisms of visual guidance of hand action in the parietal cortex of the monkey. *Cerebral Cortex*, 5:429-438.

Sansom, S. N., D. S. Griffiths, Faedo, et al. 2009. The level of the transcription factor Pax6 is essential for controlling the balance between neural stem cell self-renewal and neurogenesis. *PLoS Genetics,* 5(6):e1000511.

Sauer, F. C. 1936. The interkinetic migration of embryonic epithelial nuclei. *Journal of Morphology,* 60:1-11.

Saunders, N. R., K. M. Dziegielewska, K. Møllgård, et al. 2015. Influx mechanisms in the embryonic and adult rat choroid plexus: A transcriptome study. *Frontiers in Neuroscience*. 9:123. (PMC4412010)

Schadé, J. P. and W. B. van Groningen. 1961. Structural organization of the human cerebral cortex: Maturation of the middle frontal gyrus. *Acta Anatomica*, 47:74-111.

Schira M. M., C. W. Tyler, M. Breakspear and B. Spehar. 2009. The foveal confluence in human visual cortex. *Journal of Neuroscience*, 29:9050-9058.

Schnack, H. G., N. E. M. van Haren, R. M. Brouwer et al. 2015. Changes in thickness and surface area of the human cortex and their relationship with intelligence. *Cerebral Cortex*, 25:1608-1617.

Sherbondy, A. J., R. F. Dougherty, S. Napel and B. A. Wandell. 2008. Identifying the human optic radiation using diffusion imaging and fiber tractography. *Journal of Vision*, 81-11.

Snyder, L. H., A. P. Batista and R. A. Andersen. 1997. Coding of intention in the posterior parietal cortex. *Nature*, 386:167-170.

Stoykova, A., D. Treichel, M. Hallonet and P. Gruss. 2000. Pax6 modulates the dorsoventral patterning of the mammalian telencephalon. *Journal of Neuroscience*, 20:8042-8050.

Sturrock, R. R. 1990. A morphological study of the development of the leptomeninx in the fetal rat cerebrum. *Anatomischer Anzeiger*, 171:265-271.

Szebenyi, G., E. W. Dent, J. L. Callaway, et al. 2001. Fibroblast growth factor-2 promotes axon branching of cortical neurons by influencing morphology and behavior of the primary growth cone. *Journal of Neuroscience*, 21:3932-3941.

Taira, M., S. Mine, A. P. Georgopoulos, A. Murata and H. Sakata. 1990. Parietal cortex neurons of the monkey related to the visual guidance of hand movement. *Experimental Brain Research*, 83:29-36.

Tamai, H., H. Shinohara, T. Miyata, et al. 2007. Pax6 transcription factor is required for the interkinetic nuclear movement of neuroepithelial cells. *Genes Cells*, 12:983-996.

Tanaka, K. 2000. Mechanisms of visual object recognition studied in monkeys. *Spatial Vision*, 13:147-163.

Tanaka, K. and H. Saito. 1989. Analysis of motion of the visual field by direction, expansion/contraction, and rotation by cells clustered in the dorsal part of the medial superior temporal area of the macaque monkey. *Journal of Neurophysiology*, 62:626-641.

Tanaka, K., and H.-A. Saito, Y. Fukada and M. Moriya. 1991. Coding visual images of objects in the inferotemporal cortex of the macaque monkey. *Journal of Neurophysiology*, 66:170-189.

Tang, C. Y., E. L. Eaves, J. C. Ng et al. 2010. Brain networks for working memory and factors of intelligence assessed in males and females with fMRI and DTI. *Intelligence*, 38:293-303.

Tennyson, V. M. and G. D. Pappas. 1964. Fine structure of the developing telencephalic and myelenephalic choroid plexus in the rabbit. *Journal of Comparative Neurology*, 123:379-412.

Toga, A. W., P. M. Thompson and E. R. Sowel. 2006. Mapping brain maturation. *Trends in Neuroscience*, 29:148-159.

Torreson, H., S. S. Potter, K. Campbell. 2000. Genetic control of dorsal-ventral identity in the telencephalon : Opposing roles for Pax6 and Gsh2. *Development*, 127:4361-4371.

Travis, K., K. Ford and B. Jacobs. 2005. Regional dendritic variation in neonatal human neocortex: A quantitative Golgi study. *Developmental Neuroscience*, 27:277-287.

Travis, K. E., M. M. Curran, M. K. Leonard, et al. 2013. Age-related changes in tissue signal properties within cortical areas important for word understanding in 12- to 19-month-old infants. *Cerebral Cortex*, 24:1948-1955.

Treue, S. and J. H. Maunsell. 1999. Effects of attention on the processing of motion in macaque middle superior temporal and medial superior temporal visual cortical areas. *Journal of Neuroscience*, 19:7591-7602.

Tsao, D. Y., W. A. Freiwald, T. A. Knutsen, et al. 2003. Faces and objects in macaque cerebral cortex. *Nature Neuroscience*, 6:989-995.

Ungerleider, L. G. and M. Mishkin. 1982. Two cortical visual systems. In: D. J. Ingle et al. (eds.), *Analysis of Visual Behavior*, pp. 549-586. Cambridge, MA: MIT Press.

Van Essen, D. C. 1997. A tension-based theory of morphogenesis and compact wiring in the central nervous system. *Nature*, 385:313-318.

Van Essen, D. C. and S. M. Zeki. 1978. The topographic organization of rhesus monkey prestriate cortex. *Journal of Physiology*, 277:193-226.

Vernon, P. E. 1979. *Intelligence: Heredity and Environment*. New York: Freeman.

Vogt, C. and O. Vogt. 1902. *Beiträge zur Hirnfasernlehre*. Vol. 1. *Zur Erforschung der Hirnfaserung.* Jena: Fischer.

Vogt, C. and O. Vogt. 1904. *Beiträge zur Hirnfasernlehre*. Vol. 2. *Die Markreifung des Kindergehirns während der ersten vier Lebensmonate und ihre methodologische Bedeutung*. Jena: Fischer.

Walcher T., Q. Xie, J. Sun, et al. 2013. Functional dissection of the paired domain of Pax6 reveals molecular mechanisms coordinating neurogenesis and proliferation. *Development*, 140:1123-1136.

Wandell, B. A., S. O. Dumoulin and A. A. Brewer. 2007. Visual field maps in human cortex. *Neuron*, 56:366-383.

Wilke, M., J. H. Sohn, A. W. Byars and S. K. Holland. 2003. Bright spots: Correlations of gray matter volume with IQ in a normal pediatric population. *NeuroImage*, 20:202-215.

Woods, C. G., J. Bond and W. Enard. 2005. Autosomal primary recessive mirocephaly (MCPH): A review of clinical, molecular, and evolutionary findings. *American Journal of Human Genetics*, 76:717-728.

Yakovlev, P. I. and A.-R. Lecours. 1967. The myelogenetic cycles of regional maturation of the brain. In: A. Minkowski (ed.), *Regional Development of the Brain in Early Life*, pp. 3-70. Oxford: Blackwell.

Yamazaki, J. N., S. W Wright and P. M. Wright. 1954. Outcome of pregnancy in women exposed to the atomic bomb in Nagasaki. *American Journal of Diseases in Children*, 87:448-463.

Yun, K., S. Potter and J. L. Rubenstein. 2001. Gsh2 as Pax6 play complementary roles in dorsoventral patterning of the mammalian telencephalon. *Development*, 128:193-205.

Zeki, S. M. 1973. Colour coding in rhesus monkey prestriate cortex. *Brain Research*, 53:422-427.

Zeki, S. M. 1978. The cortical projections of foveal striate cortex in the rhesus monkey. *Journal of Physiology*, 277:227-244.

Zhang, X., C. T. Huang, J. Chen, et al. 2010. Pax6 is a human neuroectoderm cell fate determinant. *Cell, Stem Cell*, 7:90-100.